Life is pleasant. Death is peaceful. It's the transition that's troublesome.

- Isaac Asimov

University of Alberta

Investigation of the Anti-apoptotic Function and Regulation of Vaccinia Virus F1L

by

Stephanie Dawn Campbell

A thesis submitted to the Faculty of Graduate Studies and Research
in partial fulfillment of the requirements for the degree of

Doctor of Philosophy
in
Virology

Medical Microbiology and Immunology

To my parents, for their endless support, encouragement, and inspiration.

Abstract

Apoptosis, an evolutionarily conserved cell death programme, is a potent barrier against virus infection. Central to this process are mitochondria, which harbour cytochrome *c* and other apoptosis-inducing factors. Once released, these factors activate a caspase cascade that culminates in cell death. Mitochondrial integrity is tightly regulated by the Bcl-2 family of proteins, which are united by the presence of one or more conserved Bcl-2 homology, or BH, domains that are critical for protein interactions and function. Bak and Bax are the key pro-apoptotic members that engage the mitochondrial death machinery to release cytochrome *c*. These proteins are activated by pro-apoptotic BH3-only proteins and inhibited by anti-apoptotic family members, such as Mcl-1. Due to the importance of Bak and Bax, many viruses, including poxviruses, have adapted strategies to interfere with the activation of these two proteins. In the prototypic poxvirus vaccinia virus, this is accomplished by a unique anti-apoptotic protein, F1L. F1L localizes to mitochondria and prevents apoptosis induced by a variety of stimuli. This is achieved by direct binding to Bak, while Bax inhibition is believed to occur by the binding of F1L to the BH3-only protein, BimL. However, the way in which F1L binds Bak and BimL is unknown, since F1L lacks sequence homology to Bcl-2 proteins. Here, we show that F1L functions in a manner that resembles Mcl-1, the major cellular regulator of Bak. Moreover, we have identified divergent BH domains within F1L that are critical for Bak binding and anti-apoptotic activity. Given the importance of the Bcl-2 family of

proteins, many members are regulated by ubiquitination, which targets the proteins for proteasomal degradation. Similarly, we have discovered that F1L is tightly regulated by the ubiquitin-proteasome system. Our studies on F1L ubiquitination have also revealed a potential role for F1L in the regulation of mitochondrial morphology. Thus, despite divergence at the sequence level, F1L interacts with Bak in a manner nearly identical to cellular Bcl-2 family members, and, additionally, F1L is governed by the same regulatory mechanisms that control members of the Bcl-2 family.

Acknowledgement

I would first of all like to thank Michele Barry for giving me the chance to work in her lab. Michele has been a wonderful mentor and has provided me with so many opportunities to pass on the knowledge I have acquired to others. She has always believed in me, encouraged me, and provided me with room to grow. Thank you for everything.

To my lab mates, both past and present, you made work such a pleasure. For being great mentors, I would like to thank John Taylor and Brianne Couturier. And to the students who contributed to this work, namely Robyn-Lee Burton, Ninad Mehta, John Thibault, and Alastair Teale – thank you. And of course Kristin Burles, who finally figured out where the easy button belongs.

I would also like to thank my science buddy from the beginning, Nicola McFarlane, who was always available for coffee dates and pep talks. I also have an amazing group of friends who were never more than a phone call away. A HUGE thanks goes out to Tara Menon, Sarah Tippe, Jasmine John, and Ramya El-Hayouni.

And of course my two lab BFFs: Logan Banadyga and Nick van Buuren. On our first day as grad students I didn't realize how close we would become. You guys are more than just lab mates and travelling partners. You have become such close friends. Heck yeah!!!

I also need to thank my amazing boyfriend Brett Stefura for his endless encouragement and positive thoughts. I love you times a million!

Last, but definitely not least, my family. My brother Brandon continues to amaze and inspire me with his accomplishments. My mom and dad have unbelievable faith in me and have always been in my corner. For this I will forever be grateful.

Table of Contents

Table of Contents (Continued)

CHAPTER 2: Materials and Methods

Table of Contents (Continued)

Table of Contents (Continued)

Table of Contents (Continued)

Table of Contents (Continued)

List of Tables

List of Figures

CHAPTER 4: Identification and Characterization of the Functional Domains in Vaccinia Virus F1L

CHAPTER 5: F1L is Regulated by the Ubiquitin-Proteasome System

CHAPTER 6: Discussion

Appendix

List of Figures (Continued)

List of Abbreviations Used in This Study

β-TrCP – Beta-transducin-repeat-containing-protein
Δψm – inner mitochondrial membrane potential
μCi – microcurie
μL – microliter
μM – micromolar
aa – amino acid
AdV – adenovirus
AIF – apoptosis inducing factor
ASFV – African swine fever virus
ATCC – american type culture collection
ATP – adenosine triphosphate
Bak – Bcl-2 antagonist of killing
Bax – Bcl-2 associated gene X
BCA – bicinchoninic acid assay
Bcl – B-cell leukemia/lymphoma
BGMK – buffalo green monkey kidney cells
BH – Bcl-2 homology
Bid – Bcl-2 interacting domain
Bim – Bcl-2 interacting mediator of cell death (S-short, L-long, EL-extra long)
BMK – baby mouse kidney
bp – basepair
BrdU - 5-bromo-2'-deoxyuridine
BSA – bovine serum albumin
CHAPS - 3-[(3-cholamidopropyl)-dimethylammonio]-1-propanesulfonate
Cop - Copenhagen
CrmA – cytokine response modifier A
CTL – cytotoxic T lymphocyte
CV-1 – African green monkey kidney cells
Cul – cullin
DMEM – Dulbecco's modified Eagle's media
DMF – dimethylformamide
DMSO – dimethyl sulphoxide
DNA – deoxyribonucleic acid
dsDNA – double-stranded deoxyribonucleic acid
dsRNA – double-stranded ribonucleic acid
DUB – deubiquitinating enzyme
EBV – Epstein-Barr virus
ECL – enhanced chemiluminescence
EDTA – ethylenediaminetetraacetic acid
EGFP – enhanced green fluorescent protein
EGTA – ethylene glycol tetraacetic acid
ER – endoplasmic reticulum

List of Abbreviations Used in This Study (Continued)

EV – enveloped virus
EVM – ectromelia virus strain Moscow
FADD – Fas-associated death domain
FITC – fluorescein isothiocyanate
HA – haemagglutinin
HCMV – human cytomegalovirus
HEK – human embryonic kidney
HI-FBS – heat-inactivated fetal bovine serum
HRP – horseradish peroxidise
IAP – inhibitor of apoptosis protein
ICS – intracristae space
IFN – interferon
IHDW – vaccinia virus strain International Health Department
IMM – inner mitochondrial membrane
IMS – intermembrane space
IP - immunoprecipitation
IPTG – isopropyl β-D-1-thiogalactopyranoside
ITR – inverted terminal repeats
JNK – jun kinase
kb – kilobase
kDa – kilodalton
KSHV – Kaposi's sarcoma herpesvirus
LB – Luria-Bertani Broth
LMH – leghorn male hepatoma
LMP – low melting point
M – molar
MAPK – mitogen-activated protein kinase
Mcl-1 – myeloid cell leukemia 1
MCMV – mouse cytomegalovirus
MEF – mouse embryonic fibroblast
mg – milligram
MG132 – N-(benzyloxycarbonyl)leucinylleucinylleucinal (proteasome inhibitor)
MHC – major histocompatibility complex
mL – millilitre
MnSOD – manganese superoxide dismutase
MOI – multiplicity of infection
MOMP – mitochondrial outer membrane permeabilization
MV – mature virus
MVA – Modified vaccinia virus Ankara
NFκB – nuclear factor kappa B
nm - nanometer
OMM – outer mitochondrial membrane

List of Abbreviations Used in This Study (Continued)

ORF – open reading frame
PAGE – polyacrylamide gel electrophoresis
PARP – poly-ADP ribose polymerase
PBR – peripheral benzodiazepine receptor
PBS – phosphate buffered saline
PCR – polymerase chain reaction
PE - phycoerythrin
PFA – paraformaldehyde
pfu – plaque forming unit
PKR – protein kinase response
PT – permeability transition
PTP – permeability transition pore
PVDF – polyvinylidene fluoride
RE – restriction endonuclease
RING – really interesting new gene
RIPA – radioimmunoprecipitation assay
RMPI – Rosewell Park Memorial Institute
RNA – ribonucleic acid
rRNA – ribosomal ribonucleic acid
SCF – Skp1-Cullin 1-F-box
S.D. – standard deviation
SDS – sodium dodecyl sulphate
Skp1 – S-phase-kinase-associated protein 1
SMAC – second mitochondrial activator of caspases
SPI – serine protease inhibitor
SSC – standard saline citrate
STS – staurosporine
TAE – tris acetate EDTA
TBST – tris buffered saline plus Tween 20
TK – thymidine kinase
TMRE – tetramethylrhodamine ethyl ester
TNFα – tumour necrosis factor alpha
TNFR – tumour necrosis factor receptor
TRADD – tumour necrosis factor receptor associated death domain
tRNA – transfer ribonucleic acid
U – units
Ub – ubiquitin
UPS – ubiquitin-proteasome system
UV – ultraviolet
v/v – volume/volume
vMIA – viral mitochondrial inhibitor of apoptosis
VV – vaccinia virus

List of Abbreviations Used in This Study (Continued)

w/v – weight/volume
WB – western blot
WR – Western Reserve
WT – wildtype
WV – wrapped virus
X-gal – 5-bromo-4-chloro-3-indolyl-β-D-galactopyranoside
XIAP – X-linked inhibitor of apoptosis protein

CHAPTER 1: Introduction

1.1 POXVIRUSES

The *Poxviridae* family is a large family of enveloped DNA viruses that infect insects (*Entomopoxvirinae*) and vertebrates (*Chordopoxvirinae*) (Table 1.1) [1]. Poxviruses are the most complex and diverse viruses as they complete their entire life cycle in the cytoplasm of infected cells [2]. The nine recognized genera in the *Chordopoxvirinae* subfamily share similar biological features and some cause disease in humans or domesticated animals, such as sheep, goats, cows, and poultry [1,3]. The most notorious member of the *Poxviridae* family, variola virus, was the causative agent of smallpox, which caused the deaths of hundreds of millions of people and greatly shaped our world's history [4,5,6]. While only two species, variola virus (genus *Orthopoxvirus*) and molluscum contagiosum virus (genus *Molluscipoxvirus*), are specific to humans, members of the *Orthopoxvirus*, *Parapoxvirus*, and *Yatapoxvirus* genera can also infect humans; however this most often occurs zoonotically [1,7]. Although the poxvirus family is most well known for the wrath of smallpox, many members of the family are currently being studied in the areas of vaccine development and gene therapy research [1].

1.1.1 Orthopoxviruses

The *Orthopoxvirus* genus compromises twelve species and includes the most medically-relevant poxviruses (Table 1.1) [1,3,8]. Species within this genus are characterized by immunologic cross-reaction and cross-protection, yet host range and disease severity are quite diverse [1,7]. Variola virus and ectromelia virus are specific for humans and mice, respectively, and cause systemic disease in infected hosts [8]. Ectromelia virus causes a severe and often lethal disease in mice, known as mousepox, and thus serves as an excellent small animal model for smallpox infections since both diseases are highly pathogenic and transmissible [9,10]. Members such as vaccinia virus, monkeypox virus, and cowpox virus, however, infect a broad range of hosts including humans, rabbits, cows, monkeys, and rodents [1,7]. Unlike cowpox virus and vaccinia virus, which

Table 1.1 The *Poxviridae* Family.

Subfamily *Entomopoxvirinae*		
Genus	**Species**	
Alphaentomopoxvirus	Melolontha melolontha entomopoxvirus	
Betaentomopoxvirus	Amsacta moorei entomopoxvirus	
Gammaentomopoxvirus	Chironomus luridus entomopoxvirus	
Subfamily *Chordopoxvirinae*		
Genus	**Species**	**Reservoir Hosts**
Orthopoxvirus	Variola virus	Humans
	Vaccinia virus	Unknown
	Ectromelia virus	Rodents
	Monkeypox virus	Rodents, squirrels
	Cowpox virus	Rodents
	Camelpox virus	Camels
	Raccoonpox virus	Raccoons
	Horsepox virus	Unknown
	Taterapox virus	Gerbils
	Uasin Gishu poxvirus	Unknown
	Skunkpox virus	Skunks
	Volepox virus	Voles
Parapoxvirus	Orf virus	Sheep, goats
	Bovine papular stomatitis virus	Cattle
Capripoxvirus	Sheeppox virus	Sheep
	Goatpox virus	Goats
	Lumpy skin disease virus	Cattle
Suipoxvirus	Swinepox virus	Swine
Leporipoxvirus	Myxoma virus	Rabbits
	Shope fibroma virus	Rabbits
	Squirrel fibroma virus	Gray squirrel
Avipoxvirus	Fowlpox virus	Birds
Yatapoxvirus	Tanapox virus	Rodents?
	Yaba monkey tumour virus	Monkeys?
Molluscipoxvirus	Molluscum contagiosum virus	Human
Cervidpoxvirus	Deerpox virus	Deer

Adapted from [1,3].

cause localized benign infections, monkeypox virus causes a systemic disease in humans reminiscent of smallpox [11]. Fortunately, both monkeypox virus and cowpox virus infections of humans are accidental and occur only in rare instances through zoonosis after exposure to infected animal hosts, yet the incidence of monkeypox virus infections has risen and it may therefore represent an emerging disease [11]. Intriguingly, the natural host for vaccinia virus is unknown, yet the virus was widely used to immunize humans against smallpox and instrumental in the global eradication of variola virus [12,13].

1.1.1.1 Variola virus

Variola virus is the most notorious member of the *Poxviridae* family and it was the first virus to be used as a preventative antiviral measure and the first virus to be globally eradicated [6,9]. Smallpox, the disease caused by variola virus, was specific for humans and caused devastating illness typically characterized by systemic infection and raised pustular lesions on the skin [6]. Two variants of variola virus existed; variola major, which had a fatality rate of 30%, and variola minor, which killed less than 1% of infected individuals [8]. The highly transmissible nature and pathogenicity of the virus led to deaths of millions and often left survivors severely scarred and disfigured [4,8]. The demise of smallpox is accredited to British doctor Edward Jenner who, in 1796, pioneered vaccinations using cowpox virus lesions from infected milkmaids to immunize people against variola virus infections [14]. This, along with a widespread eradication program initiated by the World Health Organization, led to the last natural case of smallpox in 1977 and thus its eradication [13,15].

1.1.1.2 Vaccinia virus

Although Edward Jenner employed cowpox virus as the vaccinating agent, for the past 200 years the vaccine used to protect against variola virus has been the related orthopoxvirus, vaccinia virus (VV) [2]. The transition from cowpox virus to VV for smallpox vaccination and the origin of VV remains unclear [12,14]. It is speculated that VV could be a derivative of cowpox virus or another

virus such as buffalopox virus; alternatively, VV may represent a now extinct virus [12,14]. While the natural host of VV is unknown, the virus infects a wide range of hosts [1,7]. In humans, VV produces localized benign lesions until the virus is rapidly cleared by the immune system [1,3]. Although the first and most well recognized use of VV was its role in eradicating smallpox, VV is still being studied in disease treatment through gene delivery therapies, oncolytic therapies, and development of vaccines against poxviruses and other viruses [16,17,18]. Additionally, the 192 kilobase (kb) genome of VV encodes a plethora of immunomodulatory proteins and research on the activity of these proteins has contributed to a better understanding of host immune pathways [19,20,21,22].

1.1.2 Poxvirus Genome Organization

Poxviruses are extremely large viruses with virion sizes of approximately 350 by 270 nanometers (nm) (Fig 1.1A) [2]. While some poxviruses are ovoid-shaped, members of the *Orthopoxvirus* genus appear as large brick-shaped virions (Fig 1.1A) [1]. The viruses are wrapped in at least one lipid bilayer and various morphologically distinct virions are observed during infection, all of which contain a proteinaceous core that houses the genomic material (Fig 1.1B) [1]. The large virion size is necessary to accommodate the extremely large double-stranded (ds) DNA genome, which for chordopoxviruses ranges from 140-260kb and encodes more than 150 genes [2]. The linear genome contains inverted terminal repeats (ITRs) and at the extreme termini, the two strands of DNA are covalently linked to form hairpins (Fig 1.1C) [2]. Viral proteins involved in essential molecular functions such as replication, transcription, protein processing, and virion assembly, as well as structural proteins, are encoded by genes in the 100kb central conserved region of the genome (Fig 1.1C) [2,23]. Nearly 100 genes within the central region are conserved throughout the *Chordopoxvirinae* subfamily and these genes are often essential for virus replication *in vitro* [24]. In contrast, the genes found in the variable regions at

A

B

dsDNA genome

Viral enzymes

Lateral body

Surface
proteins

Core

Membrane

C

| ITR | Var. Region | Conserved Region | Var. Region | ITR |
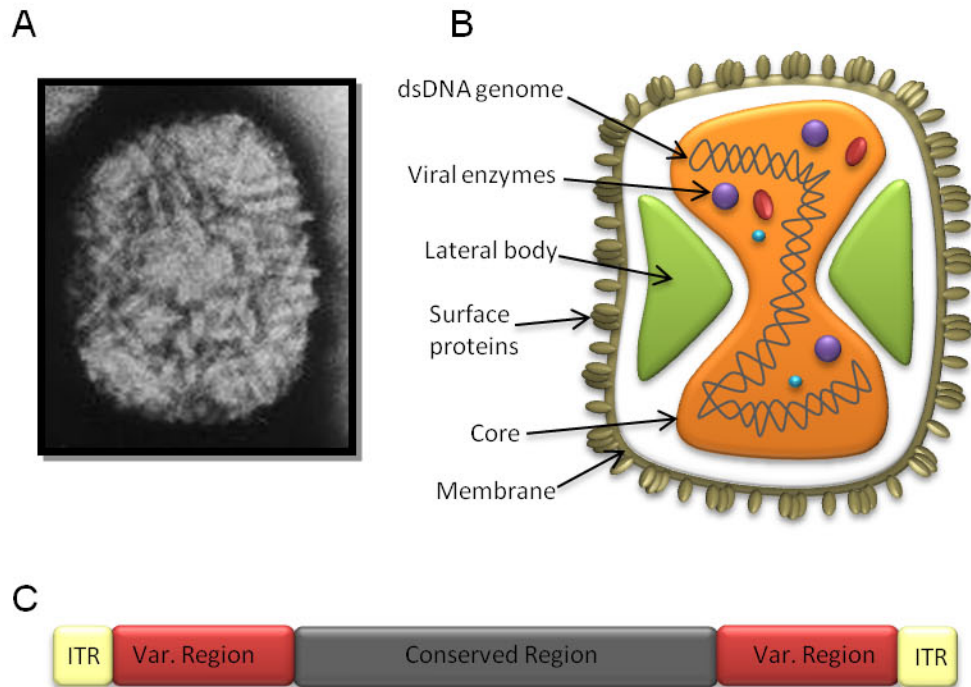
Figure 1.1 The structure and organization of poxviruses. A. Electron micrograph of a negatively stained vaccinia virus mature particle (adapted from [717]). **B.** A vaccinia virus mature virus particle contains a lipid bilayer with surface proteins important for fusion. The envelope surrounds two lateral bodies and a biconcave proteinaceous core that contains the dsDNA genome and viral proteins to initiate early gene transcription following entry. **C.** The linear dsDNA genome of poxviruses is divided into conserved and variable (Var.) regions. Conserved genes required for replication, gene expression, and virion assembly are located in the central region. The variable regions at both ends of the genome contain genes involved in immune evasion and host range specificity and these genes are highly variable throughout the *Poxviridae*. Inverted terminal repeats (ITR) located at the extreme ends contain duplicated genes and hairpins at the ends of the genome covalently link the two DNA molecules.

both ends of the genome are extremely diverse and no one gene in the variable region is conserved throughout chordopoxviruses [23,25]. These genes have roles in immune evasion and host-range determination [2,23]. Although deletion of variable genes does not usually alter virus growth *in vitro*, the gene products are usually required for subversion of the host immune response and virus virulence *in vivo* [2,23].

1.1.3 Poxvirus Life Cycle

The large genomes of poxviruses accommodate the production of many viral proteins involved in replication and transcription, which is critically important since poxviral replication takes place entirely in the cytoplasm of infected cells away from nuclear machinery [2]. Infection is initiated by one of two infectious forms, the mature virion (MV) (Fig 1.1B) or the enveloped virion (EV), which differ in the number and composition of membranes surrounding the nucleoprotein core (Fig 1.2) [2]. MVs represent the most basic virion containing one membrane wrapping the core, while EVs contain an extra membrane derived from cellular organelles [2,26]. To begin infection, MV attaches to unidentified cellular receptors and the virus membrane fuses with the plasma membrane to release the genome-containing core into the cytoplasm (Fig 1.2) [27]. For EV to enter, the outer membrane must first be disrupted prior to fusion [27]. Whether this event occurs outside of the cell or in an endosome following endocytosis is unclear; however, once the outer membrane is dissociated, the remaining membrane can fuse with the plasma or endosomal membrane to release the core [27].

In the cytoplasm, the virion core components begin dismantling in a process referred to as uncoating [2]. During uncoating, the virus-associated RNA polymerase and transcription factors present in the core begin transcribing early genes [2]. Poxviral gene expression is temporally regulated; early genes encode immune evasion proteins, a DNA-dependent DNA polymerase, and proteins involved in virus DNA replication (Fig 1.2) [2]. Replication of viral genomic DNA
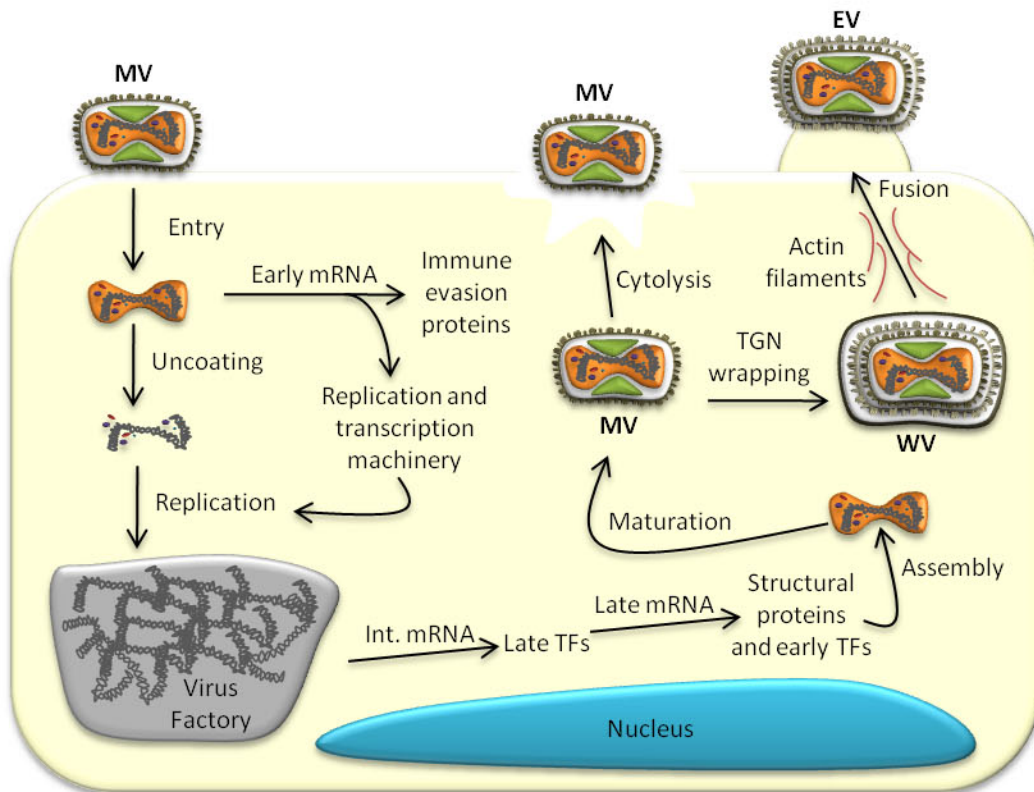
Figure 1.2 Poxvirus life cycle. Infection is initiated by binding of mature virions (MV) to unidentified cellular receptors leading to fusion of the virus membrane with the plasma membrane. Extracellular enveloped virions (EV) can also initiate infection but must lose the outermost membrane prior to fusion. Fusion releases the core into the cytoplasm and early transcription begins within the core prior to uncoating. Early mRNAs encode proteins involved in immune evasion, viral replication, and intermediate (Int.) gene expression. Viral replication takes place in discrete DNA-rich cytoplasmic sites, or viral factories. Intermediate genes encode transcription factors (TFs) for late gene expression, which produces structural proteins and early TFs that get packaged in newly synthesized virions. Notably, viral gene expression and assembly occur within viral factories. Virus assembly begins with the formation or acquisition of crescent-shaped membranes that surround the genome-containing cores to produce MV, which are released by cytolysis. MV may also get wrapped in a double membrane from the trans-Golgi network (TGN) to produce wrapped virions (WV). WVs are propelled to the cell surface on actin filaments, which produce actin pedestals on the cell surface. WVs fuse with the plasma membrane to release EV, which may diffuse away from the infected cell or remain attached as cell-associated EV. Adapted from [2].

and transcription of viral genes occur in discrete cytoplasmic regions named "viral factories" (Fig 1.2) [28,29]. Following DNA replication, intermediate genes are expressed, which consist mainly of transcription factors that facilitate late gene expression [2]. Late genes encode virus structural proteins and proteins that aid in virion assembly. Following late protein synthesis, virion morphogenesis begins in the viral factory with crescent-shaped membranes forming [2]. Whether the outer membrane of the virion arises *de novo*, or whether it is derived from an intermediate compartment between the Golgi apparatus and endoplasmic reticulum (ER) currently remains unknown [28,30]. Once the membrane is generated or acquired, immature virus particles mature into MVs upon acquisition of a genome-containing core (Fig 1.2) [2,31]. Wrapped virions (WVs) are formed from a small fraction of MVs that get wrapped by an additional double membrane from the trans-Golgi or endosomal network (Fig 1.2) [2,31]. While MVs are released through cytolysis, WVs are shuttled to the cell periphery along actin filaments where they fuse with the plasma membrane, lose their outermost membrane, and are released as EVs into the extracellular space (Fig 1.2) [2,31,32]. The exocytosed EV may also remain attached to the plasma membrane of infected cells as cell-associated EV and this form of the virus is propelled along the cell surface by microvilli to infect adjacent cells (Fig 1.2) [31,32]. This method of EV propulsion along actin pedestals is believed to be the most efficient method of cell to cell spread of the virus [33].

1.1.4 Poxviruses and Immune Evasion

1.1.4.1 The Immune Response to Poxviruses

Both innate and adaptive arms of the immune system are involved in warding off poxvirus infections [20]. On the adaptive arm, which includes cellular and humoral immunity, the cell-mediated response of cytotoxic T-lymphocytes (CTLs) is particularly important in the removal of poxvirus-infected cells [34,35]. However, before the CTL response is mounted, poxviruses are

faced with a multifaceted innate response [19,20,21,22]. Host innate defences occur extracellularly with the binding of complement proteins to the lipid envelope of EV and subsequent recruitment of antibodies for antibody-dependent neutralization [20]. Concomitantly, circulating chemokines released by infected cells lead to activation and migration of leukocytes, such as macrophages and neutrophils, to the site of infection [20,36]. Circulating cytokines, such as interferon (IFN) α, β, and γ, tumour necrosis factor α (TNFα), interleukin-1 beta (IL-1β), and interleukin-18 (IL-18), have direct antiviral, cytolytic, and pro-inflammatory functions [21,37]. Poxviruses are also faced with intracellular innate defences, one of which is the activation of the protein kinase (PKR) pathway that detects viral double-stranded RNA (dsRNA) and leads to global inhibition of protein synthesis [20]. Additionally, TNFα and IL-1β signalling pathways converge on the activation of the transcription factor NFκB that upregulates many pro-inflammatory cytokines including pro-IL-1β and pro-IL-18 that form active molecules upon proteolytic cleavage by the cysteine protease caspase 1 [20]. Importantly, the cytokines involved in the innate immune response to poxvirus infections have critical roles in the subsequent activation and shaping of the T-lymphocyte response [20,34,35].

1.1.4.2 Immune Evasion Strategies of Vaccinia Virus

In addition to genes involved in replication and mRNA synthesis, the large genomes of poxviruses contain an arsenal of immunomodulatory genes whose protein products interfere with inflammatory and antiviral host responses [19,20,21,22]. Most of these genes are present in the variable region of the genome and thus vary considerably between genera and even within species [2,23]. Because many of these genes are highly similar to their cellular counterparts, it is believed that poxviruses captured these genes from infected hosts through horizontal gene transfer [22,37]. These captured genes are then re-purposed to circumvent the host immune response.

The importance of the innate inflammatory response during poxviral infection is underscored by the number of viral gene products aimed at obstructing inflammatory pathways [19,20,21,22]. VV encodes several secreted gene products that inhibit extracellular immune defences (Table 1.2). These include complement inhibitors, chemokine binding proteins, and soluble receptors to bind IFN-α/β, IFN-γ, TNFα, IL-1β, and IL-18 [19,20,38]. To impede intracellular host defences, VV produces a large number of proteins that inhibit NF-κB activation [22], and two proteins, E3L and K3L, that prevent the sensing of viral dsRNA and activation of the PKR response (Table 1.2) [39,40,41]. Additionally, VV contains a family of serine proteases, or serpins, such as the cytokine response modifier A (CrmA) homologue SPI-2, that inhibit caspase 1 activation and thus prevent the downstream cleavage of pro-IL-1β to its active form IL-1β [42,43]. Examining the variable region of the VV genome has revealed the importance of immune evasion during the virus life cycle [19,20,21,22]. The presence of numerous immune evasion genes also highlights the cellular pathways that are active during VV infection and thus require viral targeting [19,20,21,22]. One of those cellular pathways, important not only during VV infection but also during infection with a number of poxviruses, is the activation of the cellular suicide machinery, or apoptosis.

1.2 APOPTOSIS

Apoptosis, or "cellular suicide", is a genetically programmed mechanism of self-destruction found in all multicellular organisms [44,45,46]. Originally described in 1972, apoptosis is now widely studied because of its importance in maintaining the overall integrity of multicellular organisms and preventing certain diseases and infections [47,48]. Apoptotic cell death plays fundamental roles in embryonic development, tissue homeostasis, and removal of damaged and abnormal cells [44,45,46]. Moreover, the apoptotic machinery is an active immune defence against pathogens, since circulating CTLs and natural killer (NK) cells can rapidly induce apoptosis in infected cells and infected cells themselves

Table 1.2 Vaccinia Virus Immune Evasion Genes.

Secreted Factors		
Gene	**Function**	**Source**
A39R	Semaphorin	726
A41R	Chemokine binding protein	737,740
A53R*	Soluble TNF receptor (CrmC)	461
B5R	Complement binding protein	743
B8R	Soluble IFN-γ receptor	719
B16R	Soluble IL-1β receptor	720,729
B19R	Soluble IFNα/β receptor	721,728
B28R/C22L*	Soluble TNF receptor (CrmB)	460
B29R/C23L	Chemokine binding protein	722,723
C3L	Complement binding protein	741,742
C11L	Epidermal growth factor homologue	724,725
VACWR-013*	IL-18 binding protein	730,731
Intracellular Factors		
Gene	**Function**	**Source**
A46R	NFκB inhibitor	718
A52R	NFκB inhibitor	718
B13R*	Serpin (SPI-2/CrmA), inhibits caspase 1/8	42,43
B14R	NFκB inhibitor	704,736
C12L	Serpin (SPI-1)	479,480
E3L	Binds dsRNA, inhibits PKR	39,40
H1L	Dephosphorylates STAT1, blocks IFN	739
F1L	Mitochondrial inhibitor of apoptosis	547
K1L	NFκB inhibitor	734
K2L	Serpin (SPI-3)	732,733
K3L	eIF-2 mimic, inhibits PKR	41
K7L	Inhibits NF-κB and IFN	738
M2L	NFκB inhibitor	735
N1L	NFκB inhibitor	702

*These genes are present in vaccinia virus strain Western Reserve but absent or pseudogenes in vaccinia virus strain Copenhagen.

can initiate the apoptotic program in response to cellular stress [49,50]. Defects in apoptosis are tightly linked to disease: too much apoptosis can lead to degenerative disorders and immunodeficiency, whereas too little apoptosis can result in autoimmunity and cancer [51]. Cells undergoing apoptosis display a number of characteristic morphological changes that include cell shrinkage, mitochondrial dysfunction, chromatin condensation, nuclear fragmentation, and plasma membrane blebbing [52,53]. Ultimately, the dying cell forms small membrane-bound fragments, known as apoptotic bodies, that are engulfed by phagocytic immune cells, allowing for efficient removal of the dying cell in the absence of inflammation and tissue damage [44,45,46]. The morphological features of apoptosis are primarily due to the actions of a family of intracellular proteases, known as caspases, which dismantle the cell in a controlled and efficient manner [52,54,55].

1.2.1 Caspases

Apoptotic cell death is carried out by caspases, an evolutionarily conserved family of cysteine proteases that cleave substrates after aspartic acid residues [52,54,55]. Caspases exist in healthy cells as inactive zymogens, or pro-caspases, that are, themselves, cleaved after aspartic acid residues to produce the active enzyme [52,54,55]. The earliest studies of apoptosis focused on the nematode *Caenorhabditis elegans*, which contains one caspase, CED-3, that mediates apoptotic death [56]. In mammals, the caspase family consists of 14 members with roles in apoptosis and inflammation (Fig 1.3A) [52,54]. Caspases involved in transmitting apoptotic signals are divided into two types, initiator and executioner caspases, that differ in structure, mode of activation, and substrates [52,54]. Pro-caspases are structurally divided into three domains: a pro-domain that is typically removed during activation, and a small and large subunit that comprise the active enzyme [57,58] (Fig 1.3A). The pro-domains of initiator caspases contain protein-protein interaction domains such as death effector domains (DEDs) and caspase recruitment domains (CARDs), which are critical for
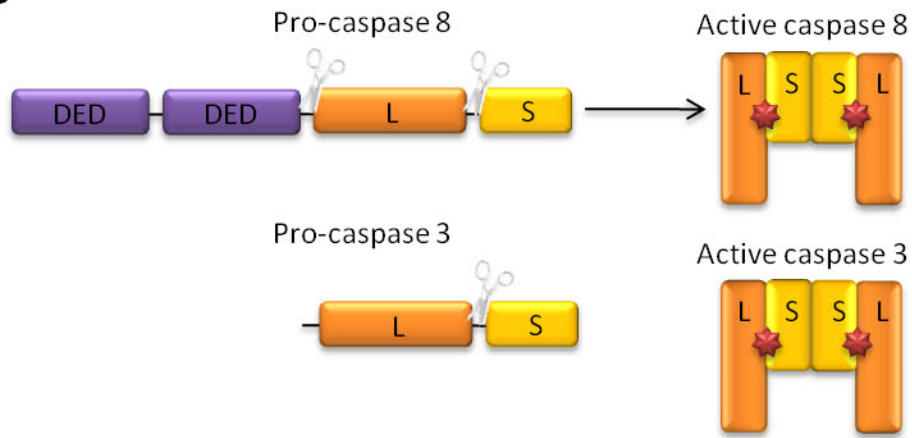
Figure 1.3 The human caspase family. A. Caspases 1, 4, 5, and 12 contain caspase recruitment domains (CARD) and are involved in inflammation, although only a small subset of people contain full-length caspase 12. Apoptotic caspases are divided into death effector domain (DED)-containing initiator caspases 8 and 10, CARD-containing initiator caspases 2 and 9, or executioner caspases 3, 6, and 7. The inhibitor c-FLIP contains DED domains and a caspase-like domain to inhibit activation of caspases 8 and 10. L; large subunit, S; small subunit. **B.** Activation of caspase 8 and 3 involves interdomain cleavages. Active caspases form tetramers with active sites highlighted with red stars. Caspases cleave after the tetrapeptide motif P1-P2-P3-P4, where P4 is an aspartic acid residue.

their activation (Fig 1.3A) [52,57]. Initiator caspases, such as caspases 8, 9, and 10, are the first to be activated upon receipt of an apoptotic stimulus [52,57]. The activation of initiator caspases occurs by recruitment to various protein complexes via the pro-domain containing DEDs or CARDs [59,60]. The formation of these protein complexes allows for proximity-induced dimerization of initiator pro-caspases, which is often followed by auto-cleavage between the pro-domain and the small and large subunit (Fig 1.3B) [59,60]. Active caspases function as heterotetramers that fold in such a way to form the active site of the enzyme [57,58].

Downstream executioner caspases, such as caspase 3, 6, and 7, are activated by initiator caspases through proteolytic cleavage (Fig 1.3B) [52,57]. While initiator caspases are mainly limited to auto-cleavage and cleavage of executioner caspases, there are approximately 400 cellular substrates that have been identified for executioner caspases in mammals [61]. Executioner caspases are responsible for cleaving structural proteins of the cytoskeleton and nuclear membrane and proteins involved in critical cellular functions, such as ribosomal subunits and DNA repair proteins [62]. Instead of degrading proteins, executioner caspases make one or several "cuts" in target proteins in order to inactivate or modify the function of the protein [61]. The cumulative effect of the proteolytic caspase cascade is the irreversible shutdown and dismantling of the cell, ultimately culminating in cell death [54,63].

1.2.1.1 Activation of Caspases by the Extrinsic Pathway

The activation of executioner caspases, such as caspase 3, occurs through two main pathways, the extrinsic and intrinsic apoptotic pathways [52,54]. The extrinsic pathway, or the death receptor pathway, is activated by the binding of extracellular "death ligands" to their cognate transmembrane receptors [59,64,65]. For example, the extrinsic pathway is activated by binding of TNFα to the TNF I receptor (TNFR1) (Fig 1.4) [66,67]. In lymphoid cells, the Fas is activated by binding of Fas ligand (FasL), which is expressed on the plasma
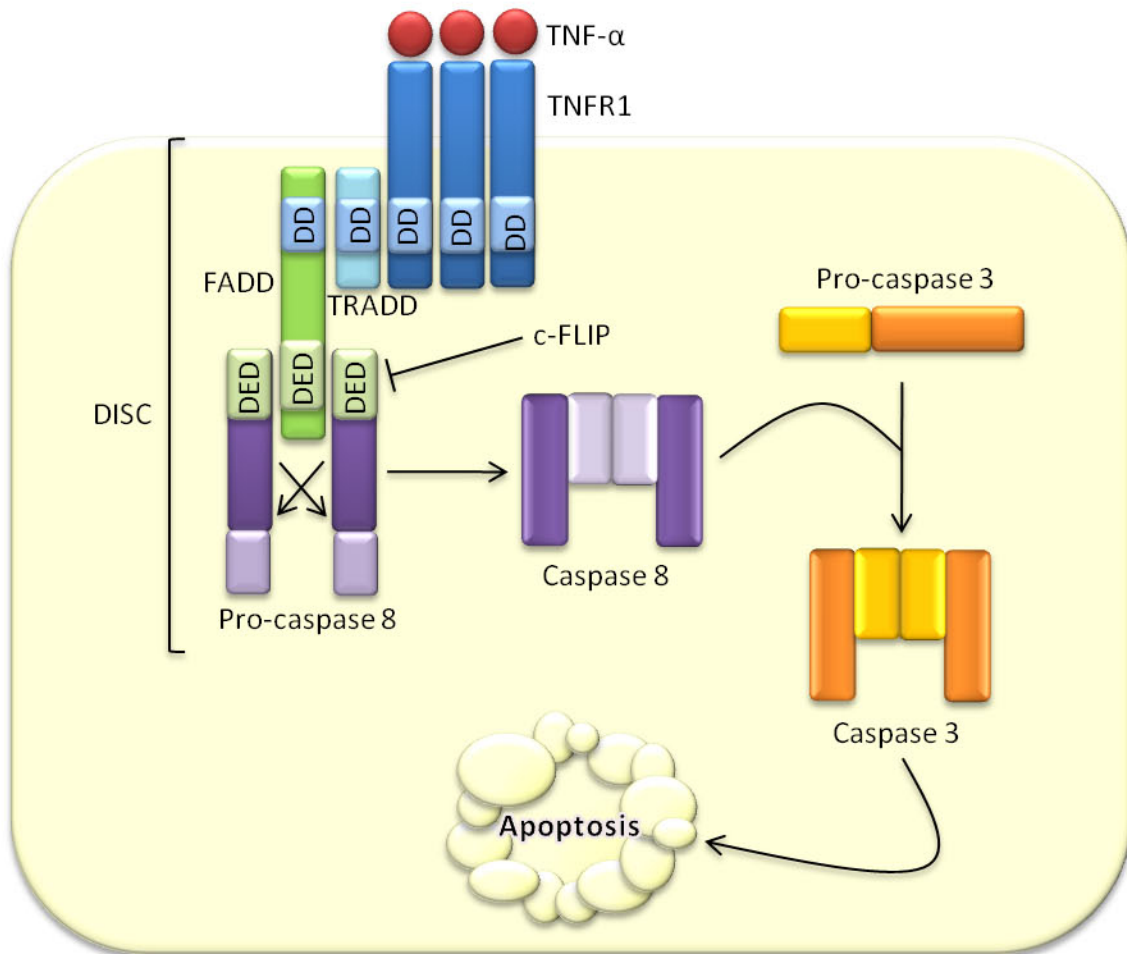
Figure 1.4 The extrinsic pathway. Binding of TNFα induces the trimerization of the TNF receptor TNFR1. The TNF-specific adaptor, TRADD, binds the death domains (DD) in TNFR1 and recruits the DD-containing adaptor protein FADD. FADD recruits pro-caspase 8 (or 10) through the death-effector domain (DED), to form the death-inducing signalling complex (DISC). Proximity-induced cleavage of pro-caspase 8 activates the caspase, which then cleaves and activates executioner caspase 3. This pathway is inhibited by c-FLIP binding either pro-caspase 8 or FADD through DED-mediated interactions.

membrane of CTLs or exists in a soluble form [68,69]. Both TNFR1 and Fas belong to the TNF receptor gene superfamily, which contain cytoplasmic death domains (DDs) [70,71]. Notably, while Fas signalling seems to exclusively result in apoptosis, signalling through TNFR1 does not always result in apoptotic death. Adaptor proteins bound to TNFR1 can recruit additional adaptor proteins that result in NF-κB activation and the upregulation of genes involved in survival and inflammation [72,73,74,75,76].

Ligand binding to Fas and TNFR1 leads to receptor trimerization and recruitment of the DD-containing adaptor protein, Fas associated death domain (FADD), which binds the DD present in the cytoplasmic region of the receptors (Fig 1.4) [77,78,79]. In the case of Fas, the interaction with FADD is direct; TNFR1, however, interacts with FADD indirectly through the DD of a second adaptor protein, TNFR1-associated death domain protein (TRADD) (Fig 1.4) [72,73]. FADD binding to death receptors results in recruitment of two initiator caspase 8 or 10 molecules, through interactions between a second domain, the DED, present in both FADD and pro-caspases 8/10 [80,81]. The complex formed by death receptors, their adaptor proteins, and pro-caspases 8/10 constitutes the death-inducing signalling complex (DISC), which is responsible for activating initiator caspases 8/10 (Fig 1.4) [79]. The close proximity of two initiator caspases results in their dimerization and auto-cleavage, releasing the DED-containing pro-domain and cleaving the linker between the small and large subunits (Fig 1.4) [82,83,84]. Active caspases 8 and 10 subsequently cleave and activate executioner caspase 3 to begin the cleavage of downstream targets [80].

Importantly, this pathway is subject to regulation by cellular FLICE/caspase 8 inhibitory protein, or c-FLIP (Fig 1.3) [85]. c-FLIP contains two N-terminal DEDs that allow it to bind both pro-caspase 8 and FADD to inhibit the activation of caspase 8 in a dominant negative fashion (Fig 1.4) [86,87,88,89,90]. Moreover, the extrinsic pathway can be activated in the absence of death receptor ligation. CTLs and NK cells release cytotoxic granules that contain

granzyme B, a serine protease that enters targeted cells and directly cleaves initiator caspase 8 and executioner caspase 3, thereby bypassing the requirement for DISC formation [91,92,93,94].

1.2.1.2 Activation of Caspases by the Intrinsic Pathway

The death receptor pathway receives signals from various immune cells and cytokines, whereas the intrinsic apoptotic pathway is triggered by intracellular stress that threatens cellular integrity [52,54]. Critical for the execution of the intrinsic signalling pathway are mitochondria [95,96,97]. Only in the mid-1990s was the link been made between mitochondria and apoptosis [98] and now the organelle is considered an essential coordinating centre for the initiation and amplification of apoptotic signals [96,99,100,101]. In response to a variety of stimuli, including DNA damage, growth factor deprivation, metabolic stress and pathogen infections, mitochondria release apoptogenic factors into the cytosol that result in activation of the initiator caspase 9 (Fig 1.5) [96,99,100,101].

One of these pro-apoptotic factors is cytochrome *c*, a 13 kilodalton (kDa) soluble protein that, upon release from mitochondria, associates with apoptotic protease activating factor-1 (Apaf-1) [60,96]. In an energy-dependent manner, cytochrome *c* binding to Apaf-1 induces Apaf-1 oligomerization into a heptameric cytosolic signalling complex known as the apoptosome (Fig 1.5) [102,103,104,105]. The apoptosome recruits the CARD-containing pro-caspase 9, which interacts with the CARD in the N-terminus of Apaf-1 [104,106]. The dimerization of caspase 9 leads to its activation and interdomain cleavage can occur; however, unlike caspases 8 and 10, cleavage of caspase 9 attenuates its enzymatic activity and the uncleaved dimer is believed to be the active form of the enzyme [82,107,108]. The release of cytochrome *c* is absolutely essential for activation of caspase 9 and subsequent activation of executioner caspase 3 (Fig 1.5) [109]. Therefore, the release of cytochrome *c* from mitochondria in
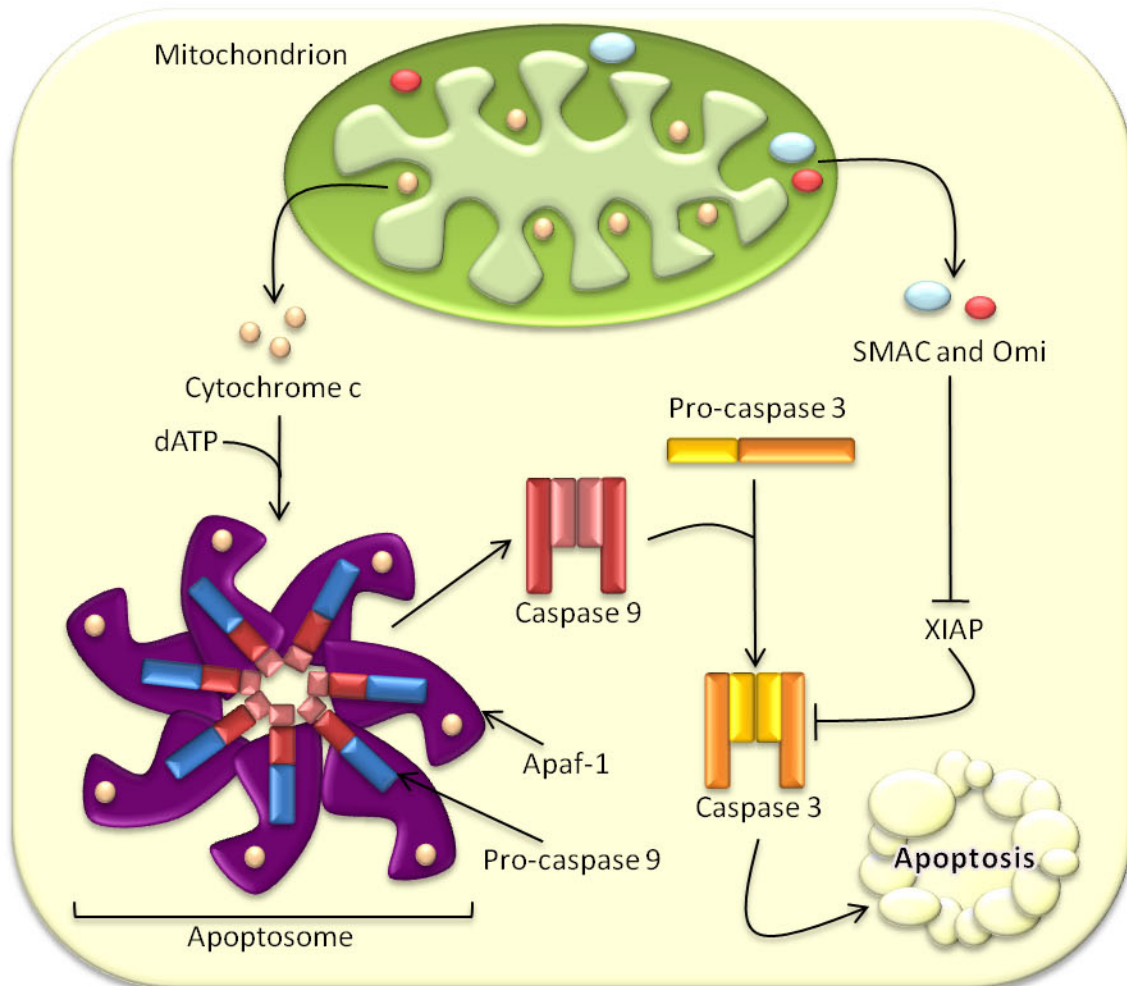
Figure 1.5 The intrinsic pathway. Mitochondria release apoptogenic factors, such as cytochrome c, SMAC, and Omi. Apaf-1 binds cytoplasmic cytochrome c and in the presence of energy, in the form of ATP, forms the heptameric apoptosome. Pro-caspase 9 is recruited to the apoptosome by the CARD domain in the N-terminus of Apaf-1, activated, and subsequently activates the executioner caspase 3. Unlike other caspases, dimerization of pro-caspase 9 is sufficient for activation, while cleavage of caspase 9 is believed to inhibit its activity. Once in the cytoplasm, SMAC and Omi interact with and inhibit XIAP in order to relieve the inhibition on caspases 3, 7, and 9.

response to intracellular stress is tightly regulated as cytochrome *c* is a potent activator of the caspase cascade [96,100,101].

Other apoptosis-inducing factors that play a role in caspase activation are released from mitochondria as well [95]. Second mitochondria-derived activator of caspases (SMAC) and Omi indirectly activate caspases by antagonizing caspase inhibitors. [110] To prevent unwanted apoptosis, active caspase 9 and caspases 3 and 7 are bound and inhibited by the inhibitor of apoptosis protein (IAP) family, which contains the prototypic member X-linked IAP, or XIAP (Fig 1.5) [111]. To achieve caspase activation, XIAP and other IAPs must be inactivated and this is accomplished by SMAC and Omi [95,110]. Once in the cytosol, SMAC and Omi promote apoptosis by binding XIAP and relieving caspase repression (Fig 1.5) [112,113,114]. In addition to molecules important for direct and indirect caspase activation, mitochondria also release apoptosis-inducing factor (AIF), and endonuclease G, both of which have roles in cleavage of nuclear DNA and, in the case of AIF, chromatin condensation [115,116].

While the end result of executioner caspase activation is common between the death receptor and mitochondrial apoptotic pathways, each pathway is initiated by different types of stimuli and activates different initiator caspases [52,54]. In some cells, such as lymphoid cells, caspase 8 is efficiently activated upon death receptor ligation and is sufficient to activate downstream executioner caspases 3 and 7. These cells are referred to as "type I cells", in which executioner caspases are effectively activated by death receptor engagement [117]. However, in so-called "type II cells", such as hepatocytes, death receptor-induced activation of caspase 8 is not capable of activating sufficient levels of caspase 3 [117]. Instead, these cells require mitochondrial amplification of the apoptotic signal in order to fully activate caspase 3 and commit cells to death. Mitochondria are required for apoptosis in response to death receptor signalling in hepatocytes due to the activity of XIAP, which, without the release of SMAC and OMI, prevents sufficient activation of

executioner caspases [118]. Thus, mitochondria are crucial for apoptosis in response to intracellular stress and, additionally, in response to external signals mediated through death receptors in type II cells [118].

1.2.2 Mitochondria and Apoptosis

1.2.2.1 Mitochondrial Origin and Role in Energy Production

Mitochondria are double-membrane organelles believed to have originated from oxygen-utilizing bacteria, closely resembling modern day α-proteobacteria (Fig 1.6A) [119]. These bacteria are thought to have entered into a symbiotic relationship after being engulfed by an archaea-like organism [120,121]. The genome of the α-proteobacterial symbiont likely underwent extensive gene loss and many of the genes were acquired by the host nucleus, resulting in a compact mitochondrial DNA (mtDNA) genome that encodes, on average, 40-50 genes [122]. In humans, the mitochondrial genome is a 16.5kb closed circular dsDNA molecular that encodes 37 genes [123,124].   Only 13 of these genes produce proteins, all of which are involved in an oxygen-dependent energy production process, known as oxidative phosphorylation, and the remaining genes produce transfer RNA and ribosomal RNA involved in mitochondrial protein synthesis [122,124,125]. In contrast to its bacterial ancestor, most mitochondrial proteins, such as cytochrome *c*, are encoded by the nucleus and synthesized in the cytosol before translocation to mitochondria [126,127].

Mitochondria are considered the "powerhouses of the cell" since they generate energy in the form of adenosine tri-phosphate (ATP) to fuel nearly all cellular processes [128,129]. These morphologically distinct organelles are compartmentalized and their unique architecture maximizes energy production (Fig 1.6B) [130,131,132]. Mitochondria are separated from the cytosol by the outer mitochondrial membrane (OMM), which is permeable to most small molecules and uses various protein transporters to facilitate import of cytoplasmically-synthesized proteins (Fig 1.6B) [95,130]. The most abundant
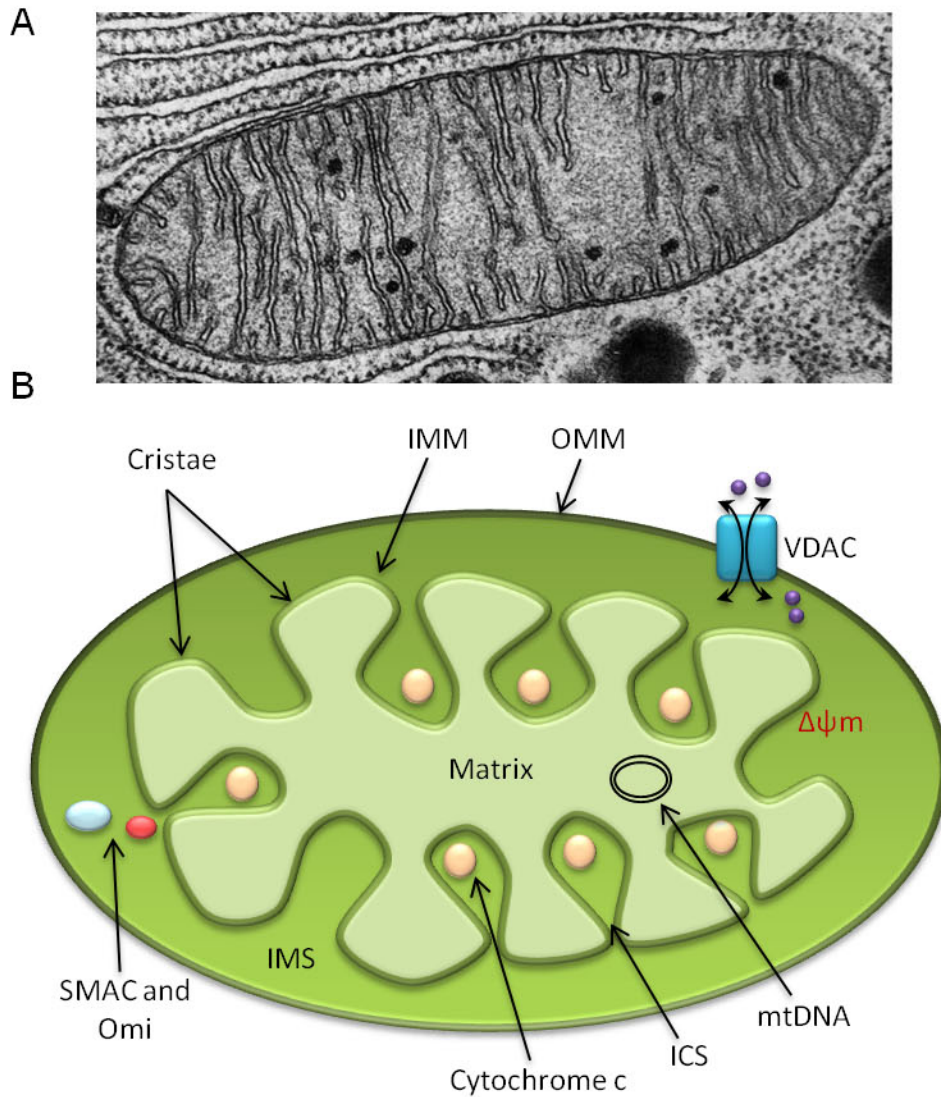
Figure 1.6 Mitochondrial architecture. A. Electron micrograph of a mitochondrion (adapted from [130]). **B.** Mitochondria are delimited by the outer mitochondrial membrane (OMM), which is permeable to small molecules due to the action of porins, such as VDAC. The inner mitochondrial membrane (IMM) delimits the matrix, which houses mitochondrial DNA (mtDNA). The IMM is the site of oxidative phosphorylation and as a result of the electron transport chain, the IMM is polarized ($\Delta\psi m$). The surface area of the IMM greatly exceeds the OMM and thus forms numerous invaginations, or cristae. Apoptogenic molecules, such as SMAC and OMI are located in the space between the IMM and OMM, the intermembrane space (IMS). Cytochrome c is housed in pockets of the IMS between cristae, known as the intracristae space (ICS).

OMM protein, the voltage-dependent anion channel (VDAC), allows for diffusion of various molecules up to 5kDa (Fig 1.6B) [133,134]. Inside mitochondria, the inner mitochondrial membrane (IMM) delimits the matrix, which houses the mtDNA and metabolic enzymes (Fig 1.6B) [95,124]. In contrast to the OMM, the IMM is highly impermeable to most metabolites and solutes, including protons [128]. The IMM is the site of energy production through a process known as oxidative phosphorylation and the impermeability of this membrane is absolutely critical for this process [128,129]. The space between the OMM and the IMM is the intermembrane space (IMS), which contains apoptogenic molecules released at the onset of apoptosis [95] (Fig 1.6B). Within the IMS, however, is an additional compartment formed by cristae, which are deep involutions of the IMM [95,130]. The narrow cavities formed between cristae make up the intracristae space (ICS), which is separated from the IMS by tight junction-like barriers and it is within the ICS that the majority of cytochrome *c* is stored in healthy cells (Fig 1.6B) [131,132]. In addition to forming the ICS and storing molecules such as cytochrome *c*, cristae also effectively increase the surface area of the IMM and thus maximize ATP generation [131,132].

During respiration, protein complexes embedded in the IMM transfer electrons through a series of oxidation and reduction reactions, and this results in pumping protons into the IMS [135,136]. Cytochrome *c* has a dual role in mitochondrial functions; in addition to activating caspases during apoptosis, cytochrome *c* is involved in electron transfer during respiration [128,129]. The pumping of protons from the matrix to the IMS generates an electrochemical gradient and establishes the IMM potential ($\Delta\psi$m) (Fig 1.6B) [128,129]. Energy in the form of ATP is generated as protons flow back into the matrix; thus, the transfer of electrons is coupled to energy production and the maintenance of $\Delta\psi$m is critical for cellular bioenergetics [95,128].

1.2.2.2 Apoptosis-induced Alterations in Mitochondria

Disrupting mitochondria can halt energy production and cause cell death due to a general shutdown of cellular process [137]. However, mitochondria play an active role in the intrinsic apoptotic pathway by releasing apoptosis-promoting factors, such as cytochrome *c*, SMAC, and Omi into the cytosol (Fig 1.5) [95]. The release of these factors coincides with numerous alterations in mitochondrial architecture and permeability, including mitochondrial fragmentation, cristae remodelling, and permeabilization of the IMM and OMM (Fig 1.7) [95].

1.2.2.2.1 Mitochondrial Fragmentation and Cristae Remodelling

Mitochondria are dynamic organelles that are regulated by the opposing and coordinating processes of fusion and fission [138,139]. Fusion of mitochondria results in a single larger mitochondrion that forms interconnected mitochondrial networks, whereas fission divides a single mitochondrion into two morphologically and functionally distinct organelles (Fig 1.8) [138,139]. In mammals, fusion is regulated by two guanosine triphosphate hydrolyzing enzymes (GTPases) in the OMM, mitofusins 1 and 2 (Mfn 1 and Mfn2), and optic atrophia 1 (Opa1), a GTPase associated with the IMM at the junctions of the ICS (Fig 1.8) [140,141]. Mfn1 and Mfn2 promote fusion of the OMM, while Opa1 fuses the IMM of two distinct mitochondria [142,143,144,145]. Fission events are also controlled by GTPases, namely dynamin-related protein 1 (Drp1), which, during fission, is recruited from the cytosol to the OMM where it interacts with its potential receptor, fission 1 (Fis1) (Fig 1.8) [146,147,148,149]. A high concentration of Drp1 results in the formation of Drp1 "rings" around mitochondria, effectively pinching off a piece of the organelle to form two physically and functionally distinct organelles (Fig 1.8) [150,151]. Importantly, the balance between fission and fusion maintains mitochondrial morphology and the equilibrium is critical for development in mammals [152,153]. During apoptosis, extensive mitochondrial fission occurs, coinciding with the recruitment of the Drp1 to the OMM (Fig 1.7) [154]. Although loss of Drp1
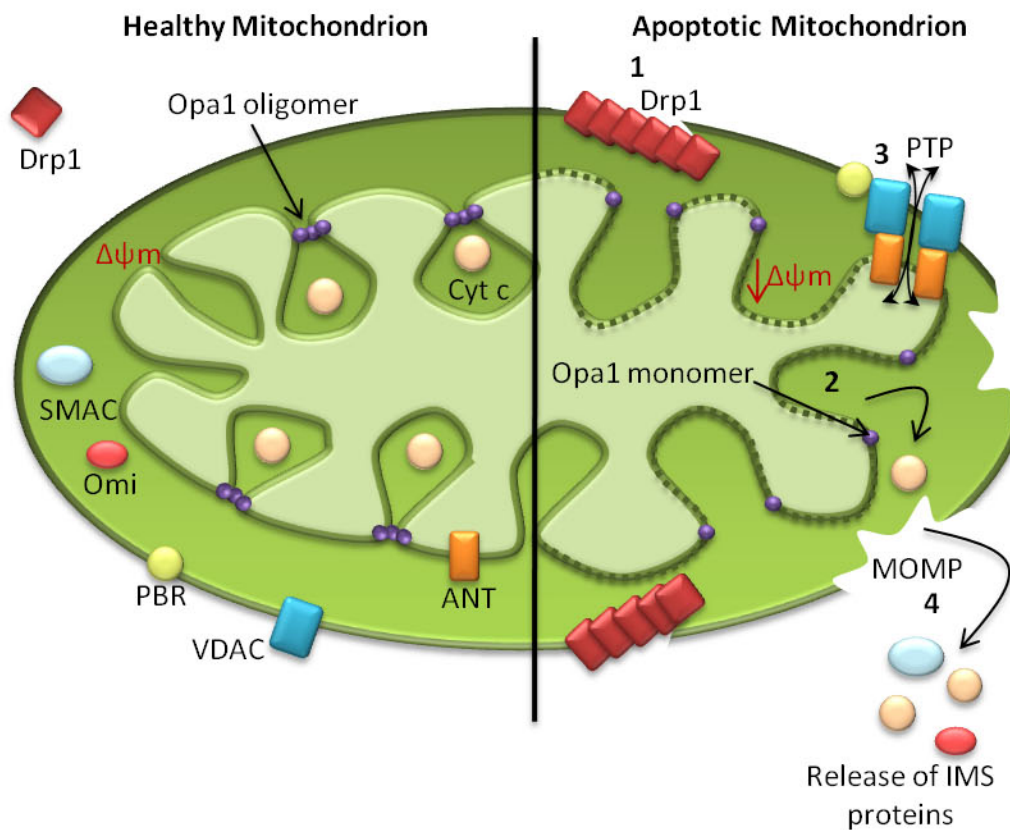
Figure 1.7 Apoptosis-induced changes in mitochondria. *Left:* In healthy cells, Δψm is intact and Opa1 oligomers form tight junction-like complexes in the ICS, which houses the majority of cytochrome c. *Right:* During apoptosis, Drp1 translocates to the OMM and promotes fission, or fragmentation, of mitochondria (**1**). Opa1 oligomers are disrupted, resulting in monomers of Opa1 in the IMM, cristae remodelling, and cytochrome c mobilization into the IMS (**2**). The newly formed PTP opens causing ΔψM collapse, IMM permeabilization, and potentially release of IMS proteins into the cytoplasm (**3**). Mitochondrial outer membrane permeabilization (MOMP) destabilizes the OMM integrity and allows for the release of IMS proteins, such as cytochrome c, SMAC, and Omi, into the cytoplasm (**4**).
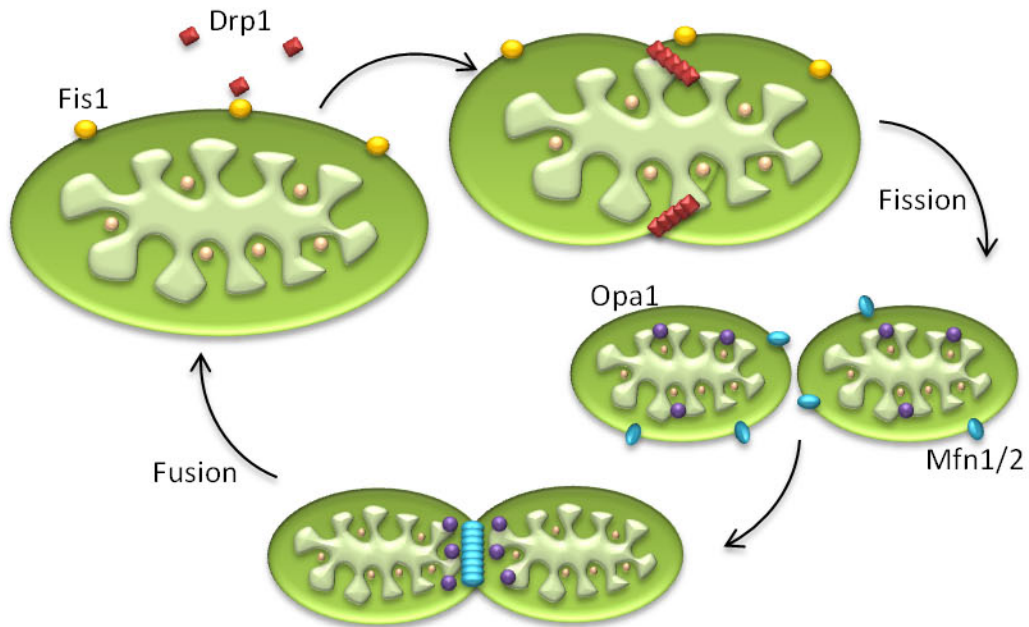
Figure 1.8 Regulation of mitochondrial dynamics. Mitochondrial fission is mediated by the binding of the GTPase Drp1 to its receptor on the OMM, Fis1. Drp1 forms rings around mitochondria in order to pinch the organelle and generate two distinct organelles. Mitochondrial fusion is achieved by the GTPases Mfn1, Mfn2, and Opa1. Mfn1 and Mfn2 mediate fusion of the OMM between two organelles, while the IMM protein Opa1 is required for fusion of the IMM.

delays fragmentation and cytochrome *c* release, apoptosis still occurs, suggesting that fission accompanies, but is not required for, cytochrome *c* release [153,155,156].

Morphological changes occur at the level of the IMM during apoptosis as well, with cristae remodelling and disruption of the ICS [95,96]. The majority of cytochrome *c* is contained within ICS and the junctions of these compartments are maintained by Opa1 oligomers (Fig 1.7) [131,132]. During apoptosis, Opa1 oligomers are disrupted, allowing for release of cytochrome *c* into the IMS; therefore, reorganization of the IMM by Opa1 is believed to play an important role in apoptotic signalling (Fig 1.7) [157,158]. The link between mitochondrial dynamics and apoptosis is not fully understood and since the two processes can be uncoupled, apoptosis can occur without the requirement of fission machinery [153,155,156]. While there may not be a direct causal relationship between apoptosis and morphological changes induced at the OMM and IMM, it remains possible that the two processes are linked in response to specific types of cell stress [139,159,160,161].

1.2.2.2.2 Mitochondrial Depolarization and Permeabilization

In addition to cristae remodelling during apoptosis, dissipation of Δψm and IMM permeabilization occur [95]. Transient Δψm loss occurs in healthy cells when respiration is inhibited; however, long lasting Δψm collapse leads to apoptosis [95,162,163]. Once an apoptotic signal reaches mitochondria, dissipation of Δψm occurs following the activation of a high conductance channel known as the permeability transition pore (PTP) that causes IMM permeabilization (Fig 1.7) [133,164]. The PTP is a large protein complex comprised of VDAC and the peripheral benzodiazepine receptor (PBR) in the OMM, adenine nucleotide transporter (ANT) in the IMM, and cyclophilin D (CypD) in the matrix (Fig 1.9) [133,164]. In its high conductance state, the PTP allows for passage of molecules up to 1.5kDa across the IMM [162]. Although
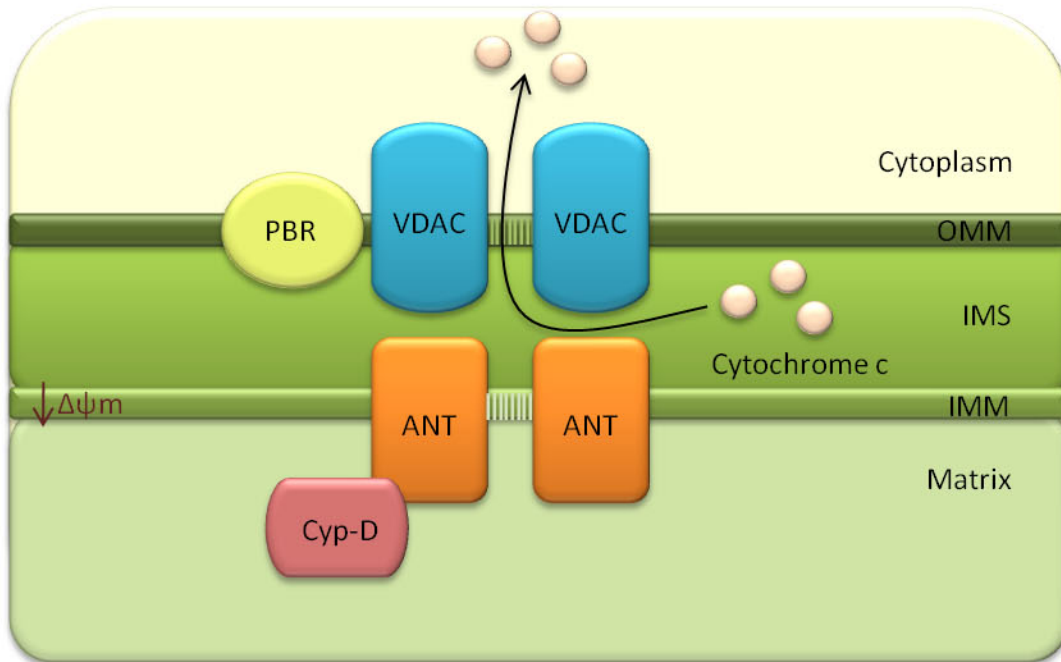
Figure 1.9 The permeability transition pore. The permeability transition pore (PTP) is a large multi-protein complex that spans the OMM and IMM. Three isoforms of voltage-dependent anion channel (VDAC) exist in the OMM, along with the peripheral benzodiazepine receptor (PBR). Two isoforms of adenine nucleotide transporter (ANT) are embedded in the IMM and cyclophilin D (Cyp-D) is located in the matrix. During apoptosis, these core components associate to form the voltage-dependent non-selective PTP, which dissipates the Δψm and potentially allows for release of mitochondrial proteins, such as cytochrome c.

activation of the PTP during apoptosis has been well documented, its exact role in the process remains controversial [165].

A critical event that occurs prior to Δψm collapse and IMM permeabilization is mitochondrial outer membrane permeabilization (MOMP), a hallmark of apoptosis [95,100,166]. MOMP promotes the release of pro-apoptotic factors, such as cytochrome *c*, into the cytosol through pores formed in the OMM (Fig 1.7) [167]. Although once thought to occur as a result of PTP opening, MOMP has since been shown to occur independently of IMM permeabilization [167,168,169]. Additionally, MOMP is absolutely required for apoptosis to occur and is widely considered the "point of no return" for apoptosis induction [166,170]. The way in which pores form in the OMM, however, is still a matter of debate and will be discussed in section 1.2.3.6. Importantly, the physical changes that occur in mitochondria during apoptosis are readily detected. Dissipation of Δψm is detected by cationic Δψm-dependent fluorochromes, such as tetramethylrhodamine ethyl ester (TMRE), that specifically accumulate in the matrix of mitochondria with an intact Δψm [171,172], whereas MOMP is often assessed by determining whether protein translocation from the IMS to the cytosol has occurred [95].

1.2.3 Mitochondrial Integrity is Regulated by the Bcl-2 Family of Proteins

The importance of MOMP in the induction of apoptosis is highlighted by the extensive regulation of the OMM by a group of proteins known as the B-cell leukemia/lymphoma (Bcl-2) family [99,100,101]. This evolutionarily conserved family is found throughout multicellular organisms, from sponges to humans [173,174]. Members of this protein family are united by the presence of one or more conserved amino acid signatures, or Bcl-2 homology (BH) domains, that mediate homo- and heterotypic interactions among members (Fig 1.10) [99,175,176]. Bcl-2 family members are classified as pro- or anti-apoptotic depending on their tendency to promote or inhibit MOMP, respectively. Pro-apoptotic members are further subdivided into BH3-only proteins, which sense

Anti-apoptotic Multi-domain Proteins

BH4 | BH3 | BH1 | BH2 | TM   Bcl-2, Bcl-xL, Mcl-1, Bcl-w, A1

Pro-apoptotic Multi-domain Proteins

BH3 | BH1 | BH2 | TM   Bak, Bax, Bok

Pro-apoptotic BH3-only Proteins

BH3 | TM   Bim, Bik, Noxa, Puma, HRK

BH3   Bid, Bad, Bmf
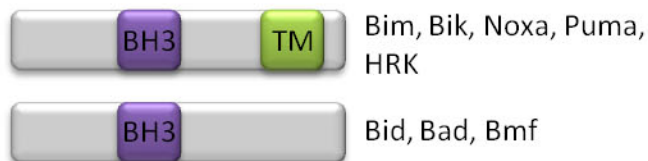
Figure 1.10 The Bcl-2 family of proteins. The Bcl-2 family is divided into anti-apoptotic and pro-apoptotic members. Anti-apoptotic members contain Bcl-2 homology (BH) domains 1-4 and a C-terminal transmembrane domain (TM), with the exception of A1, which is predicted to lack a functional TM. Although not shown, the N-terminus of Mcl-1 is much longer than the remaining anti-apoptotic members and the BH4 domain in Mcl-1 is highly divergent. Pro-apoptotic members are sub-divided into the multi-domain effector proteins and the BH3-only proteins. Bak and Bax contain BH domains 1-3 and a TM, while Bok lacks both a TM and a clear role in apoptosis. All BH3-only proteins contain a BH3 domain that is critical for their pro-apoptotic function and, in addition, most members contain tail anchors.

death signals, and multi-domain effectors, which translate the death signal from BH3-only proteins into MOMP (Fig 1.10) [99,101]. The activity of pro-apoptotic members is tightly regulated by the anti-apoptotic Bcl-2 proteins, which set a critical threshold that must be reached to initiate the apoptotic events [99,101]. The multi-domain pro-apoptotic effector proteins Bcl-2 antagonist killer 1 (Bak) and Bcl-2-associated x protein (Bax) contain BH domains 1-3 and act as the gatekeepers of the OMM (Fig 1.10) [99,101]. Both proteins exist as monomers in healthy cells, yet while Bak is a resident OMM protein by virtue of a C-terminal transmembrane domain, Bax is found in the cytosol or loosely associated with the OMM in an inactive state (Fig 1.11) [177,178]. Once activated, Bax undergoes a series of conformational changes, including exposure of its C-terminal transmembrane domain that allows for insertion into the OMM (Fig 1.11) [179,180,181,182,183]. Similarly, Bak undergoes a series of activation-induced conformational changes within the OMM [177,184,185,186]. Ultimately, the activation of Bak and Bax results in oligomerization of the two proteins, which destabilizes the OMM, leading to MOMP (Fig 1.11) [187,188]. Bak and Bax, in combination or alone, are capable of promoting MOMP and the release of apoptogenic molecules; however, either Bak of Bax must be present, since cells deficient in both proteins are refractory to apoptosis [189,190].

1.2.3.1 Activation of BH3-only Proteins

The activation of Bak and Bax is achieved by members of the pro-apoptotic BH3-only subfamily (Fig 1.11) [99,101,191]. In humans, 8 pro-apoptotic BH3-only proteins have been identified; BH3-interacting domain death agonist (Bid), Bcl-2 antagonist of cell death (Bad), Bcl-2-interacting mediator of cell death (Bim), Bcl-2 interacting killer (Bik), Harakiri (Hrk), Bcl-2-modifying factor (Bmf), Noxa, and p53 upregulated modulator of apoptosis (Puma) [191,192,193] (Fig 1.10). As the name suggests, these proteins contain a single BH3 domain that is critical for their function as sensors of cell stress [191,192,193]. Some members, such as Bid, Bad, and Bmf, are present in
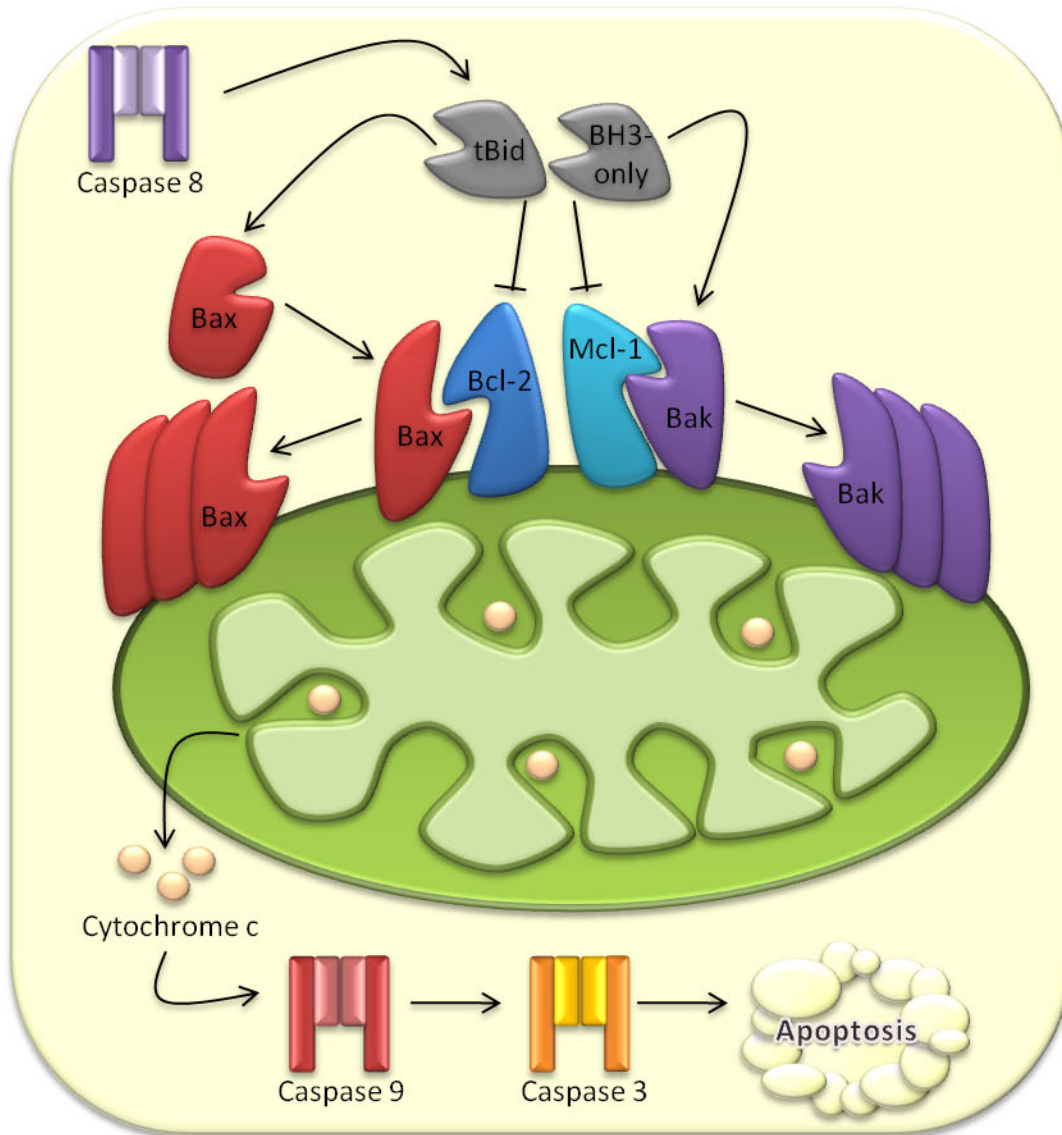
Figure 1.11 The Bcl-2 family regulates apoptosis at mitochondria. BH3-only proteins sense various stimuli; in the case of Bid, the active truncated form (tBid) is generated by caspase 8 cleavage following death receptor ligation. BH3-only proteins can directly activate the downstream effectors Bak and Bax. BH3-only proteins also bind and inactivate anti-apoptotic proteins, such as Bcl-2 and Mcl-1, in order to relieve the suppression on Bak and Bax. Unlike Bak, which is an integral OMM protein, Bax is cytoplasmic until activation by BH3-only proteins stimulates its translocation and insertion into the OMM. Upon activation, both Bax and Bak undergo structural rearrangements including exposure of the N-terminus. Activation of Bak and Bax ultimately results in their oligomerization and destabilization of the OMM. This allows for the efflux of cytochrome c that activates caspase 9 to engage the caspase cascade, culminating in cell death.

inactive forms in the cytosol of healthy cells and require post-translational modifications for activation, while others, such as Noxa and Puma, are transcriptionally upregulated following an apoptotic insult [194,195]. Interestingly, Bim is regulated transcriptionally and post-translationally. Three isoforms of Bim are produced by alternative splicing, BimEL (extra-long), BimL (long), and BimS (short) [196]. In healthy cells, BimEL and BimL are found in the cytosol bound to the dynein light chain 1 (DLC-1) component of microtubules [197,198]. During apoptosis, BimS is transcribed, BimL and BimEL are released from the cytoskeleton, and all three isoforms are able to transmit apoptotic signals to mitochondria [197,198].

BH3-only proteins are activated upon receipt of various signals, such as DNA damage, growth factor withdrawal, hypoxia, and ER stress, and each member senses specific types of cellular stress (Fig 1.12) [192,193]. Ultimately, the role of BH3-only proteins is to relay specific apoptotic signals downstream to activate Bak and Bax (Fig 1.11) [191,192,193]. Whether this occurs by a direct interaction with Bak and Bax or as result of relieving the repression by anti-apoptotic members will be discussed in section 1.2.3.5. Interestingly, the BH3-only protein Bid plays an important role in linking the extrinsic and intrinsic pathways [199]. Bid must be cleaved to produce truncated Bid (tBid) in order to become activated, and this cleavage event can be mediated by caspase 8, the initiator caspase of the death receptor pathway, or granzyme B, contained within cytotoxic granules from immune cells (Fig 1.11) [200,201,202]. Cleavage of Bid by caspase 8 occurs downstream of death receptor signalling and tBid subsequently translocates to mitochondria where it activates Bak and Bax [201,203,204,205]. Therefore, Bid is essential for linking the death receptor pathway to the mitochondrial pathway and plays an instrumental role in type II cells, which require mitochondrial amplification of the apoptotic signal following death receptor ligation [201].

1.2.3.2 Anti-apoptotic Bcl-2 Family Members Prevent Cell Death
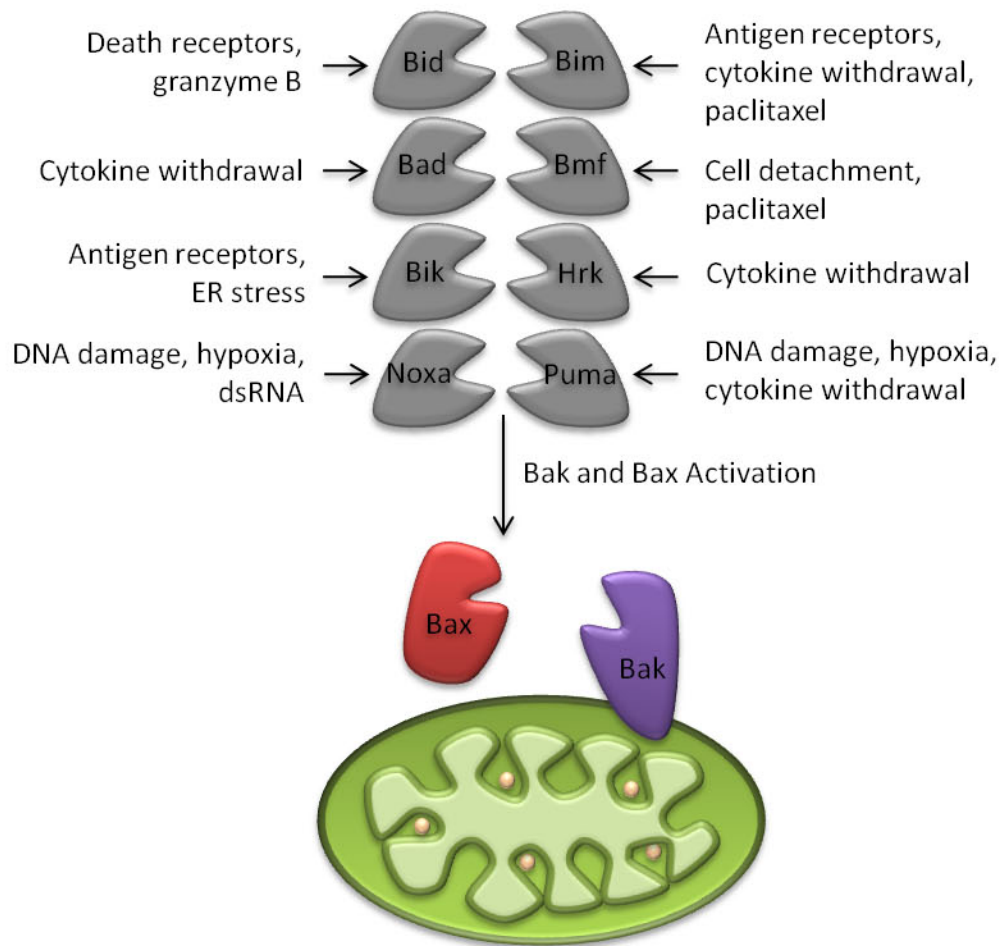
Figure 1.12 BH3-only proteins sense cellular stress. BH3-only proteins sense various types of insults that threaten the health of a cell and transmit signals downstream to activate Bak and Bax. Bid is activated by caspase 8 following death receptor signalling and thus serves as a link between the extrinsic and intrinsic pathways, which is particularly important in type II cells. In addition, Bid is also cleaved by granzyme B, a component of cytotoxic granules released by immune cells. Although not shown, three isoforms of Bim exist: BimS, BimL, and BimEL. All three contain a BH3 domain but differ in the presence of regulatory domains. DNA damage is a potent inducer of Noxa and PUMA; in addition, Noxa is activated by double-stranded RNA (dsRNA), a common by-product of viral replication and transcription.

In order to ensure the timely and proper onset of apoptosis, Bak and Bax are held in check by the anti-apoptotic members of the Bcl-2 family [99,101]. The first identified member of the family, Bcl-2, was discovered in B-cell follicular lymphomas where its transcription was highly upregulated [206,207,208]. These observations led to the notion that apoptosis is a critical tumour suppression mechanism and that overexpression of anti-apoptotic members, such as Bcl-2, can contribute to cancer development [209]. The anti-apoptotic Bcl-2 family has since been extended to include Bcl-2-related gene, long isoform (Bcl-xL), myeloid cell leukemia 1 (Mcl-1), Bcl-w, and Bcl-2-related gene A1 (A1) (Fig 1.10) [99,101]. Similar to pro-apoptotic Bak and Bax, the anti-apoptotic Bcl-2 family members contain BH domains 1-3, as well as an additional N-terminal BH4 domain, thought to serve as a regulatory domain (Fig 1.10) [210,211]. These proteins are predominantly located in the OMM and, in the case of Bcl-2, Mcl-1, and Bcl-xL, in the ER or nuclear membranes as well [178,212,213,214,215]. Additionally, a portion of some anti-apoptotic members, such as Bcl-xL, Mcl-1, and Bcl-w, are found in the cytosol until an apoptotic stimulus triggers their translocation to the OMM [178,216,217]. Anti-apoptotic members function to inhibit MOMP through direct interactions with Bak and Bax or upstream BH3-only proteins (Fig 1.11) [99,101,218]. Apoptosis occurs following BH3-only protein activation once all anti-apoptotic Bcl-2 family members have been neutralized and Bak and Bax are activated [99,101,218]. Thus, the decision between life and death of a cell rests on a delicate balance of pro- and anti-apoptotic forces and the slightest tip of the scale can seal a cell's fate [219].

1.2.3.3 Membrane Targeting of Bcl-2 Family Members

Localization to membranes is critical for the function of all Bcl-2 family members [220,221]. Although pro-apoptotic members, such as Bak and Bax, and anti-apoptotic members, such as Bcl-xL and Bcl-2, can function in the membrane of the ER and Bcl-2 can insert into the nuclear membrane, the major site of action for all members of the Bcl-2 family is the OMM [221]. Most of the multi-

domain members contain a C-terminal tail anchor that is critical for post-translational targeting to the OMM [220].   The C-terminal tail anchor is characterized by a hydrophobic transmembrane domain that spans the OMM, flanked by positively charged amino acids (Fig 1.13) [220,222].   The majority of the protein is exposed to the cytosol, while a small hydrophilic C-terminal tail is inserted into mitochondria [220,222].   The transmembrane domain varies in sequence, length, and hydrophobicity, yet all contain approximately 20 amino acids and this membrane-spanning domain is necessary and sufficient for membrane insertion [220].   Loss of the tail anchor in Bcl-2 and Bax not only inhibits mitochondrial localization of these proteins, but also abrogates their function [180,212].   Interestingly, structural analysis and binding studies on Bax and the anti-apoptotic members Bcl-xL, Bcl-w, and Mcl-1, revealed that in their inactive state, the C-terminal transmembrane domain can fold back onto the proteins making it unavailable for membrane insertion until receipt of an apoptotic stimulus [223,224,225,226].

The BH3-only proteins Bim, Bik, Noxa, Puma, and Hrk contain a C-terminal transmembrane domain required for localization to membranes [191]. Other BH3-only proteins, such as Bid, Bad, and Bmf, do not possess a C-terminal tail anchor and instead rely on post-translational modifications, interactions with mitochondrial lipids, or mitochondrial proteins for targeting and insertion into the OMM [191,220].   In the case of cytosolic Bid, which has been the focus of much research, caspase 8 cleavage exposes a glycine residue at the N-terminus of tBid that allows for myristoylation of the protein and subsequent localization of tBid to mitochondria [227].   The phospholipid cardiolipin is present at contact sites where the OMM and IMM meet and this lipid has been linked to mitochondrial targeting of Bid, as well as Bad, which bind cardiolipin through lipid-binding motifs [228,229,230,231].   In addition to myristoylation and interactions with cardiolipin, the OMM protein mitochondrial carrier homologue 2 has been identified as a binding partner of Bid and an important player in the

```
            BH4
Bcl-2   (7)  TGYDNREIVMKYIHYKLSQRGYEWDAGDVGAAEPGAAPAPGIFSSQPGHTPHPAASRDPV
Bcl-xL  (1)  MSQSNRELVVDFLSYKLSQKGYSWSQFSDVEENRTEAPEGTESEMETPSAINGNPSWHLA
Mcl-1  (174) LYRQSLEIISRYLREQATGAKDTKPMGRSGA----------------------------
Bak    (26)  QVAQDTEEVFRSYVFYRHQQEQEAEGVAAPADPEMVT-----------------------
Bax    (19)  IMKTGALLLQGFIQDRAGRMGGEAPELALDPVPQ--------------------------
             α1

                                              BH3
Bcl-2  (67)  ARTSPLQTPAAPGAAAGPALSPVPPVVHLTLRQAGDDFSRRYRRDFAEMSSQLHLTPFTA
Bcl-xL (61)  DSPAVNGATAHSSSLDAREVIP-MAAVKQALREAGDEFELRYRRAFSDLTSQLHITPGTA
Mcl-1  (205) ---------------------TSRKALETLRRVGDGVQRNHETAFQGMLRKLDIKNEDD
Bak    (63)  ---------------LPLQPSSTMGQVGRQLAIIGDDINRRYDSEFQTMLQHLQPTAENA
Bax    (53)  ------------------DASTKKLSECLKRIGDELDSNM--ELQRMIAAVDTD--SP
                                 α2                        α3

                           BH1
Bcl-2  (127) RGREATVVEELFRDG-VNWGRIVAFFEFGGVMCVESVNR-EMSPLVDNIALWMTEYLNR
Bcl-xL (120) YQSFEQVVNELFRDG-VNWGRIVAFFSFGGALCVESVDK-EMQVLVSRIAAWMATYLND
Mcl-1  (243) VKSLSRVMIHVFSDGVTNWGRIVTLISFGAFVAKHLKTI-NQESCIEPLAESITDVLV-
Bak    (108) YEYFTKIATSLFESG-INWGRVVALLGFGYRLALHVYQH-GLTGFLGQVTRFVVDFMLH
Bax    (89)  REVFFRVAADMFSDGNFNWGRVVALFYFASKLVLKALCT-KVPELIRTIMGWTLDFLRE
             α4              α5                            α6

                 BH2                                  TM
Bcl-2  (184) H-LHTWIQDNGGWDAFVELYGPSMRP-LFDFSWLSLKTLLSLALVGACITLGAYLGHK
Bcl-xL (177) H-LEPWIQENGGWDTFVELYGNNAAAESRKGQERFNRWFLTGMTVAGVVL-LGSLFSRK
Mcl-1  (300) RTKRDWLVKQRGWDGFVEFFH------VEDLEGGIRNVLLAFAGVAGVGAGLAYLIR
Bak    (165) HCIARWIAQRGGWVA---------ALNLNGPILNVLVVLGVVLLGQFVVRRFFKS
Bax    (147) R-LLGWIQDQGGWDGLLSYFG----------TPTWQTVTIFVAGVLTASLTIWKKMG
                  α7       α8
```

Figure 1.13 Bcl-2 family members contain conserved BH motifs. Sequence alignment of Bcl-2, Bcl-xL, Mcl-1, Bak, and Bax generated by AlignX. Most members contain C-terminal tail anchors that consist of approximately 20 hydrophobic amino acids that span the lipid bilayer flanked by polar and often positively charged residues, such as R, K, and H (highlighted in blue). Members contain 8 or 9 α-helices (α1 to α8 are highlighted) and up to 4 BH domains (boxed). Bak and Bax lack the regulatory BH4 domain and its presence in Mcl-1 is disputed. Mcl-1 contains a unique extended N-terminal domain of approximately 170 amino acids that is not shown. The long flexible loop is evident in Bcl-2 and Bcl-xL connecting α1 to α2. Conserved residues are highlighted in black and similar residues in grey, with the most conservation within the BH1, BH2, and BH3 domains. The characteristic "NWGR" motif in the BH1 domain and "LXXXGD" motif (where X is any amino acid) in the BH3 domain are present in all 5 proteins.

recruitment of Bid to mitochondria [232,233]. Relocalization to mitochondria is a crucial step for all BH3-only proteins, since mitochondria serve as a platform for the battle between pro- and anti-apoptotic members and the pro-apoptotic message carried by BH3-only proteins is only received once they reach the OMM [220].

1.2.3.4 Structural Conservation of Bcl-2 Family Members

All members of the Bcl-2 family contain, at the very least, a BH3 domain, and all of the multi-domain members contain up to three additional BH domains (Fig 1.10) [99,175]. Although the sequence outside of the BH domains is not conserved, the sequences of BH domains are highly conserved among all cellular Bcl-2 proteins (Fig 1.13) [176,234]. In addition to conserved functional domains, Bcl-2 family members adopt a similar overall fold (Fig 1.14A) [99,175]. To date, eight three-dimensional (3D) structures have been solved: the anti-apoptotic members Bcl-xL, Bcl-2, Bcl-w, Mcl-1, and A1, the multi-domain pro-apoptotic members Bak and Bax, and the BH3-only protein Bid [223,224,225,226,235,236,237,238,239,240,241]. All of these proteins contain eight or nine α-helices that fold into globular helical bundles referred to as the "Bcl-2 core" fold (Fig 1.14A) [99,175]. The core fold is a globular domain of approximately 20kDa and consists of six or seven amphipathic α-helices of variable lengths surrounding two central hydrophobic α-helices (α5 and α6) [99,175] (Fig 1.14A). Each helical bundle contains an elongated hydrophobic groove on the surface of the protein comprised of residues from the BH1, BH2, and BH3 domains (Fig 1.14) [99,175]. One side of the groove is composed of the BH1 domain, made up of α-helices 4 and 5, and the BH2 domain, made up of α-helices 7 and 8, while on the other side is α-helix 3 and the BH3 domain, which is contained within α-helix 2 (Fig 1.14A) [99,175]. The BH4 domain, which is found on α-helix 1, is separated from the rest of the protein by a long unstructured loop in some members, such as Bcl-2 and Bcl-xL [175,236,237]. α-helices 1 and 6 form the back of the protein as they face away from the binding pocket and both
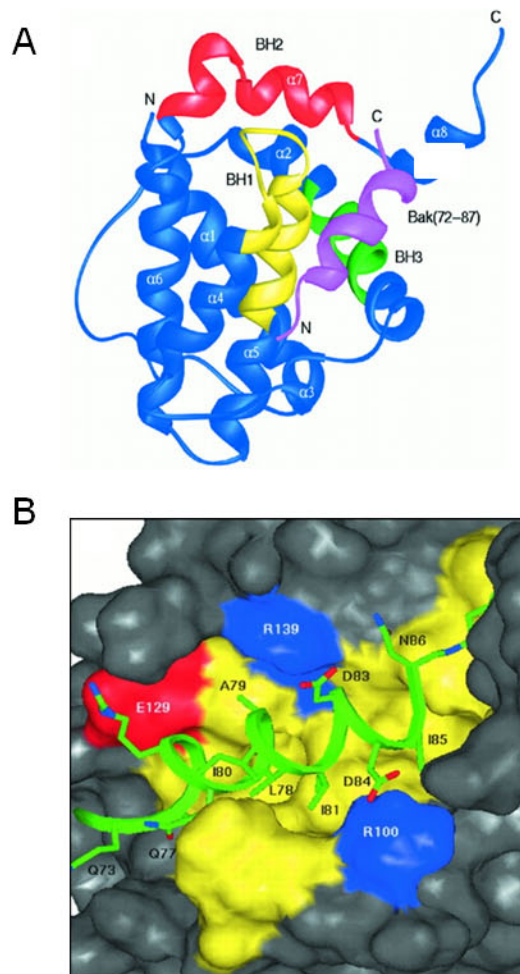
Figure 1.14 Bcl-2 family members are α-helical proteins that interact using BH domains. A. Ribbon diagram of Bcl-xL (blue) in complex with a peptide comprising the BH3 domain (residues 72-87) of Bak in purple. Although Bcl-xL contains 9 α-helices, only 8 are visible since the ninth α-helix is the transmembrane domain, which is removed for structural analysis. The long unstructured loop is apparent between the first and second α-helix. The BH1, BH2, and BH3 domains of Bcl-xL, highlighted in yellow, red, and green, respectively, make up the hydrophobic binding groove on the surface of the protein that binds the Bak BH3 peptide and on the opposite side of the molecule are α-helices 1 and 6. **B.** Surface representation of Bcl-xL bound to a Bak BH3 peptide (green) in a "lock and key" manner. Hydrophobic residues lining the bottom of the Bcl-xL binding pocket are highlighted in yellow and the residues of the Bak BH3 peptide are labelled. Charged residues on the ridge of the groove, including R139 of the conserved BH1 sequence motif NWGR, are red and blue. Both (**A**) and (**B**) are adapted from [245].

helices act to stabilize the interactions between the BH1, BH2, and BH3 domains (Fig 1.14A) [99,175].

1.2.3.4.1 Interactions Between Bcl-2 Family Members are Mediated by the BH3 Domain and Hydrophobic Binding Groove

The hydrophobic crevice on the surface of members with the Bcl-2 core fold is critical for interacting with BH3 domains from other members of the family [99,175]. BH3 domains or synthesized peptides comprising the BH3 motif bind the hydrophobic binding pocket as an amphipathic helix [226,239,242,243,244,245,246]. This interaction was first observed with Bcl-xL binding a BH3 peptide derived from Bak (Fig 1.14B) [245]. The majority of the contacts made between the BH3 peptide and the bottom of the binding cleft are mediated by hydrophobic residues, while interactions with the ridge of the cleft are mediated by charged amino acid side chains (Fig 1.14B) [245]. The amino acid signature and the overall structure of the BH3 binding groove dictate the binding profile, and thus the function, of the protein since only complementary BH3 motifs can bind [99,175].

1.2.3.4.2 Most BH3-only Proteins are Intrinsically Unstructured

The Bcl-2 core fold is observed throughout the multi-domain Bcl-2 family members and in the BH3-only protein Bid [99,175,234]. Interestingly, Bid is the only BH3-only protein that displays structural conservation with the multi-domain Bcl-2 family members [240,241]. Despite lacking identifiable domains other than the BH3 domain, Bid contains a hydrophobic surface groove, albeit it not as long or as deep as those of the multi-domain Bcl-2 family members [240,241]. Moreover, Bid can homo-oligomerize in lipid bilayers [247,248]. In contrast to Bid, secondary structure predictions indicate that all other BH3-only proteins are intrinsically unstructured and, moreover, do not appear to be evolutionarily related to other Bcl-2 family members [234]. Bad, Bmf, and Bim are highly disordered, yet they adopt a structured conformation upon binding to other Bcl-2 family members [249]. Binding-induced conformational changes is a

growing theme in the Bcl-2 family literature, as most members of the family likely change or adopt a specific conformation upon binding other proteins, as well as the OMM [250,251,252,253].

1.2.3.4.3 BH1, BH2, and BH3 Domains are Critical for Bcl-2 Family Interactions

The BH3 domain is the unifying feature among the Bcl-2 protein family: it represents the minimal functional unit and, as such, is critical for protein function [99,175,234]. Synthesized BH3 peptides from Bid and Bim are capable of activating Bak and Bax in mitochondria or lipid micelles that mimic mitochondria [254,255,256]. The multi-domain pro-apoptotic effectors Bak and Bax require an intact BH3 domain for the formation of homo-oligomers and also for interacting with members of the anti-apoptotic sub-family [257,258]. Anti-apoptotic Bcl-2 family members require conserved sequences within the BH1 and BH2 domains to mediate binding and inhibition of pro-apoptotic counterparts [259,260,261,262]. The BH1 domain, which is highly conserved, is characterized by the "NWGR" motif that plays a role in both protein structure and function, as mutating the tryptophan residue of Bcl-xL disrupts the fold of the protein, while mutating arginine inhibits binding of pro-apoptotic proteins and BH3 peptides (Fig 1.13) [245].

1.2.3.5 Three Models for Bak and Bax Activation

The permeabilization of the OMM is considered the point of no return [166,170]; therefore, the activation of Bak and Bax, which are the central executioners of MOMP, is tightly controlled [99,101]. Despite the importance of Bak and Bax activity, the exact way in which these proteins become activated has yet to be fully resolved [99,218]. It is clear that diverse signalling from BH3-only proteins converges on Bak and Bax, but this is met with resistance as Bak and Bax are negatively regulated by pro-survival members of the Bcl-2 family [99,101,218]. The most contentious point revolves around how Bak and Bax are activated by BH3-only proteins and what role anti-apoptotic proteins play in the system [99,218].

Two models were initially proposed to explain how Bak and Bax are activated during apoptosis (Fig 1.15) [99,219,263]. The indirect, or neutralization, model states that Bak and Bax are constitutively bound and suppressed by anti-apoptotic proteins, such as Bcl-2 or Mcl-1, until the anti-apoptotic protein is neutralized by binding of BH3-only proteins (Fig 1.15A) [264,265,266,267,268]. In order for apoptosis to occur, BH3-only proteins must bind and suppress all anti-apoptotic members, and therefore, in this model, Bak and Bax are indirectly activated by BH3-only proteins [264,265,266,267]. Due to differences in binding affinities, some BH3-only proteins, such as Bim, tBid, and Puma are promiscuous and bind all anti-apoptotic proteins, whereas the other BH3-only proteins are more selective: Bik and Bmf bind Bcl-2, Bcl-w, Bcl-xL, and Mcl-1, Bad binds Bcl-2, Bcl-w, and Bcl-xL, while Hrk binds Bcl-xL, and Noxa is specific for Mcl-1 and A1 (Fig 1.15A) [264].

In contrast to the indirect model, the direct model of Bak and Bax activation states that some BH3-only proteins, such as Bim, tBid, and Puma, are referred to as activators and have the capacity to bind and activate Bak and Bax directly (Fig 1.15B) [255,256,269,270,271]. In this model, the role of anti-apoptotic proteins is not to sequester Bak and Bax, but instead to bind the activator BH3-only proteins [255,256,269]. Apoptosis occurs once pro-survival members are bound and suppressed by the remaining BH3-only proteins, referred to as sensitizers (Fig 1.15B) [256,269,272]. The binding of sensitizer BH3-only proteins to anti-apoptotic proteins releases the activator BH3-only proteins, which are then free to bind and activate Bak and Bax [256,269,272].

More recently, a third model has been proposed to take into account the environment in which these interactions occur [218,273,274]. The embedded together model suggests that interactions among Bcl-2 family members only occur in the presence of a membrane since membrane binding induces critical conformational changes in these proteins (Fig 1.15C) [253,275,276]. This model agrees with the classification of BH3-only proteins into activators and sensitizers

A **Indirect (Neutralization) Model**
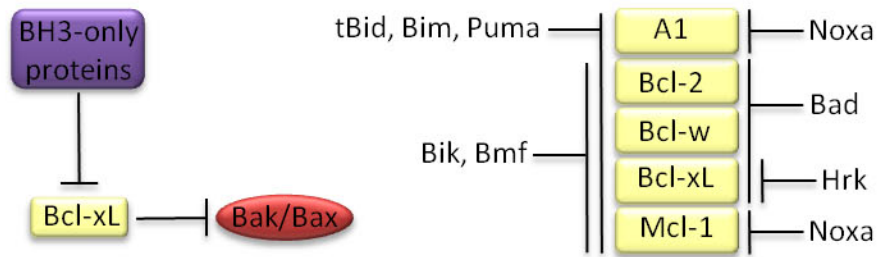
Promiscuous: tBid, Bim, Puma
Selective: Bik, Bad, Bmf, Noxa, Hrk

B **Direct Model**
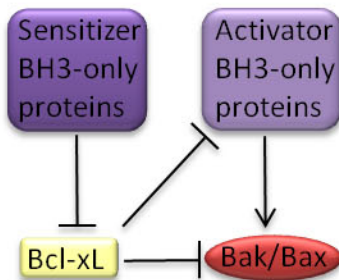
Activator: tBid, Bim, Puma
Sensitizer: Bik, Bad, Bmf, Noxa

C **Embedded Together Model**
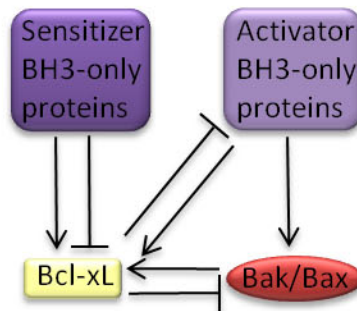
Figure 1.15 Three models for Bak and Bax activation. **A.** *Left:* In the indirect model Bak/Bax are the primary binding targets of anti-apoptotic proteins, represented here as Bcl-xL. BH3-only proteins bind and neutralize Bcl-xL to alleviate the repression of Bak/Bax; therefore, all anti-apoptotic members must be suppressed before Bak/Bax activation occurs. *Right:* tBid, Bim, and Puma are promiscuous as they engage all anti-apoptotic proteins, while the remaining BH3-only proteins are more selective. **B.** In the direct model, Bcl-xL primarily binds activator BH3-only proteins (tBid, Bim, and Puma) until sensitizer BH3-only proteins bind Bcl-xL and displace activator BH3-only proteins. Bak/Bax are activated by direct binding of activator BH3-only proteins once Bcl-xL is bound and neutralized by sensitizer BH3-only proteins. **C.** The embedded together model adopts the sensitizer and activator classification system but states that all interactions occur in a membrane. In this model, Bcl-xL functions equally in binding Bak/Bax and the activator BH3-only proteins. Additionally, the consequences of BH3-only proteins binding to Bcl-xL differs; binding of the activator tBid to Bcl-xL sequesters tBid and prevents it from directly activating Bak/Bax, whereas binding of the sensitizer Bad to Bcl-xL prevents Bcl-xL from inhibiting activator BH3-only proteins and thus Bak/Bax.

with the former able to bind and activate Bak and Bax directly [274]. The model also proposes that anti-apoptotic proteins are able to bind both BH3-only proteins and the effectors Bak and Bax [275,276,277]. Most likely, aspects from all three models are correct [254,278]. Membrane-induced conformational changes occur in many Bcl-2 family members, and in agreement with the embedded together model, these structural changes are likely to influence protein-protein interactions [250,251,252,253]. Direct binding between the BH3-only proteins Bim and Bid and either Bak or Bax has been demonstrated, strengthening the idea that BH3-only proteins can directly activate the effector proteins [235,279]. Additionally, anti-apoptotic proteins likely have a role in inhibiting members of the BH3-only protein family, as well as Bak and Bax [278]. It is therefore likely that BH3-only proteins have dual roles in binding Bak and Bax and anti-apoptotic members [218,273]. Indeed, the pro-apoptotic ability of Bim is not attributed solely to Bax binding or neutralization of anti-apoptotic proteins; instead, both activities are required for apoptosis [278].

1.2.3.5.1 Activation of Bax

Bax is cytoplasmic or loosely associated with the OMM in healthy cells since the C-terminal α-helix 9 of Bax occupies the BH3 binding groove of the protein [178,225]. It has been recently established that Bax shuttles back and forth between the cytosol and mitochondria, an event that is mediated and accompanied by the mirrored shuttling of Bcl-xL [280]. The first step in Bax activation involves translocation and integration into the OMM [178,179,180], which is believed to be the rate-limiting step [276]. This is initiated by a number of conformational changes, including exposure of the N-terminus, which can be readily detected by the conformation-specific antibody anti-Bax 6A7 [181,281]. Simultaneous exposure of the C-terminal tail anchor allows for membrane insertion and liberates the BH3 binding groove [179]. Membrane insertion of Bax is believed to require an interaction with membrane-embedded BH3-only proteins, such as tBid [255,276]. Following Bax insertion into mitochondria, Bax

undergoes further structural rearrangements, and Bax monomers interact to form higher-order oligomers, which facilitate MOMP and cytochrome *c* release [182,183,187,255].

1.2.3.5.2 Activation of Bak

In contrast to Bax, Bak is anchored in the OMM in healthy cells by virtue of its C-terminal transmembrane domain [177]. The mitochondrial localization of Bak bypasses the requirement for translocation and membrane insertion steps and, therefore, Bak activation typically displays faster kinetics compared to Bax [282]. Although the BH3 binding groove of Bak is not occupied by its C-terminal transmembrane domain, the cleft is slightly occluded and thus unable to accept a donor BH3 motif until activated [235]. Therefore, Bak too requires conformational changes to achieve a fully active state. Importantly, because Bak is integrated in membranes in healthy cells, Bak is sequestered on the OMM by the anti-apoptotic molecules Mcl-1 and Bcl-xL (Fig 1.16) [266]. In order for Bak activation to occur, the protein must first be released from the restraints of these proteins [266].

The binding of BH3-only proteins, such as tBid, can initiate the activation of Bak, yet the direct binding of BH3-only proteins to Bak has previously been difficult to detect [99]. The binding site of tBid has been mapped within the BH3 binding groove of Bak, indicating that the tBid-Bak interaction likely follows conventional BH3:groove interactions [235] and, moreover, tBid binding to Bak induces a conformational changes in Bak [283]. Similarly, BH3 domains from the BH3-only proteins Bim and Noxa bind the hydrophobic binding pocket of Bak, although the interaction is transient [284]. Like Bax, Bak undergoes extensive rearrangements at the N-terminus that can be detected by the anti-Bak AB-1 antibody, which is specific for residues 23-38 that are normally hidden within the molecule (Fig 1.16) [177,184]. In addition to N-terminal exposure, the BH3 domain of Bak becomes exposed [185], which is initially sequestered by binding the hydrophobic groove of anti-apoptotic members Mcl-1 and Bcl-xL [245].
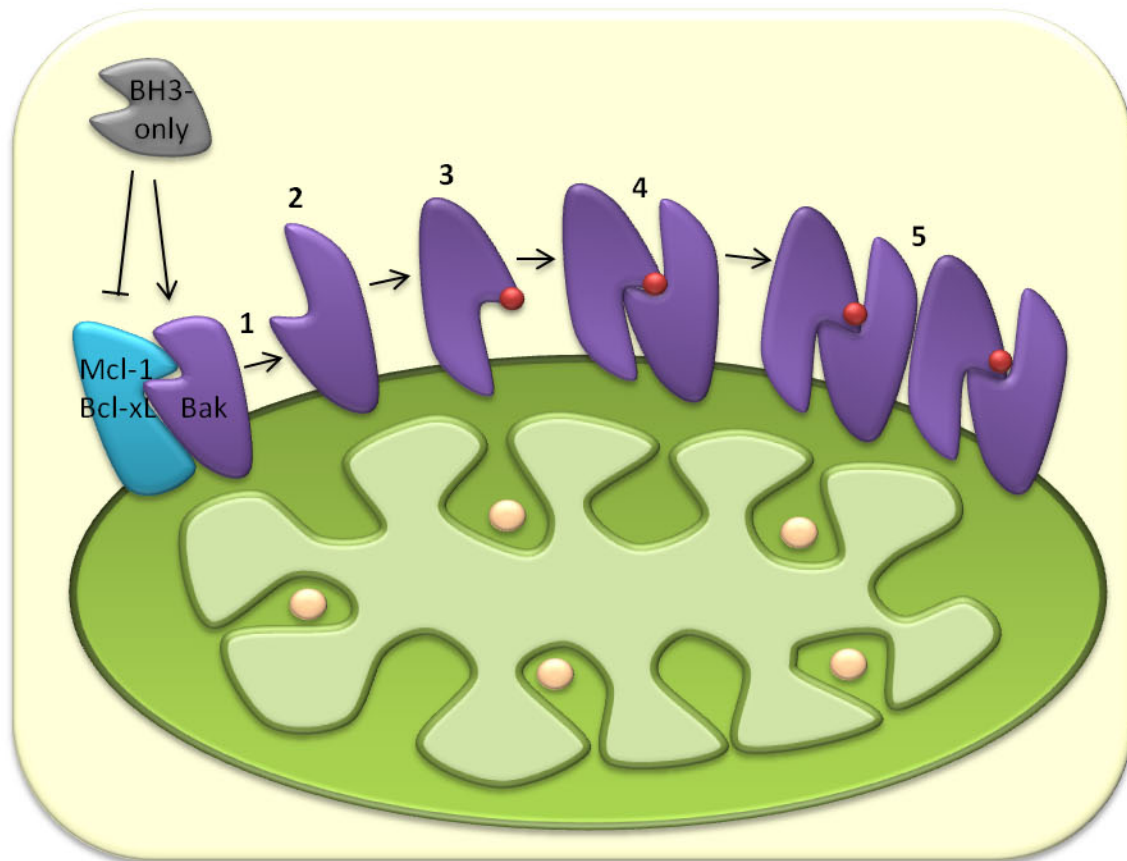
Figure 1.16 The step-wise activation of Bak. Bak is bound to Mcl-1 or Bcl-xL (or potentially VDAC2, not shown) in the OMM until the activation of BH3-only proteins disrupts the complex by binding the anti-apoptotic proteins and/or Bak (**1**).   Once free, Bak undergoes structural rearrangements at the N-terminus, an event detected by the conformation-specific antibody anti-Bak AB-1 (**2**). The Bak BH3 domain (red dot) becomes exposed (**3**), and in a process of auto-activation, inserts into the binding groove of a neighbouring Bak molecule to form a symmetric dimer (**4**). Bak dimers interact to form tetramers through interactions with the rear side of the molecule, mediated by α-helices 1 and 6 (**5**). This process is believed to repeat to form higher order Bak oligomers until a critical threshold is reached and the OMM is destabilized.

However, neutralization of anti-apoptotic members by BH3-only proteins eventually outcompetes the interaction between anti-apoptotic proteins and Bak, allowing for activated Bak molecules free of repression [266]. Through a process of auto-activation, activated Bak monomers interact with and activate neighbouring Bak molecules by burying the exposed BH3 domain into the binding groove of the inactive neighbour (Fig 1.16) [185,283]. This results in exposure of the BH3 domain from the second partner, which reciprocally inserts into the binding groove of the first Bak molecule to form a dimer [185,285]. Indeed, mutation of Bak α-helices 2, 4, and 5, which comprise the BH3 binding cleft, does not affect N-terminal exposure but inhibits homo-oligomerization of Bak [185]. The formation of Bak homodimers via BH3:groove interactions is believed to precede the formation of higher order oligomers [286]. The favoured two-interface model states that Bak homodimers interact with neighbouring homodimers through interactions mediated by the back of the molecule (Fig 1.16) [186]. Alpha-helix 6 of one Bak molecule is required to bind α-helix 6 of another Bak molecule, resulting in the linkage of two symmetric Bak homodimers into higher-order oligomers (Fig 1.16) [186]. Although the exact number and size of oligomers required to induce MOMP is not clear, Bak oligomerization inevitably results in destabilization of the OMM and MOMP [286].

1.2.3.5.3 Regulation of Bak by Mcl-1 and Bcl-xL

In healthy cells, Bak is held in an inactive state by anti-apoptotic members of the Bcl-2 family, namely Mcl-1 and Bcl-xL, and perhaps A1 [243,266]. Before Bak activation can occur, the activity of Mcl-1 and Bcl-xL must be suppressed by BH3-only proteins (Fig 1.16) [266]. It is clear from the structure of Bcl-xL bound to a BH3 peptide from Bak that the Bak BH3 domain inserts into the hydrophobic binding pocket of Bcl-xL (Fig 1.14B) [245]. Therefore, it is likely that BH3-only proteins bind to Mcl-1 and Bcl-xL and compete with Bak for binding to the hydrophobic cleft, effectively displacing the Bak BH3 region from the binding

groove [287,288]. Interestingly, although lacking an obvious BH3 domain, the transcription factor p53 has been demonstrated to relieve Bak of repression by Mcl-1 [289]. Although the primary apoptotic functions of p53 involve transcription-dependent activities, p53 binds to Bak that is in complex with Mcl-1 and results in Bak oligomerization, further suggesting that disruption of the Bak-Mcl-1 complex is a necessary step prior to Bak activation [289]. Furthermore, while Mcl-1 is regarded as the major regulator of Bak, both Mcl-1 and Bcl-xL must be neutralized before Bak is activated, although the role of Bcl-xL in Bak inhibition appears to be secondary to the role of Mcl-1 [266].

1.2.3.5.4 Regulation of Bak by VDAC

In addition to the inhibitory functions provided by Mcl-1 and Bcl-xL, the negative regulation of Bak has been attributed to members outside of the Bcl-2 family. VDAC2, an isoform of the mitochondrial porin VDAC, has been implicated as a major binding partner of Bak [290,291,292]. However, the precise outcome of this interaction is disputed. It has been reported that VDAC2 binds Bak on the OMM and prevents Bak activation until the complex is disrupted by binding of BH3-only proteins, such as tBid and Bim [290]. The interaction between Bak and VDAC2 does not resemble the way in which Bak binds anti-apoptotic Bcl-2 family members. Point mutations in the BH1 and BH3 domains of Bak disrupt binding to VDAC2, suggesting that the hydrophobic binding groove of Bak mediates the interaction with VDAC2 [290]. Conversely, VDAC2 has also been reported to interact with the hydrophobic transmembrane domain of Bak in the OMM [291]. In contrast to the inhibitory role proposed for VDAC2, other groups suggest another role for VDAC2, whereby the mitochondrial porin promotes apoptosis [292]. VDAC2 may recruit newly synthesized Bak from the cytosol to the OMM, in a manner similar to the recruitment of Bax by tBid following an apoptotic stimulus [276]. The interaction with VDAC2 causes a conformational change in Bak to expose the transmembrane segment that inserts into the OMM [293] and this recruitment of nascent Bak by VDAC2 has been implicated in tBid-induced

apoptosis [292]. In this model, VDAC2 functions to ensure Bak is inserted into the OMM to receive death signals from tBid [292]. Despite the presented models for VDAC2 and Bak, genetic studies have revealed that deletion of all three *vdac* isoforms (*vdac1, vdac2, and vdac3*) has no significant effect on mitochondrial-dependent apoptosis [294]. Thus, it is presently unclear whether VDAC2 inhibits or activates Bak activity during cell death, or whether VDAC2 is completely dispensable for Bak regulation and activity.

1.2.3.5.5 Activation of Bak and Bax by Non-Protein Factors

Bak and Bax are activated by a number of proteins, although it is now accepted that both proteins can be activated by non-protein factors, such as heat and detergents [99]. Exposing isolated mitochondria to increasing temperatures results in the activation and oligomerization of both Bak and Bax [295]. Additionally, lysing cells in non-ionic detergents results in conformational changes in Bax that can be detected by the activation-specific antibody anti-Bax 6A7 [181,281] and more recently, non-ionic detergents have been shown to induce conformational changes in Bak [296]. Because of this, studies involving Bcl-2 family members are often conducted in zwitterionic detergents to preserve the native conformation of proteins [178,181]. The sensitivity of Bak and Bax to mild heat and detergents is likely due to the conformational changes induced by the treatments. In this way, heat and lipids yield the same outcome as BH3-only proteins.

1.2.3.6 Mechanisms of MOMP and Cytochrome *c* Release

Both Bak and Bax are capable of forming oligomers in membranes [187,188] and oligomerization is required for pore formation during mitochondria-dependent apoptosis [185,297]. Bak and Bax are thought to form supramolecular openings that permit the translocation of a variety of IMS proteins across the normally impermeable OMM [255,298]. However, the way in which pores are formed in the OMM and the nature of these openings have not yet been resolved but these are areas of considerable interest [95,96,100].

There are various models proposed for poration of the OMM: Bak and Bax regulate pre-existing pores, Bak and Bax form proteinaceous pores, Bak and Bax are involved in the formation of a large multi-protein channel, or Bak and Bax stimulate the formation of lipidic pores (Fig 1.17) [95,96,100]. Additionally, it has recently been proposed that Bak and Bax may associate with the mitochondrial fission and fusion machinery during MOMP [95,160,299].

1.2.3.6.1 Bak and Bax May Modulate Pre-existing Pores

There is accumulating evidence for a role of VDAC, an integrated porin in the OMM, in apoptosis [300,301,302]. It was initially believed that MOMP occurs following matrix swelling and rupture of the OMM. This could occur following closure of VDAC on the OMM, which would result in the influx of charged solutes and osmotic swelling of the matrix [303,304,305]. Conversely, data now support the opening of VDAC during apoptosis to promote the efflux of IMS proteins, such as cytochrome *c* [306,307]. In fact, VDAC oligomers form pores large enough for the transport of cytochrome *c* and VDAC oligomerization is coupled to apoptosis [308,309]. Alternatively, yet not mutually exclusively, VDAC may promote apoptosis by associating with ANT and PBR to form the multi-protein PTP, which spans the IMM and OMM [133,164]. Opening of the PTP, a large voltage-dependent, non-selective channel, dissipates Δψm and has been linked to MOMP (Fig 1.17) [134,310,311]. Supporting a role for PTP opening in MOMP induction is the extensive cross-talk between components of the PTP and the Bcl-2 family. VDAC1 and VDAC2 have been shown to positively regulate the activation of Bax in a manner independent of Bak [302,312], whereas VDAC2 recruits Bak to mitochondria to promote Bid-induced apoptosis [313]. Importantly, VDAC and the PTP components may serve as downstream targets of activated Bak and Bax; both effector proteins promote VDAC opening while anti-apoptotic members, such as Bcl-2 and Bcl-xL, interact with and inhibit ANT and VDAC [306,314,315]. Together, the data suggest a pro-apoptotic role for components of the PTP. Ultimately, however, a definitive role for VDAC and
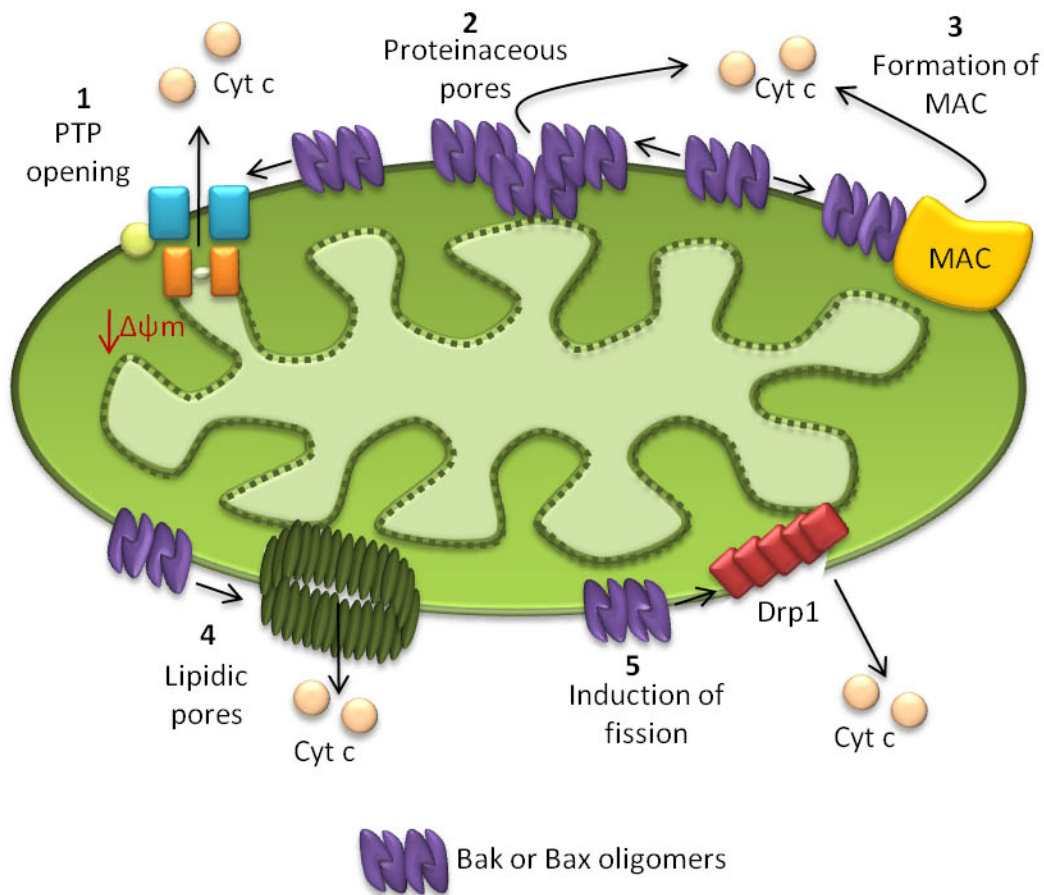
Figure 1.17 Mechanisms of mitochondrial outer membrane permeabilization. Bak and Bax oligomers may activate the multi-protein PTP, which spans the IMM and OMM, effectively causing $\Delta\psi$M collapse and permeabilization of IMM and OMM (**1**). Bak and Bax oligomers may associate to form proteinaceous pores in the OMM (**2**), or they may associate with other unknown proteins to form the large mitochondrial apoptosis-induced channel (MAC) (**3**). The insertion of Bak and Bax into the OMM may destabilize the membrane, causing positive curvature and eventual fusion of the inner and outer leaflets of the OMM to form a lipid pore large enough for the efflux of apoptotic proteins (**4**). Bak and Bax oligomers have been documented at fission sites with the GTPase Drp1; thus, the promotion of fission may cause the release of cytochrome c following Bak and Bax activation (**5**).

the PTP in apoptosis initiation has not been elucidated [165]. While VDAC is required for PTP opening and cytochrome *c* release in response to certain stimuli [300,302,316], VDAC is dispensable for apoptosis induced by calcium and oxidative stress [294]. Similar results have been recorded for ANT, which plays a role in calcium-induced ΔψM collapse but is not required for apoptosis in response to other stimuli [317]. Cytochrome *c* release occurs independently of the PTP [318,319]; therefore, the observation that PTP opening occurs during apoptosis may take place in response to specific apoptotic stimuli, such as cisplatin and endostatin, or as an event downstream of MOMP [95,133,164,165].

1.2.3.6.2 Bak and Bax May Form Proteinaceous Channels

The first structure solved for Bcl-2 family members revealed striking similarities between Bcl-xL and the pore-forming domain of bacterial toxins, such as diphtheria toxin [236,320]. This sparked the idea that members of the Bcl-2 family may porate the OMM on their own. Indeed, Bax and Bid, as well as the anti-apoptotic members Bcl-xL and Bcl-2, are all capable of forming pores in artificial membranes [248,321,322,323,324,325]. Thus, Bak and Bax oligomers may form pores large enough to support the translocation of IMS proteins (Fig 1.17). In support of this model, Bax, Bcl-2, and Bcl-xL all insert α-helices 5, 6, and 9 into membranes upon activation, though it has not yet been determined if, in the case of Bax, this contributes to pore formation [250,251,252,275,326]. In synthetic vesicles, Bax forms oligomers capable of transporting molecules up to 250kDa [255,276,321,327]. Although the exact number of molecules required for pore formation has yet to be established, Bak and Bax oligomers containing at least 18 molecules have been described [186,328] and oligomers consisting of over 100 Bak and Bax molecules have been observed in dying cells [329,330]. A major caveat of the proteinaceous pore model is the difficulty visualizing proteinaceous pores containing Bak and Bax on membranes and determining whether or not pores formed by Bak and Bax are large enough to facility the transport of large IMS proteins [101].

1.2.3.6.3 Bak and Bax May Form the Mitochondrial Apoptosis-induced Channel

Bax oligomers have been implicated in the formation of a supramolecular high-conductance channel referred to as the mitochondrial apoptosis-induced channel (MAC) (Fig 1.17) [331]. MAC forms early during apoptosis and, unlike the PTP, is not voltage dependent [332]. Over time, MAC increases in size, suggesting that recruitment of Bak and Bax oligomers results in the formation of a large channel to facilitate MOMP [332,333]. Indeed, the channels formed by MAC facilitate the release of cytochrome *c* [332]. Bak and Bax are redundant for MAC activity, yet at least one of the proteins must be present [332]. However, apart from Bak and Bax, the other components of MAC, as well the steps involved in its formation, are currently unknown [334,335].

1.2.3.6.4 Bak and Bax May Form Lipidic Pores

The alternative possibility exists that Bak and Bax oligomers may instead associate with membrane lipids to form lipid-based pores (Fig 1.17) [96,100,336]. Lipidic pores could form following the insertion and oligomerization of Bak and Bax molecules [337,338,339]. At a high enough concentration, these peptides destabilize the lipid bilayer by increasing the surface tension [337,338,340]. As a result of the positive membrane curvature, the inner and outer leaflets of the membrane fuse to form a pore composed of lipid and protein [337,338,340]. In support of this model, lipids play a role in Bax-induced membrane poration [228,255,276] and lipids that induce membrane curvature promote the pore-forming activity of Bax [338,340]. Importantly, whereas proteinaceous pores are restricted in size and conductance, lipidic pores can grow in size to facilitate the release of cytochrome *c* and larger IMS proteins, further supporting the role of lipid pores in MOMP [228,337,340].

1.2.3.6.5 Bak and Bax May Regulate Mitochondrial Dynamics

During apoptosis, massive fragmentation of mitochondria occurs, suggesting a link between enhanced fission rates and MOMP [139,159,160,161]. Drp1, the GTPase required for mitochondrial fission, shuttles between cytosol

and mitochondria (Fig 1.8) until an apoptotic stimulus induces Drp1 recruitment to mitochondria at discrete sites where fission is initiated (Fig 1.7) [154]. Bax accumulates at these fission sites, indicating that Bax may engage the fission machinery to induce MOMP [341], and in addition, Drp1 has been implicated in the formation of Bax oligomers at fission sites [342]. A role for Bak in promoting fission has also been observed, since mitochondrial fragmentation is decreased in Bak-deficient cells [343]. Intriguingly, both Bak and Bax promote Drp1-mediated fission during apoptosis, implying that Bak and Bax function upstream of fission and fusion machinery to promote MOMP [344]. The proposed role for mitochondrial dynamics in mediating MOMP, however, has been met with criticism since depletion of the fission protein Drp1 delays, but does not prevent, cytochrome c release or Bak/Bax-dependent apoptosis [153,155,156]. These data suggest that Drp-1-mediated fragmentation may not initiate MOMP, but simply accompany the process. A second explanation for the extensive fragmentation observed during apoptosis stems from the housekeeping functions of Bak and Bax. In healthy cells, the fission and fusion machinery cooperate with members of the Bcl-2 family to regulate mitochondrial morphology [139,159,160,345,346]. Bak and Bax promote mitochondrial fusion through interactions with the fusion protein Mfn2 until receipt of an apoptotic stimulus induces extensive mitochondrial fission [347]. Indeed, fusion is blocked during Bax activation [348]. Therefore, the massive mitochondrial fragmentation observed during apoptosis may be a result of activated Bak and Bax no longer promoting fusion.

Perhaps the most convincing evidence for the role of the fission and fusion machinery in the execution of apoptosis involves changes in the morphology of the IMM during cristae remodelling [157]. During apoptosis, Opa1 oligomers are disrupted, allowing for cristae remodelling and mobilization of cytochrome c into the IMS (Fig 1.7) [157,158]. This represents a critical step that occurs prior to the translocation of cytochrome c through pores in the OMM

[96].   Interestingly, Opa1-mediated cristae opening and mobilization of cytochrome *c* is dependent on Bak and Bax activation [349]. In addition, the release of cytochrome *c*, but not other IMS proteins, is delayed in Drp1-deficient cells [155,156].   Together, these data suggest that activated Bak and Bax promote mitochondrial fission, which is required for downstream cristae remodelling and release of cytochrome *c* into the IMS [155,156,349]. However, further investigation into whether mitochondrial fragmentation causes MOMP, results from MOMP, or simply accompanies MOMP is required and the role of Bak and Bax in regulating mitochondrial dynamics in healthy and apoptotic cells requires future study [139,159,160,345,346].

1.2.4 Regulation of Apoptosis

Because of its critical role in development, tissue homeostasis, and defence against pathogens, apoptosis is tightly regulated [99,101]. Proteins involved in the mitochondrial pathway are regulated by transcription, protein folding, and interactions with other proteins, in order to ensure the timely onset of apoptosis [99,101,195]. Additionally, various post-translational mechanisms govern the activity of proteins involved in activating and inhibiting apoptosis. These include protein cleavage, phosphorylation, and ubiquitination [99,101,195].

1.2.4.1 Transcription and Structure

Regulation of the Bcl-2 family is observed at the level of transcription for Bax, as well as the BH3-only proteins Bim, Noxa, and Puma [194,195]. An additional level of regulation occurs following transcription via alternative splicing, which generates distinct isoforms. For example, of the three major isoforms of Bim, BimS is the most potent and less abundant form, while BimEL is the least potent and most predominant form [196,197]. In the case of Mcl-1, alternative splicing yields two isoforms with opposing functions.   Mcl-1 is predominantly expressed as Mcl-1 long (Mcl-1L), the anti-apoptotic isoform that regulates Bak activity [350]; however, the expression of Mcl-1 short (Mcl-1S),

although minor, produces a pro-apoptotic protein [351,352]. In addition to transcription, some members of the Bcl-2 family are regulated by virtue of their structure. Buried C-termini of Bax, Bcl-xL, Bcl-w, and Mcl-1, inside their hydrophobic binding grooves effectively retain these proteins as inactive molecules in the cytoplasm until an activating conformational change occurs [223,224,225,226].

1.2.4.2 Protein-Protein Interactions

One critical regulatory mechanism is the complex network of interactions among the Bcl-2 family, as well as with other cellular proteins [99,101,195]. For instance, BimL and BimEL are inhibited in healthy cells through interaction with DLC-1 of the cytoskeletal network [197,198]. Cytoplasmic retention is observed for Bad, which is bound to 14-3-3, and Bmf, which binds the cytoskeletal protein dynein light chain 2 (DLC-2) [353]. In the case of the mitochondrial gatekeepers Bak and Bax, interactions with anti-apoptotic Bcl-2 family members are essential to control their activation [99,100,101,218]. This is especially important for Bak because it resides in the OMM in healthy cells and therefore must be sequestered by Mcl-1, Bcl-xL, and perhaps VDAC2 [266,289,290,354].

1.2.4.3 Post-translational Modifications

Various post-translational modifications regulate the activity of Bcl-2 family members [99,101,195]. Cleavage mediated by caspase 8 or granzyme B is a crucial activating step for production of tBid from Bid [200,201,202]. Conversely, inactivating cleavage events occur in some anti-apoptotic members, such as Bcl-2 and Bcl-xL, which are cleaved by caspase 3 in the flexible loop connecting α-helices 1 and 2, producing truncated proteins lacking the BH4 domain [355,356]. The BH4-deficient fragments are potently pro-apoptotic and believed to function as part of a positive feedback loop to ensure apoptosis occurs [355,356]. Like cleavage, phosphorylation can have activating or inhibitory effects on Bcl-2 family members. The interaction between Bad and 14-3-3 in the cytosol is mediated by phosphorylation of Bad until an apoptotic

signal, such as growth factor withdrawal, leads to Bad dephosphorylation, release from 14-3-3, and mitochondrial translocation [229,357,358]. Phosphorylation of Bcl-2 and Bim can activate or inhibit the proteins depending on the stimuli and kinases involved. Whereas Bcl-2 phosphorylation by the mitogen-activated protein kinase (MAPK) pathway stabilizes the protein [359,360,361], phosphorylation of Bcl-2 in the long unstructured loop leads to functional inactivation of the protein [362,363,364]. Similarly, Jun kinase (JNK) phosphorylates and activates BimEL to promote apoptosis in neurons [365,366], whereas phosphorylation of BimEL by the MAPK pathway dampens protein activity [367,368,369]. Specifically, once phosphorylated by the MAPK pathway, Bim is degraded in a manner dependent on the cellular ubiquitin-proteasome system [368,370].

1.3 THE UBIQUITIN-PROTEASOME SYSTEM

The ubiquitin-proteasome system (UPS) is involved in nearly every aspect of the cell, from transcription and cell division to inflammation and apoptosis [371,372,373]. Targeted proteins are covalently linked to ubiquitin, an evolutionarily conserved 76 amino acid protein [374,375,376]. Ubiquitin linkage is achieved by an enzymatic cascade carried out by three enzymes (Fig 1.18). Ubiquitin is first activated in an energy-dependent process by one of two E1 ubiquitin activating enzymes and then transferred to one of a hundred E2 ubiquitin conjugating enzymes [371,372]. The third enzyme, the E3 ubiquitin ligase, catalyzes the transfer of ubiquitin from the E2 enzyme to a lysine residue on a substrate, forming an isopeptide bond [371,372]. There are over 600 predicted ubiquitin ligases in the human genome [377] and these enzymes are critical for not only mediating the transfer of ubiquitin onto substrates, but also for conferring substrate specificity [371,372]. Importantly, ubiquitination is a reversible process and through the action of nearly 100 deubiquitinating enzymes (DUBs), ubiquitin can be removed from substrates (Fig 1.18) [378].
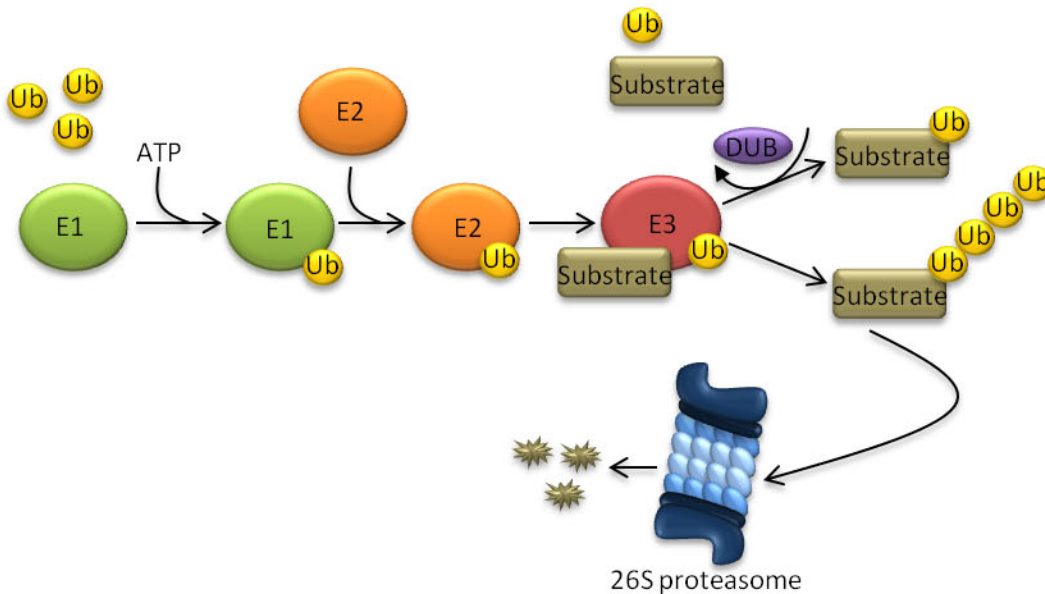
Figure 1.18 The ubiquitination cascade. In an ATP-dependent process, ubiquitin is conjugated onto an E1 activating enzyme. Ubiquitin is transferred to an E2 conjugating enzyme, which then associates with one of many E3 ligases. E3 ligases typically contain HECT or RING finger domains, the latter of which can exist as single subunit or multi-component complexes. The E3 ligase recruits substrates either directly or through adaptor proteins and catalyses the transfer of ubiquitin onto a lysine residue in the substrate, resulting in covalent modification of the substrate. This process is reversible through the action of de-ubiquitinating enzymes, which hydrolyze the isopeptide bond between ubiquitin and the tagged protein. Substrates can be monoubiquitinated on one or multiple lysine residues, or alternatively, the protein can be modified with polyubiquitin chains of 4 or more ubiquitin molecules. Although there are exceptions, polyubiquitin chains typically target the protein for degradation by the 26S proteasome.

The reaction catalyzed by E3 ubiquitin ligases can be repeated to produce polyubiquitin chains by linking an incoming ubiquitin moiety onto a lysine residue in the preceding ubiquitin molecule (Fig 1.18) [371,372]. Ubiquitin contains seven lysine residues, all capable of forming linkages *in vivo*, and the lysine residue in ubiquitin used to form polyubiquitin chains has a significant effect on the fate of the protein (Fig 1.19A) [379,380,381]. Whereas polyubiquitin chains formed through K63 typically alter protein function or localization, polyubiquitin chains formed on K48 of ubiquitin target the ubiquitinated protein to the multi-catalytic 26S proteasome for degradation (Fig 1.19A) [379,381,382,383]. Notably, not all proteins are tagged with polyubiquitin chains; proteins altered by single or multiple monoubiquitination events are associated with DNA repair and endocytic functions [373].

1.3.1 E3 Ubiquitin Ligases: HECT and RING Domains

Two main classes of ubiquitin ligases exist, both containing evolutionarily conserved domains that are essential for ubiquitination activity [371]. The Homologous to E6-AP Carboxyl Terminus (HECT) domain-containing E3 ligases are exemplified by the cellular E6-associated protein (E6-AP), which associates with the papillomavirus virus protein E6 to promote p53 ubiquitination and degradation during infection [384]. The human genome encodes approximately 30 putative HECT domain-containing E3 ligases [377], all unified by the presence of a conserved 350 amino acid HECT domain [385]. These ubiquitin ligases use a conserved cysteine residue in the HECT domain to form a covalent bond with ubiquitin before transferring the ubiquitin molecule onto target proteins [385].

In contrast to HECT E3 ligases, the second major group of E3 ligases contain Really Interesting New Gene (RING) domains and transfer ubiquitin directly from E2 enzymes onto target proteins [386]. Over 600 genes in the human genome are suspected to encode ubiquitin ligases containing RING finger domains [386]. The RING finger contains conserved cysteine and histidine residues that coordinate the binding of two zinc ions and are critical for catalytic
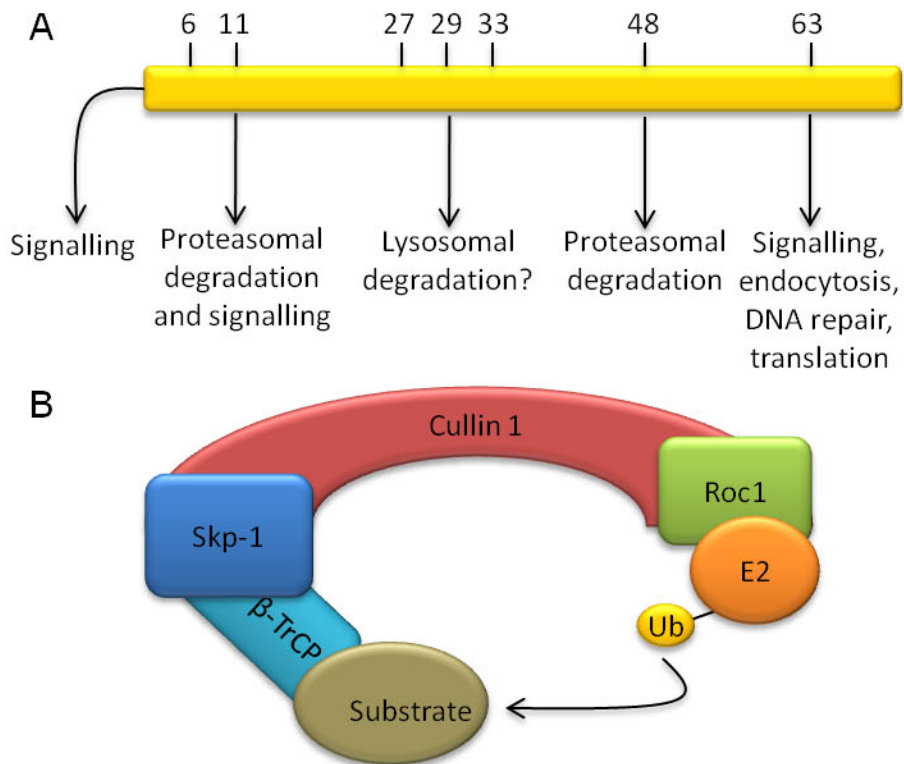
Figure 1.19 Ubiquitin linkages and the SCF complex. A. Ubiquitin contains 7 lysines that can form linkages. K48-linked chains target a protein for proteasomal degradation, while K63-linked chains are involved in various signalling events, such as NFκB activation and endocytosis. Chains formed on K11 have been implicated in proteasomal degradation and signalling. K29 linkages may be involved in lysosomal degradation. Linear ubiquitin chains formed through the N-terminal methionine have also been observed. **B.** In the SCF$^{β-TrCP}$ complex, cullin-1 acts as a scaffold to recruit the RING-finger protein Roc1, the E2-ubiqutin complex, and the substrate protein. The substrate is recruited by the F-box protein β-TrCP, which interacts with the E3 ligase machinery through the adaptor protein Skp1.

activity [387]. RING-based E3 ligases can function as single proteins that contain the RING domain and substrate recognition domain in one polypeptide or as multi-protein complexes [371,386]. An example of a single-subunit RING domain-containing E3 ligase is XIAP, the prototypic member of the IAP family, which not only binds and inactivates caspases 3, 7, and 9, but polyubiquitinates these caspases to promote their degradation [111,388].

In multi-subunit E3 ligases, the RING finger domain and the substrate recognition domain are found on separate proteins and, moreover, most contain a member of the cullin family of proteins to bring both domains into close proximity [386,389]. Cullin proteins act as molecular scaffolds to recruit Roc1, a RING finger protein, the E2 enzyme conjugated to ubiquitin, and one or two substrate adaptor proteins, which bind and recruit specific substrates [386,389,390,391]. The best studied multi-component E3 ligase is the SCF, or Skp1-Cullin 1-F-box, complex (Fig 1.19B) [392]. The RING finger Roc1 and the E2-ubiquitin complex bind the C-terminus of Cullin-1 (Cul-1) [393,394]. At the N-terminus of Cul-1, the linker protein Skp1 (S-phase-kinase-associated protein-1) binds and recruits one of many substrate adaptor proteins containing F-box domains (Fig 1.19B) [395,396,397,398]. F-box domain-containing proteins contain a second interaction motif, such as WD40 repeats or a leucine-rich domain, that directly interacts with the target protein, which is typically a phosphoprotein [399,400,401]. One such F-box protein is β-transducin-repeat-containing-protein (β-TrCP), which forms the SCF$^{\beta\text{-TrCP}}$ complex responsible for ubiquitination and the eventual destruction of substrates such as β-catenin and the inhibitor of NFκB, IκB [402,403,404,405].

1.3.2 The 26S Proteasome

Many polyubiquitinated proteins are often targeted to a large multi-protein complex, the 26S proteasome, for degradation (Fig 1.20) [382,406]. The proteasome is a large cylindrical complex that is responsible for the proteolysis of numerous unrelated proteins, yet it is specialized to ensure timely and specific
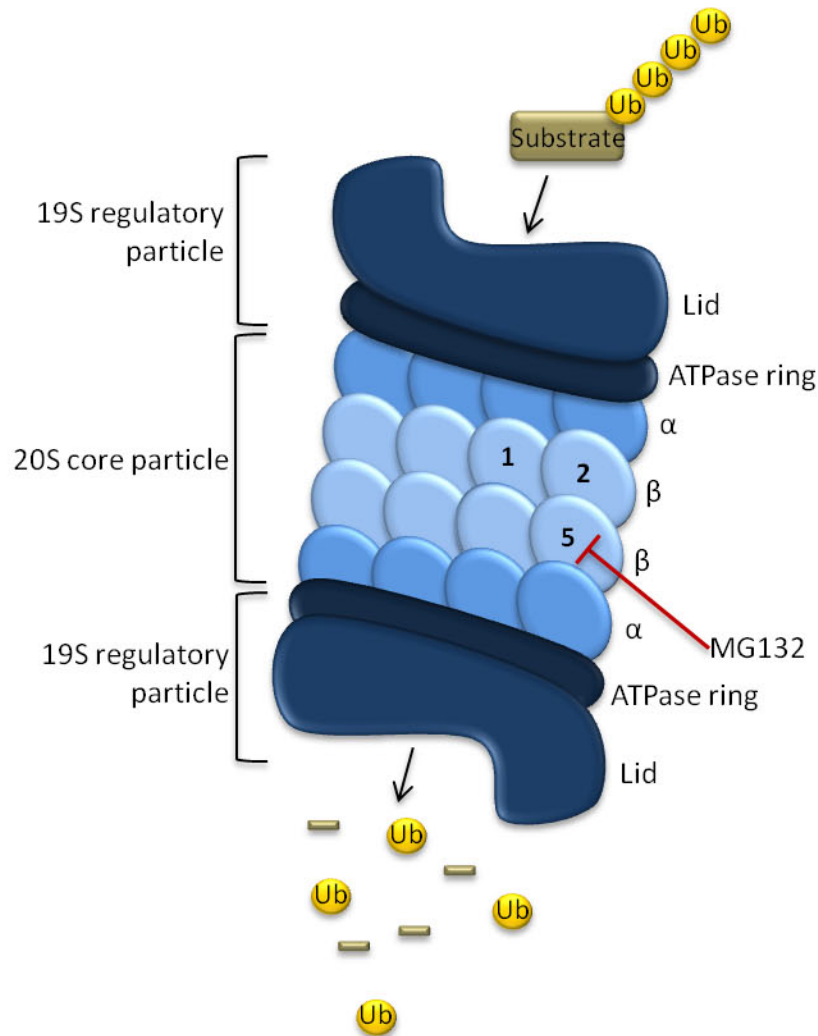
Figure 1.20 The 26S proteasome. The 20S core of the proteasome contains 4 stacked rings composed of α-subunits and β-subunits that form a barrel-like structure with a narrow central cavity. β-subunits make up the center of the 20S core and three β-subunits in each ring contain catalytic activity responsible for processively degrading proteins into small peptides: β1, β2, and β5 have caspase-like, trypsin-like, and chymotrypsin-like activities, respectively. α-subunits are responsible for recruiting the 19S regulatory particle to one or both ends of the core particle. The regulatory particle contains a lid which recruits polyubiquitinated proteins via ubiquitin-binding domains and an ATPase ring to unfold the protein before entering the 20S core. The peptide aldehyde MG132 targets the chymotrypsin-like activity of the β5 subunits to effectively inhibit proteasome activity.

protein degradation [382,406,407]. The complex consists of a 20S core particle composed of four heptameric rings that form a barrel shape (Fig 1.20) [408,409]. The outermost rings are made up of α-subunits, which provide a docking site for the regulatory particle, whereas the catalytic activity is contained within the two inner rings that are composed of β-subunits [408,409]. Of the seven β-subunits, three have catalytic activity: β1 has caspase-like activity, β2 has trypsin-like activity, and β5 has chymotrypsin-like activity (Fig 1.20) [410]. The broad specificity of the β-subunits, the narrow channel of the core particle, and the concentrated catalytic sites ensures that all proteins that enter the proteasome are processively degraded to small peptides, typically ranging in size from 3-22 amino acids [411]. Many chemical inhibitors have been developed to inhibit proteasome function [412,413]. The first and most widely used inhibitors were synthetic peptide aldehydes, such as MG132, which inhibit the proteasome by targeting the chymotrypsin-like β5 subunits (Fig 1.20) [414,415]. MG132 is a potent inhibitor of the proteasome that is readily taken up by cells and whose action can be easily reversed upon removal of the peptide inhibitor [414,415].

Importantly, the catalytic β-subunits face inside the channel and therefore access inside the proteasome is highly restricted by the 19S regulatory particle, which flanks one or both sides of the 20S core [408,409]. The 19S regulatory unit, which consists of a lid and a base, controls protein entry into the inner catalytic chamber and the ATPase activity of the base partially unfolds the polypeptide to allow entry into the narrow channel [382,406,407]. In addition to a polyubiquitin chain, which is recognized by ubiquitin receptors on the base, it is believed that proteins to be degraded must also have an unstructured region in order to access the proteasome [416]. Importantly, ubiquitin is recycled by the action of DUBs in the 19S subunit, which remove the entire polyubiquitin chain from the target protein, an event that is believed to be necessary for proteasomal entry and peptide unfolding [417,418].

1.3.3 Control of Apoptosis by the Ubiquitin-Proteasome System

There is growing evidence for an important role of the UPS in governing the apoptotic cascade [419]. In addition to XIAP and other members of the IAP family, which target active caspases for proteasomal degradation [111,388], cullin-based E3 ligases also target caspases. Pro-caspase 3 is a target for the SCF$^{\beta\text{-TrCP}}$ complex, which mediates degradation of the protein [420], whereas proteolytic processing and activation of caspase 8 following death receptor ligation is assisted by another member of the cullin family, the cullin 3 (Cul-3)-based E3 ligase complex [421].

Both pro- and anti-apoptotic members of the Bcl-2 family are targeted for destruction by the UPS. Following phosphorylation of BimEL by the MAPK pathway, the phosphoprotein is recruited to the SCF$^{\beta\text{-TrCP}}$ complex, which promotes its polyubiquitination and degradation [422]. Although degradation of tBid has been reported [423], more recently, the UPS has been implicated in enhancing the pro-apoptotic activity of Bid [424]. Following initial cleavage by caspase 8 or 10, tBid remains associated with the inhibitory N-terminus [425,426] until the latter fragment is ubiquitinated and degraded to promote activation of tBid [424]. Proteasomal degradation also regulates the effector protein Bax, particularly in tumourigenic cells [427,428,429], and additionally, a potently apoptotic splice variant of Bax, Baxβ, is under stringent control by the UPS [430]. The role of the UPS in regulating cell death is not restricted to pro-apoptotic proteins; dephosphorylated Bcl-2 is sensitive to proteasomal degradation [359], although S-nitrosylation by nitric oxide inhibits Bcl-2 degradation and thus promotes cell survival [431]. Together, these results point to an essential role for the UPS in controlling the levels and activity of Bcl-2 family members. To date, however, the best described role for the UPS in apoptotic signalling involves the regulation of the anti-apoptotic protein Mcl-1.

1.3.3.4 The Activity of Mcl-1 is Tightly Governed by the Ubiquitin-Proteasome System

Mcl-1 plays an important role in preventing apoptosis by binding Bak and various BH3-only proteins, including Bim, Bid, Noxa, Puma, and Bik [287,288,432]. Mcl-1 constitutively binds Bak to prevent cell death; thus, the disruption of the Bak-Mcl-1 complex is a necessary step to initiate Bak activation (Fig 1.16) [266,289,354]. Interestingly, Mcl-1 is an extremely labile protein and under certain conditions, such as ultraviolet (UV) irradiation, the dissociation of Mcl-1 from Bak is immediately followed by Mcl-1 degradation (Fig 1.21) [216,266,354]. The induction of a DNA damage response is a common cause of rapid Mcl-1 destruction, as infection with adenovirus (AdV) results in DNA damage and proteasomal degradation of Mcl-1 [354]. This is perhaps due to BH3-only proteins that are activated in response to DNA damaging insults, such as the p53-induced Noxa [433,434]. Indeed, the binding of BH3-only proteins appears to play an important role in the fate of Mcl-1; although Bim binding is associated with stable Mcl-1 protein levels, Noxa binding induces rapid proteasomal degradation of Mcl-1 (Fig 1.21) [266,435,436]. Recently, Mule, a unique BH3-only protein with ubiquitin ligase activity, has been implicated in Mcl-1 turnover in healthy and stressed cells [437,438]. Mule not only constitutively controls the levels of Mcl-1, but also plays a pro-apoptotic role by degrading Mcl-1 following treatment with DNA damaging agents [437,438]. In addition to Mule activity during a DNA damage response, Mcl-1 degradation also occurs during growth factor withdrawal, and this is mediated by the SCF$^{\beta\text{-TrCP}}$ complex or the SCF complex in association with a different F-box protein, FBW7 [439,440]. Prior to recognition by the SCF complex, however, Mcl-1 is phosphorylated by the glycogen synthase-3 (GSK-3), a kinase that is activated during growth factor deprivation [440,441,442]. The intricate regulation of Mcl-1, along with the fact that the protein is upregulated in various tumours [287,288], highlights the integral role the protein has in preventing apoptosis. Additionally, since the increase or decrease of both pro- and anti-apoptotic
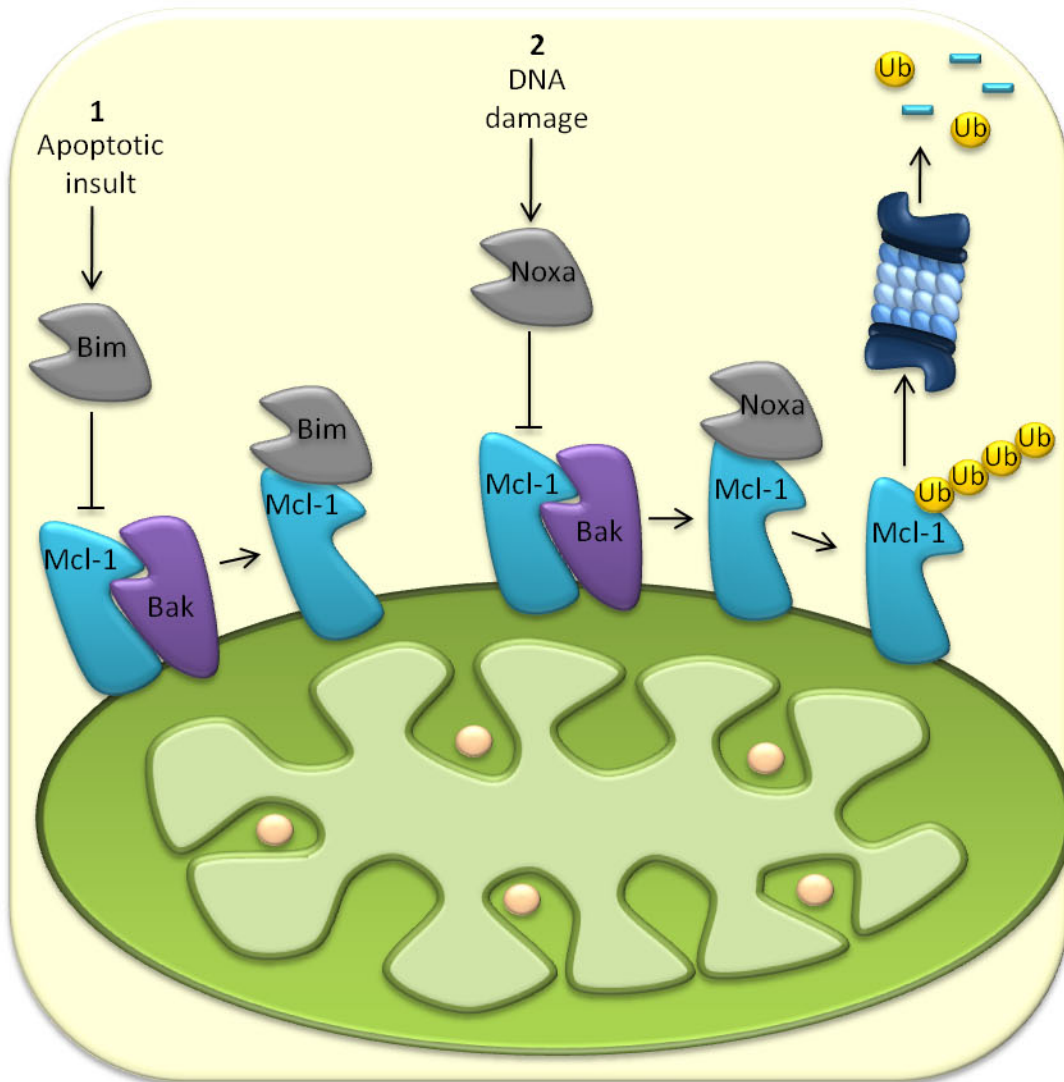
Figure 1.21 Regulation of the anti-apoptotic protein Mcl-1. Mcl-1 is a major regulator of Bak activity. In healthy cells, Mcl-1 binds Bak on the OMM until an apoptotic insult activates BH3-only proteins, such as Bim (**1**). Bim disrupts the Bak-Mcl-1 complex by binding Mcl-1, an interaction that stabilizes both Mcl-1 and Bim. Displaced Bak is free of suppression and undergoes activation. Apoptotic stimuli that cause DNA damage, such as UV irradiation, activate a specific set of BH3-only proteins, such as Noxa (**2**). Noxa binding to Mcl-1 also disrupts the Bak-Mcl-1 complex to displace Bak and allow Bak activation to occur. However, through an unknown mechanism, the interaction between Noxa and Mcl-1 targets Mcl-1 for rapid polyubiquitination and degradation by the 26S proteasome.

members can influence the activation of Bak and Bax, the UPS plays a critical role in determining the fate of a cell.

1.4 POXVIRAL INHIBITORS OF APOPTOSIS

Apoptosis is a potent defence against invading pathogens, particularly viruses [52,54,443]. Cytotoxic immune cells, such as CTLs and NK cells, patrol the host and rapidly induce apoptosis in cells showing signs of infection [49,50]. Additionally, all cells of the human body have the intrinsic ability to sense viral infection and activate the apoptotic machinery in order to prevent replication and spread of the virus to neighbouring cells [52,54]. Thus, viruses have adopted various strategies to interfere with apoptosis. In fact, poxviruses encode an arsenal of proteins aimed at interfering with the apoptotic cascade at nearly every step (Table 1.3) [63,444].

1.4.1 Downregulation of Major Histocompatibility Complex

During infection, the major histocompatibility complex (MHC) class I presents viral peptides produced in the infected cell on the cell surface [445]. Upon recognizing MHC class I bearing viral peptides, along with the T-lymphocyte co-receptor CD4, CTLs become activated and induce apoptosis of the infected cell through death receptor ligation and the release of granzyme B [49]. In order to prevent detection by patrolling CTLs, poxvirus-infected cells prevent MHC class I from presenting viral peptides on the cell surface and thus "hide" infected cells from the host immune system [444,446]. In myxoma virus, this is achieved by the RING finger-containing protein M153R, which downregulates MHC class I, as well as Fas and the T-lymphocyte co-receptor CD4, from the cell surface [447,448]. In a manner dependent on its RING domain, M153R functions as a membrane bound E3 ligase to mediate the ubiquitination and degradation of MHC class I and CD4 in order to escape detection by immune cells [448]. While M153R-like proteins are found in other members of the *Leporipoxvirus*, *Suipoxvirus*, and *Yatapoxvirus* family, orthopoxviruses lack M153R homologues [444]. Cowpox virus, a member of the *Orthopoxvirus* genus, inhibits MHC class I

Table 1.3 Poxviral Inhibitors of Apoptosis.

Function	Protein	Genus
MHC-1 downregulation	M153R (MV-LAP)	*Leporipoxvirus, Suipoxvirus, Yatapoxvirus*
	CPXV12, CPXV203	*Orthopoxvirus*
Soluble TNF receptors	MT-2, ST-2	*Leporipoxvirus*
	CrmB, CrmC, CrmD, CrmE	*Orthopoxvirus*
	TPV-2L	*Yatapoxvirus*
vFLIPs	MC159, MC160	*Molluscipoxvirus*
Serpin, inhibit caspases 1 and 8	CrmA/SPI-2	*Orthopoxvirus*
	SP-1, SP-3	*Orthopoxvirus*
	Serp1, Serp2	*Leporipoxvirus*
Viral IAPs	AMV-IAP	*Betaentomopoxvirus*
	MSV242 and MSV248	*Alphaentomopoxvirus*
Anti-apoptotic E3 ligases	p28/N1R	*Orthopoxvirus, Leporipoxvirus, Capripoxvirus, Suipoxvirus, Yatapoxvirus*
Anti-apoptotic inhibitor at Golgi apparatus	vGAAP	*Orthopoxvirus*
vBcl-2 Homologues	FPV039/CNPV058	*Avipoxvirus*
Unique Mitochondrial Inhibitors of Apoptosis	M11L	*Leporipoxvirus*
	DPV022	*Cervidpoxvirus*
	ORFV125	*Parapoxvirus*
	F1L	*Orthopoxvirus*

Adapted from [63].

trafficking in order to prevent surface expression of MHC class I altogether [449]. Recently, two gene products, CPXV12 and CPXV203, have been identified as the proteins responsible for impeding MHC class I transport to the cell surface [450,451,452]; thus, it is apparent that members of the poxvirus family have evolved multiple mechanisms to achieve immune stealth.

1.4.2 Soluble TNF Receptors

In addition to its role in inflammation, the TNF receptor pathway activates caspase 8 and initiates apoptosis [64,453]. In order to prevent TNFα from binding TNFR on the surface of infected cells, poxviruses produce secreted mimics of the TNFR [38,63,444]. Myxoma virus M-T2 and Shope fibroma virus S-T2 were the first TNFR decoys discovered [454,455,456]. Once secreted, these TNFR mimics bind TNFα to prevent TNFα-induced apoptosis of infected cells [457,458]. The importance of M-T2 was exemplified by its requirement for apoptosis inhibition upon infection of rabbit cells and for virus virulence in European rabbits [455,459]. Other members of the poxvirus family encode soluble TNFR decoys, such as A53R and B28R/C22L, in VV (Table 1.2). A53R and B28R/C22L are orthologous to cytokine response modifier C (CrmC) and CrmB in cowpox virus, respectively [460,461]. In addition to CrmB and CrmC, cowpox virus also encodes two other TNFR homologues, CrmD and CrmE, [462,463,464]. Interestingly, tanapoxvirus, a member of the *Yatapoxvirus* genus, encodes a soluble TNFα binding protein, TPV-2L, that does not display any homology to cellular TNFRs but binds TNFα with high affinity [465].

1.4.3 Inhibition of Death Receptor Signalling and Caspase Activation

The fundamental role of death receptor signalling in combating poxvirus infection is further underscored by the extensive manipulation of TNFR and Fas signalling pathways [63,444]. Molluscum contagiosum virus prevents death receptor signalling at the level of pro-caspase 8 processing, similar to the dominant negative activity of c-FLIP (Fig 1.4) [85]. MC159 and MC160 are viral homologues of c-FLIP, termed v-FLIPS, and contain domains homologous to the

DED present in both pro-caspase 8 and the adaptor proteins FADD and TRADD [466,467,468]. Through these domains, MC159 and MC160 interact with FADD and pro-caspase 8 to prevent caspase 8 activation following the ligation of death receptors [466,467,468,469,470,471].

Since caspase activation is a critical event in the initiation of apoptosis, many poxviruses impede the function of active caspases [63,444,472]. CrmA of cowpox virus is the best studied poxviral caspase inhibitor. CrmA is homologous to members of the cellular serine protease inhibitor, or serpin, superfamily, which form irreversible complexes with serine proteases [473,474]. Interestingly, CrmA inhibits both serine and cysteine proteases and therefore caspases are a major target [475,476]. Similar to other serpins, CrmA acts as a pseudo-substrate and forms covalent bonds with the active site of caspases [473]. The caspases targeted by CrmA are caspase 1, which is involved in pro-inflammatory pathway by processing pro-IL-1β and pro-1L-18, and caspase 8, the initiator caspase of the death receptor pathway [81,477,478]. Moreover, CrmA inhibits granzyme B, a direct activator of both caspases and Bid [476]. The role of serpins, such as CrmA, are believed to play a major role in preventing death receptor signalling, since other members of the *Orthopoxvirus* genus encode one or more of these proteins [63,444]. In addition to encoding SPI-2, a CrmA orthologue that inhibits caspase 1 activation and TNFα- and FasL-induced apoptosis [42,43], VV encodes two additional protease inhibitors, SPI-1 and SPI-3 [479,480,481], while myxoma virus encodes two serpins, Serp-1 and Serp-2 [482].

While serpins act as pseudo-substrates for caspase 8, some poxviruses have devised other strategies to interfere with caspase activity [63,444]. The genomes of insect poxviruses contain genes bearing strong homology with cellular IAPs [483,484]. Similar to cellular IAPs, such as XIAP, the poxviral genes contain baculovirus IAP repeat regions and a RING finger domain [485,486]. Indeed, AMV-IAP from Amsacta moorei inhibits caspases 3 and 9 to effectively

inhibit apoptosis *in vitro* [487,488]. Whether or not the poxviral IAPs mediate ubiquitination and degradation of caspases is unclear, however, and the role of the RING finger domain has not yet been determined.

1.4.4 Poxviral Anti-apoptotic Proteins of Unknown Function

Poxviral IAPs and the ubiquitin ligase M153R are not the only RING domain-containing proteins implicated in preventing apoptosis. Members of the *Orthopoxvirus* genus encode the RING finger E3 ligase p28 that is crucial for virus virulence [489]. Outside the orthopoxviruses, many other members of the *Chordopoxvirinae* encode the p28 homologue N1R, which was initially characterized in Shope fibroma virus [490]. Although the anti-apoptotic mechanism of p28 is unclear, it functions as an E3 ligase to mediate ubiquitination and both p28 and N1R prevent apoptosis in response to UV irradiation [490,491,492,493]. Moreover, a recently identified anti-apoptotic protein was identified in VV and camelpox virus that functions at the Golgi apparatus [494]. vGAAP, or viral Golgi anti-apoptotic protein, and its cellular homologue human GAAP, have been reported to inhibit death receptor and mitochondrial-induced apoptotic programs; however, the importance of Golgi localization and the way in which the inhibition occurs remains to be established [494].

1.5 VIRAL SUBVERSION OF THE MITOCHONDRIAL APOPTOTIC PATHWAY

Mitochondria play a central role in the execution and amplification of the apoptosis and, accordingly, many viruses have evolved strategies to interfere with mitochondrial machinery [495,496]. In order to prevent the release of apoptogenic molecules from mitochondria, poxviruses and many other large DNA viruses encode viral Bcl-2 (vBcl-2) homologues that function similarly to cellular anti-apoptotic proteins [495,496]. Importantly, vBcl-2 proteins display amino acid sequence similarity with cellular counterparts and each vBcl-2 contains, at the very least, a recognizable BH1 motif and often a domain responsible for mitochondrial localization [497,498].

1.5.1 Gammaherpesvirus Bcl-2 Proteins

All known gammaherpesviruses encode at least one Bcl-2 homologue; these include Kaposi's sarcoma-associated herpesvirus (KSHV) Bcl-2, Epstein-Barr virus (EBV) BHRF1 and BALF1, and murine gammaherpesvirus-68 (MHV-68) M11 [499,500,501,502,503]. KSHV Bcl-2, BHRF1, and BALF1 all contain conserved BH1 and BH2 domains, while M11 possesses a single BH1 domain [498]. In the case of KSHV Bcl-2, mutations within the conserved "NWGR" motif in the BH1 domain have structural and functional consequences, similar to cellular Bcl-2 [504]. Importantly, all gammaherpesviruses vBcl-2 proteins contain hydrophobic transmembrane domains at the C-terminus, which allow for mitochondrial targeting [498]. Many studies have focused on the inhibition of apoptosis by KSHV Bcl-2 and EBV BHRF1, which both prevent Bak and Bax activation [499,500,505,506]. However, the mechanism used by each vBcl-2 appears to differ. Although KSHV Bcl-2 binds Bak and Bax BH3 peptides in binding assays, interaction with full-length proteins has not been observed [500,504]. In contrast, EBV BHRF1 binds Bak but not Bax [505,506]. The way in which these proteins inhibit effector molecules without a direct interaction is likely due to binding of distinct BH3-only proteins [507]. KSHV Bcl-2 binds BH3 peptides from Bid, Bim, Noxa, Bik, Puma, and Bmf, while EBV BHRF1 interacts with Bim, Bid, and Puma BH3 domains [506,507]. Thus, subtle differences exist in the binding profiles of these proteins and it is apparent that targeting upstream BH3-only proteins may be an important anti-apoptotic strategy. The second vBcl-2 homologue in EBV, BALF1, interacts with Bak and Bax [502], yet BALF1 antagonizes the anti-apoptotic effects of BHRF1 and therefore may serve as an apoptotic inducer [508].

Remarkably, the homology between KSHV Bcl-2, BHRF1, M11, and cellular Bcl-2 proteins extends beyond the sequence level. KSHV Bcl-2, BHRF1, and M11 adopt Bcl-2-like structures that all contain hydrophobic binding grooves, and in the case of BHRF1, the protein structure has been solved in

complex with BH3 peptides from Bak and Bim [504,509,510,511]. The structures also reveal the absence of the flexible loop that is present in cellular Bcl-2 and Bcl-xL between α-helices 1 and 2 [236,237]. The absence of the flexible loop in vBcl-2 homologues renders the proteins resistant to caspase cleavage and inactivating phosphorylation, unlike their cellular counterparts [512]. Thus, vBcl-2 proteins adopt Bcl-2-like folds, yet have escaped the negative regulation that controls cellular anti-apoptotic proteins and are therefore more potent inhibitors of apoptosis.

1.5.2 Bcl-2 Homologues of African Swine Fever Virus and Adenovirus

In addition to gammaherpesviruses, both African swine fever virus (ASFV) and AdV encode vBcl-2 homologues with conserved sequence similarity to cellular counterparts [513,514]. The ASFV Bcl-2 homologue, A179L, contains conserved BH1 and BH2 domains and prevents apoptosis in ASFV-infected cells [513,515]. It has been reported that A179L inhibits apoptosis not only through interactions with Bak and Bax, but also a wide range of BH3-only proteins with the exception of Bid and Noxa [516]. AdV E1B-19K contains a BH1 domain and prevents apoptosis induced by AdV infection and in response to a variety of stimuli, such as TNFα and DNA damage [354,514,517,518,519]. E1B-19K interacts with both Bak and Bax and the BH3-only protein Bik [518,520,521]. Intriguingly, the interaction between E1B-19K and Bak occurs after Mcl-1 is displaced from Bak and degraded, as a consequence of the DNA damage response induced during AdV infection [354]. Although the structures of A179L and E1B-19K have not been solved, the sequence and functional homology to cellular anti-apoptotic proteins suggests that these proteins likely adopt Bcl-2-like folds [497,498]. Indeed, mutations within the BH1 domains of A179L and E1B-19K abrogate their anti-apoptotic activity [517,522]. In contrast to cellular Bcl-2 proteins and members of the gammaherpesvirus family though, A179L and perhaps E1B-19K lack defined transmembrane domains [497,498]. How exactly

these two proteins inhibit mitochondrial events without a characteristic mitochondrial targeting sequence requires further investigation.

1.5.3 Non-Homologous Viral Bcl-2 Proteins

Human cytomegalovirus (HCMV) and murine cytomegalovirus (MCMV) inhibit the mitochondrial apoptotic pathway, yet the sequences of these viruses do not reveal the presence of vBcl-2 homologues [495,496]. Instead, HCMV encodes a unique apoptotic inhibitor, viral mitochondria-localized inhibitor of apoptosis (vMIA), which localizes to mitochondrial and ER membranes by virtue of its N-terminal mitochondrial targeting sequence [523,524,525]. vMIA is a selective inhibitor of Bax, yet intriguingly, vMIA inhibits Bax after the translocation and oligomerization of Bax in the OMM [523,524]. The structure of vMIA has not been solved, although secondary sequence predictions and computational modeling indicate that vMIA likely folds like Bcl-xL [526]. Moreover, highly divergent BH domains have also been identified in this protein [526]. However, instead of interacting in a conventional manner with the BH3 region of Bax, vMIA is suspected to interact with a region between the BH2 and BH3 domains of Bax through electrostatic interactions [526]. The reason for this binding site and its significance await further clarification.

The apoptotic inhibitor in MCMV, m38.5, functions similarly to vMIA in that it specifically interacts with and inhibits Bax following the recruitment of Bax to mitochondria [527,528,529]. Although functionally similar, vMIA and m38.5 do not share significant amino acid similarity [527,528,529]. Curiously, both vMIA and m38.5 specifically inhibit Bax, but not Bak-induced death, raising the possibility of a Bak-specific inhibitor in HCMV and MCMV [523,524,527,528,529]. Indeed, a second inhibitor has been identified in MCMV, m41.1, which specifically interferes with Bak-induced apoptosis [530], although whether a functional orthologue of m41.1 exists in HCMV to complement the Bax-specific inhibition by vMIA remains unclear.

1.5.4 Poxviruses Encode Mitochondrial Inhibitors of Apoptosis

Due to the importance of mitochondria, poxviruses have also devised strategies to interfere with this organelle [63,444]. Based on sequence homology, only members of the *Avipoxvirus* genus, which includes fowlpox virus and canarypox virus, contain true vBcl-2 proteins [531,532]. Investigation into the anti-apoptotic mechanisms employed by the remaining poxviruses has therefore yielded novel inhibitors that lack sequence identity to cellular Bcl-2 proteins (Table 1.3) [495,496].

1.5.4.1 Fowlpox Virus FPV039

Fowlpox virus, a virus specific for poultry, contains the vBcl-2 homologue FPV039, which inhibits apoptosis in response to TNFα, staurosporine (STS), and VV infection [533]. Moreover, FPV039 interacts with Bak and activated Bax, as well as the BH3-only proteins BimL and Bik, further highlighting the diverse binding profiles of vBcl-2 proteins [533,534]. FPV039 inhibits the conformational activation of both Bak and Bax and potently prevents loss of Δψm [533,534]. In addition to a C-terminal transmembrane domain that is critical for mitochondrial localization and anti-apoptotic activity, FPV039 contains conserved BH1 and BH2 domains [533]. Although sequence analysis does not reveal the presence of a conserved BH3 motif, deletion of the predicted α-helix 2 in FPV039, which corresponds to the BH3 domain in cellular anti-apoptotic proteins, abrogates Bak binding [533]. Thus, FPV039 is a vBcl-2 homologue that shares sequence and functional homology with cellular anti-apoptotic proteins.

1.5.4.2 Myxoma Virus M11L

The discovery of novel apoptotic inhibitors within the poxvirus family was sparked by the discovery of myxoma virus M11L. The protein was identified as a mitochondrial inhibitor of apoptosis that is crucial for inhibiting myxoma virus-induced apoptosis [535]. M11L was initially found to interact with PBR, a component of the PTP, in order to prevent mitochondrial depolarization [536]. Subsequently, M11L has been shown to interact constitutively with Bak and inducibly with the conformationally active form of Bax following Bax

translocation to mitochondria [537,538]. Similar to FPV039, M11L also interacts with the BH3-only protein Bim but this interaction is highly specific and no interaction is observed between M11L and any other BH3-only proteins [539]. At the amino acid level, M11L lacks conserved regions found within members of the cellular Bcl-2 family and vBcl-2 proteins, so the way in which M11L interacts with members of the Bcl-2 family, such as Bak, Bax, and Bim, was originally unclear. The discovery of a divergent BH3-like domain in M11L offered a potential hint [538]. Remarkably, the structure of M11L revealed that although sequence motifs have not been strongly maintained, the overall fold of M11L closely resembles that of Bcl-xL [539,540]. The structure of M11L includes a hydrophobic binding groove that mediates binding to a BH3 peptide from Bak [539]. Although M11L lacks the conserved "NWGR" motif that characterizes the BH1 domain, it is believed to contain hydrophobic residues that are structurally and functionally equivalent [539,540]. Thus, M11L represents the first described non-vBcl-2 poxviral protein that lacks sequence identity but maintains structural and functional similarity with the Bcl-2 family of proteins.

1.5.4.3 Deerpox Virus DPV022 and Orf Virus ORFV125

Since the characterization of myxoma virus M11L, other non-vBcl-2 proteins have been identified within the poxvirus family. Deerpox virus, the sole member of the recently classified *Cervidpoxvirus* family, encodes a mitochondrial protein that shares limited amino acid similarity with M11L [541,542]. Indeed, DPV022 inhibits both Bak and Bax activation and, similar to M11L, interacts directly with Bak and Bax [541]. Unlike M11L, however, DPV022 interacts with the inactive form of Bax and the ability of DPV022 to interact with BH3-only proteins is a question that has not yet been addressed.

Members of the *Parapoxvirus* genus lack a true vBcl-2 protein or proteins that resemble M11L or DPV022. Instead, ORFV125 has recently been identified as an apoptotic inhibitor encoded by Orf virus [543]. ORFV125 localizes to mitochondria via a C-terminal transmembrane domain and inhibits cytochrome *c*

release and caspase activation following UV irradiation [543]. ORV125 inhibits Bak and Bax, but unlike FPV039 and M11L, ORFV125 does not interact with Bak [543,544]. Instead, ORFV125 interacts with the active form of Bax and a variety of BH3-only proteins [543,544]. Although ORFV125 lacks significant sequence homology with Bcl-2 family members, structural modeling predicts the 3D fold of ORFV125 resembles that of Bcl-w [544]. Thus, poxvirus families, with the exception of avipoxviruses, do not encode vBcl-2 proteins, but instead encode novel inhibitors, some of which have been identified and characterized as functional anti-apoptotic proteins. The above data indicate that interfering with cell death, particularly at the level of mitochondria, is a vital strategy during poxvirus infection.

1.5.4.4 Vaccinia Virus F1L

VV, the prototypic orthopoxvirus, prevents apoptotic events at mitochondria, yet the way in which the virus achieved this was previously unclear [545]. VV does not encode a true vBcl-2 homologue, nor does it contain an M11L-like protein [546]. This lead to the discovery of F1L, a unique inhibitor of the mitochondrial pathway, that is found exclusively in members of the *Orthopoxvirus* genus [547]. F1L is a 226 amino acid protein that contains a C-terminal transmembrane domain, comprised of residues 206-226 (Fig 1.22A) [547,548]. The transmembrane domain is responsible for the exclusive localization of F1L to the OMM, and moreover, mitochondrial localization is absolutely essential for the anti-apoptotic activity of the protein [547,548]. F1L potently prevents apoptosis in response to a variety of stimuli, such as FasL, TNFα, STS, UV irradiation, and VV infection itself [547,548,549,550]. The integral role of F1L in preventing apoptosis is highlighted by the fact that a VV devoid of F1L, VVΔF1L, induces apoptosis during infection and sensitizes infected cells to cell death induced by external stimuli, such as STS [550].

F1L inhibits cytochrome *c* release from mitochondria and blocks upstream events, including MOMP and the activation of both Bak and Bax (Fig

A
```
1                                                  50
MLSMFMCNNIVDYVDDIDNGIVQDIEDEASNNVDHDYVYPLPENMVYRFD

51                                                 100
KSTNILDYLSTERDHVMMAVRYYMSKQRLDDLYRQLPTKTRSYIDIINIY

101                                                150
CDKVSNDYNRDMNIMYDMASTKSFTVYDINNEVNTILMDNKGLGVRLATI

151                                                200
SFITELGRRCMNPVKTIKMFTLLSHTICDDCFVDYITDISPPDNTIPNTS

201                      226
TREYLKLIGITAIMFATYKTLKYMIG
```

B
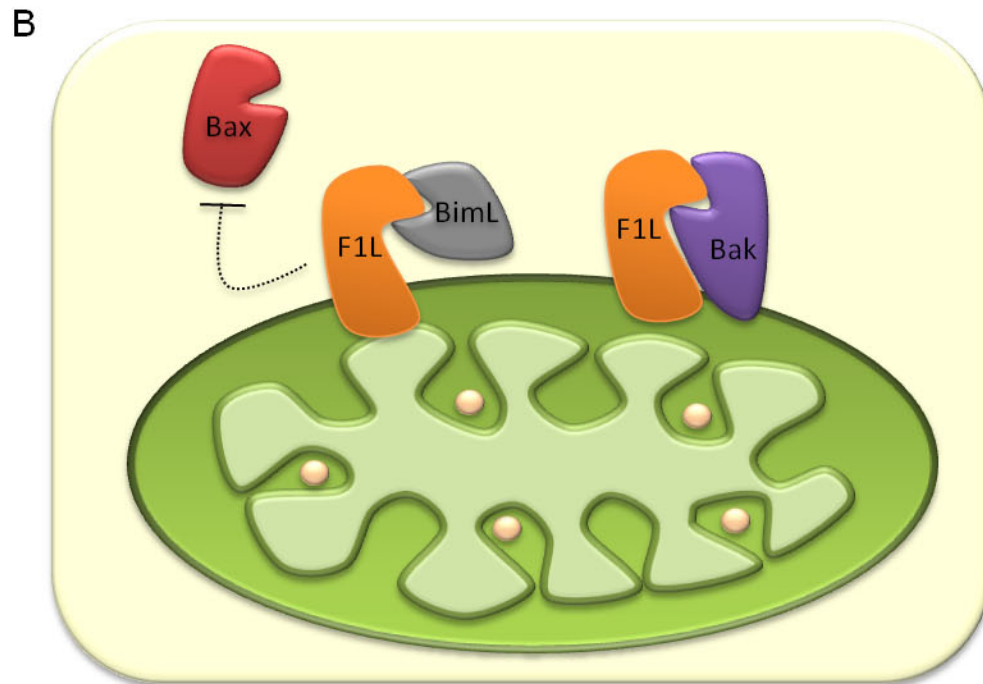
Figure 1.22 Vaccinia virus F1L is a unique inhibitor of mitochondrial-induced apoptosis. **A.** The amino acid sequence of F1L from vaccinia virus strain Copenhagen. F1L contains 226 amino acids but lacks obvious sequence homology to cellular and viral Bcl-2 proteins, with the exception of a C-terminal tail anchor. The 12 amino acid transmembrane domain, which is flanked by positively charged lysine residues, is highlighted. The 8 amino acid hydrophilic domain inserts into mitochondria. **B.** F1L localizes exclusively to mitochondria and interacts constitutively with Bak to prevent Bak N-terminal exposure and subsequent activation. F1L does not interact with Bax but prevents Bax activation, likely by constitutively binding the BH3-only protein BimL.

1.22B) [547,549,550]. Bak has been identified as a major binding partner of F1L and the constitutive interaction between F1L and Bak is observed in the presence and absence of VV infection [550,551]. In contrast, F1L inhibits Bax in the absence of a direct interaction [552]. Instead, F1L is believed to inhibit Bax by binding and inhibiting the upstream BH3-only protein BimL, a binding pattern distinct from previously reported poxviral apoptotic inhibitors (Fig 1.22B) [549]. In addition to associating with Bak and BimL, F1L has recently been deemed a caspase 9 inhibitor, a function attributed to the N-terminal 15 residues of F1L [553,554]. However, the physiological relevance of this interaction remains to be established since F1L inhibits Bak and Bax activation and thus potently inhibits the release of cytochrome *c*, a molecule required for activating caspase 9.

The way in which F1L binds Bak and BimL is uncertain, since besides possessing a C-terminal tail anchor, F1L does not display sequence homology with cellular or viral Bcl-2 proteins [547]. Although F1L and M11L do not share significant regions of amino acid similarity, both share limited regions of homology with DPV022, suggesting all three proteins are evolutionarily related [541]. Recently, the crystal structure of F1L from modified VV Ankara (MVA) was solved and revealed that despite limited sequence homology, F1L adopts a Bcl-2-like fold (Fig 1.23A) [555]. F1L forms a helical bundle characteristic of cellular multi-domain Bcl-2 family members, complete with a hydrophobic BH3 binding cleft (Fig 1.23B) [555]. However, three distinct differences are observed in the structure of F1L. First, F1L contains a novel α-helix in the N-terminus, α0, that is not present in Bcl-2 family members (Fig 1.23A). Second, F1L does not contain the regulatory flexible loop observed in the structures of Bcl-2 and Bcl-xL [236,237]. Lastly, unlike cellular family members, F1L adopts a domain-swapped dimer in which the second α-helix (α1) of one monomer forms the structure of a second monomer (Fig 1.23A) [555]. The significance of F1L dimer formation has yet to be determined and, additionally, the regions of F1L that interact with cellular Bcl-2 family members, such as Bak and BimL, await further validation.
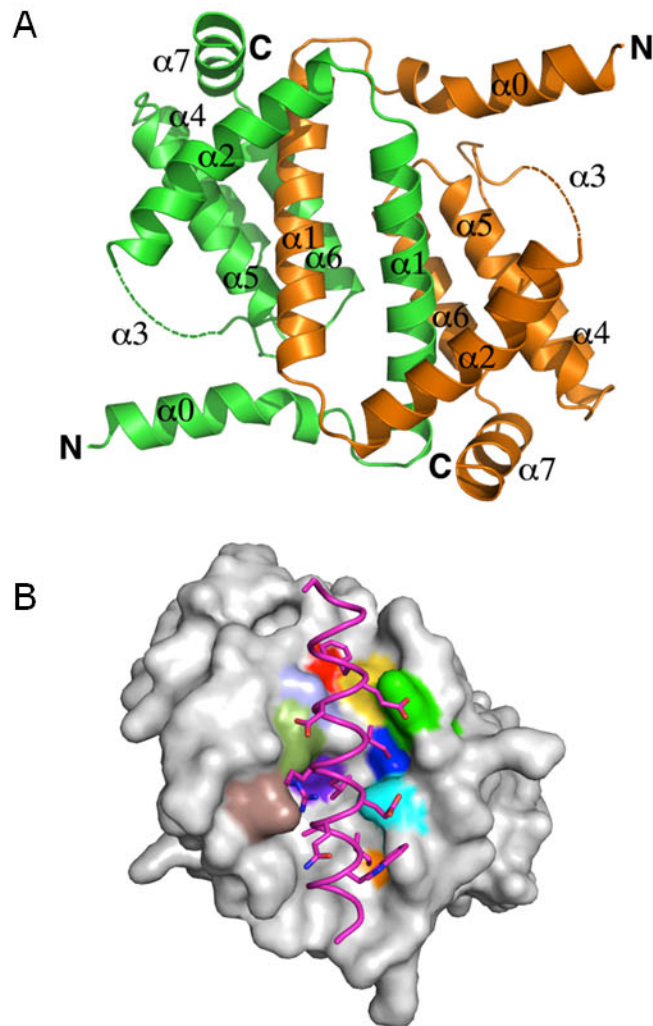
Figure 1.23 F1L adopts a Bcl-2 like fold. A. Ribbon diagram of F1L from modified vaccinia virus strain Ankara (MVA) adapted from [555]. F1L forms a helical bundle highly reminiscent of Bcl-2 family members. Unlike the Bcl-2 family, F1L forms a domain-swapped dimer; the second helix, α1, of one monomer is swapped into the structure of the second monomer. Not included in the structure is α3, which is highly disordered, and N-terminal residues 1-17 and C-terminal residues 187-222, which correspond to residues 1-22 and 201-226, respectively, from vaccinia virus strain Copenhagen F1L. **B.** Surface representation of MVA F1L bound to a BH3 peptide of Bak (magenta) [677]. F1L contains a hydrophobic binding groove on the surface of the molecule with residues of the binding groove highlighted in different colors and binds BH3 peptides in a manner similar to cellular anti-apoptotic proteins.

1.6 THESIS OBJECTIVES

Since Mcl-1 is not only a major regulator of Bak, but Bim as well, the role of F1L seemingly parallels that of Mcl-1. While Mcl-1 is a major target during AdV infection, during which it is degraded and replaced by the vBcl-2 E1B-19K [354], the fate of Mcl-1 during VV is unknown. Thus, our goal is to understand the role of Mcl-1 during infection with VV and further investigate the apparent similarities between F1L and Mcl-1, particularly regarding the inhibition of Bak. While F1L and Mcl-1 both function as major regulators of Bak and Bim, the way in which F1L binds cellular Bcl-2 family members is unclear. Thus, functional domains within F1L will be characterized to understand how F1L interacts with its cellular partners Bak and BimL, as F1L adopts a Bcl-2 like fold without containing characteristic BH motifs [555]. Following the structural and functional studies of F1L, the regulation of the protein will be assessed. Given the integral role of the UPS in controlling the levels and activity of cellular Bcl-2 family members [556,557,558,559], the potential regulation of F1L by the UPS will be assessed. Thesis objectives are summarized as follows:

1. Determine the role of the cellular regulator of Bak, Mcl-1, during VV infection.

2. Identify and characterize functional domains in the VV-encoded protein F1L.

3. Investigate the potential regulation of VV-encoded protein F1L by the cellular UPS.

CHAPTER 2: Materials and Methods

2.1 CELL LINES

All cell lines used in this study are listed in Table 2.1. HeLa, human embryonic kidney (HEK) 293T, chicken leghorn male hepatoma (LMH), buffalo green monkey kidney cells (BGMK), National Institute of Health 3T3 (NIH/3T3), African green monkey kidney (CV-1) and HuTK⁻-143B cells were obtained from the ATCC. BGMK cells were cultured in Dulbecco's modified Eagle's medium (DMEM) (Invitrogen) containing 10% newborn calf serum (Invitrogen), 2mM $_L$-glutamine (Invitrogen), 50units/mL penicillin (Invitrogen), and 50µg/mL streptomycin (Invitrogen). HeLa, HEK 293T, LMH, NIH/3T3, CV-1, and HuTK⁻-143B cells, as well as Bak-deficient baby mouse kidney (BMK) cells, generously provided by Dr. E. White (Rutgers University, Piscataway, NJ) [560], were cultured in DMEM (Invitrogen) containing 10% heat inactivated fetal bovine serum (HI-FBS) (Invitrogen), 2mM $_L$-glutamine (Invitrogen), 50units/mL penicillin (Invitrogen), and 50µg/mL streptomycin (Invitrogen). HuTK⁻-143B cell media was supplemented with 25µg/mL 5-bromo-2'-deoxyuridine (BrdU) (Sigma-Aldrich). Jurkat cells also obtained from ATCC were cultured in Rosewell Park Memorial Institute (RPMI) 1640 medium (Invitrogen) supplemented with 10% HI-FBS, 2mM $_L$-glutamine, 50units/mL penicillin, 50µg/mL streptomycin, and 100µM 2-mercaptoethanol (Bioshop). Jurkat cells overexpressing Bcl-2 were generated previously [200] and Bak- and Bax-deficient Jurkat cells were a gift from Dr. H. Rabinowich (University of Pittsburgh School of Medicine, Pittsburgh, PA) [561]. Dr. S. Korsmeyer kindly provided mouse embryonic fibroblasts (MEFs), which were cultured in DMEM containing 10% HI-FBS, 2mM $_L$-glutamine, 50units/mL penicillin, 50µg/mL streptomycin, and 100µM minimal essential medium non-essential amino acids (Invitrogen) [190]. All cells were maintained at 37°C in the presence of 5% carbon dioxide (CO_2).

2.2 DNA METHODOLOGY

2.2.1 Polymerase Chain Reaction

Table 2.1 Cell Lines Used in This Study.

Cell Line	Cell Type	Characteristics	Source
BGMK	Buffalo green monkey kidney cell		ATCC
BMK (Bak-/-)	Baby mouse kidney cell	Deficient in Bak	[560]
CV-1	Monkey kidney fibroblast		ATCC
HEK 293T	Human embryonic kidney cell		ATCC
HeLa	Human fibroblast		ATCC
Jurkat	Immortalized human T lymphocyte		ATCC
Jurkat (Bax-/-Bak-/-)	Immortalized human T lymphocyte	Bak- and Bax-deficient	[561]
Jurkat Bcl-2	Immortalized human T lymphocyte	Overexpress Bcl-2	[200]
LMH	Chicken hepatocellular carcinoma epithelial cell		ATCC
MEF	Mouse embryonic fibroblast		[190]
NIH/3T3	Mouse embryonic fibroblast		ATCC
TK⁻ -143B	Human 143B osterosarcoma cell	Deficient in thymidine kinase	ATCC

Polymerase Chain Reactions (PCR) were carried out in 50μL volumes containing 100mM Tris-HCl (pH 8.85), 250mM KCl, 50mM $(NH_4)_2SO_4$, 20mM $MgSO_4$, 1pmole of each primer, 10mM deoxyribonucleotide triphosphates (dNTPs) (Invitrogen), and 2.5U *Taq* DNA polymerase (Invitrogen) or Pwo DNA polymerase (Roche Diagnostics). Each reaction contained 10ng of plasmid DNA or 100ng of viral DNA. All primers used in this study are listed in Table 2.2. Reactions were performed using a Techgene thermal cycler (Techne) using the following parameters: 2 minute initial denaturation at 95°C followed by 30 cycles of melting at 95°C (30 seconds), primer annealing at 55°C (30 seconds) and primer extension at 72°C for 1 minute/kb. Alternatively, PCR was performed in 50μL volumes of 60mM Tris-SO_4 (pH 9.0 @ 25°C), 20mM $(NH_4)_2SO_4$, 2mM $MgSO_4$, 3% glycerol, 0.06% Nonidet P-40 (NP-40), and 0.05% Tween-20, 1pmole of each primer, 10mM dNTPs (Invitrogen), 10ng of plasmid DNA, and 2.5U LongAmp *Taq* DNA polymerase (New England Biolabs). Reactions were performed as described above except primer extension was carried out at 65°C.

2.2.2 Agarose Gel Electrophoresis and Gel Extraction

PCR products and restriction endonuclease digested products were purified by agarose gel electrophoresis and gel extraction. 1% weight/volume (w/v) agarose gels were prepared with agarose (Invitrogen) in 1x TAE buffer containing 40mM Tris-acetate and 1mM EDTA. DNA was prepared in sample loading dye containing 5% glycerol (Fisher Scientific), 0.04% w/v bromophenol blue (BioRad), 0.04% w/v xylene cyanol (Sigma-Aldrich), 10mM EDTA (pH 7.5), and gels were electrophoresed at 100V in 1X TAE buffer. Gels were stained with 10μg/mL ethidum bromide (Sigma-Aldrich) for 10 minutes at room temperature. Agarose gels were visualized using ImageQuant 300 and ImageQuant 300 Capture software (GE Healthcare) and bands were excised.

Excised DNA was purified using a QIAquick Gel Extraction Kit (Qiagen) using the manufacturer's protocol. In brief, the DNA-containing agarose gel was resuspended in 3 volumes of solubilization buffer and incubated at 50°C for 10

Table 2.2 Oligonucleotides Used in This Study.

Primer Name	Primer Sequence (5' to 3')	Rest. Site	Description	Source
FLAG-Bak *Hin*dIII FOR	AAGCTTATG**GACTACAA AGACGATGACGACAAG** ATGGCTTCGGGGCAAGG C	*Hin*dIII	Used to generate FLAG-BakΔBH3 in pcDNA3	IDT
Bak O/L REV (aa71)	TGAGTCATAGCGCATGG TGCTGC TAGGTTGCAG	N/A	Used to generate FLAG-BakΔBH3 in pcDNA3	IDT
Bak FOR (aa88)	CGCTATGACTCA GAGTTCCAG	N/A	Used to generate FLAG-BakΔBH3 in pcDNA3	IDT
Bak *Eco*RI REV	GAATTCTCATGATTTGAA GAATCTTCG	*Eco*RI	Used to generate FLAG-BakΔBH3 in pcDNA3	IDT
EVM004 *Eco*RI FOR	GAATTCTCATGAGTGAT TACTATTTT	*Eco*RI	Used to clone EVM004 into pEGFP-C3	Qiagen
EVM004 *Bam*HI REV	GGATCCTTAATAATACCT AGAAAATAT	*Bam*HI	Used to clone EVM004 into pEGFP-C3 and pSC66	Qiagen
EGFP-EVM004 *Sal*I FOR	GTCGACATGGTGAGCAA GGGCGAGGAGCTG	*Sal*I	Used to clone EGFP-EVM004 into pSC66 (specific for EGFP)	Qiagen
FIL *Eco*RI FOR	GAATTCTCATGTTGTCG ATGTTTATG	*Eco*RI	Used for PCR to clone F1LΔBH1 and F1LΔBH3 into pEGFP-C3	Qiagen
F1L *Bam*HI REV	GGATCCTTATCCTATCAT GTATTTG	*Bam*HI	Used for PCR to clone F1L(84-226), F1L(109-226), F1LΔBH1, and F1LΔBH3 into pEGFP-C3	Qiagen
F1L(84) *Eco*RI FOR	GAATTCTCAGACAGTTG CCCACAAAGAC	*Eco*RI	Used to clone F1L(84-226) into pEGFP-C3	Qiagen
F1L(109) *Eco*RI FOR	GAATTCTCAATAGGGAC ATGAATATCAT	*Eco*RI	Used to clone F1L(109-226) into pEGFP-C3	IDT
F1LΔBH3 FOR (aa109)	AATAGGGACATGAATAT CAT	N/A	Internal primer-BH3	Qiagen
F1LΔBH3 O/L REV (aa92)	CATGTCCCTATTTGATCT AGTCTTTGTGGGCA	N/A	Internal primer-BH3	Qiagen
F1LΔBH1 FOR (aa157)	GGTAGACGATGTATGAA TCC	N/A	Internal primer-BH1	Qiagen
F1LΔBH1 O/L REV (aa143)	ACATCGTCTACCCAACCC CTTGTTATCCATTA	N/A	Internal primer-BH1	Qiagen

Table 2.2 Continued.

WT FLAG-F1L *Sal*I FOR	<u>GTCGAC</u>ATG**GACTACAA AGACGATGACGACAAG** TTGTCGATGTTTATGTGT	*Sal*I	Used to clone FLAG-F1LΔBH1 into pSC66	IDT
FLAG-F1L(84) *Sal*I FOR	<u>GTCGAC</u>ATG**GACTACAA AGACGATGACGACAAG** AGACAGTTGCCCACAAA GACT	*Sal*I	Used to clone FLAG-F1L(84-226) into pSC66	IDT
FLAG-F1L(109) *Sal*I FOR	<u>GTCGAC</u>ATG**GACTACAA AGACGATGACGACAAG** AATAGGGACATGAATAT C	*Sal*I	Used to clone FLAG-F1L(109-226) into pSC66	IDT
F1L *Not*I REV	<u>GCGGCC</u>GCTTATCCTAT CATGTATTTGAGAGT	*Not*I	Used to clone FLAG-F1L(84-226), (109-226), and ΔBH1 into pSC66	IDT
F1L(V104A) FOR	CAACATATATTGTGATA AAGCAAGTAATGATTAT AATAGGG	N/A	Used for site directed mutagenesis	IDT
F1L(V104A) REV	CCCTATTATAATCATTAC TTGCTTTATCACAATATA TGTTG	N/A	Used for site directed mutagenesis	IDT
F1L(G144F) FOR	GGATAACAAGGGGTTGT TTGTAAGATTGGCG	N/A	Used for site directed mutagenesis	IDT
F1L(G144F) REV	CGCCAATCTTACAAACA ACCCCTTGTTATCC	N/A	Used for site directed mutagenesis	IDT
F1L(F152A) FOR	GGCGACAATTTCAGCTA TAACCGAATTGGG	N/A	Used for site directed mutagenesis	IDT
F1L(F152A) REV	CCCAATTCGGTTATAGCT GAAATTGTCGCC	N/A	Used for site directed mutagenesis	IDT
F1L(A119W) FOR	GACATGAATATCATGTA TGATATGTGGTCTACAA AATCATTTAC	N/A	Used for site directed mutagenesis	IDT
F1L(A119W) REV	GTAAATGATTTTGTAGA CCACATATCATACATGAT ATTCATGTC	N/A	Used for site directed mutagenesis	IDT
F1L(V145F) FOR	GGATAACAAGGGGTTG GGTTTCAGATTGGCGAC	N/A	Used for site directed mutagenesis	IDT
F1L(V145F) REV	GTCGCCAATCTGAAACC CAACCCCTTGTTATCC	N/A	Used for site directed mutagenesis	IDT
F1L(Y108E) FOR	GTGATAAAGTTAGTAAT GATGAGAATAGGGACAT GAATATCATG	N/A	Used for site directed mutagenesis	IDT
F1L(Y108E) REV	CATGATATTCATGTCCCT ATTCTCATCATTACTAAC TTTATCAC	N/A	Used for site directed mutagenesis	IDT

Table 2.2 Continued.

F1L(M115W) FOR	GGGACATGAATATCTGG TATGATATGGCATC	N/A	Used for site directed mutagenesis	IDT
F1L(M115W) REV	GATGCCATATCATACCA GATATTCATGTCCC	N/A	Used for site directed mutagenesis	IDT
F1L(L147F) FOR	GGGGTTGGGTGTAAGA TTTGCGACAATTTCATTT ATAACC	N/A	Used for site directed mutagenesis	IDT
F1L(L147F) REV	GGTTATAAATGAAATTG TCGCAAATCTTACACCCA ACCCC	N/A	Used for site directed mutagenesis	IDT
F1L(T149L) FOR	GGGTGTAAGATTGGCGC TCATTTCATTTATAACCG	N/A	Used for site directed mutagenesis	IDT
F1L(T149L) REV	CGGTTATAAATGAAATG AGCGCCAATCTTACACC C	N/A	Used for site directed mutagenesis	IDT
F1L(M112W) FOR	GATTATAATAGGGACTG GAATATCATGTATGATA TGGC	N/A	Used for site directed mutagenesis	IDT
F1L(M112W) REV	GCCATATCATACATGAT ATTCCAGTCCCTATTATA ATC	N/A	Used for site directed mutagenesis	IDT
F1L(I136F) FOR	CGAAGTTAATACTTTCCT AATGGATAACAAGGGG	N/A	Used for site directed mutagenesis	IDT
F1L(I136F) REV	CCCCTTGTTATCCATTAG GAAAGTATTAACTTCG	N/A	Used for site directed mutagenesis	IDT
F1L(F124W) FOR	GGCATCTACAAAATCAT GGACAGTTTATGACATA AATAACG	N/A	Used for site directed mutagenesis	IDT
F1L(F124W) REV	CGTTATTTATGTCATAAA CTGTCCATGATTTTGTAG ATGCC	N/A	Used for site directed mutagenesis	IDT
F1L(M118R) FOR	GACATGAATATCATGTA TGATAGGGCATCTACAA AATC	N/A	Used for site directed mutagenesis	IDT
F1L(M118R) REV	GATTTTGTAGATGCCCT ATCATACATGATATTCAT GTC	N/A	Used for site directed mutagenesis	IDT
F1L(N140F) FOR	CTATACTAATGGATTTCA AGGGGTTGGGTG	N/A	Used for site directed mutagenesis	IDT
F1L(N140F) REV	CACCCAACCCCTTGAAAT CCATTAGTATAG	N/A	Used for site directed mutagenesis	IDT
F1L(I129F) FOR	CAGTTTATGACTTCAATA ACGAAGTTAATACTATA CTAATGG	N/A	Used for site directed mutagenesis	IDT

Table 2.2 Continued.

F1L(I129F) REV	CCATTAGTATAGTATTAA CTTCGTTATTGAAGTCAT AAACTG	N/A	Used for site directed mutagenesis	IDT
F1L(K122R) FOR	GGCATCTACAAGGTCAT TTACAGTTTATG	N/A	Used for site directed mutagenesis	IDT
F1L(K122R) REV	CATAAACTGTAAATGAC CTTGTAGATGCC	N/A	Used for site directed mutagenesis	IDT
F1L(K165R/K 168R) FOR	CGATGTATGAATCCAGT ACGAACTATACGAATGT TTACTCTACTATCGC	N/A	Used for site directed mutagenesis	IDT
F1L(K165R/K 168R) REV	GCGATAGTAGAGTAAAC ATTCGTATAGTTCGTACT GGATTCATACATCG	N/A	Used for site directed mutagenesis	IDT
F1L(K103R) FOR	GATATTATCAACATATAT TGTGATCGAGTTAGTAA TGATTATAATAGGG	N/A	Used for site directed mutagenesis	IDT
F1L(K103R) REV	CCCTATTATAATCATTAC TAACTCGATCACAATATA TGTTGATAATATC	N/A	Used for site directed mutagenesis	IDT
F1L(K89R) FOR	GTATAGACAGTTGCCCA CACGGACTAGATCATAT ATAG	N/A	Used for site directed mutagenesis	IDT
F1L(K89R) REV	CTATATATGATCTAGTCC GTGTGGGCAACTGTCTA TAC	N/A	Used for site directed mutagenesis	IDT
F1L(K141R) FOR	CTAATGGATAACAGGGG GTTGGGTGTAAGATTGG CG	N/A	Used for site directed mutagenesis	IDT
F1L(K141) REV	CGCCAATCTTACACCCAA CCCCCTGTTATCCATTAG	N/A	Used for site directed mutagenesis	IDT
F1L(K51R) FOR	GGTATATAGATTTGACA GGTCCACTAACATACTC G	N/A	Used for site directed mutagenesis	IDT
F1L(K51R) REV	CGAGTATGTTAGTGGAC CTGTCAAATCTATATACC	N/A	Used for site directed mutagenesis	IDT
F1L(K76R) FOR	GGCTGTTCGATACTATA TGAGTAGGCAACGTTTA GACGAC	N/A	Used for site directed mutagenesis	IDT
F1L(K76R) REV	GTCGTCTAAACGTTGCC TACTCATATAGTATCGAA CAGCC	N/A	Used for site directed mutagenesis	IDT
F1L(K206R) FOR	CGCGTGAATATCTAAGG CTTATTGGCATC	N/A	Used for site directed mutagenesis	IDT
F1L(K206R) REV	GATGCCAATAAGCCTTA GATATTCACGCG	N/A	Used for site directed mutagenesis	IDT

Table 2.2 Continued.

pEGFP FOR	CATGGTCCTGCTGGAGTTCG	N/A	Used to sequence constructs in pEGFP	IDT
pEGFP REV	GCAAGTAAAACCTCTACAAATGTGG	N/A	Used to sequence constructs in pEGFP	IDT
Mcl-1 *Sal*I FOR	<u>GTCGAC</u>ATG**GACTACAAAGACGATGACGATAAA**	*Sal*I	Used to clone Mcl-1 into pSC66; specific to the FLAG tag in pcDNA-FLAG-Mcl-1	IDT
Mcl-1 *Nhe*I REV	<u>GCTAGC</u>CTATCTTATTAGATATGCCAA	*Nhe*I	Designed to clone Mcl-1 into pSC66 but not used	IDT
Mcl-1 *Eco*RI FOR	<u>GAATTC</u>TCATGTTTGGCCTCAAAAGA	*Eco*RI	Used to clone Mcl-1 into EGFP	IDT
Mcl-1 *Bam*HI REV	<u>GGATCC</u>CTATCTTATTAGATATGCCAA	*Bam*HI	Used to clone Mcl-1 into pSC66 and pEGFP	IDT
FLAG-Mcl-1 *Hind*III FOR	<u>AAGCTT</u>ATG**GACTACAAAGACGATGACGACAAG**TTTGGCCTCAAAAGAAAC	*Hind*III	Used to clone FLAG-Mcl-1 into pcDNA3	IDT
Mcl-1 *Eco*RI REV	<u>GAATTC</u>CTATCTTATTAGATATGCCAA	*Eco*RI	Used to clone FLAG-Mcl-1 into pcDNA3	IDT
pSC66(+70) *Sma*I FOR	CGTGATAGGTATCGATGAAGGACAG	N/A	Used to sequence constructs in pSC66	Qiagen
pSC66(-100) *Sma*I REV	GGGTGGGTTTGGAATTAGTGAAAGC	N/A	Used to sequence constructs in pSC66	Qiagen

Restriction cut sites are underlined, FLAG sequences are bolded, Rest – Restriction, FOR – forward primer, REV – reverse primer, IDT – Integrated DNA Technologies, N/A – not available

minutes. The solubilized gel was then passed over a QIAquick DNA column, washed in ethanol, and DNA bound to the column was eluted in 30μL of 10mM Tris (pH 8.0) by centrifugation at 17,000xg for 1 minute. Agarose gel electrophoresis was used to assess purity of the extracted DNA.

2.2.3 DNA Ligations

For ligations into pGEM-T, the blunt ends of gel extracted PCR products amplified with Pwo DNA polymerase (Roche Diagnostics) were first modified using an A-addition kit (QIAGEN). The modified DNA was T-A ligated into pGEM-T Vector System (Promega) according to manufacturer's instructions. In brief, reactions consisted of 2μL of gel extracted PCR product, 50ng of pGEM-T, 3U T4 DNA ligase, and 5μL of 2X rapid ligation buffer containing 60mM Tris-HCl (pH 7.8), 20mM MgCl$_2$, 20mM DTT, 2mM ATP, and 10% polyethylene glycol. PCR products generated with *Taq* DNA polymerase (Invitrogen) and LongAmp *Taq* DNA polymerase (New England Biolabs) did not require modifications and were ligated directly into pGEM-T. Ligations into pEGFP-C3, pcDNA3, and pSC66 were carried out using 400U T4 ligase (New England Biolabs) with insert to vector ratios of 3:1 or 6:1 in 10μL or 20μL volumes. All ligation reactions were incubated overnight at 4°C prior to bacterial transformation.

2.2.4 Competent Cells and Bacterial Transformation

Chemically competent *Escherichia coli* (*E. coli*) DH5α were prepared as described [562]. Ligations were transformed into DH5α *E. coli* or Mach1 T1 Phage-Resistant Chemically Competent *E. coli* (Invitrogen) by heat shock transformation. Competent DH5α or Mach1 *E. coli* cells were incubated with plasmid DNA on ice for 30 minutes and then placed at 42°C for 1 minute followed by a 2 minute recovery on ice. Transformed bacteria were recovered in 250μL of SOC media containing 20mg/mL tryptone, 5mg/mL yeast extract, 0.5mg/mL NaCl, 2.5mM KCl (pH 7.0) at 37°C for 1 hour before plating on Luria-Bertani (LB) broth agar plates containing 100μg/mL ampicillin (Sigma-Aldrich) or 30μg/mL kanamycin (Sigma-Aldrich). For blue-white screening of pGEM-T-

containing clones, LB-agar plates containing ampicillin were supplemented with 80µg/mL 5-bromo-4-chloro-3-indolyl-β-D-galactopyranoside (X-gal) (Rose Scientific) and 0.5mM isopropyl β-D-1-thiogalactopyranoside (IPTG) (Rose Scientific).

2.2.5 Plasmid DNA Isolation

Plasmid DNA used for cloning was isolated from 5mL overnight cultures of LB broth containing 100µg/mL ampicillin or 60µg/mL kanamycin using alkaline hydrolysis [562]. Briefly, 1.5mL of bacteria were pelleted and resuspended in 100µL of resuspension buffer containing 50mM glucose, 25mM Tris (pH 8.0), and 10mM EDTA. Bacteria were lysed in 200µL of lysis buffer containing 1% sodium docecyl sulphate (SDS) (Fisher Scientific) and 200mM NaOH for five minutes at room temperature. Membranes and proteins were precipitated on ice for five minutes by adding neutralization buffer containing 3M potassium acetate and 11.5% glacial acetic acid. Precipitates were centrifuged at 18,000xg for 15 minutes and supernatants were extracted with phenol:chloroform (1:1). The aqueous phase was again extracted with an equal volume of choloroform and DNA was precipitated with the addition of 2.5 volumes of 95% ethanol at -20°C for 20 minutes. DNA was pelleted by centrifugation at 18,000xg at 4°C and pellets were resuspended in double distilled (dd) H$_2$0.

High-purity plasmid DNA used for sequencing and transfections was prepared by inoculating 400mL of LB broth containing 100µg/mL of ampicillin or 60µg/mL of kanamycin with *E. coli* DH5α cells containing the plasmid of interest. Bacteria were grown overnight at 37°C. For low copy plasmids, such as pSC66, logarithmic phase cultures were treated with 170µg/mL of chloramphenical (Sigma-Aldrich) for 18 hours. Plasmid DNA was isolated using a Plasmid Maxi kit (Qiagen) according to manufacturer's instructions. DNA yields were determined by optical density at 280nm using a spectrophotometer (Eppendorf) and purity was assessed by agarose gel electrophoresis.

2.2.6 Restriction Endonuclease Digestion

All restriction endonucleases and reaction buffers were purchased from Invitrogen or New England Biolabs. Digest reactions were performed in 10μL volumes and were supplemented with 10μg RNAse (Sigma-Aldrich). Reactions were carried out at 37°C for 1 hour using plasmid DNA isolated from alkaline hydrolysis or plasmid maxi kits (section 2.2.5).

2.2.7 Site-Directed Mutagenesis

Polymerase chain reaction was used to generate point mutations in pSC66-FLAG-F1L or pEGFP-F1L using QuikChange II Site-Directed Mutagenesis Kit (Stratagene) as per manufacturer's instructions. Each reaction contained 10x reaction buffer, 2.5U *PfuUltra* high fidelity DNA polymerase, 10ng of template DNA, 1pmole of each primer, and 10mM dNTPs. Thermal cycling parameters were as follows: initial denaturation for 30 seconds at 95°C followed by 18 cycles of denaturation (30 seconds at 95°C), primer annealing (1 minute at 55°C), and extension (8 minutes at 68°C for pSC66-F1L or 6 minutes at 68°C for pEGFP-F1L). PCR products were subsequently treated with 10U/μL of the restriction endonuclease *Dpn*I for 1 hour at 37°C to selectively digest parental methylated and hemimethylated DNA. Newly synthesized mutant-containing DNA was transformed into *E. coli* XL1-Blue supercompetent cells (Stratagene) by heat pulsing the reactions for 45 seconds at 42°C followed by a 2 minute recovery on ice. Transformation reactions were recovered in NZY+ broth (pH 7.5) containing 10mg/mL NZ amine (casein hydrolysate), 5mg/mL yeast extract, 5mg/mL NaCl, 12.5mM MgCl$_2$, 12.5mM MgSO$_4$, and 20mM glucose for 1 hour at 37°C. Reactions containing pSC66-FLAG-F1L were plated on LB-ampicillin agar plates, while reactions containing pEGFP-F1L were plated on LB-kanamycin agar plates and incubated overnight at 37°C. Following plasmid DNA isolation, positive clones were identified by PCR using the pSC66(+70) *Sma*I forward primer and the pSC66(-100) *Sma*I reverse primer for mutations made in pSC66-FLAG-F1L or pEGFP forward and reverse primers for mutations made in pEGFP-F1L (Table 2.2).

2.2.8 DNA Sequencing and Computer Analysis

Plasmid DNA isolated from Plasmid Maxi kits and isolated viral DNA were sequenced to ensure fidelity. Sequencing reactions were performed by The Molecular Biology Services Unit (Department of Biological Sciences, University of Alberta), or The Applied Genomics Centre (University of Alberta). Primers used for sequencing were the T7 primer, SP6 primer, pSC66(+70) *Sma*I forward primer, pSC66(-100) *Sma*I reverse primer, and pEGFP forward and reverse primers (Table 2.2). Sequencing reactions were analyzed by FinchTV (Geospiza) and basic local alignment search tool (BLAST) programs offered by the National Center for Biotechnology Information [563].

2.3 CLONING

2.3.1 Plasmids

All plasmid DNA was stored at -20°C. pGEM-T (Promega) was used for all T-A cloning reactions and pEGFP-C3 (Clontech) was the vector used for generating N-terminal EGFP fusion proteins. pSC66, which contains a synthetic poxviral early/late promoter [564], was provided by Dr. E. Long (National Institute of Allergy and Infectious Diseases, Bethesda, MB) [565] and pcDNA3 was supplied by Invitrogen. pEGFP-F1L, pEGFP-F1L(206-226), pEGFP-Bcl-xL, pSC66-EGFP-F1L, pSC66-EGFP-F1L/B6R, pSC66-EGFP-F1L(1-206), psC66-EGFP-F1L(206-226), and pSC66-FLAG-F1L were generated previously [534,547,548,550]. pcDNA3-FLAG-Bak was a gift from Dr. G. Shore (McGill University, Montreal, QC) [283], while pEGFP-p28 was generated in our lab using p28 from VV strain International Health Department (IHDW) that had been codon optimized by GeneArt [566]. FLAG-p28 was amplified from codon optimized p28 and subcloned into pEGFP-C1 to create pEGFP-p28 containing a FLAG sequence linking EGFP and p28. HA-Ubiquitin-K48 was generated in our lab [566] by subcloning HA-Ubiquitin-K48 from pEF-HA-Ubiquitin-K48 (a gift from Z. Chen, Southwestern Medical Center, Dallas, TX) into pBluescript II (Stratagene) and pcDNA3-HA-ubiquitin was supplied by Dr. J. Hiscott (McGill University, Montreal, QC). pCR3.1-Mcl-1 was

provided by Dr. H. Rabinowich (University of Pittsburgh School of Medicine, Pittsburgh, PA) [567] and pcDNA3-HA-Bak was provided by Dr. Grant McFadden (University of Florida, Gainesville, FL) [538]. Wildtype pcDNA-Bak and the Bak point mutants pcDNA-BakmtBH1 (W125A, G126E, R127A), pcDNA-BakmtBH2 (G175E, G176E, W177A), and pcDNA-BakmtBH3 (L78A, D83A), were a kind gift from Dr. D. George (University of Pennsylvania School of Medicine, Philadelphia, PA) [289]. All other vectors were constructed in sections 2.3.2-2.3.7. All vectors used in this study are represented in Table 2.3.

2.3.2 Generation of pSC66-FLAG-Mcl-1. FLAG-Mcl-1 was amplified from pcDNA3-FLAG-Mcl-1 (provided by Dr. Gordon Shore, McGill University, Montreal, QC) [437] using the Mcl-1 *Sal*I forward primer and the Mcl-1 *Bam*HI reverse primer. The PCR product was ligated into pGEM-T (Promega) and FLAG-Mcl-1 was then subcloned into pSC66 as a *Sal*I fragment, which placed the gene under the control of a poxviral early/promoter [564].

2.3.3 Generation of F1L BH Domain Mutants. F1L(84-226) and F1L(109-226) were generated from the pEGFP-F1L template using the F1L(84) *Eco*RI forward primer and the F1L(109) *Eco*RI forward primer, respectively, and the F1L *Bam*HI reverse primer. Residues 144-156 of F1L were deleted to generate F1LΔBH1 with overlapping PCR using the F1L *Eco*RI forward primer and the internal F1LΔBH1 O/L reverse primer (aa143) to generate the N-terminal fragment. The internal F1LΔBH1 O/L forward primer (aa157) and F1L *Bam*HI reverse primer were used to generate the C-terminal fragment. The resulting PCR fragments were amplified together using the F1L *Eco*RI forward and F1L *Bam*HI reverse primers. F1LΔBH3 lacking residues 93-108 was generated in a similar manner to F1LΔBH1, with the exception of the internal F1LΔBH3 O/L reverse primer (aa92) and the internal F1LΔBH3 forward primer (aa109). F1L(84-226), F1L(109-226), F1LΔBH1, and F1LΔBH3 PCR products were T-A cloned into pGEM-T (Promega) and subcloned into pEGFP-C3 (Clontech) as *Eco*RI/*Bam*HI fragments. These mutants are illustrated in Figure 2.1.

Table 2.3 Vectors Used in This Study.

Plasmid	Characteristics	Source
pGEM-T	TA cloning vector; CMV promoter	Promega
pcDNA3	CMV and T7 promoter	Invitrogen
pcDNA3.1-Bak	Untagged wildtype Bak	[289]
pcDNA3.1-BakmtBH1	3 mutations in BH1 domain: W125A, G126E, R127A	[289]
pcDNA3.1-BakmtBH2	3 mutations in BH2 domain: G175E, G176E, W177A	[289]
pcDNA3.1-BakmtBH3	2 mutation in BH3 domain: L78A, D83A	[289]
pcDNA-FLAG-Bak	FLAG-tagged wildtype Bak	[283]
pcDNA-FLAG-BakΔBH3	FLAG-tagged Bak lacking BH3 domain (72-87)	This study
pcDNA-HA-Bak	HA-tagged wildtype Bak	[538]
pEGFP-C3	Empty EGFP vector with CMV promoter	Clontech
pEGFP-Bcl-xL	Human Bcl-xL	[534]
pEGFP-F1L	Wildtype F1L from VV(Cop)	[547]
pEGFP-F1L(206-226)	F1L-tail lacking the first 205 amino acids	[548]
pEGFP-F1L(109-226)	F1L lacking the first 108 amino acids	This study
pEGFP-F1L(84-226)	F1L lacking the first 83 amino acids	This study
pEGFP-F1LΔBH1	F1L lacking the putative BH1 domain (144-156)	This study
pEGFP-F1LΔBH3	F1L lacking the putative BH3 domain (93-108)	This study
pEGFP-F1L(V104A)	F1L with V104A mutation	This study
pEGFP-F1L(G144F)	F1L with G144F mutation	This study
pEGFP-F1L(F152A)	F1L with F152A mutation	This study
pEGFP-F1L(A119W)	F1L with A119W mutation	This study
pEGFP-F1L(V145F)	F1L with V145F mutation	This study
pEGFP-F1L(L147F)	F1L with L147Fmutation	This study
pEGFP-F1L(T149L)	F1L with T149L mutation	This study
pEGFP-F1L(M112W)	F1L with M112Wmutation	This study
pEGFP-F1L(M115W)	F1L with M115W mutation	This study
pEGFP-F1L(M118R)	F1L with M118R mutation	This study
pEGFP-F1L(I129F)	F1L with I129F mutation	This study
pEGFP-F1L(Y108E)	F1L with Y108E mutation	This study
pEGFP-F1L(F124W)	F1L with F124W mutation	This study
pEGFP-F1L(I136F)	F1L with I136F mutation	This study
pEGFP-F1L(N140F)	F1L with N140F mutation	This study
pEGFP-F1L(3K-R)	F1L with 3 mutations: K122R/K165R/K168R	This study

Table 2.3 Continued.

pEGFP-F1L(4K-R)	F1L with 4 mutations: K122R/K165R/K168R /K103R	This study
pEGFP-F1L(5K-R)	F1L with 5 mutations: K122R/K165R/K168R /K103R/K89R	This study
pEGFP-F1L(6K-R)	F1L with 6 mutations: K122R/K165R/K168R /K103R/K89R/K51R	This study
pEGFP-F1L(7K-R)	F1L with 7 mutations: K122R/K165R/K168R /K103R/K89R/K51R/K76R	This study
pEGFP-F1L(8K-R)	F1L with 8 mutations: K122R/K165R/K168R /K103R/K89R/K51R/K76R/K141R	This study
pEGFP-F1L(9K-R)	F1L with 9 mutations: K122R/K165R/K168R /K103R/K89R/K51R/K76R/K141R/K206R	This study
pSC66	Empty vector; contains *lacZ*; multi-cloning site flanked by TK regions	E.Long [564]
pSC66-EGFP-F1L	EGFP-tagged F1L from VV(Cop) under T7.5 promoter	[548]
pSC66-EGFP-F1L/B6R	EGFP-tagged F1L (amino acids 1-198) and amino acids 143-174 of VV(Cop) B6R	[576]
pSC66-EGFP-F1L (206-226)	EGFP-tagged F1L-tail lacking the first 205 amino acids	[576]
pSC66-EGFP-F1L (1-206)	EGFP-tagged F1L lacking the tail anchor (207-226)	[576]
pSC66-EGFP-EVM004	EGFP-EVM004 (ectromelia virus BTB protein)	This study
pSC66-FLAG-EVM004	FLAG-EVM004 (ectromelia virus BTB protein)	[571]
pSC66-FLAG-EVM005	FLAG-EVM005 (ectromelia virus F-box/ ankyrin protein)	[571]
pSC66-FLAG-EVM150	FLAG-EVM150 (ectromelia virus BTB/kelch protein)	[572]
pSC66-FLAG-F1L	Wildtype FLAG-F1L	[547]
pSC66-FLAG-F1L(84-226)	FLAG-F1L(84-226)	This study
pSC66-FLAG-F1L(109-226)	FLAG-F1L(109-226)	This study
pSC66-FLAG-F1LΔBH1	FLAG-F1LΔBH1 (Δ144-156)	This study
pSC66-FLAG-F1L(3K-R)	FLAG-F1L(3K-R); K122R/K165R/K168R	This study
pSC66-FLAG-F1L(4K-R)	FLAG-F1L(4K-R); K122R/K165R/K168R/ K103R	This study
pSC66-FLAG-F1L(5K-R)	FLAG-F1L(5K-R); K122R/K165R/K168R/ K103R/K89R	This study
pSC66-FLAG-F1L(6K-R)	FLAG-F1L(6K-R); K122R/K165R/K168R/ K103R/K89R/K51R	This study
pSC66-FLAG-F1L(7K-R)	FLAG-F1L(7K-R); K122R/K165R/K168R/ K103R/K89R/K51R/K76R	This study

Table 2.3 Continued.

pSC66-FLAG-F1L(8K-R)	FLAG-F1L(8K-R); K122R/K165R/K168R/ K103R/K89R/K51R/K76R/K141R	This study
pSC66-FLAG-F1L(9K-R)	FLAG-F1L(9K-R); K122R/K165R/K168R/ K103R/K89R/K51R/K76R/K141R/K206R	This study
pSC66-FLAG-F1L(A119W)	FLAG-F1L(A119W)	This study
pSC66-FLAG-F1L(G144F)	FLAG-F1L(G144F)	This study
pSC66-FLAG-F1L(I136F)	FLAG-F1L(I136F)	This study
pSC66-FLAG-F1L(K122R)	FLAG-F1L(K122R)	This study
pSC66-FLAG-F1L(K122R/K103R)	FLAG-F1L(K122R/K103R)	This study
pSC66-FLAG-F1L(K122R/K89R)	FLAG-F1L(K122R/K89R)	This study
pSC66-FLAG-F1L(K206R)	FLAG-F1L(K206R)	This study
pSC66-FLAG-F1L(L147F)	FLAG-F1L(L147F)	This study
pSC66-FLAG-F1L(M112W)	FLAG-F1L(M112W)	This study
pSC66-FLAG-F1L(M115W)	FLAG-F1L(M115W)	This study
pSC66-FLAG-F1L(T149L)	FLAG-F1L(T149L)	This study
pSC66-FLAG-F1L(V104A)	FLAG-F1L(V104A)	This study
pSC66-FLAG-F1L(V145F)	FLAG-F1L(V145F)	This study
pSC66-FLAG-F1L(Y108E)	FLAG-F1L(Y108E)	This study
pSC66-FLAG-F1L(M118R)	FLAG-F1L(M118R)	This study
pSC66-FLAG-F1L(I129F)	FLAG-F1L(I129F)	This study
pSC66-FLAG-F1L(N140F)	FLAG-F1L(N140F)	This study
pSC66-FLAG-F1L(F152A)	FLAG-F1L(F152A)	This study
pSC66-FLAG-FPV039	FLAG-FPV039; Bcl-2 homologue from fowlpox virus	[533]
pCR3.1-Mcl-1	Untagged human wildtype Mcl-1 (long isoform)	[567]
pSC66-FLAG-Mcl-1	FLAG-tagged human Mcl-1 (long isoform)	This study

Table 2.3 Continued.

pEGFP-p28	p28 E3 ligase from VV strain IHDW	[566]
pcDNA3.1-HA-Ub	Wildtype ubiquitin with an N-terminal HA tag	J. Hiscott
pBluescript-HA-K48-Ub	Ubiquitin with all lysines mutated except for K48; N-terminal HA tag	[566]
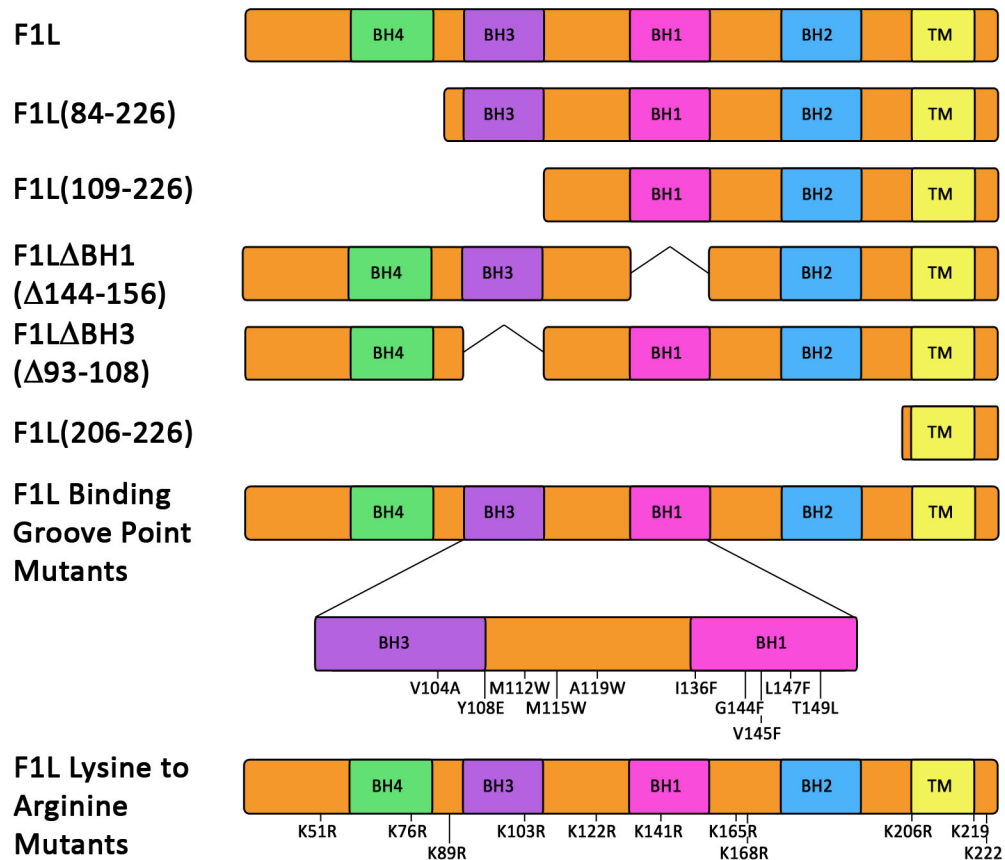
Figure 2.1 F1L mutants generated in this study. Wildtype F1L is illustrated with the BH1, BH2, BH3, and BH4 domains highlighted in pink, blue, purple, and green, respectively. The transmembrane domain (TM) is shown in yellow. The N-terminal mutant F1L(84-226) lacks the putative BH4 domain, while F1L(109-226) lacks the BH3 and BH4 domains. F1LΔBH1 (Δ144-156) and F1LΔBH3 (Δ93-108) are lacking the BH1 or BH3 domain, respectively. F1L(206-226) was generated previously and consists of the C-terminus of F1L [548]. The 10 point mutations made in the binding groove of F1L, between the BH1 and BH3 domains, are highlighted, along with lysine to arginine mutations that span the entire protein.

To generate FLAG-tagged versions of these F1L mutants in pSC66, FLAG-F1L(84-226) and FLAG-F1L(109-226) were generated from the wildtype pEGFP-F1L template with the FLAG-F1L(84) *Sal*I forward and FLAG-F1L(109) *Sal*I forward primers, respectively. FLAG-F1LΔBH1 and FLAG-F1LΔBH3 were generated from pEGFP-F1LΔBH1 and pEGFP-F1LΔBH3, respectively, using the WT FLAG-F1L *Sal*I forward primer. The reverse primer used for all four constructs above was the F1L *Not*I reverse primer. FLAG-F1L(84-226), FLAG-F1L(109-226), FLAG-F1LΔBH1, and FLAG-F1LΔBH3 PCR products were cloned into pGEM-T (Promega) and subsequently subcloned into pSC66 as *Sal*I/*Not*I fragments.

2.3.4 Generation of pcDNA-FLAG-BakΔBH3. pcDNA3-FLAG-Bak, received from Dr. G. Shore (McGill University, Montreal, QC) [283], was used to create a Bak construct lacking residues 72-87 comprising the BH3 domain, FLAG-BakΔBH3 [258]. The FLAG-Bak *Hind*II forward primer and the internal Bak O/L reverse primer (aa71) were used to generate the N-terminal fragment. The C-terminal segment was amplified using the internal Bak forward primer (aa88) and the Bak *Eco*RI reverse primer. The resulting PCR products were combined and amplified together using the FLAG-Bak *Hind*III forward primer and the Bak *Eco*RI reverse primer, ligated into pGEM-T and subcloned into pcDNA3 (Invitrogen) as a *Hind*III/*Eco*RI fragment to generate pcDNA3-FLAG-BakΔBH3.

2.3.5 Generation of pSC66-EGFP-EVM004. pEGFP-EVM004 was generated by PCR using ectromelia virus strain Moscow DNA and EVM004 *Eco*RI forward and reverse primers. The PCR product was ligated into pGEM-T and subcloned into pEGFP-C3 as an *Eco*RI/*Bam*HI fragment. To produce pSC66-EGFP-EVM004, the EGFP-specific forward primer, EGFP *Sal*I forward, and the EVM004 *Bam*HI reverse primer were used to amplify the EGFP-EVM004 fragment from pEGFP-EVM004. The PCR product was ligated into pGEM-T and the *Sal*I fragment was subcloned into pSC66.

2.3.6 Generation of F1L Binding Groove Point Mutants. To generate point mutations in the binding groove of F1L, the previously created pSC66-FLAG-F1L

plasmid [547] was used as a template to make point mutations using F1L(V104A) forward and reverse primers for pSC66-FLAG-F1L(V104A) and F1L(G144F) forward and reverse primers for pSC66-FLAG-F1L(G144F) using QuikChange II site-directed mutagenesis kit (Stratagene). The same mutagenesis technique was used to produce pSC66-FLAG-F1L(Y108E) with F1L(Y108E) forward and reverse primers, pSC66-FLAG-F1L(M112W) with F1L(M112W) forward and reverse primers, pSC66-FLAG-F1L(M115W) with F1L(M115W) forward and reverse primers, pSC66-FLAG-F1L(M118R) with F1L(M118R) forward and reverse primers, pSC66-FLAG-F1L(A119W) with F1L(A119W) forward and reverse primers, pSC66-FLAG-F1L(I129F) with F1L(I129F) forward and reverse primers, pSC66-FLAG-F1L(I136F) with F1L(I136F) forward and reverse primers, pSC66-FLAG-F1L(N140F) with F1L(N140F) forward and reverse primers, pSC66-FLAG-F1L(V145F) with F1L(V145F) forward and reverse primers, pSC66-FLAG-F1L(L147F) with F1L(L147F) forward and reverse primers, pSC66-FLAG-F1L(T149L) with F1L(T149L) forward and reverse primers, and pSC66-FLAG-F1L(F152A) with F1L(F152A) forward and reverse primers. All F1L binding groove mutants are illustrated in Figure 2.1.

EGFP-tagged F1L containing point mutations in the binding groove were constructed using the QuikChange II site-directed mutagenesis kit described above. In brief, pEGFP-F1L was used as a template with the primer pairs for V104A, G144F, Y108E, M112W, M115W, M118R, A119W, I129F, I136F, N140F, V145F, L147F, T149L, and F152A listed above. In addition, pEGFP-F1L(F124W) was generated with F1L(F124W) forward and reverse primers.

2.3.7 Generation of F1L Lysine to Arginine Mutants. Lysine to arginine mutations were introduced into FLAG-F1L using QuikChange II site-directed mutagenesis (Stratagene) as described above (Figure 2.1). The F1L(K122R) forward and reverse primers were used to generate pSC66-FLAG-F1L(K122R) using pSC66-FLAG-F1L as a template. pSC66-FLAG-F1L(K122R/K165R/K168R) was produced from pSC66-FLAG-F1L(K122R) using the F1L(K165R/K168R) forward

and reverse primers and this construct was renamed pSC66-FLAG-F1L(3K-R) due to mutation of three lysine residues. To generate pSC66-FLAG-F1L(4K-R), pSC66-FLAG-F1L(3K-R) was used as a template to introduce K103R using F1L(K103R) forward and reverse primers. pSC66-FLAG-F1L(5K-R) was generated using pSC66-FLAG-F1L(4K-R) as template DNA with F1L(K89R) forward and reverse primers. To create pSC66-FLAG-F1L(6K-R), K51R was introduced into pSC66-FLAG-F1L(5K-R) using F1L(K51R) forward and reverse primers. pSC66-FLAG-F1L(7K-R) was generated by introducing K76R into pSC66-FLAG-F1L(6K-R) using F1L(K76R) forward and reverse primers. Using pSC66-FLAG-F1L(7K-R) with F1L(K141R) forward and reverse primers, pSC66-FLAG-F1L(8K-R) was produced by introducing the K141R mutation. To generate a construct lacking all nine cytoplasmic-exposed lysines, pSC66-FLAG-F1L(9K-R), the template pSC66-FLAG-F1L(8K-R) was used along with F1L(K206R) forward and reverse primers to introduce the K206R mutation. F1L(K206R) forward and reverse primers were also used to create a single point mutant, pSC66-FLAG-F1L(K206R), using pSC66-FLAG-F1L as a template.

F1L mutants bearing lysine to arginine mutations were also constructed in the pEGFP-C3 backbone. A DNA fragment amplified from pSC66-FLAG-F1L(3K-R) using F1L *Eco*RI forward and F1L *Bam*HI reverse primers was T-A ligated into pGEM-T and subcloned into pEGFP to generate pEGFP-F1L(3K-R). The same primers were used with pSC66-FLAG-F1L(4K-R), pSC66-FLAG-F1L(5K-R), pSC66-FLAG-F1L(6K-R), pSC66-FLAG-F1L(7K-R), pSC66-FLAG-F1L(8K-R), and pSC66-FLAG-F1L(9K-R) to generate pEGFP-F1L(4K-R), pEGFP-F1L(5K-R), pEGFP-F1L(6K-R), pEGFP-F1L(7K-R), pEGFP-F1L(8K-R), and pEGFP-F1L(9K-R).

2.4 TRANSFECTIONS

2.4.1 General Transfection Protocol

Transfection of 1×10^6 HeLa, HEK 293T, and Bak-/- BMK cells was accomplished using Lipofectamine 2000 (Invitrogen) according to manufacterer's specifications. Plasmid DNA (0.5-2μg) and 5μL of Lipofectamine were separately

diluted in 500µL OptiMEM (Invitrogen) for 5 minutes at room temperature. Plasmid DNA was gently mixed with Lipofectamine 2000 and the mixture was further incubated for 15 minutes at room temperature. Cell monolayers were washed in 1mL of OptiMEM and 0.5mL of the DNA-lipid mixture was added to the cells in combination with 0.5mL of OptiMEM. Transfections were incubated at 37^oC and 5% CO_2 for 2 hours before adding recovery media containing DMEM, 20% HI-FBS, and 2mM $_L$-glutamine and cells were returned to 37^oC for 16 hours. Transfection of 18mm coverslips (Fisher Scientific) containing $5x10^5$ HeLa cells for live and fixed cell imaging was performed in a similar manner with the following changes. Plasmid DNA (2µg) and 5µL of Lipofectamine 2000 were each diluted in 250µL OptiMEM. Following the incubation of the DNA-lipid mixture, 500µL was added to coverslips directly following the OptiMEM wash and transfections were carried out for 18 hours at 37^oC and CO_2.

2.4.2 General Infection-Transfection Protocol

Fourteen hour infection-transfection experiments were performed to express proteins from pSC66 in the context of VV infection. For fixed cell imaging, HeLa cells ($5x10^5$) seeded on 18mm coverslips were washed in 1mL of OptiMEM and infected with the appropriate virus at a multiplicity of infection (MOI) of 5 in 500µL of OptiMEM. Cells were incubated at 37^oC for one hour with rocking every 10 minutes. During this time, 2µg of DNA was combined with 5µL of Lipofectamine 2000 in a total volume of 500µL as described in section 2.4.1. Virus media was removed from cells and cell monolayers were washed in 1mL of OptiMEM before the addition of 500µL of the DNA-lipid mixture. After two hours at 37^oC, 20% HI-FBS recovery media (1:1) was added to the cells and the transfections were returned to 37^oC and 5% CO_2. Similarly, $7x10^6$ HEK 293T cells were simultaneously infected and transfected for immunoprecipitation analysis. In this case, cells were virally infected at an MOI of 5 in 3.5mL OptiMEM. DNA (14µg) and 35µL of Lipofectamine 2000 were diluted in 1.75mL of OptiMEM and subsequently combined in a total volume of 3.5mL. After one hour of infection,

the entire DNA-lipid mixture was added to the virus-containing media on the cell monolayer for a total volume of 7mL.

2.5 VIRUSES – GENERATION AND PROPOGATION

2.5.1 Viruses Used

All viruses used and generated in this study are listed in Table 2.4. Viruses were stored at -80°C. Prior to use, viruses were thawed at 37°C and sonicated for 20 seconds with 0.5 second pulses (on/off cycles) using a Sonic Dismembrator (Misonix Inc.). VV strain Copenhagen (VV(Cop)), VV strain Copenhagen expressing β-galactosidase in place of the viral thymidine kinase (TK) gene (VV), and VV strain Copenhagen expressing the EGFP fluorescent protein in place of TK (VVEGFP) were kindly provided by Dr. G. McFadden (University of Florida, Gainesville, FL). Recombinant VV strain Western Reserve (VV(WR)) expressing T7 DNA polymerase (VVT7) was a gift from Dr. B. Moss (National Institute of Allergy and Infectious Diseases) [568,569]. VV strain Copenhagen deficient in F1L (VVΔF1L) was generated by insertion of EGFP into the F1L open reading frame [550]. All viruses were propagated in buffalo green monkey kidney (BGMK) cells described in section 2.5.3. VV-HA-ubiquitin was generated previously by inserting HA-tagged human ubiquitin into the TK locus of VV(WR) [493]. VVΔF1L-FLAG-EVM025(E255) and VVΔF1L-FLAG-FPV039 were generated by inserting FLAG-EVM025(255-456) from ectromelia virus or FLAG-FPV039 from fowlpox, respectively, into the TK locus of VVΔF1L [533,570]. FLAG-EVM025(255-456) lacks the large DNGIVQDI repeat-containing N-terminus of EVM025. Residues 255-456 does not contain any repeats but includes the remaining C-terminus, which is 95% identical to F1L in VV(Cop) [570]. VV-FLAG-EVM004, VV-FLAG-EVM005, and VV-FLAG-EVM150 were generated by inserting FLAG-EVM004, FLAG-EVM005, or FLAG-EVM150, all from ectromelia virus, into the TK locus of VV(Cop) [571,572]. VV-HA-Cul1ΔRoc1, which expresses an HA-tagged Cul-1 lacking a functional Roc1-binding domain (amino acids 610-615), was generated by inserting HA-Cul1ΔRoc1 [571] into the TK locus of VV(Cop) [573]. Similarly,

Table 2.4 Viruses Used in This Study.

Virus	Background	Characteristics	Source
VV(Cop)	VV(Cop)	Wildtype vaccinia virus	G. McFadden
VV	VV(Cop)	Wildtype vaccinia virus, expresses β-galactosidase	G. McFadden
VVEGFP	VV(Cop)	Wildtype vaccinia virus, expresses EGFP	G. McFadden
VV-FLAG-F1L	VV(Cop)	Expresses FLAG-F1L	This study
VVΔF1L	VV(Cop)	F1L open reading frame replaced with EGFP	[550]
VVΔF1L-FLAG-Mcl-1	VVΔF1L	Lacks F1L, expresses FLAG-Mcl-1	This study
VVΔF1L-FLAG-FPV039	VVΔF1L	Lacks F1L, expresses FLAG-FPV039	[533]
VVΔF1L-FLAG-EVM025	VVΔF1L	Lacks F1L, expresses FLAG-EVM025(255-456)	[570]
VVΔF1L-FLAG-F1L(V104A)	VVΔF1L	Lacks F1L, expresses FLAG-F1L(V104A)	This study
VVΔF1L-FLAG-F1L(G144F)	VVΔF1L	Lacks F1L, expresses FLAG-F1L(G144F)	This study
VVΔF1L-FLAG-F1L(Y108E)	VVΔF1L	Lacks F1L, expresses FLAG-F1L(Y108E)	This study
VVΔF1L-FLAG-F1L(M112W)	VVΔF1L	Lacks F1L, expresses FLAG-F1L(M112W)	This study
VVΔF1L-FLAG-F1L(M115W)	VVΔF1L	Lacks F1L, expresses FLAG-F1L(M115W)	This study
VVΔF1L-FLAG-F1L(M118R)	VVΔF1L	Lacks F1L, expresses FLAG-F1L(M118R)	This study
VVΔF1L-FLAG-F1L(A119W)	VVΔF1L	Lacks F1L, expresses FLAG-F1L(A119W)	This study
VVΔF1L-FLAG-F1L(F124W)	VVΔF1L	Lacks F1L, expresses FLAG-F1L(F124W)	This study
VVΔF1L-FLAG-F1L(I129F)	VVΔF1L	Lacks F1L, expresses FLAG-F1L(I129F)	This study
VVΔF1L-FLAG-F1L(I136F)	VVΔF1L	Lacks F1L, expresses FLAG-F1L(I136F)	This study
VVΔF1L-FLAG-F1L(N140F)	VVΔF1L	Lacks F1L, expresses FLAG-F1L(N140F)	This study
VVΔF1L-FLAG-F1L(V145F)	VVΔF1L	Lacks F1L, expresses FLAG-F1L(V145F)	This study
VVΔF1L-FLAG-F1L(L147F)	VVΔF1L	Lacks F1L, expresses FLAG-F1L(L147F)	This study

Table 2.4 Continued.

VVΔF1L-FLAG-F1L(T149L)	VVΔF1L	Lacks F1L, expresses FLAG-F1L(T149L)	This study
VVΔF1L-FLAG-F1L(F152A)	VVΔF1L	Lacks F1L, expresses FLAG-F1L(F152A)	This study
VVΔF1L-FLAG-F1L(8K-R)	VVΔF1L	Lacks F1L, expresses FLAG-F1L(8K-R)	This study
VVΔF1L-FLAG-F1L(9K-R)	VVΔF1L	Lacks F1L, expresses FLAG-F1L(9K-R)	This study
VV-FLAG-EVM150	VV(Cop)	Expresses FLAG-EVM150	[572]
VV-FLAG-EVM004	VV(Cop)	Expresses FLAG-EVM004	[571]
VV-HA-Ubiquitin	VV(WR)	Expresses HA-ubiquitin	[493]
VV-FLAG-EVM005	VV(Cop)	Expresses FLAG-EVM005	[571]
VV-HA-Cul1ΔRoc1	VV(Cop)	Expresses HA-Cul1ΔRoc1	[573]
VV-Myc-Cul3ΔRoc1	VV(Cop)	Expresses Myc-Cul3ΔRoc1	[574]
VVT7	VV(WR)	Expresses T7 DNA polymerase from T7 bacteriophage	[568,569]

Cop – Vaccinia virus strain Copenhagen

WR – Vaccinia virus strain Western Reserve

VV-Myc-Cul3ΔRoc1 was produced by inserting pSC66-Myc-Cul3ΔRoc1, which expresses a Myc-tagged dominant-negative Cul-3 (Δ597-615), into the VV(Cop) TK locus [574]. The remaining viruses in this study were generated as discussed in section 2.5.6.

2.5.2 General Virus Infection Protocol

Infections of $1x10^6$ HeLa were performed as follows. Media was removed from the cells and 0.5mL of fresh media was added to the cell monolayer before virus infection at an MOI of 5 or 10. Cells were incubated at 37^oC for one hour with rocking every 10 minutes. One hour after infection, 1.5mL of fresh media was added to the cells for the remainder of the infection at 37^oC and 5% CO_2. In some instances, such as time course studies for Mcl-1 protein stability (section 2.8.1) and virus growth curves (section 2.5.8), virus media was removed after the first hour and cells were washed with 1mL of phosphate buffered saline (PBS) containing 4.3mM Na_2HPO_4, 1.4mM KH_2PO_4, 137mM NaCl, 2.7mM KCl (pH 7.4), before the addition of fresh media. In cases where proteasome inhibition was required, cells were pretreated with 10μM MG132 (Sigma-Aldrich) for one hour prior to virus infection. Following MG132 treatment, cells were washed in 1mL of PBS before the addition of virus. One hour after infection, virus media was removed and replaced with 1mL of fresh media containing 10μM MG132 for the duration of the infection.

For infections of $7x10^6$ HeLa or HEK 293T cells for immunoprecipitation studies, virus was added at an MOI of 5 or 10 in 3.5mL of media and after one hour at 37^oC, 6.5mL of media was added to the cells. Virus infections for confocal microscopy were performed by infecting $5x10^5$ HeLa cells on 18mm coverslips (Fisher Scientific). Cells were infected for 1 hour in 500μL of media at 37^oC and 500μL of media was added to the cells for the remainder of the infection.

To infect suspension Jurkat cells ($1x10^6$ or $2x10^6$), cells were counted in a haemocytometer (Fisher Scientific) and resuspended at a concentration of $5x10^3$ cells/mL for Bak and Bax activation assays or $1x10^4$ cells/mL for cytochrome *c*

release assays. Virus was added to 200μL of the cell suspension in 10mL round bottom tubes (Fisher Scientific) and cells were incubated at $37^{\circ}C$ in a continuous rotator. After one hour of infection, cells were transferred to a tissue culture 6 well plate containing 800μL of media per well and placed at $37^{\circ}C$ and 5% CO_2.

2.5.3 Virus Propagation and Isolation

All viruses were amplified by infecting roller bottles containing approximately $3x10^8$ BGMK cells at an MOI of 1. Virus was harvested in standard saline citrate (SSC) buffer containing 150mM NaCl and 15mM trisodium citrate and resuspended in 20mL of ice-cold swelling buffer containing 10mM Tris (pH 8) and 2mM $MgCl_2$. Following 3 rounds of freezing at $-80^{\circ}C$ and thawing at $37^{\circ}C$, virus was isolated by dounce homogenization using a B pestle (Bellco Biotechnology) on ice in order to disrupt the plasma membrane but preserve the integrity of the nuclear membrane. After 100 strokes, homogenates were centrifuged at 300xg for 5 minutes and supernatants were collected. Pellets were resuspended in 10mL of swelling buffer and dounce homogenized with 60 strokes before centrifugation at 300xg for 5 minutes. Supernatants were pooled and subject to centrifugation at 10,000xg at $4^{\circ}C$ for 1 hour and virus pellets were resuspended in DMEM. Viral titers were determined as described in section 2.5.4.

2.5.4 Quantification of Virus

To determine the number of plaque forming units (pfu) per mL of each virus stock, BGMK cells were infected with a virus dilution series. The virus stock was diluted 100-fold by resuspending 10μL of virus stock in 990μL of media. A serial dilution of 10^{-3} to 10^{-8} was achieved by continuous removal of 100μL of previously diluted virus into 900μL of media. These six dilutions were used to infect $1x10^6$ BGMK cells in duplicate. Infected monolayers were fixed 24-48 hours post infection in neutral buffered formalin containing 4% volume/volume (v/v) formaldehyde (Sigma-Aldrich) (pH 7.4), 1.45M NaCl, 550mM Na_2HPO_4, and 350mM NaH_2PO_4. Plaque formation was observed following staining with crystal violet solution containing 0.1% w/v crystal violet (Sigma-Aldrich) and 20%

v/v ethanol solution. Visible, isolated plaques were counted and viral titres were calculated by multiplying the number of plaques in one well with the reciprocal dilution factor used to infect that well and then dividing by the volume of medium used to infect that well [(number of plaques)x(1/dilution factor)/volume]. The pfu/mL for duplicate plates was averaged to obtain the titer of each virus stock. For all infections the MOI was calculated by multiplying the number of cells in a monolayer by the desired number of particle forming units per cell and then dividing by the titer of the virus stock [(number of cells)x(pfu)/(virus titer)].

2.5.5 Isolation of Viral Genomic DNA

Phenol:chloroform extraction following SDS lysis was used to isolate viral and cellular DNA from infected cells. BGMK cells ($1x10^6$) were infected at an MOI of 5 for 16 hours. Media was removed from the infected monolayers and cells were incubated with 1mL of cell lysis buffer containing 50mM Tris-HCl (pH 8.0), 4mM EDTA, 4mM $CaCl_2$, 1.2% SDS, and 0.2mg/mL proteinase K (Roche Diagnostics) for 4-16 hours at 37^oC. The lysed solution was transferred to a microfuge tube and DNA was extracted following vigorous vortexing with phenol:chloroform (1:1) and centrifugation at 9000xg for 10 minutes. A portion of the aqueous layer (300μL) was transferred to a new microfuge tube and to this tube was added 50μL of 3M NaAc (pH 5) and 2.5 volumes of 95% ethanol. After thorough vortexing, DNA was precipitated at -80^oC for 15 minutes and DNA was pelleted by centrifugation at 18,000xg for 15 minutes. The DNA pellet was air-dried and resuspended in 50μL of ddH_2O before being used in PCR.

2.5.6 Generation of Recombinant Viruses

Recombinant VV-FLAG-F1L was created by homologous recombination into the TK locus of VV(Cop). CV-1 cells ($1x10^6$) were transfected with pSC66-FLAG-F1L and simultaneously infected with VV(Cop). pSC66-FLAG-F1L consists of FLAG-F1L and *lacZ*, both under the control of synthetic poxviral promoters, flanked by regions of the VV TK gene (Fig 2.2). Double crossover events between pSC66-
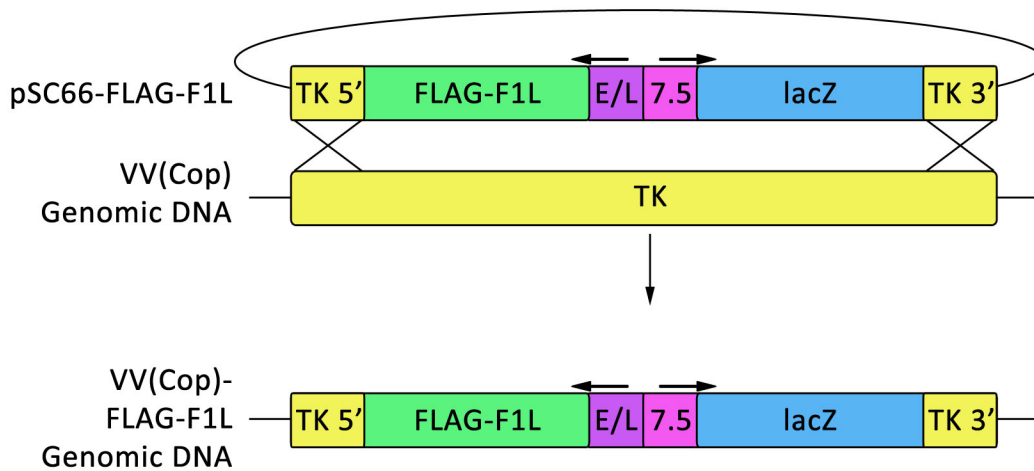
Figure 2.2 Generation of recombinant vaccinia viruses. To generate VV-FLAG-F1L, cells were transfected with pSC66-FLAG-F1L and simultaneously infected with vaccinia virus strain Copenhagen, VV(Cop). The pSC66-FLAG-F1L vector expresses lacZ, the cDNA encoding for β-galactosidase, under the control of a poxviral 7.5 promoter (7.5). The flanking promoter is a strong synthetic poxviral early/late (E/L) promoter that drives the expression of the gene of interest, FLAG-F1L in this case. The regions coding for FLAG-F1L and β-galactosidase are flanked by the 5' and 3' regions of the vaccinia virus thymidine kinase (TK) gene. These regions of homology allow for recombination into the TK gene of the VV(Cop) DNA genome in infected-transfected cells. The resulting recombinant virus, VV-FLAG-F1L, contains coding regions for FLAG-F1L and lacZ and lacks a functional TK gene.

FLAG-F1L and the endogenous TK gene in VV(Cop) will result in a *lacZ*-positive, TK-negative recombinant virus (Fig 2.2) [564]. In brief, CV-1 cells were infected with VV(Cop) at an MOI of 0.05 in OptiMEM (Invitrogen) for one hour at 37°C. During this hour, pSC66-FLAG-F1L (5µg) and 10µL of Lipofectin (Invitrogen) were each diluted in 100µL of OptiMEM and incubated for 45 minutes at room temperature. The DNA and Lipofectin solutions were then mixed, incubated for 15 minutes at room temperature, and added to infected CV-1 cell monolayers. Following a 5 hour incubation at 37°C, 1mL of recovery media was added to the cells. Fourty-eight hours post infection-transfection, cells were harvested in SSC, centrifuged at 1000xg, and resuspended in ice-cold swelling buffer.

Recombinant viruses were identified by titering out serial dilutions on CV-1 cells. Twenty-four to 48 hours post infection, cells were overlaid in the presence of X-gal (Rose Scientific) to visualize recombinant β-galactosidase-positive viruses (see section 2.5.7). Following plaque purification, viruses were titered on human TK$^-$-143B cells, which lack a functional TK gene, in the presence of 25µg/mL BrdU (Sigma-Aldrich) to allow for growth of only cells and viruses that lack TK. Purified viruses were subsequently amplified in CV-1 cells and the expression of FLAG-F1L was confirmed by western blotting with anti-FLAG M2.

Recombinant VVΔF1L-FLAG-Mcl-1, VVΔF1L-FLAG-F1L(V014A), VVΔF1L-FLAG-F1L(G144F), VVΔF1L-FLAG-F1L(Y108E), VVΔF1L-FLAG-F1L(M112W), VVΔF1L-FLAG-F1L(M115W), VVΔF1L-FLAG-F1L(M118R), VVΔF1L-FLAG-F1L(A119W), VVΔF1L-FLAG-F1L(I129F), VVΔF1L-FLAG-F1L(I136F), VVΔF1L-FLAG-F1L(N140F), VVΔF1L-FLAG-F1L(V145F), VVΔF1L-FLAG-F1L(L147F), VVΔF1L-FLAG-F1L(T149L), VVΔF1L-FLAG-F1L(F152A), VVΔF1L-FLAG-F1L(8K-R), and VVΔF1L-FLAG-F1L(9K-R) were generated using the protocol described above with the replacement of CV-1 cells with BGMK cells for the initial infection/transfection event. Additionally, recombinant viruses were generated using VVΔF1L as the parental virus. The plasmid DNA used to generate these viruses was pSC66-FLAG-Mcl-1, pSC66-FLAG-F1L(V104A), pSC66-FLAG-F1L(G144F), pSC66-FLAG-F1L(Y108E), pSC66-

FLAG-F1L(M112W), pSC66-FLAG-F1L(M115W), pSC66-FLAG-F1L(M118R), pSC66-FLAG-F1L(A119W), pSC66-FLAG-F1L(I129F), pSC66-FLAG-F1L(I136F), pSC66-FLAG-F1L(N140F), pSC66-FLAG-F1L(V145F), pSC66-FLAG-F1L(L147F), pSC66-FLAG-F1L(T149L), pSC66-FLAG-F1L(F152A), pSC66-FLAG-F1L(8K-R), or pSC66-FLAG-F1L(9K-R).

2.5.7 Agarose Overlay and Plaque Purification

For recombinant virus selection, virus-infected BGMK, CV-1, or TK⁻-143B cell monolayers were overlaid with a low melting point (LMP) agarose overlay containing 2.5mL 2X DMEM (2.7% w/v DMEM, 88mM $NaHCO_3$), 2.5mL of 2.5% w/v LMP agarose (Sigma-Aldrich), and 1mL of HI-FBS. In order to visualize *lacZ*-expressing recombinant viruses, 100μL of 100mg/mL X-gal dissolved in dimethylformamide (Sigma-Aldrich) was added to the overlay. Agarose overlays were cooled at room temperature before incubation overnight at 37°C and 5% CO_2. Blue plaques expressing *lacZ* were selected the following day using a Pasteur pipet and each plaque was suspended in 50μL of swelling buffer. Plaques containing virus-infected cells were freeze thawed with three cycles at -80°C and 37°C to lyse the cells and release infectious virus. Prior to infection, an equal volume of 2X DMEM was added to the plaque suspension and plaques were sonicated as described in section 2.5.1.

2.5.8 Plaque Assays and Growth Curves

To monitor virus growth, monolayers of $1x10^6$ BGMK cells were infected with serial dilutions of VV, VVΔF1L, VVΔF1L-FLAG-F1L(8K-R), or VVΔF1L-FLAG-F1L(9K-R). One hour after infection, virus-containing media was removed and cells were maintained in fresh media for 42 hours at 37°C and 5% CO_2. Cells were then fixed in neutral buffered formalin and stained with crystal violet solution. The area of each plaque was measured using Fiji software and 20 plaques were counted for each virus. Graphical representation of plaque size was obtained using GraphPad Prism version 5 and statistical significance was calculated using

2-tailed paired t-tests (GraphPad Software, La Jolla California USA, www.graphpad.com).

Multi-step growth curves were performed by infecting 1×10^6 BGMK cells with VV, VVΔF1L, VVΔF1L-FLAG-F1L(8K-R), or VVΔF1L-FLAG-F1L(9K-R) at an MOI of 0.01, in triplicate. After one hour of infection, virus-infected cells were washed in PBS before adding back fresh media. Adherent and floating cells were collected in SSC at 12, 24, 36, 48, and 72 hours post infection, washed in PBS, and pellets were resusupended in swelling buffer following centrifugation at 1000xg. Samples were subject to three cycles of freezing at -80^oC and thawing at 37^oC before 1:1 dilution in 2X DMEM. Each sample was serially diluted and used to infect a monolayer of BGMK cells in duplicate, as described in section 2.5.4. Fourty-two hours post-infection, cell monolayers were fixed in neutral buffered formalin and stained with crystal violet solution. Viral titres were determined by counting isolated plaques and the mean viral titer and standard deviation were calculated for each sample using GraphPad Prism version 5 (GraphPad Software, La Jolla California USA, www.graphpad.com).

2.6 PROTEIN METHODOLOGY

2.6.1 Antibodies

All antibodies used in this study are listed in Table 2.5, along with source and working concentrations.

2.6.2 Protein Sequence Analysis and Domain Prediction

Protein sequences were obtained from NCBI database and the Poxvirus Bioinformatics Resource. Multiple sequence alignments were generated using AlignX (Invitrogen) and Clustal W [575]. F1L BH domains were identified by correlating F1L sequence features, in particular hydrophobic spacing, to structural constraints of known Bcl-2 protein structures together with conservation patterns in a multiple sequence alignment. Sequences used were VV(Cop) F1L sequence (AAA48014), human Bcl-xL (NP_612815), human Bcl-2 (1GJH_A), human Mcl-1 (NP_068779), human Bax (NP_620116), human Bak

Table 2.5 Antibodies Used in This Study.

Antibody	Species	Dilution/ Amount	Source
Flow Cytometry			
anti-Bak AB-1	Mouse	2µg/mL	Oncogene Research Products
anti-Bax 6A7	Mouse	2µg/mL	BD Biosciences
anti-NK1.1 (PK136)	Mouse	2µg/mL	K. Kane and [583]
PE-conjugated anti-mouse	Goat	1:100	Jackson Immunoresearch
Immunoprecipitation			
anti-Bak NT	Rabbit	2ug	Upstate
anti-EGFP	Goat	1µL	L. Berthiaume
anti-FLAG M2	Mouse	1µg	Sigma-Aldrich
anti-Mcl-1	Rabbit	2µg	Assay Designs
Microscopy			
anti-cytochrome c	Mouse	1:150	BD Pharmingen
anti-FLAG M2	Rabbit	1:200	Sigma-Aldrich
anti-HA (12CA5)	Mouse	1:200	Roche Diagnostics
anti-Mcl-1	Rabbit	1:100	Assay Designs
anti-Ubiquitin (FK2)	Mouse	1:200	Enzo Life Sciences
AlexaFluor546 anti-mouse	Goat	1:400	Jackson Immunoresearch
AlexaFluor488 anti-rabbit	Goat	1:400	Jackson Immunoresearch
Western Blot			
anti-β-tubulin	Mouse	1:4000	ECM Bioscience
anti-Bak	Mouse	1:500	BD Pharmingen
anti-Bak NT	Rabbit	1:2000	Upstate
anti-cytochrome c	Mouse	1:1000	BD Pharmingen
anti-EGFP	Mouse	1:5000	Covance
anti-F1L (306)	Rabbit	1:5000	[548]
anti-FLAG M2	Mouse	1:5000	Sigma-Aldrich
anti-phospho-histone H2AX	Mouse	1:1000	Upstate
anti-I3L	Mouse	1:20	[684]
anti-I5L	Rabbit	1:5000	[571]
anti-Mcl-1 (RC13)	Mouse	1:250	Fisher Scientific
anti-MnSOD (110)	Rabbit	1:5000	Stressgen
anti-Myc (9E10)	Mouse	1:2500	M. Barry
anti-PARP	Mouse	1:2000	BD Pharmingen
anti-Ubiquitin (FK2)	Mouse	1:2000	Enzo Life Sciences
anti-mouse-HRP	Donkey	1:25,000	Jackson Immunoresearch
anti-rabbit-HRP	Donkey	1:25,000	Jackson Immunoresearch

(2IMS_A), myxoma virus M11L (NP_051725), monkeypox virus C7L (NP_536460), yaba monkey tumor virus 16L (NP_938273), lumpy skin disease virus 017 (NP_150451), sheep poxvirus 014 (NP_659590), shope fibroma virus 011L (NP_051900), and swinepox virus 012 (NP_570172).

F1L images highlighting the residues of the binding groove and surface lysine residues were provided by Dr. M. Kvansakul (La Trobe University, Australia) based on the crystal structure of MVA F1L (Protein Data Base accession code 2vty) [555]. Figures were generated in Pymol (The PyMOL Molecular Graphics System, Version 1.2r3pre, Schrödinger, LLC) using the coordinates of the MVA F1L:Bim complex (Dr. M. Kvansakul, personal communication).

2.6.3 Immunoprecipitations to Detect Protein Interactions

All immunoprecipitations were carried out 18 hours post transfection, 14 hours post infection-transfection, or 12 hours post infection, unless stated otherwise. Cells were washed in 1X PBS prior to lysis in CHAPS (3-[(3-cholamidopropyl)-dimethylammonio]-1-propanesulfonate) lysis buffer containing 2% w/v CHAPS (Sigma-Aldrich), 150mM NaCl, and 50mM Tris (pH 8.0) for examining interactions with Bcl-2 family members. Alternatively, immunoprecipitations involving ubiquitin or ubiquitination machinery were lysed in NP-40 lysis buffer containing 1% NP-40 v/v (Sigma-Aldrich), 150mM NaCl, and 50mM Tris (pH 8.0), or radioimmunoprecipitation (RIPA) buffer containing 150mM NaCl, 50mM Tris (pH 8.0), 1% v/v NP-40, 0.5% w/v deoxycholate (Sigma-Aldrich), and 0.1% w/v SDS (Fisher Scientific). All lysis buffers contained complete EDTA-free protease inhibitor cocktail tablets (Roche Diagnostics). Lysis occurred at 4°C for 2 hours before insoluble components were pelleted by centrifugation at 9000xg for 10 minutes. Soluble fractions were extracted and a portion of this was reserved for examining protein expression following acetone precipitation (section 2.6.4). For transfections, 20% of the supernatant was reserved, whereas 5% was retained for infections or infection-transfection experiments. The appropriate concentration of antibody (Table 2.5) was added to the remainder of the soluble

fraction for 2 hours at 4°C. Following incubation with antibody, 20-30µL of a 1:1 mixture of lysis buffer to protein A- or protein G-conjugated sepharose beads (GE Healthcare) was added and immune complexes were allowed to form at 4°C for 1 hour. Complexes were isolated by centrifugation (300xg for 30 seconds) followed by three washes in 200-500µL of lysis buffer. Supernatant was gently removed and the beads were resuspended in SDS sample buffer.

2.6.3.1 Examining Interactions Between F1L, Bak, and Mcl-1. To examine the interaction between F1L and endogenous Bak during virus infection, 1.4×10^7 HeLa, HEK 293T, MEF, Jurkat, or LMH cells were infected with VV-FLAG-F1L or VVΔF1L at an MOI of 5. Following CHAPS lysis, soluble fractions were immunoprecipitated with rabbit anti-Bak NT antibody (Upstate). To determine the region of Bak responsible for binding Mcl-1 and F1L, 1×10^6 HEK 293T cells were transfected with pEGFP-C3, pEGFP-F1L, pCR3.1-Mcl-1, pcDNA3-FLAG-Bak, or pcDNA3-FLAG-BakΔBH3 with Lipofectamine 2000. Cells were lysed in 2% CHAPS lysis buffer and immunoprecipitated with rabbit anti-Mcl-1 (Assay Designs) or goat anti-GFP (Dr. Luc Berthiaume, University of Alberta, Edmonton, Alberta). The effect of Bak point mutations on interaction with F1L was assessed by transfecting 1×10^6 Bak-deficient BMKs with pEGFP-C3, pEGFP-F1L, or pEGFP-Bcl-xL and wildtype pcDNA-Bak, pcDNA-BakmtBH1, pcDNA-BakmtBH2, or pcDNA-BakmtBH3. Following transfection, cells were lysed in 2% CHAPS lysis buffer and goat anti-GFP was used to immunoprecipitate complexes. The interaction between endogenous Bak and Mcl-1 was assessed by infecting 1.4×10^7 HEK 293T cells with VV, VV-FLAG-F1L, or VVΔF1L at an MOI of 10 for 3, 6, or 12 hours. Following lysis in 2% CHAPS lysis buffer, Mcl-1 was immunoprecipitated with rabbit anti-Mcl-1 (Assay Designs). Alternatively, 1.4×10^7 HeLa cells were treated with 2µM STS (Sigma-Aldrich) before immunoprecipitation with rabbit anti-Mcl-1 (Assay Designs).

2.6.3.2 Identifying Regions and Residues of F1L Responsible for Interacting with Bak. To examine regions of F1L that interact with Bak, 1×10^6 HEK 293T cells were

transfected with pcDNA-HA-Bak along with pEGFP-C3 (Clontech), pEGFP-F1L, pEGFP-F1L(84-226), pEGFP-F1L(109-226), pEGFP-F1LΔBH1, or pEGFP-F1LΔBH3 with Lipofectamine 2000. Cells were lysed in 2% CHAPS lysis buffer and immunoprecipitated with goat anti-GFP antibody (Dr. Luc Berthiaume, University of Alberta, Edmonton, Alberta). The interaction between endogenous Bak and FLAG-F1L or FLAG-F1L bearing BH mutations during infection was assessed by infecting 7×10^6 HEK 293T cells with VV at an MOI of 5. These cells were simultaneously transfected with pSC66, pSC66-FLAG-F1L, pSC66-FLAG-F1L(84-226), pSC66-FLAG-F1L(109-226), or pSC66-FLAG-F1LΔBH1 and immune complexes were isolated with mouse anti-FLAG M2 (Sigma Aldrich) following lysis in 2% CHAPS lysis buffer. Point mutations within the BH domains of F1L were first assessed for Bak binding by infecting 7×10^6 HEK 293T cells with VV at an MOI of 5 and transfecting with pSC66, pSC66-FLAG-F1L, pSC66-FLAG-F1L(V104A), or pSC66-FLAG-F1L(G144F). Immune complexes were isolated with mouse anti-FLAG M2 in 2% CHAPS lysis buffer. To determine residues in the F1L binding groove that were responsible for binding Bak, 7×10^6 HEK 293T cells were mock-infected or infected with VVΔF1L, VVFLAG-F1L, VVΔF1L-FLAG-F1L(V104A), VVΔF1L-FLAG-F1L(G144F), VVΔF1L-FLAG-F1L(Y108E), VVΔF1L-FLAG-F1L(M112W), VVΔF1L-FLAG-F1L(M115W), VVΔF1L-FLAG-F1L(A119W), VVΔF1L-FLAG-F1L(I136F), VVΔF1L-FLAG-F1L(V145F), VVΔF1L-FLAG-F1L(L147F), or VVΔF1L-FLAG-F1L(T149L) at an MOI of 5. FLAG-tagged protein complexes were isolated in 2% CHAPS lysis buffer using mouse anti-FLAG M2. In order to establish if lysine to arginine mutations in F1L altered Bak binding, 7×10^6 HeLa cells were mock-infected or infected at an MOI of 5 with VV-FLAG-F1L, VVΔF1L-FLAG-F1L(8K-R), or VVΔF1L-FLAG-F1L(9K-R). Cells were subsequently lysed in 2% CHAPS lysis buffer and subject to immunoprecipitation with mouse anti-FLAG M2.

2.6.3.3 Examining the Association Between F1L and Ubiquitin. For silver staining and mass spectrometric analysis, 1.4×10^7 HeLa cells were infected with VV or VV-FLAG-F1L at an MOI of 5. Cells were lysed in 1% NP-40 lysis buffer and

subjected to mouse anti-FLAG M2 immunoprecipitation. To examine the association between F1L and overexpressed ubiquitin, 7×10^6 HeLa cells were mock-infected or infected with VV-FLAG-EVM004, VV-FLAG-EVM150, VV-FLAG-F1L, VVΔF1L-FLAG-EVM025(E255), or VVΔF1L-FLAG-FPV039 at an MOI of 5. Cells were co-infected with VV-HA-Ubiquitin at an MOI of 5 to overexpress HA-tagged ubiquitin. Cells were lysed in 1% NP-40 lysis buffer and FLAG-tagged proteins were immunoprecipitated with mouse anti-FLAG M2. The association between F1L and endogenously-expressed ubiquitin was examined by infecting 7×10^6 HeLa cells at an MOI of 5 with VV-FLAG-EVM004, VV-FLAG-EVM150, VV-FLAG-F1L, VVΔF1L-FLAG-EVM025(E255), or VVΔF1L-FLAG-FPV039. Following infection, cells were lysed in either 1% NP-40 or RIPA lysis buffer and mouse anti-FLAG M2 was used for immunoprecipitation. To determine if the SCF ubiquitin ligase was responsible for ubiquitination of F1L, 7×10^6 HEK 293T cells were infected with VV-FLAG-EVM004, VV-FLAG-F1L, or VVΔF1L-FLAG-FPV039 at an MOI of 5. Cells were co-infected with either VV or VV-HA-Cul1ΔRoc1, a dominant negative form of Cul-1 lacking the Roc1 binding domain, at an MOI of 5, before mouse anti-FLAG M2 immunoprecipitation in 1% NP-40 lysis buffer. Similarly, the role of Cul-3 based ubiquitin ligases on F1L ubiquitination was assessed as described above by infecting HEK 293T cells with VV-FLAG-EVM004, VV-FLAG-EVM150, VV-FLAG-F1L, or VVΔF1L-FLAG-FPV039 at an MOI of 5 and co-infecting cells with VV or VV-Myc-Cul3ΔRoc1 at an MOI of 5. The effect of lysine to arginine mutations on the level of F1L ubiquitination was assessed by infecting 7×10^6 HEK 293T cells with VV at an MOI of 5 and simultaneously transfecting the cells with pSC66-FLAG-F1L, pSC66-FLAG-F1L(3K-R), pSC66-FLAG-F1L(4K-R), pSC66-FLAG-F1L(5K-R), pSC66-FLAG-F1L(6K-R), pSC66-FLAG-F1L(7K-R), pSC66-FLAG-F1L(8K-R), pSC66-FLAG-F1L(9K-R), or pSC66-FLAG-F1L(K206R). Following infection-transfection, cells were lysed in 1% NP-40 or RIPA lysis buffer and immunoprecipitation was performed with mouse anti-FLAG M2. In order to establish which region of F1L was conjugated to ubiquitin, HEK 293T cells (7×10^6) were infected with VV at an

MOI of 5 and simultaneously transfected with EGFP-tagged mutants of F1L in pSC66 or pSC66-EGFP-EVM004 as a control. In contrast to wildtype pSC66-EGFP-F1L, pSC66-EGFP-F1L/B6R contains the first 198 amino acids of F1L and amino acids 143-174 of B6R, an ER localized protein from VV [576], pSC66-EGFP-F1L(1-206) lacks the hydrophobic transmembrane domain of F1L, and pSC66-EGFP-F1L(206-226) contains only the transmembrane domain of F1L [548]. Infected and transfected cells were immunoprecipitated with mouse anti-FLAG M2 following 1% NP-40 lysis.

2.6.4 Acetone Precipitation of Proteins

Post-nuclear supernatants from immunoprecipitations (section 2.6.3) were precipitated using acetone precipitation. Five volumes of ice-cold acetone (Fisher Scientific) were added to supernatants and protein precipitation occurred at -20°C during a 30 minute incubation. Precipitates were centrifuged at 11,000xg for 10 minutes at 4°C and pellets were air-dried and resuspended in 60μL of SDS sample buffer.

2.6.5 Confocal Microscopy

2.6.5.1 Live Cell Microscopy to Assess Mitochondrial Localization of F1L BH Mutants.
Localization of F1L BH domain mutants was ascertained by transfecting 5×10^{5} HeLa cells on 18mm coverslips in modified 3.5cm cell culture dishes (Corning) with 2μg of pEGFP, pEGFP-F1L, pEGFP-F1L(84-226), pEGFP-F1L(109-226), pEGFP-F1LΔBH1, or pEGFP-F1LΔBH3 as described in section 2.4.1. Live cells were stained with 15ng/mL of MitoTracker Red CMXRos (Invitrogen) for 30 minutes at 37°C before visualization using a Zeiss LSM510 laser scanning confocal microscope. EGFP fluorescence was detected at 488nm and mitochondria stained with MitoTracker were detected at 543nm.

2.6.5.2 Fixed Cell Microscopy to Assess Mitochondrial Localization of Mcl-1.
To determine the subcellular localization of Mcl-1, HeLa cells were transfected with 2μg of pCR3.1-Mcl-1 alone or in the presence of pEGFP or pEGFP-F1L for 18 hours using Lipofectamine 2000. Cells were fixed for 5 minutes in 4% w/v

paraformaldehyde (PFA) (Sigma-Aldrich) in PBS and permeabilized for 10 minutes in 1% v/v NP-40 in PBS. Cells were incubated with mouse anti-cytochrome *c* (BD PharMingen) and rabbit anti-Mcl-1 (Assay Designs) for 1 hour at room temperature. Cells were subsequently stained with Alexa488 goat anti-mouse (Jackson Immunoresearch) and Alexa546 goat anti-rabbit (Jackson Immunoresearch) secondary antibodies for 1 hour at room temperature. Between fixing, permeabilization, staining, and mounting steps, cells were washed in PBS containing 1% v/v HI-FBS. Stained coverslips were mounted onto microscope slides (Fisher Scientific) using mounting medium containing 4mg/mL N-propyl-gallate (Sigma-Aldrich) and 50% glycerol before visualization using laser scanning microscopy on a Zeiss LSM510 microscope. EGFP fluorescence and Alexa488 staining were detected at 488nm and Alexa 546 staining was detected with a laser wavelength of 543nm and all images were analyzed using LSM510 imaging software (Zeiss).

2.6.5.3 Fixed Cell Microscopy to Assess Mitochondrial Localization of Lysine-deficient F1L Mutants. Localization of lysine-deficient F1L constructs was assessed by infecting 18mm coverslips of HeLa cells with VVT7 at an MOI of 5 and transfecting 2μg of pSC66-FLAG-F1L, pSC66-FLAG-F1L(8K-R), pSC66-FLAG-F1L(9K-R), or pSC66-FLAG-F1L(K206R) for 14 hours. Alternatively, HeLa cells were mock-infected or infected with VVΔF1L, VV-FLAG-F1L, VVΔF1L-FLAG-F1L(8K-R), or VVΔF1L-FLAG-F1L(9K-R) for 12 hours at an MOI of 5.   Cells were fixed in 4% PFA for 5 minutes, permeabilized in 1% NP-40 for 10 minutes, and blocked in 30% v/v goat serum (Invitrogen) in PBS for 30 minutes. Following washes in PBS containing 1% HI-FBS, coverslips were stained for 1 hour with rabbit anti-FLAG M2 (Sigma Aldrich) alone or in combination with mouse anti-cytochrome *c* (BD Pharmingen) at room temperature. Alexa488 goat anti-mouse and Alexa546 goat anti-rabbit secondary antibodies were incubated with coverslips for 1 hour at room temperature and coverslips were mounted onto microscope slides (Fisher Scientific) with mowiol mounting medium containing

0.096g/mL mowiol (Calbiochem), 0.24g/mL glycerol, 0.48% v/v PBS (pH 7.4), and 0.1% v/v N-propyl-gallate (Sigma-Aldrich). Mounting medium also contained 4'6-diamino-2-phenylindole (DAPI) for visualization of DNA-rich nuclei and virus factories. Using a Zeiss LSM710 laser scanning microscope, DAPI was detected at 405nm, EGFP fluorescence and Alexa488 staining at 488nm, and Alexa546 staining at 543nm, and images were analyzed with Zen 2009 Light Edition software (Zeiss). The localization patterns of FLAG-F1L, FLAG-F1L(8K-R), and FLAG-F1L(9K-R) were classified as reticular, punctate, or aggregated and punctate. Localization patterns were quantified by counting 200 cells in triplicate and the means and standard deviations were graphically represented using GraphPad Prism version 5 (GraphPad Software, La Jolla California USA, www.graphpad.com).

2.6.5.4 Fixed Cell Microscopy to Assess Colocalization Between F1L and HA-tagged Ubiquitin Constructs. Co-localization studies between F1L and HA-tagged ubiquitin constructs were carried out by infecting 18mm coverslips of HeLa cells with VV or VV-FLAG-F1L at an MOI of 4 and VVT7 at an MOI of 1. Cells were simultaneously transfected for 14 hours with 2µg of pcDNA3.1-HA-Ub or pBluescript-HA-Ub-K48, both under the control of the T7 promoter and thus their expression was dependent on T7 DNA polymerase from VVT7 [568,569]. As described in section 2.6.5.3, cells were fixed in 4% PFA, permeabilized in 1% NP-40, and blocked in 30% goat serum. Coverslips were stained with anti-HA (Roche Diagnostics) and Alexa488 goat anti-mouse to visualize HA-ubiquitin, while rabbit anti-FLAG M2 and Alexa546 goat anti-rabbit antibodies were used to detect FLAG-F1L. Cells were mounted in mowiol mounting medium and visualized with an LSM710 microscope using lasers wavelengths of 405nm, 488nm, or 543 nm, to detect DAPI, Alexa488 staining, or Alexa546 staining, respectively.

2.6.5.5 Fixed Cell Microscopy to Assess Colocalization Between F1L and Conjugated Ubiquitin. To establish whether F1L co-localized with conjugated ubiquitin, 18mm coverslips of HeLa cells were mock-infected or infected with VV,

VV-FLAG-EVM004, or VV-FLAG-F1L at an MOI of 5 for 12 hours. Alternatively, cells were infected with VV at an MOI of 5 and simultaneously transfected with 2µg of pSC66-FLAG-F1L, pSC66-FLAG-F1L(8K-R), or pSC66-FLAG-F1L(9K-R) for 14 hours. Cells were fixed, permeabilized, blocked, stained, and mounted as described in section 2.6.5.3. Conjugated ubiquitin was detected with mouse anti-ubiquitin (FK2) (Enzo Life Sciences) [577] and Alexa488 goat anti-mouse antibodies, while FLAG-tagged proteins were visualized by staining with rabbit anti-FLAG M2 (Sigma-Aldrich) and Alexa546 goat anti-rabbit antibodies. Detection of DAPI staining occurred at 405nm, Alexa488 staining at 488nm, and Alexa546 staining at 543nm using an LSM710 microscope and Zen 2009 Light Edition software (Zeiss). Colocalization of FLAG-F1L, FLAG-F1L(8K-R), and FLAG-F1L(9K-R) with conjugated ubiquitin was quantified by counting 200 cells in triplicate. Means and standard deviations were calculated and represented in graphical form with GraphPad Prism version 5 (GraphPad Software, La Jolla California USA, www.graphpad.com).

2.6.6 Silver Staining and Mass Spectrometry

Anti-FLAG immunoprecipitates were subjected to SDS-PAGE on a Hoefer electrophoresis unit SE 600 series (GE Healthcare). The acrylamide gel was silver stained using the following adapted protocol [578,579]. The gel was fixed in 50% methanol/5% acetic acid solution for 20 minutes and washed with 50% methanol for 25 minutes followed by five washes with milli-Q water for a total of 25 minutes. Sodium thiosulfate (0.02%) was used to sensitize the gel for 1 minute, followed by two 1 minute washes with milli-Q water. The gel was stained with 0.1% cold silver nitrate for 25 minutes. Following two 1 minute washes in milli-Q water, the gel was developed during a 10 minute incubation with 2% sodium carbonate anhydrous and 37% formaldehyde. The developing reaction was stopped with 5% acetic acid solution for 20 minutes. The resulting gel was stored in milli-Q water until protein bands were excised. Individual bands were then subjected to enzymatic digestion and mass spectrometry for peptide

identification by the Mass Spectrometry Facility (Dept. of Chemistry, University of Alberta).

2.6.7 Bicinchoninic Acid Assay for Protein Quantification

Protein concentrations for purified mitochondrial and cytoplasmic fractions were determined by bicinchoninic acid (BCA) assay (Pierce) according to manufacturer's specifications. A standard curve was established using increasing concentrations of bovine serum albumin (BSA) (Roche Diagnostics). Both standard and protein samples were incubated in 200µl of BCA reagent at 37^oC for 30 minutes. The absorbance of each sample was read using a 96-well plate reader equipped with a 570nm filter (Softmax Inc.). Optical densities were plotted against the standard curve to determine protein concentration.

2.6.8 SDS-Polyacrylamide Gel Electrophoresis

Protein samples were prepared in SDS sample buffer containing 62.5mM Tris (pH 6.8), 30% v/v glycerol, 2% w/v SDS, 50mM 2-mercaptoethanol (Bioshop), and 0.1% w/v bromophenol blue and boiled at 95^oC for 10 minutes.   Protein samples were subjected to SDS-Polyacrylamide Gel Electrophoresis (SDS-PAGE) using the Mini-PROTEAN Cell (BioRad). Samples were resolved at 150-200V in Tris-glycine running buffer containing 25mM Tris, 190mM glycine, and 3.5mM SDS. Pre-stained low range molecular weight markers (Fermentas) were used as size indicators.

2.6.9 Semi-dry Transfer

Proteins resolved by SDS-PAGE were transferred to nitrocellulose membranes (GE Water and Process Technologies) or polyvinylidene difluoride (PVDF) membranes (GE Healthcare) for 2 hours at 450mA using a semi-dry transfer apparatus (Tyler Research). Prior to transfer, PVDF membranes were activated in methanol for 20 seconds according to manufacturer's specifications.   All membranes were blocked in 5% w/v skim milk and Tris-buffered saline plus Tween-20 (TBST) containing 200mM Tris, 1.4M NaCl (pH 7.5), and 1% v/v Tween-20 (Fisher Scientific) for 3 to 18 hours at room temperature or 4^oC with the

exception of membranes blotted with mouse anti-ubiquitin (FK2), which were blocked in 1% w/v BSA (Roche Diagnostics) and TBST for 3 hours at room temperature.

2.6.10 Western Blotting

Nitrocellulose and PVDF membranes were incubated with primary antibodies listed in Table 2.5 diluted in either TBST or TBST containing 5% w/v skim milk. Membranes were incubated with antibody for 3 hours at room temperature or overnight at 4°C with continuous rocking. Membranes were washed for 15 minutes in TBST before the addition of horseradish peroxidise-conjugated secondary antibodies (Table 2.5) for 1 hour at room temperature. Membranes were washed four times in TBST for 1.5 hours before proteins were visualized using enhanced chemiluminescence (GE Healthcare) according to manufacturer's directions.

2.7 APOPTOSIS ASSAYS

2.7.1 Loss of Mitochondrial Membrane Potential

To test the anti-apoptotic ability of F1L mutants in the absence of infection, 1×10^{6} HeLa cells were transfected with 2μg of pEGFP, pEGFP-F1L, pEGFP-F1L(84-226), pEGFP-F1L(109-226), pEGFP-F1LΔBH1, pEGFP-F1LΔBH3, or pEGFP-F1L(206-226) with Lipofectamine 2000 (Invitrogen), prepared 1:50 in OptiMEM (Invitrogen) according to manufacturer's instructions. Eighteen hours post transfection, cells were treated with 10ng/mL of TNFα (Roche Diagnostics) and 5μg/mL cycloheximide (MP Biomedicals) for 6 hours. Following the apoptotic trigger, cells were stained with 0.2μM tetramethylrhodamine, ethyl ester (TMRE) (Invitrogen), a fluorescent dye that accumulates in mitochondria with intact Δψm [171,172]. After 30 minutes with TMRE, cells were trypsinized and washed with 1% HI-FBS (Invitrogen) in PBS. Cell viability was assessed by two colour flow cytometry (FACScan; Becton Dickinson) using the FL-2 channel equipped with a 585nm filter (42nm band pass) to measure TMRE fluorescence and the FL-1 channel equipped with a 488nm filter (42nm band pass) to measure EGFP

fluorescence. Data were acquired on 20,000 cells with fluorescent signals on logarithmic gain and samples were analyzed using Cell Quest software. Experiments were performed in triplicate and percent killing of GFP-positive cells was measured by subtracting TNFα-treated TMRE-positive cells from untreated TMRE-positive cells [(GFP+, TMRE+, untreated)-(GFP+, TMRE+, TNFα-treated)].

2.7.2 Mitochondrial Isolation

HeLa cells ($7x10^6$) were infected with wildtype VV, VV-FLAG-F1L or VVΔF1L at an MOI of 10 for 24 hours. Alternatively, $1.4x10^7$ HeLa cells were treated with 200mJ/cm^2 UV-C and harvested up to 6 hours post treatment. Mitochondria were harvested using a protocol adapted from [580]. Cells were washed and resuspended in 1mL of hypotonic lysis buffer containing 250mM sucrose, 20mM HEPES (pH 7.5), 10mM KCl, 1.5mM MgCl$_2$, 1mM EDTA and 1mM EGTA. Cells were incubated on ice for 30 minutes and passed through a 22-gauge needle. Crude membranes were pelleted at 750xg for 10 minutes. The pellet was resuspended in 1mL of hypotonic lysis buffer and once again passed through a 22-gauge needle. Following centrifugation at 750xg for 10 minutes, soluble fractions containing mitochondria were pelleted at 10,000xg for 15 minutes at 4°C. Isolated mitochondria were lysed at 4°C for an hour in 2% CHAPS lysis buffer and protein concentration in supernatant and mitochondrial fractions was determined by standard BCA assay (section 2.6.7).

2.7.3 PARP Cleavage

In order to detect cleavage of poly-ADP ribose polymerase (PARP), $1x10^6$ Jurkat cells were infected with VVEGFP, VVΔF1L, or VVΔF1L-FLAG-Mcl-1 at an MOI of 10. Alternatively, $1x10^6$ Jurkat cells were infected at an MOI of 10 with VVEGFP, VVΔF1L, VVΔF1L-FLAG-F1L(8K-R), or VVΔF1L-FLAG-F1L(9K-R). Whole cell lysates were collected at 5, 10, 15, and in some instances, 20 hours post infection and lysed in SDS sample buffer containing 8M urea.

2.7.4 Cytochrome *c* Release Assay

Jurkat cells ($2x10^6$) were infected with VVEGFP, VVΔF1L, or VVΔF1L-FLAG-Mcl-1 at an MOI of 10. At 4, 8, or 12 hours post infection, cells were permeabilized with lysis buffer containing 75mM NaCl, 1mM NaH$_2$PO$_4$, 8mM Na$_2$HPO$_4$, 250mM sucrose, and 190μg digitonin/mL (Sigma-Aldrich) for 10 min on ice [581,582]. Mitochondria-containing pellets and cytosolic supernatant fractions were separated by centrifugation at 10,000xg for 5 minutes and mitochondrial pellet fractions were resuspended in Triton X-100 lysis buffer containing 25mM Tris (pH 8.0) and 0.1% v/v Triton X-100 (Fisher Scientific). Cytosolic and mitochondrial fractions were then subject to SDS-PAGE (section 2.6.8).

2.7.5 Bak and Bax Conformational Analysis by Flow Cytometry

For detection of activated Bak, $1x10^6$ Jurkat cells, Bcl-2 expressing Jurkat cells, or Bak- and Bax-deficient Jurkat cells were infected at an MOI of 10 with VVEGFP, VVΔF1L, VVΔF1L-FLAG-Mcl-1, VVΔF1L-FLAG-F1L(V104A), VVΔF1L-FLAG-F1L(G144F), VVΔF1L-FLAG-F1L(Y108E), VVΔF1L-FLAG-F1L(M112W), VVΔF1L-FLAG-F1L(M115W), VVΔF1L-FLAG-F1L(A119W), VVΔF1L-FLAG-F1L(I136F), VVΔF1L-FLAG-F1L(V145F), VVΔF1L-FLAG-F1L(L147F), VVΔF1L-FLAG-F1L(T149L), VVΔF1L-FLAG-F1L(8K-R), or VVΔF1L-FLAG-F1L(9K-R) for 4 hours. To induce apoptosis, cells were treated with 0.25μM STS for 1.5 hours before fixation in 0.25% PFA. Cells were permeabilized with 500μg/mL digitonin (Sigma-Aldrich) and then stained with a conformation-specific anti-Bak AB-1 antibody (Oncogene Research Products) [177,184] or an isotype control antibody specific for NK1.1 (PK136) [583]. Phycoerythrin (PE)-conjugated anti-mouse antibody was used to counterstain cells (Jackson ImmunoResearch) before analysis by flow cytometry (FACScan; Becton Dickinson) using the FL-2 channel equipped with a 585 nm filter (42 nm band pass). Data were analyzed using CellQuest software. For detection of activated Bax, $1x10^6$ Jurkat cells were infected with VVEGFP, VVΔF1L, or VVΔF1L-FLAG-Mcl-1 for 6 hours before treatment with 2μM STS for 2 hours. Cells were fixed and permeabilized as above and the conformation-

specific anti-Bax 6A7 (BD Biosciences) [181,281] and PE-conjugated anti-mouse antibodies were used to detect activated Bax.

2.7.6 Induction of a DNA Damage Response

To determine whether VV induced a DNA damage response, 1×10^6 HeLa cells were mock-infected or infected with VV, VVΔF1L, or VV-FLAG-F1L at an MOI of 10 for 6 hours. Cells were then mock-treated, treated with 100µM etoposide (Sigma-Aldrich), or 200mJ/cm^2 UV-C using a Stratalinker UV Crosslinker (Stratagene) to trigger a DNA damage response and whole cell lysates were harvested in SDS sample buffer up to 6 hours post treatment.

2.8 UBIQUITIN AND PROTEIN STABILITY ASSAYS

2.8.1 Protein Stability, Proteasome Inhibition and Ubiquitin Laddering

All whole cell lysates were prepared by directly washing cells in 1mL of PBS, lysing cells in SDS sample buffer (section 2.6.8) and boiling at 95°C for 10 minutes. Alternatively, infected cells were harvested in 1mL of SSC, centrifuged at 500xg for 5 minutes prior to PBS wash and resuspension in SDS sample buffer. To monitor the stability of Mcl-1 protein levels, HeLa cells (1×10^6) were infected at an MOI of 10 with VV, VVΔF1L, or VV-FLAG-F1L. Total cell lysates were collected at various time points up to 24 hours post infection. To determine Mcl-1 stability following UV treatment, 1×10^6 HeLa cells were washed in PBS and treated with 200mJ/cm^2 UV-C in the presence of PBS. Following UV-C treatment, media was added back to the cells during the recovery period and whole cell lysates were collected at various times post treatment. HeLa cells were also pre-treated with 10µM MG132 (Sigma-Aldrich) one hour prior to UV-C treatment to prevent the degradation of Mcl-1. To examine the accumulation of FLAG-F1L protein levels during infection, HeLa cells were mock-infected or infected with VV-FLAG-F1L at an MOI of 5. At 4, 8, or 12 hours post infection, whole cell lysates were prepared in SDS sample buffer. The effect of MG132 on endogenous F1L protein levels was assessed by pre-treating 1×10^6 HeLa cells with 10µM MG132. Cells were then washed in PBS and infected with VV,

VVEGFP, or VVΔF1L at an MOI of 10. One hour post infection, 10µM MG132 was added back for the remainder of the infection and whole cell lysates were harvested up to 12 hours post infection. To examine the high molecular weight laddering pattern of FLAG-F1L(8K-R) and FLAG-F1L(9K-R), $1x10^6$ HeLa cells were mock-infected or infected with VVΔF1L, VV-FLAG-F1L, VVΔF1L-FLAG-F1L(8K-R), or VVΔF1L-FLAG-F1L(9K-R) at an MOI of 5 for 16 hours prior to whole cell lysate preparation and SDS-PAGE.

2.8.2 Measuring Protein Stabilization with Flow Cytometry

The stability of F1L was assessed by flow cytometry in the presence of MG132 (Sigma-Aldrich). HeLa cells ($1x10^6$) were transfected with 2µg pEGFP, 0.75µg pEGFP-F1L, or 2µg pEGFP-p28, a ubiquitin ligase from VV(IHDW) [584], as a control. Transfections were carried out with Lipofectamine 2000 as described in section 2.4.1. Eighteen hours post-transfection, cells were treated with 10µM MG132 for 6 hours followed by staining with 0.2µM TMRE with 30 minutes. Cells were harvested, washed, and analyzed by two colour flow cytometry (FACScan; Becton Dickinson) using the FL-1 and FL-2 channels as described above. Protein stabilization was determined by comparing the total EGFP-positive population treated with MG132 to the total untreated EGFP-positive population [(EGFP-positive cells + MG132) – (EGFP-positive cells – MG132)]. Each experiment was performed in triplicate and the means for each sample were plotted with standard deviations. Stabilization of EGFP-tagged protein levels was confirmed by setting up a duplicate transfection and harvesting whole cell lysates 16 hours post transfection. Lysates were collected in SDS sample buffer and subject to SDS-PAGE to monitor EGFP-tagged protein levels (section 2.6.8).

2.8.3 Pulse-Chase Assay

For metabolic labelling of proteins in half-life studies, $1x10^6$ HeLa cells were infected with VV-FLAG-F1L or VVΔF1L-FLAG-F1L(9K-R) at an MOI of 5 for 12 hours. Prior to labelling, cells were starved of methionine and cysteine by incubating cells in DMEM lacking ∟-methionine and ∟-cysteine (Invitrogen) for 30

minutes.   Cells were then radiolabelled with 45 µCi of ^{35}S-containing $_L$-methionine and $_L$-cysteine for 30 minutes.   Following removal of the ^{35}S, cells were washed in PBS and recovered with complete media containing 5µg/mL cycloheximide (MP Biomedicals) to inhibit further protein synthesis or complete media containing 5µg/mL cycloheximide and 10µM MG132 (Sigma-Aldrich) to inhibit protein synthesis and the 26S proteasome.   Cells were harvested up to 12 hours post treatment with cycloheximide or cycloheximide and MG132 and lysed in 1% NP-40 lysis buffer.   Mouse anti-FLAG M2 (Sigma-Aldrich) and protein G sepharose (GE Healthcare) were used to immunoprecipitate FLAG-F1L or FLAG-F1L(9K-R) as described in section 2.6.3.   Immunoprecipitates were resolved by SDS-PAGE and autoradiography was used to visualize the radiolabelled proteins.

CHAPTER 3: Investigating the Role of Mcl-1 During Vaccinia Virus Infection

The cloning of pcDNA-FLAG-BakΔBH3 was performed by D. Quilty, an undergraduate honours student mentored by S. Campbell. All of the experiments contained in this chapter were performed by S. Campbell. The original manuscript was written by S. Campbell and a major editorial contribution was made by Dr. M. Barry.

3.1 INTRODUCTION

Mcl-1 is a major regulator of Bak activity [266,289,354]. In healthy cells, Bak is found in a complex with Mcl-1 on the OMM and this interaction relies on the BH3 motif of Bak [266,289]. Upon receipt of an apoptotic stimulus, Bak dissociates from the restraints of Mcl-1 (Fig 1.16) [266,289,354]. Once free, Bak undergoes activation and oligomerizes to promote the release of cytochrome *c* (Fig 1.11) [266,289,354]. In addition to Bak, Mcl-1 binds a variety of BH3-only proteins [585]. BH3-only proteins, such as Noxa, Puma, and Bik, bind and neutralize Mcl-1 and release Bak [266,586,587,588,589]. Conversely, the interaction between Mcl-1 and BH3-only proteins, such as Bim, tBid, and Bik, has been demonstrated to inhibit the pro-apoptotic function of these BH3-only proteins, thus preventing Bak activation [567,587,590,591,592,593,594]. The binding of Mcl-1 to Bim, for example, inhibits Bim function and prevents Bim from activating Bak [587,594]. Subsequent binding of Noxa to Mcl-1 displaces Bim from the restraints of Mcl-1 and allows for Bak activation [587,594]. Therefore, Mcl-1 prevents cell death by directly binding and inhibiting Bak and acting as a sink for activator BH3-only proteins, effectively inhibiting Bak activation indirectly as well. Apoptosis is initiated when sensitizer BH3-only proteins, such as Noxa, bind to Mcl-1 to release Bak and also BH3-only proteins, such as Bim.

The importance of Mcl-1 in mediating cell survival is highlighted by the fact that Mcl-1 is upregulated in many cancers, such as B cell lymphoma, chronic lymphocytic leukemia, chronic myeloid leukemia, and multiple myeloma [287,288]. The integral anti-apoptotic role of Mcl-1 has also been implicated in the maintenance and survival of both B- and T-lymphocytes [595] and survival of hematopoietic stem cells [596]. However, Mcl-1 displays a few marked differences compared to other Bcl-2 family members. Mcl-1 deficiency results in peri-implantation lethality [597], unlike other Bcl-2 family members, whose absence often yields viable cells and mice albeit with developmental defects

[189,598]. Moreover, in contrast to other cellular anti-apoptotic proteins, Mcl-1 is a very labile protein that responds rapidly to various apoptotic stimuli and thus the intricate regulation of Mcl-1 is an area of extensive research [287,288,432].

The regulation of Mcl-1 occurs at the levels of transcription, post-transcription, and post-translation [287,288,432]. The upregulation of the *mcl-1* gene occurs in response to various growth factors and cytokines, such as IL-6, IL-15, and IFN-α [599,600,601,602,603]. Once transcription of *mcl-1* occurs, alternative splicing of the mRNA yields Mcl-1 short isoform (Mcl-1S), which lacks the BH1, BH2, and transmembrane domains [351,352] and Mcl-1 extra short isoform (Mcl-1ES), which lacks the N-terminus [604]. Unlike full-length anti-apoptotic Mcl-1, both Mcl-1S and Mcl-1ES have been attributed pro-apoptotic activity. Although the precise mechanisms and significance of Mcl-1S and Mcl-1ES are not completely clear, both isoforms are able to dimerize with and inhibit full-length Mcl-1 [351,352,604]. Dimerization-induced inhibition of full-length Mcl-1 by Mcl-1S and Mcl-1ES is supported by the more recent finding that the Mcl-1 BH3 helix can bind and inhibit a second Mcl-1 molecule by interfering with Bak binding [605].

Following translation of Mcl-1, the protein is subject to numerous alterations, including cleavage, ubiquitination, and phosphorylation [287,288,432]. Caspase cleavage of Mcl-1 occurs in the N-terminus at D127 and D157 and this abrogates the anti-apoptotic function of the protein [606,607]. Death receptor signalling activates caspase 3 and caspase 8, which cleave Mcl-1 and disrupt the Bim-Mcl-1 complex, allowing for Bim activation of Bak and Bax [593]. Disruption of the Bim-Mcl-1 complex also occurs following granzyme B cleavage of Mcl-1, which cleaves the protein at D117, D127, and D157 [567,592]. The cleaved C-terminus of Mcl-1 may possess pro-apoptotic activity; however, whether caspase cleavage simply inactivates Mcl-1 to release Bak or generates a pro-apoptotic Mcl-1 molecule currently remains unresolved [606,607,608,609,610].

Mcl-1 differs structurally from other Bcl-2 family members in that it contains a large N-terminal sequence with no homology to other members [350]. The unique N-terminal region contains two proline, glutamic acid, serine, threonine (PEST) sequences, which are typically associated with short-lived proteins targeted by the UPS [611]. The caspase cleavage sites, D127 and D157, reside in the PEST sequences, yet loss of the PEST domains does not appear to enhance the stability of Mcl-1, raising questions about the importance of the PEST domains in Mcl-1 regulation [608]. It is clear, however, that Mcl-1 is highly labile and under strict regulation by the UPS [216,354]. Following genotoxic stimuli, such as UV irradiation and etoposide, Mcl-1 is rapidly degraded (Fig 1.21) [216,266,354]. This degradation is dependent on the UPS as proteasome inhibitors restore Mcl-1 levels and protect cells from apoptosis induced by DNA damaging agents [216,266]. In addition, UV treatment obstructs Mcl-1 protein synthesis, which co-ordinately reduces the amount of Mcl-1 available to inhibit UV-induced apoptosis [216]. The rapid turnover of Mcl-1 also occurs during the DNA damage response induced by AdV infection, yet apoptosis is prevented in virally-infected cells by the interaction between Bak and the vBcl-2 protein E1B-19K [354]. Notably, neutralization of both Mcl-1 and Bcl-xL is necessary to induce apoptosis in response to DNA damage [266,612]. However, Mcl-1 dissociation from Bak and subsequent degradation of Mcl-1 are required for Bcl-xL translocation from the cytosol to the OMM, where it interacts with Bak [216,266]. Furthermore, Bcl-xL displays a weaker affinity for a Bak BH3 peptide compared to Mcl-1 [266]. Based on these data, Bcl-xL is thought to serve a back up, or secondary, role in preventing Bak activation [266].

The specific signals that instigate Mcl-1 ubiquitination and degradation and the mechanism by which this occurs is not completely understood, although it is likely that binding partners influence the fate of Mcl-1. Indeed, Mcl-1 is not always targeted for degradation following an apoptotic stimulus; the release of Bak from Mcl-1 is sufficient to induce apoptosis [435]. Thus, the reason for rapid

Mcl-1 turnover remains elusive. Importantly, the degradation of Mcl-1 occurs following its dissociation from Bak, suggesting that the free form of Mcl-1 is sensitive to ubiquitination [354,436,437]. Noxa is upregulated during a DNA damage response and Noxa binding to Mcl-1 results not only in the release of Bak, but also the rapid degradation of Mcl-1 [266]. In contrast, the BH3-only proteins Bim and Puma stabilize Mcl-1 through direct binding [435,436,613]. The interaction between Mcl-1 and Bim offers reciprocal protection from the 26S proteasome, since the Bim-Mcl-1 interaction prevents degradation of BimL and BimEL and a mutant form of BimEL that cannot bind Mcl-1 demonstrates an enhanced turnover rate [367,436].

Recently, the ubiquitin ligase Mule has been implicated in mediating polyubiquitination of Mcl-1 [437,438]. Mule is a unique 482kDa HECT domain-containing ligase that contains a BH3 domain most similar to the Bak BH3 domain, which is critical for interaction with Mcl-1 [437,438]. Mule ubiquitinates Mcl-1 on 5 lysine residues (K5, K40, K136, K194, and K197) and controls the constitutive turnover of Mcl-1 in healthy cells [438]. Moreover, Mule rapidly ubiquitinates Mcl-1 in response to DNA damage and treatment with chemotherapeutic agents to promote apoptosis [438]. The BH3 motif of Mule interacts specifically with Mcl-1; therefore, binding of BH3-only proteins, such as Bim and Puma, are believed to stabilize Mcl-1 by competitively preventing Mule access [242,437,613]. Mule and Mcl-1 are believed to interact in the conventional BH3:groove manner [437,438]. Somewhat surprisingly, the N-terminus of Mcl-1 is also required for Mule binding and an Mcl-1 mutant lacking the extreme N-terminal residues is more stable than wildtype Mcl-1 [614,615]. These data suggest that in addition to the BH3 binding groove, Mcl-1 contains a second motif in the N-terminus that is required for Mule binding.

Mcl-1 degradation can also occur independently of Mule [439,440]. In this case, Mcl-1 is phosphorylated by the glycogen synthase kinase-3 (GSK-3), a kinase that is activated during times of growth factor deprivation and in

response to UV light and STS treatment [440,441,442]. Following IL-3 withdrawal, GSK-3 phosphorylates S159 in Mcl-1 to allow for recognition of Mcl-1 by the SCF complex [439,440,441]. The SCF machinery interacts with Mcl-1 through the adaptor proteins β-TrCP or FBW7, both of which mediate polyubiquitination and eventual destruction of Mcl-1 by the 26S proteasome [439,440]. The degradation of Mcl-1 is an irreversible event that tips the balance towards cell death, yet an additional level of regulation exists following ubiquitination of Mcl-1. Polyubiquitin chains can be removed from Mcl-1 by the DUB USP9X in order to stabilize the protein and enhance cellular survival [616].

Phosphorylation of Mcl-1 by GSK-3 is critical for recognition by the SCF complex [439,440]. Although phosphorylation of Mcl-1 by GSK-3 results in rapid turnover, not all phosphorylation events yield the same outcome. Phosphorylation of Mcl-1 by the MAPK pathway decreases turnover, phosphorylation by JNK inactivates the function of Mcl-1, while phosphorylation by cyclin-dependent kinases during mitotic arrest enhances the anti-apoptotic activity of Mcl-1 [617,618,619]. Co-ordination of kinase activity has also been proposed, since prior phosphorylation of Mcl-1 by JNK is required for GSK-3-mediated phosphorylation to occur [620].

Given the extensive regulation of Mcl-1, its importance in maintaining Bak in an inactive state until receipt of an apoptotic stimulus appears crucial [287,288,432]. Indeed, disruption of the Bak-Mcl-1 complex is a critical step preceding Bak oligomerization and cytochrome *c* release [266,289,354]. During infection with VV, F1L interacts with Bak and maintains Bak in an inactive state [550,551]. Since deletion of F1L produces a pro-apoptotic virus, F1L is essential for preventing Bak activation and inhibiting virus-induced apoptosis [550]. Both Mcl-1 and F1L inhibit apoptosis, at least in part, by interacting with Bak; thus, we sought to determine the role of Mcl-1 during VV infection and investigate the functional similarities between Mcl-1 and F1L.

3.2 THE INTERACTION BETWEEN F1L AND BAK IS CONSERVED ACROSS SPECIES

We have previously shown that F1L inhibits loss of Δψm and cytochrome *c* release by inhibiting the pro-apoptotic activity of both Bak and Bax [547,549,550]. Although F1L inhibits both proteins, F1L interacts constitutively with only Bak, implicating Bak as an important binding partner [550,551]. Despite the ability of F1L to interact with Bak by immunoprecipitation, F1L displays low micromolar affinity for the Bak BH3 peptide in binding studies [555]. Therefore, we further investigated the ability of F1L to bind endogenous Bak in a range of human cell lines. Cells were mock-infected or infected with VV-FLAG-F1L, a recombinant VV expressing FLAG-tagged F1L, or VVΔF1L, which is devoid of F1L. Twelve hours post infection, cells were lysed in 2% CHAPS, a detergent that maintains the native state of Bcl-2 family members, and endogenous Bak was precipitated with an anti-Bak antibody [178,181]. Western blotting with an anti-FLAG antibody revealed that Bak co-immunoprecipitated FLAG-F1L in HeLa, HEK 293T and Jurkat cells, indicating that F1L was able to interact with endogenous Bak in a variety of cellular contexts (Fig 3.1). Using mouse embryonic fibroblast (MEF) and chicken hepatoma (LMH) cell lines, we also tested the binding of F1L to mouse and chicken Bak, which display 77% and 60% identity to human Bak, respectively [533,621]. In both cases, immunoprecipitates western blotted with anti-FLAG revealed that FLAG-F1L interacted with chicken Bak, as previously shown [533], and murine Bak (Fig 3.1). As expected, FLAG-F1L was not immunoprecipitated with Bak in mock-infected or VVΔF1L-infected cells (Fig 3.1). Immunoprecipitates were western blotted with anti-Bak to illustrate that human, mouse, and chicken Bak were efficiently pulled down and expression of FLAG-F1L and Bak was confirmed by western blotting lysates with anti-FLAG and anti-Bak, respectively (Fig 3.1). Together, these data suggested that despite low affinity for the Bak BH3 peptide in binding assays [555], the constitutive interaction between F1L and Bak was highly conserved during virus infection, since in addition to binding Bak in human cell lines, FLAG-F1L interacted with both chicken and murine Bak.
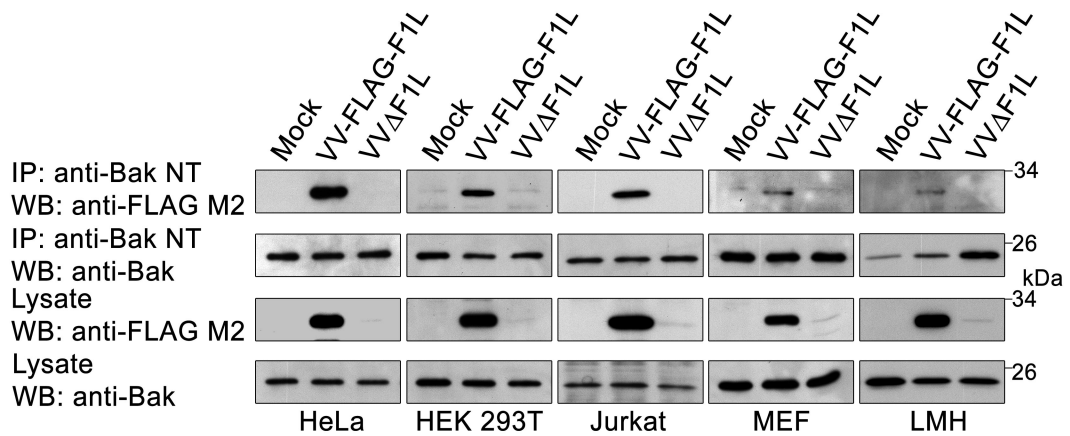
Figure 3.1 F1L interacts with human, murine, and chicken Bak. HeLa, HEK 293T, Jurkat, MEF, or LMH cells were mock-infected or infected with VV-FLAG-F1L or VVΔF1L at an MOI of 5. Cellular lysates were harvested 12 hours post infection, lysed in 2% CHAPS buffer and immunoprecipitated with anti-Bak NT. Both immunoprecipitates and lysates were western blotted with anti-FLAG M2 and anti-Bak.

3.3 F1L AND MCL-1 INTERACT WITH THE BH3 DOMAIN OF BAK

In healthy cells, Bak is in a complex with Mcl-1 until an apoptotic stimulus causes the dissociation of Mcl-1 to promote Bak activation [266,289,354]. In order to dissect the regions in Bak that are required for interaction with Mcl-1 and F1L, we generated a FLAG-tagged Bak construct lacking the BH3 domain, FLAG-BakΔBH3, by deleting amino acids 72 to 87 [258]. The importance of the Bak BH3 domain in mediating interaction with Mcl-1 was assessed by co-transfecting HEK 293T cells with pCR3.1-Mcl-1 and pcDNA-FLAG-Bak or pcDNA-FLAG-BakΔBH3. Co-immunoprecipitation with an anti-Mcl-1 antibody and western blotting with anti-FLAG revealed that while an interaction was observed between FLAG-Bak and Mcl-1, deletion of the Bak BH3 domain completely abrogated binding to Mcl-1 (Fig 3.2). The loss of interaction between Mcl-1 and FLAG-BakΔBH3 was not due to a lack of immunoprecipitated Mcl-1, since Mcl-1 was detected in the immunoprecipitates (Fig 3.2). As controls, lysates were western blotted with anti-FLAG and anti-Mcl-1 to demonstrate equivalent expression levels of FLAG-Bak constructs and Mcl-1, respectively (Fig 3.2).

To determine if the binding regions in Bak were shared between F1L and Mcl-1, HEK 293T cells were co-transfected with either FLAG-Bak or FLAG-BakΔBH3, along with pEGFP or pEGFP-F1L. Immunoprecipitation with an anti-EGFP antibody and western blotting with anti-FLAG indicated that EGFP-F1L interacted strongly with FLAG-Bak, whereas the interaction between EGFP-F1L and FLAG-BakΔBH3 was not detected (Fig. 3.3). Neither FLAG-Bak nor FLAG-BakΔBH3 co-immunoprecipitated EGFP, confirming the specificity of the interaction (Fig 3.3). Both EGFP and EGFP-F1L were present in immunoprecipitates and lysates probed with anti-EGFP, and lysates western blotted with anti-FLAG confirmed the expression of FLAG-Bak and FLAG-BakΔBH3 (Fig 3.3).

To further investigate the regions in Bak required for F1L binding, we used three additional Bak mutants that contain point mutations in the BH1, BH2,
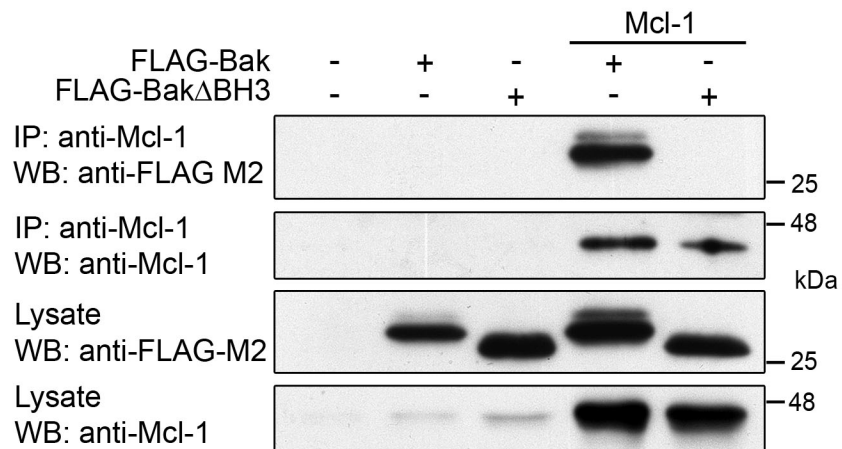
Figure 3.2 Mcl-1 interacts with the BH3 domain of Bak. HEK 293T cells were transiently transfected with pcDNA-FLAG-Bak or pcDNA-FLAG-BakΔBH3 in the presence or absence of pCR3.1-Mcl-1. Sixteen hours post transfection, cells were lysed in 2% CHAPS buffer and anti-Mcl-1 was used for immunoprecipitation. Both immunoprecipitates and lysates were western blotted with anti-FLAG M2 and anti-Mcl-1.
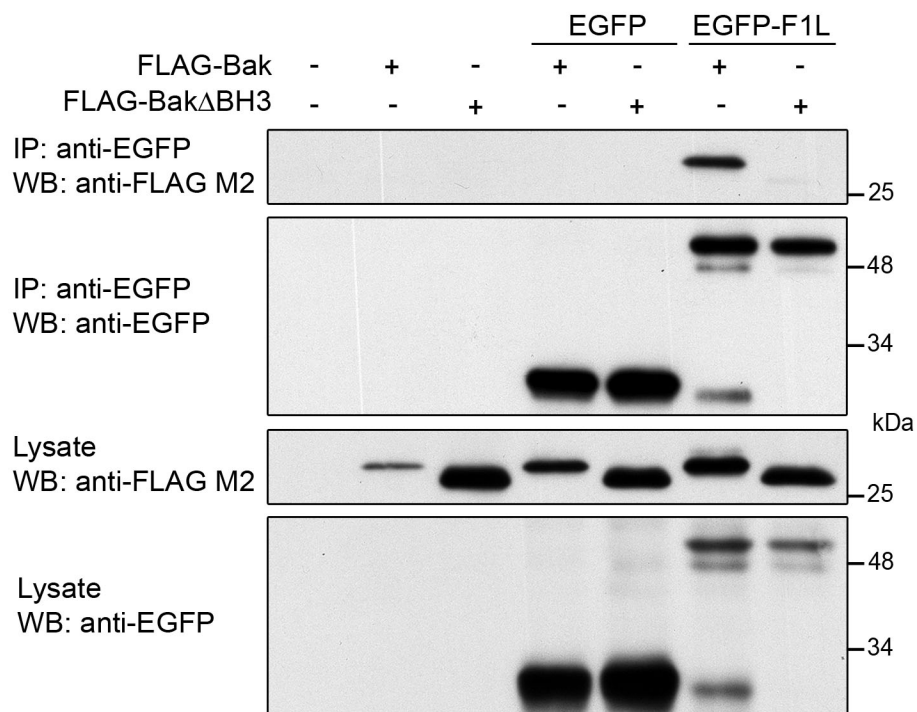
Figure 3.3 F1L interacts with the BH3 domain of Bak. HEK 293T cells were transiently transfected for 16 hours with pEGFP or pEGFP-F1L, along with pcDNA-FLAG-Bak or pcDNA-FLAG-BakΔBH3. Sixteen hours post transfection, cells were lysed in 2% CHAPS and immunoprecipitated with anti-EGFP. Anti-FLAG M2 and anti-EGFP were used to western blot immunoprecipitates and lysates.

or BH3 domains. Wildtype pcDNA-Bak, pcDNA-BakmtBH1 (W125A, G126E, R127A), pcDNA-BakmtBH2 (G175E, G176E, W177A), and pcDNA-BakmtBH3 (L78A, D83A) were co-transfected with either pEGFP, pEGFP-F1L, or pEGFP-Bcl-xL in Bak-deficient BMK cells [289]. In this case, EGFP-Bcl-xL was used as a control, since like Mcl-1, Bcl-xL interacts with Bak and maintains Bak in an inactive state [266]. Lysis in 2% CHAPS and immunoprecipitation with anti-EGFP revealed that EGFP-F1L co-precipitated both wildtype Bak and BakmtBH1 equally when immunoprecipitates were western blotted with anti-Bak (Fig 3.4). However, in contrast to wildtype Bak, the interaction between F1L and BakmtBH2 was slightly reduced, while FLAG-BakmtBH3 barely interacted with EGFP-F1L (Fig 3.4). Thus, L78 and D83 in the BH3 domain of Bak played a critical role in binding F1L, further demonstrating the importance of the Bak BH3 domain. Similarly, immunoprecipitates probed with anti-Bak revealed that EGFP-Bcl-xL bound to wildtype Bak, BakmtBH1, and BakmtBH2 (Fig 3.4). Bcl-xL binding to BakmtBH3, however, was severely reduced compared to the interaction between Bcl-xL and wildtype Bak (Fig 3.4). EGFP, EGFP-F1L, and EGFP-Bcl-xL were all immunoprecipitated equally and lysates demonstrated expression of all Bak constructs and EGFP-tagged proteins (Fig 3.4). Thus, similar to cellular Bcl-2 proteins, such as Mcl-1 and Bcl-xL, F1L bound the BH3 domain of Bak and deletion or point mutations in this domain abrogated the interaction between F1L and Bak.

3.4 VACCINIA VIRUS INFECTION DISRUPTS THE BAK-MCL-1 COMPLEX

The interaction between Mcl-1 and Bak is essential for controlling Bak activation, and thus influences whether a cell will undergo apoptosis. To test this, we examined the dissociation of Mcl-1 from Bak in response to STS treatment. HeLa cells were treated with 2μM STS and cells were harvested up to 3 hours post treatment and subject to anti-Mcl-1 immunoprecipitation. Western blotting with anti-Bak revealed an interaction between Mcl-1 and Bak in the absence of STS but this interaction was barely detectable 2 hours post STS
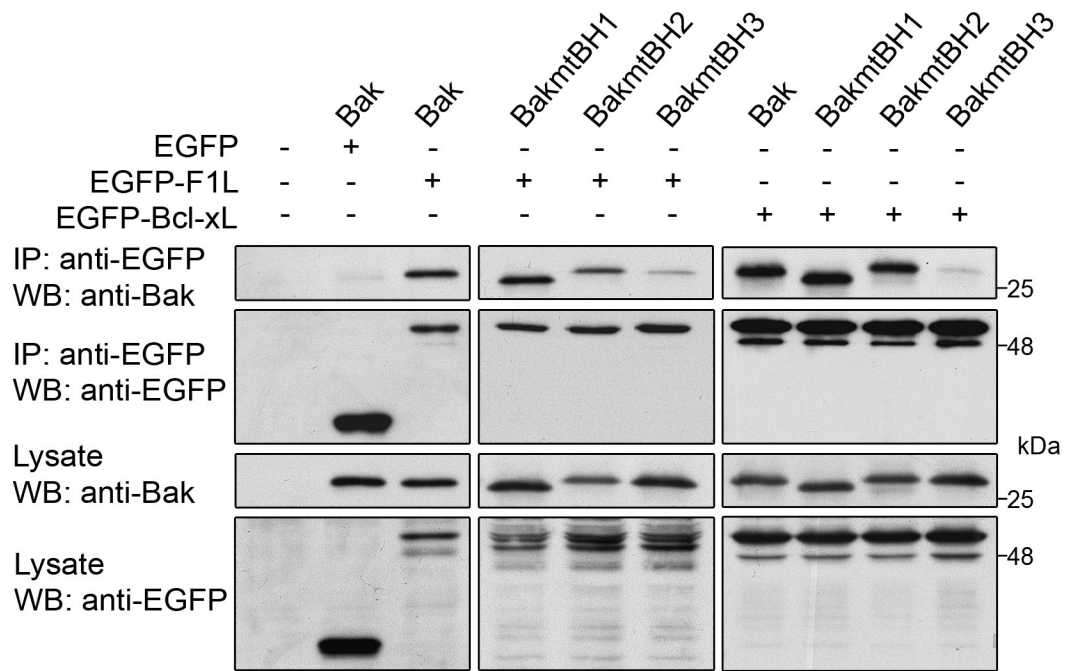
Figure 3.4 Point mutations in the Bak BH3 domain abrogate F1L binding. Bak-deficient BMK cells were transiently transfected with pEGFP, pEGFP-F1L, or pEGFP-Bcl-xL, and either pcDNA-Bak, pcDNA-BakmtBH1, pcDNA-BakmtBH2, or pcDNA-BakmtBH3. Sixteen hours post transfection, cells were lysed in 2% CHAPS buffer and anti-EGFP was used for immunoprecipitation. Immunoprecipitates and lysates were western blotted with anti-Bak and anti-EGFP.

treatment (Fig 3.5A). Bak protein levels were unaltered during STS treatment, which was demonstrated by western blotting lysates with anti-Bak (Fig 3.5A). While Mcl-1 protein levels remained relatively stable in immunoprecipitates and lysates, slightly less Mcl-1 was detected at 2 and 3 hours post STS treatment (Fig 3.5A). Thus, STS caused dissociation of Mcl-1 from Bak, and, moreover, a small portion of Mcl-1 appeared to be degraded following treatment with STS.

Given that Mcl-1 binds and prevents Bak activation in the absence of infection and F1L constitutively bound Bak during infection (Fig 3.1), we sought to determine the fate of the Bak-Mcl-1 association during VV infection. To this end, HEK 293T cells were mock-infected or infected with either wildtype VV that endogenously expresses F1L, VV-FLAG-F1L, or VVΔF1L. Following lysis, Mcl-1 was immunoprecipitated with anti-Mcl-1, demonstrated in the anti-Mcl-1 western blot (Fig 3.5B). Western blotting for endogenous Bak with anti-Bak revealed a strong interaction between Mcl-1 and Bak in mock-infected cells (Fig. 3.5B). However, the Bak-Mcl-1 complex was disrupted in cells infected with VV and VV-FLAG-F1L. Infection with the pro-apoptotic virus, VVΔF1L, also disrupted the Bak-Mcl-1 complex, likely due to apoptosis induced in the absence of F1L, as previously reported [550]. The loss of interaction between Bak and Mcl-1 was likely not due to a general decrease in Mcl-1 protein levels, since both Bak and Mcl-1 were present in mock-infected and virus-infected lysates (Fig 3.5B).

To examine the kinetics of the VV-dependent dissociation between Mcl-1 and Bak, we performed anti-Mcl-1 immunoprecipitations at various times over a 12 hour period in mock-infected HeLa cells and HeLa cells infected with VV or VVΔF1L.   The Bak-Mcl-1 complex remained relatively stable over 12 hours in mock-infected cells, visualized in anti-Mcl-1 immunoprecipitates probed with anti-Bak (Fig. 3.5C). However, in VV-infected cells, the interaction between Mcl-1 and Bak was diminished by 6 hours post infection and the same trend of dissociation, with slightly faster kinetics, was observed in cells infected with the pro-apoptotic virus, VVΔF1L. The decreased level of Bak bound to Mcl-1 was not
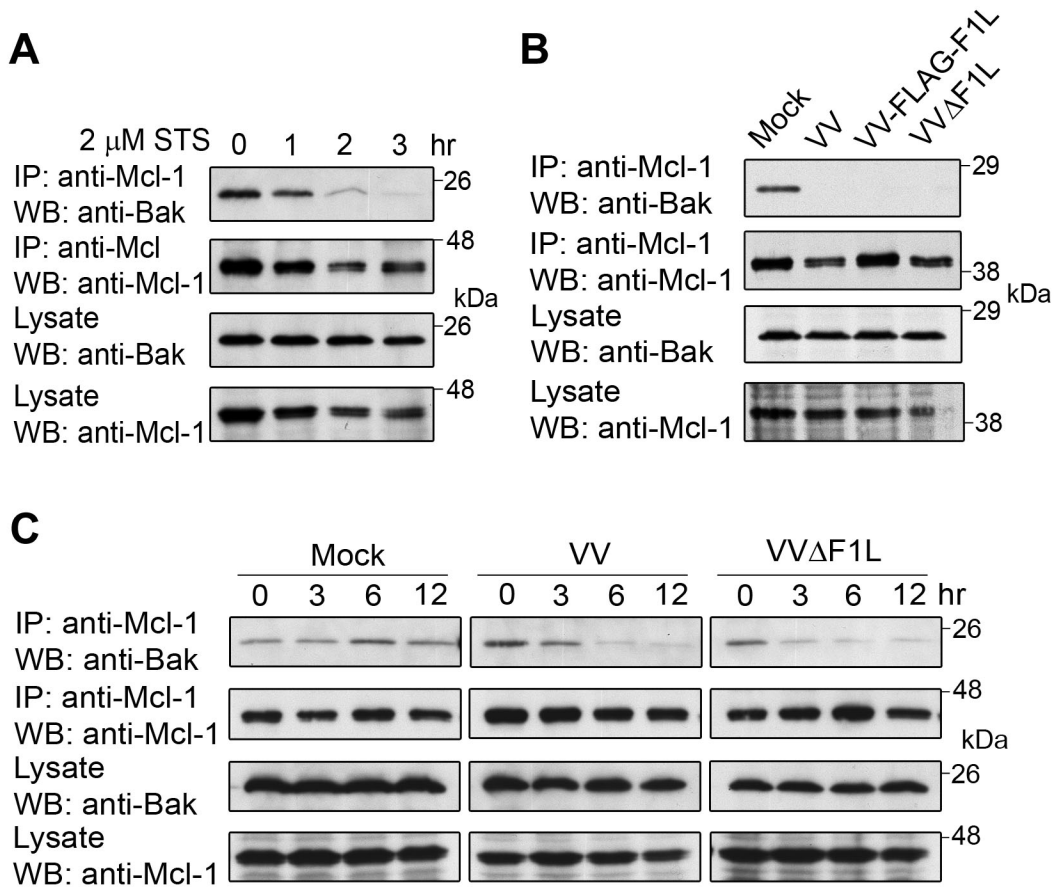
Figure 3.5 Vaccinia virus infection disrupts the Bak-Mcl-1 complex. A. HeLa cells were treated with 2µM staurosporine (STS) for 1, 2, or 3 hours to induce apoptosis. Cells were lysed in 2% CHAPS and Mcl-1 was immunoprecipitated with anti-Mcl-1. Immunoprecipitates and lysates were western blotted with anti-Bak and anti-Mcl-1. **B.** HEK 293T cells were mock-infected or infected with VV, VV-FLAG-F1L, or VVΔF1L at an MOI of 10. Twelve hours post infection, cells were lysed in 2% CHAPS buffer and subjected to anti-Mcl-1 immunoprecipitation. Immunoprecipitates and lysates were western blotted as in (**A**). **C.** HEK 293T cells were infected as described in (**B**). Cells were lysed at 3, 6, and 12 hours post infection in 2% CHAPS buffer and anti-Mcl-1 was used for immunoprecipitation. Immunoprecipitates and lysates were western blotted as in (**A**).

due to a loss of Bak protein, as lysates western blotted with anti-Bak revealed sustained Bak levels (Fig 3.5C). Western blotting with anti-Mcl-1 demonstrated equivalent levels of Mcl-1 in immunoprecipitates and lysates in mock-infected, VV- and VVΔF1L-infected cells (Fig 3.5C). Together, these data revealed that VV infection disrupted the Bak-Mcl-1 complex. The slightly faster dissociation of Bak and Mcl-1 observed with VVΔF1L was likely a result of the apoptosis induced with this virus, since other apoptotic stimuli, such as STS, also disrupted the Bak-Mcl-1 complex (Fig 3.5A)

3.5 MCL-1 IS NOT RAPIDLY DEGRADED DURING VACCINIA VIRUS INFECTION

3.5.1 Mcl-1 is rapidly degraded following UV treatment, but not virus infection.

During treatment with apoptotic stimuli, such as UV irradiation, Mcl-1 dissociates from Bak and unbound Mcl-1 is ubiquitinated and degraded in a proteasome-dependent manner [216,266,289,354]. To demonstrate this, we treated HeLa cells with UV light and harvested whole cell lysates up to six hours post treatment. Western blotting with anti-Mcl-1 illustrated a decrease in Mcl-1 protein levels by two hours post UV treatment (Fig 3.6A). As a control, cells were pretreated with 10μM MG132, a chemical inhibitor of the 26S proteasome [622], prior to UV treatment. Treatment with MG132 enhanced Mcl-1 protein levels in the absence of UV light and, additionally, MG132 prevented Mcl-1 degradation following UV treatment (Fig 3.6A). Thus, Mcl-1 is sensitive to genotoxic stimuli, as UV exposure resulted in the rapid proteasomal degradation of Mcl-1. To determine that apoptosis induced by UV did not compromise cellular integrity by 6 hours post treatment, western blotting with anti-Bak served as a protein loading control (Fig 3.6A).

To investigate the stability of Mcl-1 during VV infection, we mock-infected HeLa cells or infected with VV, VVΔF1L, or VV-FLAG-F1L and harvested cell lysates at various times post infection. Western blotting with anti-Mcl-1 illustrated that in cells infected with VV, VVΔF1L, or VVFLAG-F1L, Mcl-1 remained relatively stable during the course of infection (Fig. 3.6B). Virus infection was

A

B
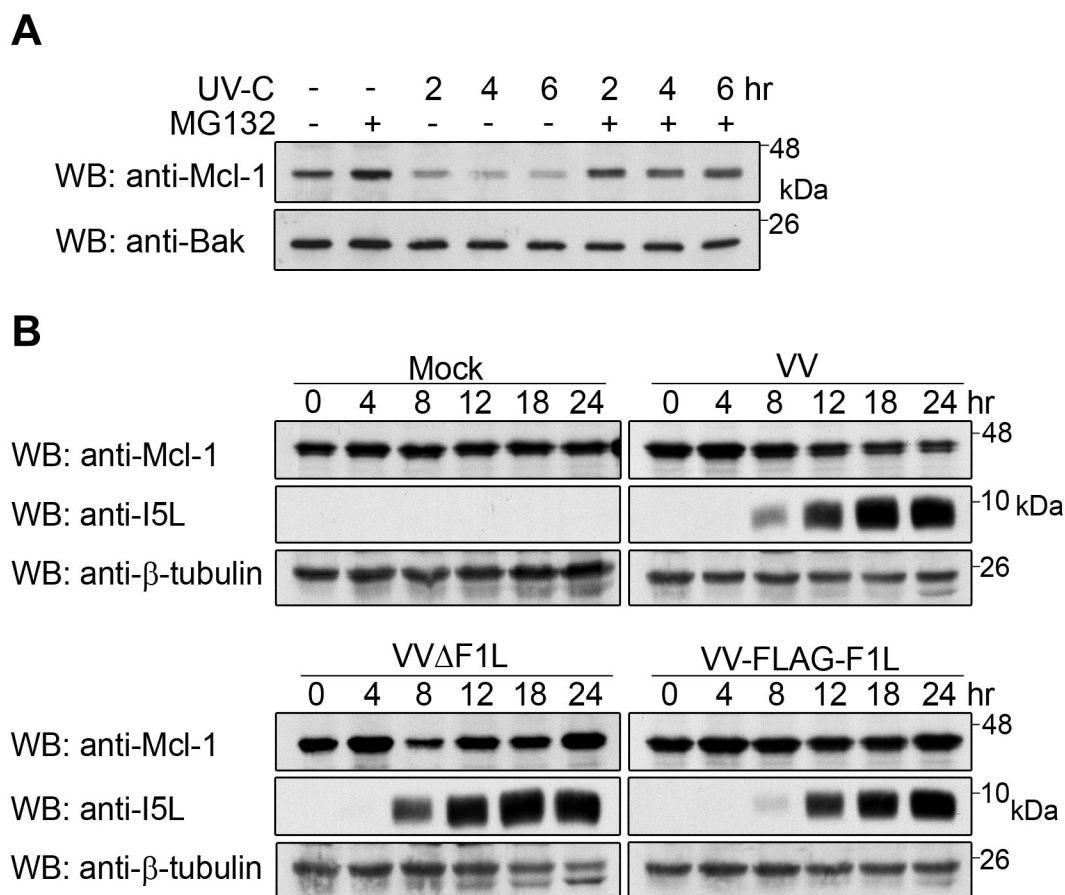
Figure 3.6 Mcl-1 is not rapidly degraded during vaccinia virus infection. A. HeLa cells were treated with 200mJ/cm^2 UV-C in the absence or presence of 10μM MG132 to inhibit the proteasome. Cell lysates were harvested at 2, 4, or 6 hours post UV treatment, subjected to SDS-PAGE, and western blotted with anti-Mcl-1 and anti-Bak. **B.** HeLa cells were mock-infected or infected with VV, VVΔF1L, or VV-FLAG-F1L at an MOI of 10. Cell lysates were harvested up to 24 hours post infected and western blotted with anti-Mcl-1, anti-I5L, or anti-β-tubulin.

confirmed by western blotting with anti-I5L, which detected the VV late protein I5L [571], while western blotting with anti-β-tubulin served as a loading control (Fig 3.6B). Therefore, despite being displaced from Bak during VV infection, Mcl-1 protein levels remained relatively stable, in contrast to the rapid loss of Mcl-1 following treatment with UV light.

3.5.2 Vaccinia virus does not induce a DNA damage response. Both UV light and virus infection are triggers of cellular stress. However, only UV irradiation resulted in rapid degradation of Mcl-1 (Fig 3.6) [216]. Since UV light causes a potent DNA damage response [623,624], we sought to determine whether the reason for Mcl-1 stability during VV infection was due to the absence of DNA damage. To address this, HeLa cells were mock-infected or infected with VV, VV-FLAG-F1L, or VVΔF1L. At 6 hours post infection, cells were mock-treated or treated with either etoposide or UV light, both of which result in considerable DNA damage. Cell lysates were harvested up to 6 hours following treatment with etoposide or UV and subject to SDS-PAGE. Using an antibody specific for phosphorylated histone H2AX as a marker for DNA double-strand breaks [625,626], we found no evidence of a DNA damage response in mock-infected or VV, VV-FLAG-F1L-, or VVΔF1L-infected cells up to 12 hours post infection (Fig 3.7). However, treatment of mock-infected or virus-infected cells with etoposide and UV-C resulted in DNA lesions, which were demonstrated by the phosphorylation of histone H2AX (Fig 3.7). The absence of phosphorylated histone H2AX during VV, VV-FLAG-F1L, and VVΔF1L infection indicated that virus infection alone did not stimulate a DNA damage response. Moreover, phosphorylated histone H2AX in virus-infected cells following etoposide or UV treatment demonstrated that VV was unable to prevent the DNA response following treatment with DNA damaging agents. Together, these data suggest that Mcl-1 was not rapidly degraded during VV infection, since unlike UV treatment, VV did not stimulate a DNA damage response.

3.6 MCL-1 REMAINS AT MITOCHONDRIA DURING VACCINIA VIRUS INFECTION
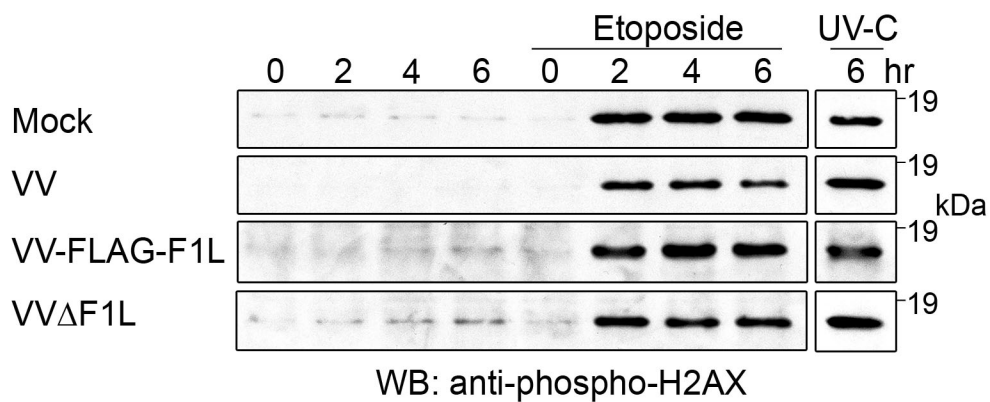
Figure 3.7 Vaccinia virus infection does not stimulate a DNA damage response. Mock-infected HeLa cells or HeLa cells infected at an MOI of 10 for 6 hours with VV, VV-FLAG-F1L, or VVΔF1L were treated with 100μM etoposide or 200mJ/cm^2 UV-C. Whole cell lysates were harvested at 0, 2, 4, or 6 hours post etoposide treatment or 6 hours post UV-C treatment and samples were western blotted with an antibody specific for phosphorylated histone H2AX (anti-phospho-H2AX) to demonstrate the induction of a DNA damage response.

Our observations indicated that the dissociation of Mcl-1 from Bak during VV infection was not followed by rapid degradation of Mcl-1 (Figs 3.5 and 3.6). Furthermore, in uninfected cells, the expression of EGFP-F1L did not alter the mitochondrial localization of Mcl-1 (Fig A.1). To further investigate the effect of VV infection on Mcl-1, we assessed the mitochondrial localization of Mcl-1. HeLa cells were either mock-infected or infected with VV, VVΔF1L, or VV-FLAG-F1L prior to mitochondrial fractionation. We verified the purity of the supernatant and mitochondrial fractions by western blotting for the mitochondrial-resident protein, manganese superoxide dismutase (MnSOD) [627]. In mock-infected and virus-infected cells, MnSOD was present in mitochondrial, but not supernatant, fractions (Fig 3.8A). To detect Mcl-1 levels at mitochondria, isolated supernatant and mitochondrial fractions were western blotted for Mcl-1. Upon infection with VV, VVΔF1L, or VVFLAG-F1L, Mcl-1 remained at mitochondria, similar to mock-infected cells (Fig 3.8A). In contrast, treatment of HeLa cells with UV-C prior to mitochondrial isolation resulted in a gradual loss of Mcl-1 from mitochondria (Fig 3.8B). While Mcl-1 was observed at mitochondria 2 hours post UV treatment, the presence of Mcl-1 was greatly reduced by 4 and 6 hours (Fig 3.8B), consistent with the degradation of Mcl-1 observed in UV-treated whole cell lysates (Fig 3.6A). Thus, unlike UV treatment, disruption of the Bak-Mcl-1 complex during VV infection did not result in the loss of Mcl-1 from mitochondria.

3.7 MCL-1 COMPENSATES FOR THE LOSS OF F1L DURING VACCINIA VIRUS INFECTION

3.7.1 Mcl-1 inhibits virus-induced apoptosis. The ability of F1L to bind Bak and the BH3-only protein BimL and inhibit apoptosis closely resembles the activity of Mcl-1 [266,567,592]. This functional similarity suggested that F1L may replace the anti-apoptotic role of Mcl-1 during infection by interacting with Bak and Bim and inhibiting cytochrome *c* release. To test whether Mcl-1 could compensate for the loss of F1L during VVΔF1L infection, we generated VVΔF1L-FLAG-Mcl-1, a recombinant F1L-deficient virus expressing FLAG-tagged Mcl-1, to determine
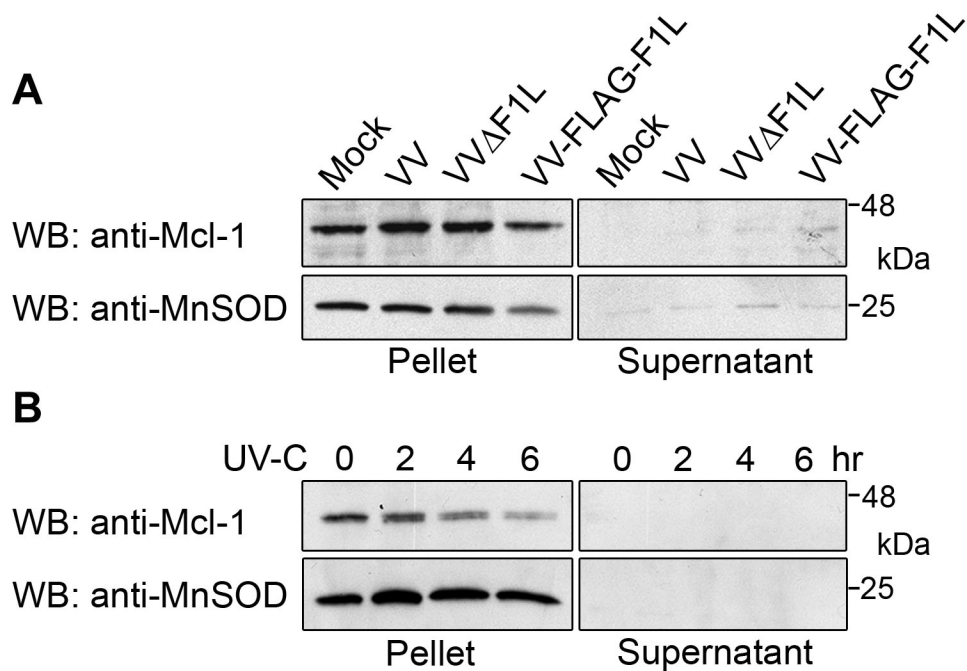
Figure 3.8 Mcl-1 remains at mitochondria during vaccinia virus infection. A. HeLa cells were mock-infected or infected with VV, VVΔF1L, or VV-FLAG-F1L at an MOI of 10 for 24 hours, and mitochondria were isolated. Ten micrograms of supernatant and mitochondrial pellet fractions were subject to SDS-PAGE and western blotted with anti-Mcl-1 and anti-manganese superoxide dismutase (MnSOD). **B.** HeLa cells were treated with 200mJ/cm^2 UV-C and mitochondria were isolated up to 6 hours post UV treatment. Supernatant and mitochondrial fractions were western blotted as in (**A**).

whether VVΔF1L-FLAG-Mcl-1 could prevent virus-induced apoptosis. Jurkat cells were analyzed for PARP cleavage following infection with VVΔF1L-FLAG-Mcl-1, the parental virus VVΔF1L, or wildtype VV expressing EGFP, VVEGFP. As expected, infection with VVEGFP failed to induce apoptosis, indicated by the presence of full-length PARP up to 15 hours post infection; however, infection with VVΔF1L resulted in a decrease of full-length PARP at 10 and 15 hours post infection and an increase in the amount of cleaved PARP (Fig 3.9A). In contrast to VVΔF1L, infection with VVΔF1L-FLAG-Mcl-1 did not induce PARP cleavage, demonstrating that Mcl-1 protected from virus-induced apoptosis in the absence of F1L. As controls, the expression of FLAG-Mcl-1 was detected by western blotting with anti-FLAG, and infection was confirmed using an antibody to the late viral protein I5L (Fig 3.9A).

To investigate events upstream of PARP cleavage, we determined whether Mcl-1 could replace the function of F1L by monitoring cytochrome c release during virus infection. Jurkat cells infected with VVEGFP, VVΔF1L, or VVΔF1L-FLAG-Mcl-1 were separated into cytosolic and mitochondria-containing fractions and western blotted with anti-cytochrome c. In VVEGFP-infected cells, cytochrome c release was completely inhibited (Fig 3.9B). In contrast, cytochrome c was predominantly found in cytosolic fractions after 12 hours of infection with VVΔF1L, signifying a loss of mitochondrial integrity (Fig 3.9B). Notably, VVΔF1L-FLAG-Mcl-1 protected against the release of cytochrome c and the protein was contained within mitochondria up to 12 hours post infection (Fig 3.9B). As a control, pellet and supernatant fractions were western blotted for Bak, which served as a mitochondrial marker (Fig 3.9B). Together, these data suggested that the presence of Mcl-1 preserved mitochondrial integrity and downstream apoptosis in the absence of F1L during VV infection.

3.7.2 Mcl-1 inhibits Bak and Bax activation during virus infection. The activation of Bak and Bax is an essential step that precedes the release of cytochrome c from mitochondria [177,187,188,189,190]. Both proteins undergo
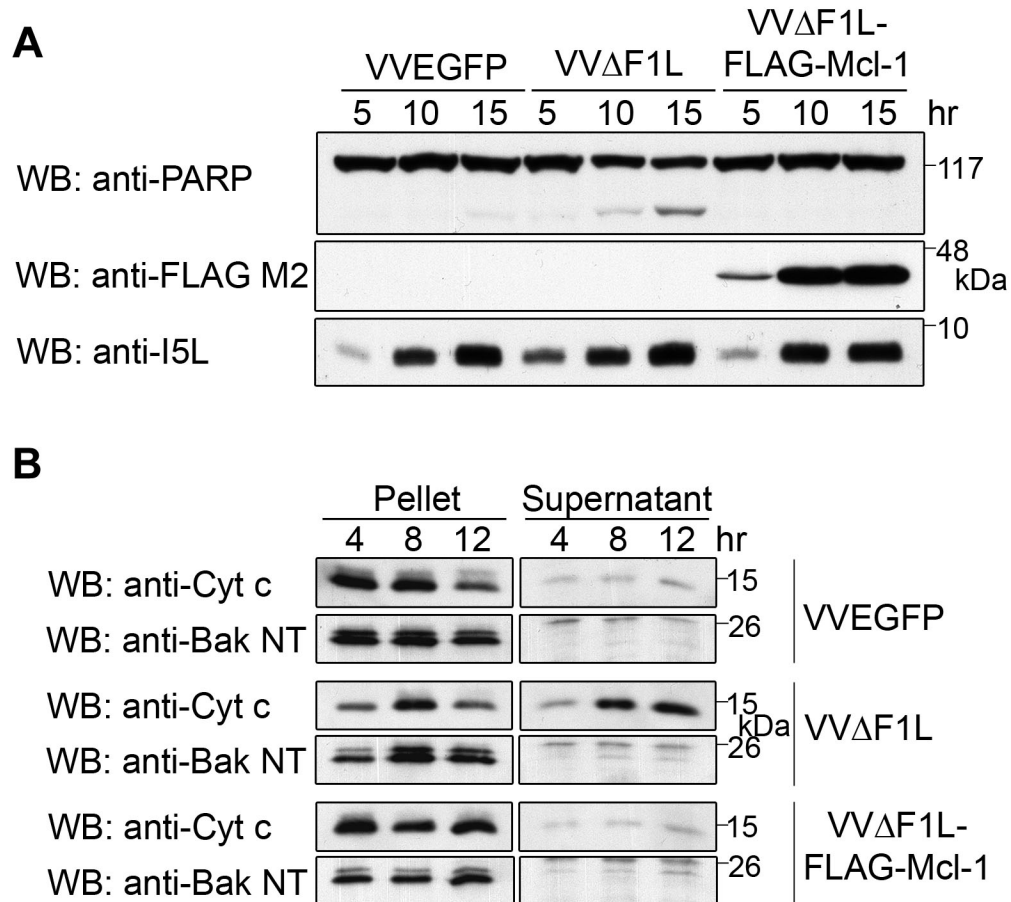
Figure 3.9 Mcl-1 prevents apoptosis induced by VVΔF1L. A. Jurkat cells were infected at an MOI of 10 with VVEGFP, VVΔF1L, or VVΔF1L-FLAG-Mcl-1. Cell lysates were harvested at 5, 10, and 15 hours post infection and western blotted with anti-PARP, anti-FLAG M2, and anti-I5L. **B.** Jurkat cells were infected with VVEGFP, VVΔF1L, or VVΔF1L-FLAG-Mcl-1 at an MOI of 10 for 4, 8, or 12 hours. Mitochondria-containing pellets and cytosolic supernatants were separated after lysis with digitonin. Pellet fractions were resuspended in 0.1% Triton lysis buffer and both pellet and supernatant fractions were western blotted with anti-cytochrome c (anti-Cyt c) and anti-Bak NT.

a series of conformational changes including the exposure of the N-terminus [177,181,184,281]. During infection, F1L prevents Bak activation through direct interaction and the absence of F1L during infection results in full activation of Bak and subsequent apoptosis [550,551]. To establish whether VVΔF1L-FLAG-Mcl-1 could prevent VVΔF1L-induced Bak activation, we infected Jurkat cells with VVEGFP, VVΔF1L, or VVΔF1L-FLAG-Mcl-1 for 4 hours. Infected cells were also treated with STS to determine if VVΔF1L-FLAG-Mcl-1 could prevent Bak activation in response to an external stimulus, in addition to virus-induced apoptosis. Virus-induced and STS-induced apoptosis in infected Jurkat cells were assayed by monitoring Bak activation using a conformation specific antibody, anti-Bak AB-1, that detects the N-terminal exposure of Bak following its activation during apoptosis [177,184]. As shown in figure 3.10 panel a, mock-infected Jurkat cells treated with STS demonstrated an increase in anti-Bak AB-1 fluorescence, indicative of Bak activation and exposure of its N-terminus. Jurkat cells infected with VVEGFP did not undergo Bak activation, and these cells were protected from STS-induced Bak activation (Fig 3.10 panel b). However, VVΔF1L-infected cells demonstrated an increase in Bak AB-1 fluorescence as expected, since this virus induces apoptosis upon infection (Fig 3.10 panel c) [550]. Bak activation was even more pronounced following STS treatment in VVΔF1L-infected cells, highlighting the inability of this pro-apoptotic virus to protect from external apoptotic stimuli (Fig 3.10 panel c). In contrast to VVΔF1L, the presence of Mcl-1 in VVΔF1L-FLAG-Mcl-1 was sufficient to prevent Bak activation during infection and in response to STS treatment (Fig 3.10 panel d). This suggested that the expression of Mcl-1 rendered VVΔF1L protective against both virus- and STS-induced Bak activation and subsequent apoptosis. The measurement of Bak N-terminal exposure was specific because an isotype control antibody did not display an increase in fluorescence following STS treatment (Fig 3.10 panel e). As shown previously, Bcl-2 overexpressing Jurkat cells infected with VVΔF1L and treated with STS prevented Bak activation (Fig 3.10 panels j-m) [533,550]. The
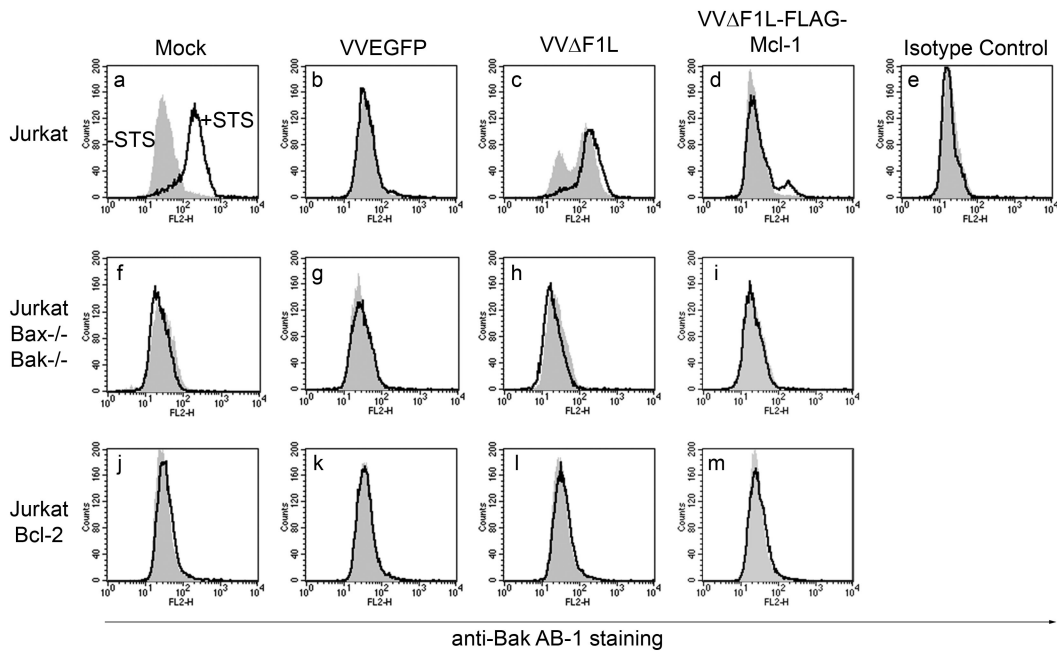
Figure 3.10 Mcl-1 inhibits Bak activation during VVΔF1L infection. Jurkat cells
(**a-e**), Jurkat cells devoid of Bax and Bak (**f-i**), and Jurkat cells overexpressing Bcl-2
(**j-m**) were mock-infected or infected with VVEGFP, VVΔF1L, or VVΔ
F1L-FLAG-Mcl-1 for 4 hours at an MOI of 10. Cells were then treated with 250nM
STS for 1.5 hours to induce apoptosis. Bak N-terminal exposure was monitored
by staining cells with the conformation-specific anti-Bak AB-1 antibody or
anti-NK1.1, an isotype control antibody. Shaded histograms, untreated cells;
open histograms, STS-treated cells.

155

specificity of the assay was confirmed using Jurkat cells deficient in Bak and Bax [561], which displayed no increase in anti-Bak AB-1 fluorescence following VVΔF1L infection and STS treatment (Fig 3.10 panels f-i). Together, these data indicated that although F1L prevented the activation of Bak during VV infection, Mcl-1 can replace this activity and protect against virus- and STS-induced apoptosis during VVΔF1L infection.

In order to effectively inhibit apoptosis, both Bak and Bax must be impeded since each protein alone is sufficient to mediate death signals resulting in cytochrome *c* release [189,190]. Although F1L does not interact with Bax directly, Bax activation is inhibited by F1L during VV infection [549]. To determine whether Mcl-1 could prevent Bax activation during VVΔF1L infection, Jurkat cells were mock-infected or infected with VVEGFP, VVΔF1L, or VVΔF1L-FLAG-Mcl-1 for 6 hours. As described above, infected cells were treated with STS for an additional 2 hours and the conformation-specific Bax antibody, anti-Bax 6A7, was used to monitor Bax activation [181,281]. While mock-infected cells did not contain active Bax unless treated with STS, Bax remained inactive in VVEGFP-infected cells, even in the presence of STS (Fig 3.11 panels a and b). While very little Bax was activated at 6 hours post infection with VVΔF1L, the F1L-deficient virus was unable to prevent Bax activation in response to STS treatment, as described previously (Fig 3.11 panel c) [534,549]. However, VVΔF1L-FLAG-Mcl-1 completely prevented Bax activation during infection in the presence and absence of STS (Fig 3.11 panel d), indicating that Mcl-1 compensated for the lack of F1L by inhibiting the activation of both Bak and Bax during infection, thereby preventing apoptosis. Thus, the anti-apoptotic mechanisms of F1L and Mcl-1 appear to be highly similar, despite the lack of sequence conservation between F1L and all cellular Bcl-2 family members.

3.8 DISCUSSION

The activation of Bak and Bax are critical events that initiate MOMP and, as such, the activity of these two proteins is tightly regulated [100,101]. In
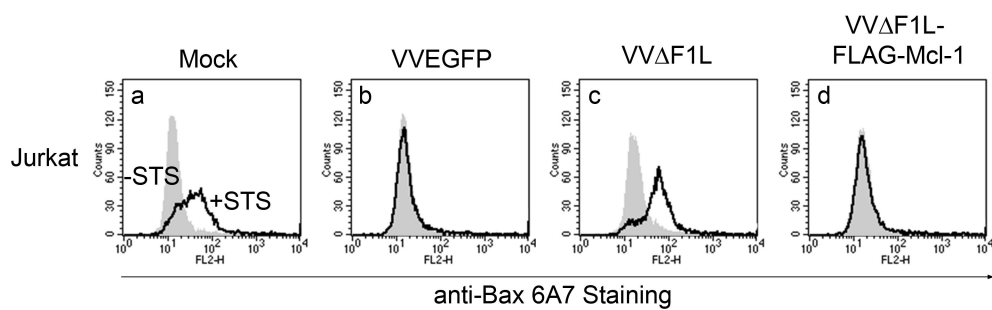
Figure 3.11 Mcl-1 inhibits Bax activation during VVΔF1L infection. Jurkat cells were mock-infected (**a**) or infected with VVEGFP (**b**), VVΔF1L (**c**), or VVΔ F1L-FLAG-Mcl-1 (**d**) at an MOI of 10 for 6 hours. To induce apoptosis, cells were treated with 2μm STS for 2 hours before staining with the conformation-specific anti-Bax 6A7 antibody to detect Bax activation. Shaded histograms, untreated cells; open histograms, STS-treated cells.

conjunction with Bcl-xL, Mcl-1 constitutively interacts with Bak to prevent its activation [266,289,354]. In order for Bak activation to occur, the protein must be released from the restraints of Mcl-1 [266,289,354]. The dissociation from Bak is often accompanied by the destruction of Mcl-1, yet the latter event is not necessary for Bak activation [216,266,354,435].

Virus infection is a potent trigger of apoptosis and in order to overcome this barrier, VV produces F1L, an anti-apoptotic protein that localizes to mitochondria and interferes with Bak and Bax activation [547,548,549,550,551]. F1L constitutively interacts with Bak and a virus devoid of F1L can no longer prevent activation-induced conformational changes in Bak [550,551]. We have demonstrated that the interaction between F1L and Bak was evolutionarily conserved, as F1L was able to bind human, murine, and chicken Bak (Fig 3.1). We have also confirmed that F1L required the Bak BH3 domain for interaction, in a similar manner to Mcl-1 and Bcl-xL (Figs 3.2-3.4) [266,289]. Binding to the Bak BH3 domain has also been reported for KSHV Bcl-2, which bound Bak BH3 peptides but failed to bind a BH3 domain bearing the L78A mutation [504]. The shared requirement of F1L and Mcl-1 for the Bak BH3 domain suggested that F1L may out-compete Mcl-1 for Bak binding. In agreement with this idea, Bak and Mcl-1 dissociated during VV infection (Fig 3.5). If F1L actively displaced Mcl-1, the disruption of the Bak-Mcl-1 complex observed during infection with VVΔF1L was likely due to the apoptotic response initiated by the virus in the absence of F1L. Alternatively, disruption of the Bak-Mcl-1 complex may occur in response to VV infection and F1L may be required to bind and sequester Bak after its dissociation from Mcl-1, similar to AdV E1B-19K [354].

In contrast to the rapid loss of Mcl-1 after UV irradiation, Mcl-1 displacement from Bak during VV infection did not result in Mcl-1 degradation, and moreover, Mcl-1 remained at mitochondria (Figs 3.6 and 3.8) [216,266,354]. The stabilization of Mcl-1 was consistent with the observation that VV infection did not induce a DNA damage response (Fig 3.7). In contrast, AdV infection

induces a DNA damage response that results in rapid degradation of Mcl-1; in this case, however, Bak is inhibited by binding E1B-19K [354]. Perhaps the differences in the fate of Mcl-1 during VV and AdV infection may rely on the specific BH3-only proteins that are activated in response to each virus, which could either stabilize Mcl-1 or trigger its rapid degradation. Indeed, the structures of Mcl-1 bound to stabilizing BH3 peptides from Bim and Puma and the degradation-inducing BH3 peptide from Noxa have been solved [242,243]. The residues in the Noxa BH3 domain that are critical for mediating Mcl-1 destruction have been mapped to the C-terminal region of the peptide [242]. Interestingly, however, binding of the BH3 ligands from Bim, Puma, and Noxa does not cause significant changes in the structure of Mcl-1; therefore, the signal for Mcl-1 degradation is not simply a conformational change upon binding of the Noxa BH3 motif [242,243]. Although the degradation signal remains elusive, it is likely that Noxa is upregulated in response to the DNA damage response initiated by AdV infection, resulting in Mcl-1 destruction [354]. Based on the stabilization of Mcl-1 during VV infection, BH3-only proteins other than Noxa or Mule may be responsible for disrupting the Bak-Mcl-1 complex in response to VV, although these BH3-only proteins await further identification.

Intriguingly, the mechanistic similarities between F1L and Mcl-1 were highlighted by a recombinant VVΔF1L expressing FLAG-Mcl-1. Mcl-1 was able to replace the function of F1L during infection with VVΔF1L, as demonstrated by the inhibition of Bak, cytochrome *c* release, and PARP cleavage (Figs 3.9-3.11). Moreover, Mcl-1 compensated for the loss of F1L by preventing Bax activation (Fig 3.12); however, similar to F1L, the interaction between Mcl-1 and Bax is not necessary for Bax inhibition [552,628]. Together, these data highlight the functional similarities between Mcl-1 and F1L, despite lacking sequence similarity. Additionally, the above data underscore the importance of inhibiting Bak activation in response to VV infection and propose a role for F1L in replacing Mcl-1 in order to maintain Bak in an inactive state.

CHAPTER 4: Identification and Characterization of the Functional Domains in Vaccinia Virus F1L

A portion of this chapter has been published:

Campbell, S., B. Hazes, M. Kvansakul, P. Colman, and M. Barry. 2010. Vaccinia virus F1L interacts with Bak using highly divergent Bcl-2 homology domains and replaces the function of Mcl-1. Journal of Biological Chemistry **285:**4695-4708.

The protein alignment in Figure 4.1 was generated by Dr. B. Hazes (University of Alberta, Edmonton, Alberta) and the schematic diagram of F1L in Figure 4.7 was provided by Dr. M. Kvansakul (La Trobe University, Melbourne, Australia). The cloning of F1L(84-226) into pEGFP-C3 was initiated by D. Quilty, an undergraduate honours student mentored by S. Campbell. Nancy Hu, a graduate student mentored by S. Campbell, produced pSC66-FLAG-F1L(V104A). Robyn Burton, an undergraduate honours student, Alastair Teale, a summer student, and Ninad Mehta, a graduate student, initiated cloning of recombinant vaccinia viruses bearing V104A, G144F, A119W, M115W, I129F, and T149L mutations in F1L, all under the mentorship of S. Campbell. The remaining experiments contained in this chapter were performed by S. Campbell. The original manuscript was written by S. Campbell and a major editorial contribution was made by Dr. M. Barry.

4.1 INTRODUCTION

The Bcl-2 family of proteins regulate the intrinsic pathway of apoptosis and all members contain at least one BH domain (Fig 1.10) [100,101]. Multi-domain members of the Bcl-2 family, along with the BH3-only protein Bid, share a conserved α-helical fold consisting of 8 or 9 α-helices (Fig 1.14) [175]. This core fold forms a hydrophobic pocket that acts as a receptor for BH3 motifs from neighbouring molecules and this conventional BH3:groove interface is the basis for the majority of homo- and heterotypic interactions among the family (Fig 1.14) [175,629]. Unlike the core fold in multi-domain members, the naturally disordered BH3 domain undergoes major conformational changes upon binding the hydrophobic binding pocket to yield a structured amphipathic helix [249]. Most members of the Bcl-2 family also possess C-terminal tail anchors that are necessary and sufficient for membrane targeting primarily, but not exclusively, to mitochondria [220,221].

While sequence identity within the Bcl-2 family is quite low, sequences within BH domains are highly conserved and critical for protein function (Fig 1.13) [175]. In anti-apoptotic members, the BH1, BH2, and BH3 domains fold to form the binding cleft that binds BH3 motifs from the effectors Bak and Bax or BH3-only proteins [175,629]. The seminal structure of Bcl-xL bound to a BH3 peptide from Bak demonstrated that the interaction involves hydrophobic contacts between the amphipathic BH3 helix of Bak with hydrophobic residues lining the binding groove of Bcl-xL (Fig 1.14) [245]. In addition, electrostatic contacts between the amphipathic BH3 motif and the polar residues lining the sides of the binding pocket also strengthen the interaction [245]. Both hydrophobic and ionic interactions are also implicated in the binding of Bcl-2 and the Bax BH3 peptide [630], Bcl-w and the Bid BH3 peptide [631], A1 and the Bim BH3 peptide [239], and Mcl-1 with BH3 peptides derived from Bim, Noxa, and Puma [242,243,632]. The specific chemical properties of the residues involved in these interactions ultimately confer specificity in binding of BH3 peptides to

binding grooves of anti-apoptotic proteins. Binding profiles of BH3-only proteins have been extensively studied [264,269] and the structure of anti-apoptotic members, such as Mcl-1, is slightly flexible in order to allow for binding to multiple BH3 ligands [243,632]. There are residues, however, that are absolutely critical for protein binding and function. In the case of Bak and Bax, the BH3 domain is absolutely required for these proteins to oligomerize and induce apoptosis [258,633]. Anti-apoptotic members require residues primarily within the BH1 and BH2 domains to form the proper environment within the BH3 binding groove to inhibit the action of both Bak and Bax and likely BH3-only proteins [260,634,635,636,637].

As the interactions among the Bcl-2 family of proteins dictate the fate of a cell, many viruses have co-opted Bcl-2 homologues to interfere with the cell death programme in favour of virus replication [496,497,638]. vBcl-2 proteins display obvious sequence similarity with cellular anti-apoptotic proteins, particularly within BH domains [497]. Based on sequence conservation, many vBcl-2 homologues have been identified in large DNA viruses: KSHV Bcl-2 [500], EBV BHRF1 [639,640], MHV-68 M11 [503], AdV E1B-19K [519,641,642], ASFV A179L [513], and fowlpox virus FPV039 [533]. Moreover, KSHV Bcl-2, EBV BHRF1, and MHV-68 M11 adopt a helical bundle fold strikingly similar to Bcl-2 family members [504,509,510,511]. However, it has become increasingly apparent that divergence at the sequence level has occurred in many viral anti-apoptotic proteins, yet the overall 3D structure remains conserved. This has been clearly shown for myxoma virus M11L, which adopts a Bcl-2 like fold [539,540]. Moreover, HCMV vMIA and Orf virus ORFV125 do not display significant sequence similarity with Bcl-2 family members, yet the proteins are believed to adopt a fold reminiscent of Bcl-2 proteins based on secondary structure predictions [526,543,544,643].

In VV, F1L is responsible for obstructing mitochondrial events in order to ensure apoptosis is inhibited [547,548,549,550,551,644]. F1L functions in a

similar manner to cellular Bcl-2 proteins by inhibiting the activation of Bak and Bax through interactions with Bak and BimL (Fig 1.22) [549,550,551]. Moreover, the interaction between F1L and Bak was dependent on the Bak BH3 motif, indicating that F1L interacted with the same structural motifs in Bak as cellular anti-apoptotic proteins, such as Mcl-1 and Bcl-xL (Figs 3.2-3.4). Inspection of the F1L sequence, however, did not reveal significant similarity to cellular or viral Bcl-2 proteins so the way in which F1L interacts with Bak and BimL was unclear. In order to investigate the interactions between F1L and its major interacting partner Bak, the F1L sequence was analyzed for putative BH domains that may reside within the protein. Concomitantly, the structure of MVA F1L was solved and revealed that despite limited sequence homology to cellular Bcl-2 family members, F1L adopted a Bcl-2-like fold (Fig 1.23) [555]. Thus, we sought to characterize the functional domains in F1L that are important for binding and anti-apoptotic activity and validate the domains proposed in the recently solved structure of F1L.

4.2 F1L CONTAINS HIGHLY DIVERGENT BH DOMAINS

Cellular anti-apoptotic cellular Bcl-2 proteins, such as Bcl-xL and Mcl-1, interact with Bak using highly conserved BH1, BH2, and BH3 domains, which form a hydrophobic pocket to accept the Bak BH3 domain [223,236]. Overall, little sequence similarity is observed between F1L and cellular Bcl-2 proteins. Additionally, F1L bares little sequence identity to other poxviral anti-apoptotic proteins outside of the *Orthopoxvirus* genus [546]. Despite this, F1L is a potent anti-apoptotic protein capable of interacting with the cellular Bcl-2 family members Bak and BimL [549,550,551]. Although F1L lacks significant sequence identity to the highly conserved consensus sequences of Bcl-2 proteins, sequence patterns with properties compatible with the known structure of BH domains were delineated. By correlating the F1L sequence to structural constraints of known Bcl-2 protein structures, we predicted the location of putative BH domains in F1L (Fig 4.1). Similar to cellular Bcl-2 proteins, F1L was

```
BCL-XL    (1)  --------------------------------------------------
VACV F1L  (1)  MLSMFMCNNIVDYVDDIDNGIVQDIEDEASNNVDHDYVYPLPENMVYRFD
MPXV C7L  (1)  MLSMFMYNNIIDYVH------VHDIEDEASDNDDRDYVYPLPENMVYRFD
MYXV M11L (1)  --------------------------------------------------
SFV GP11L (1)  --------------------------------------------------

                                     BH4                        BH3
BCL-XL    (1)  ----------MSQSNRELVVDFLSYKLSQKGYSW--IPMAAVKQALREA
VACV F1L  (51) KSTNILDYLSTERDHVMMAVRYYMSKQRLDDLYRQLPTKTRSYIDIINIY
MPXV C7L  (45) KSTNILDYLSTERDHVMMAVQYYMSKQRLDDLYGQLPTKTRSYVDIINTY
MYXV M11L (1)  ----------MMSRLKTAVYDYLNDVDITEC------TEMDLLCQLSNC
SFV GP11L (1)  -----------MSRLKEVVYTYLNGGDITEC------TEIDLLCQLVNC
                        α1                              α2

                 *    *   *   *                         * BH1
BCL-XL    (38) GDEFELRYRRAFSDLTSQLHITPGTAYQSFEQVVNELFRDGV---NWGRI
VACV F1L  (101) CDKVSNDYNRDMNIMYDMAST----KSFTVYDINNEVNTILMDNKGLGVR
MPXV C7L  (95) CDKVNNDYNSDMNIMCDMAST----ESFTVYDINNEVNTILMNNKGLGVR
MYXV M11L (34) CDFINETYAKNYDTLYDIMERDI--LSYNIVNIKNTLTFALR-DASPSVK
SFV GP11L (33) CNFINNTYAKNYDVLCDIMERDI--LSYNIENIKKALGFALL-DASPSVK
                       α3              α4                    α5

                                                   BH2
BCL-XL    (85) VAFFSFGGALCVESVDKE-MQVLVSRIAAWMATYLNDHLEPWIQENGGWD
VACV F1L  (147) LATISFITELGRRCMNP---VKTIKMFTLLSHTICDDCFVDYITDIS-PP
MPXV C7L  (141) LATISFITELGRRCMNP---VETIKMFTLLSHTICDDYFVDYITYISTPR
MYXV M11L (81) LATLTLLASVIKKLNKI---QHTDAAMFSEVIDGIVAEEQQVIGFIQKKC
SFV GP11L (80) LATLALLSIILKKLNKI---RHTEACVFSDVIDGITAEENKVIGFIQEKY
                              α6                    α7    α8

                              TM
BCL-XL    (135) TFVELYGNNAAAESRKGQERFNRWFLTGMTVAGVVLLGSLFSRK----
VACV F1L  (194) DNTIPNTSTREYL---------KLIGITAIMFATYKTLKYMIG-----
MPXV C7L  (189) DNAIH--STREYL---------KIMGIAVIMFATYKTLKYMIG-----
MYXV M11L (129) KYNTTYYNVRSGGC--------KISVYLTAAVVG-FVAYGILKWYR--
SFV GP11L (128) KYNTTYYNKRS----------KLPVYLSTAMVATLIVYGVIKWRRGT
```

Figure 4.1 F1L contains divergent BH domains. Protein sequences of human Bcl-xL, vaccinia virus strain Copenhagen (VACV) F1L, monkey poxvirus (MPXV) C7L, myxoma virus (MYXV) M11L, and Shope fibroma virus (SFV) GP11L were aligned based on spacing of hydrophobic residues (highlighted in grey). The eight predicted α-helices in F1L are delineated by α1 to α8. Putative BH1, BH2, BH3, and BH4 domains were identified in F1L, C7L, M11L, and GP11L based on corresponding domains in the cellular anti-apoptotic protein Bcl-xL (BH domains are boxed). The residues in Bcl-xL that are required for interaction with other cellular Bcl-2 proteins are indicated with asterisks. All five proteins contain C-terminal hydrophobic transmembrane (TM) domains.

predicted to contain eight α-helices. Identification of four putative BH domains in F1L was based on the conservation of hydrophobic residues that line the binding groove of Bcl-xL. In fact, the positions of many hydrophobic residues in Bcl-xL were not only conserved in F1L, but in the anti-apoptotic proteins of monkeypox virus, myxoma virus, and Shope fibroma virus as well (Fig 4.1). The identification of putative BH domains in F1L was based on conserved structural constraints of cellular Bcl-2 proteins and the conservation of hydrophobic residues in other poxviral anti-apoptotic proteins. However, the newly identified F1L BH domains displayed little sequence conservation with BH domains of cellular anti-apoptotic and pro-apoptotic Bcl-2 family members (Fig 4.2). Yet, importantly, the predicted BH domains we identified in F1L were confirmed by the crystal structure of MVA F1L [555].

4.3 F1L BH MUTANTS RETAIN MITOCHONDRIAL LOCALIZATION

To determine the importance of the predicted BH domains for the function of F1L, we generated a panel of EGFP-tagged F1L constructs, two of which contained large N-terminal deletions (Fig 2.1). EGFP-F1L(84-226) lacked the first 83 amino acids including the BH4 domain, whereas EGFP-F1L(109-226) lacked the first 108 amino acids, spanning the BH3 and BH4 domains. To specifically target select BH domains, we also created EGFP-tagged F1L mutants devoid of either the BH1 or BH3 domains: EGFP-F1LΔBH1 lacked amino acids 144 to 156, and EGFP-F1LΔBH3 lacked amino acids 93 to 108 (Fig 2.1). In order to establish the effect of F1L mutations on subcellular targeting, the localization of F1L BH mutants was examined. To this end, HeLa cells were transiently transfected with pEGFP, pEGFP-F1L, pEGFP-F1L(84-226), pEGFP-F1L(109-226), pEGFP-F1LΔBH1, or pEGFP-F1LΔBH3. Live cells were stained with the mitochondria-selective dye, MitoTracker [645], and both EGFP fluorescence and MitoTracker staining were visualized by live cell confocal microscopy. EGFP fluorescence was detected in both the cell and nucleus of transfected cells, with no mitochondrial colocalization (Fig 4.3 panels a-c). In comparison, EGFP-F1L

```
                          BH1                                    BH2                                    BH3
Human Bcl-2 (137-155) LFRDGV-NWGRIVAFFEFGG   (188-199) WIQDNGGWDAFV-   (93-107)  VHLTLRQAGDDFSRR-
Human Bcl-xL (130-148) LFRDGV-NWGRIVAFFSFGG   (181-192) WIQENGGWDTFV-   (86-100)  VKQALREAGDEFELR-
Human Mcl-1  (253-272) VFSDGVTNWGRIVTLISFGA   (305-316) WLVKQRGWDGFV-   (209-223) ALETLRRVGDGVQRN-
  Human Bak  (118-136) LFESGI-NWGRVVALLGFGY   (170-181) WLAQRGGWVAAL-   (74-88)   VGRQLAIIGDDINRR-
  Human Bax   (99-118) MFSDGNFNWGRVVALFYFAS   (151-162) WIQDQGGWDGLL-   (59-73)   LSECLKRIGDELDSN-
  VVCop F1L  (135-154) TILMDNKGLGVRLATISFIT   (179-190) DDCF-VDYITDIS   (93-108)  YIDIINIYCDKVSNDY
  Consensus            LF DGV NWGRIVALFSFG              WIQDNGGWDAFV               V    LR AGDDF RR

                          BH4
Human Bcl-2  (10-28)   DNREIVMKYIMYKLSQRGY
Human Bcl-xL (4-22)    SNRELVVDFLSYKLSQKGY
Human Bcl-w  (9-27)    DTRALVADFVGYKLRQKGY
  VVCop F1L  (64-82)   DHVMMAVRYYMSKQRLDDL
  Consensus            D R LV   YKL QKGY
```

Figure 4.2 The putative BH domains in F1L display little sequence conservation with cellular Bcl-2 proteins. Amino acid sequences of BH1, BH2, and BH3 domains from VV Copenhagen (Cop) F1L and human anti-apoptotic proteins Bcl-2, Bcl-xL, and Mcl-1, and human pro-apoptotic proteins Bak and Bax. The divergent BH4 domain of F1L was aligned with human anti-apoptotic proteins Bcl-2, Bcl-xL, and Bcl-w, which contain consensus BH4 domains. Conserved residues are highlighted in black, similar residues in grey, and consensus sequences are provided underneath each alignment.

	EGFP	MitoTracker	Merge
EGFP	a	b	c
EGFP-F1L	d	e	f
EGFP-F1L (84-226)	g	h	i
EGFP-F1L (109-226)	j	k	l
EGFP-F1L ΔBH1	m	n	o
EGFP-F1L ΔBH3	p	q	r

Figure 4.3 F1L BH domain mutants localize to mitochondria. To determine the subcellular localization of F1L BH mutants, HeLa cells were transfected with pEGFP (**a-c**), pEGFP-F1L (**d-f**), pEGFP-F1L(84-226) (**g-i**), pEGFP-F1L(109-226) (**j-l**), pEGFP-F1LΔBH1 (**m-o**), or pEGFP-F1LΔBH3 (**p-r**) for 18 hours. Cells were stained with MitoTracker to visualize mitochondria and EGFP and MitoTracker fluorescence were analyzed by live cell confocal microscopy. Bar=15μm.

adopted a reticular pattern that colocalized completely with MitoTracker, indicating that EGFP-F1L was present at mitochondria (Fig 4.3 panels d-f). Mutation of large N-terminal fragments in F1L did not appear to alter mitochondrial localization as both EGFP-F1L(84-226) and EGFP-F1L(109-226) colocalized with MitoTracker (Fig 4.3 panels g-l). Additionally, deleting either the BH1 or BH3 domain from F1L had no effect on mitochondrial localization (Fig 4.3 panels m-r). Therefore, each F1L BH mutant was capable of targeting to mitochondria, likely due to the presence of an intact C-terminal transmembrane domain.

4.4 MUTATING BH DOMAINS IN F1L ABROGATES ANTI-APOPTOTIC ACTIVITY

Deletion of the BH1 domain, BH3 domain, or the first 108 amino acids in F1L did not alter subcellular localization (Fig 4.3). To determine whether the mitochondrial-localized F1L BH mutants were still functional, each mutant was assessed for anti-apoptotic activity. HeLa cells were transfected with pEGFP, pEGFP-F1L, pEGFP-F1L(84-226), pEGFP-F1L(109-226), pEGFP-F1LΔBH1, or pEGFP-F1LΔBH3. As a control, we transfected cells with the transmembrane domain of F1L appended to EGFP, EGFP-F1L(206-226), which localizes to mitochondria but fails to inhibit apoptosis (Fig 2.1) [548]. Following transfection, cells were treated with TNFα to stimulate apoptosis for 6 hours. Cell viability was measured with TMRE, a mitochondrial-specific fluorophore that is dependent on Δψm; thus, depolarized mitochondria in apoptotic cells do not retain the selective dye [171,172]. The survival and inflammatory pathways activated by TNFα require protein synthesis, whereas inhibition of protein synthesis sensitizes cells to the apoptotic arm of the TNFα pathway, which does not require RNA or protein production [74,75,76]. Therefore, addition of cycloheximide, a protein synthesis inhibitor, promoted the apoptotic signalling arm of TNFα. Apoptosis was assessed by examining EGFP-positive cells for TMRE fluorescence in the absence and presence of TNFα by flow cytometry. Data from three independent experiments are represented in figure 4.4A. Approximately 50% of EGFP-

A

B

WB: anti-EGFP
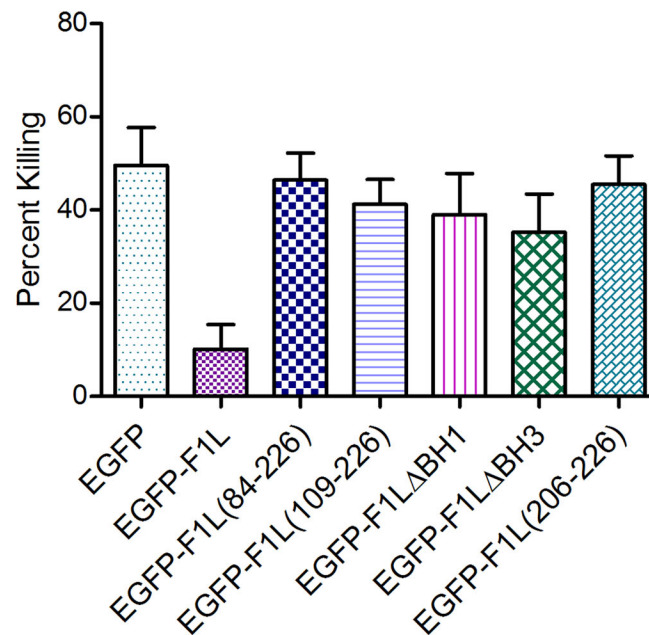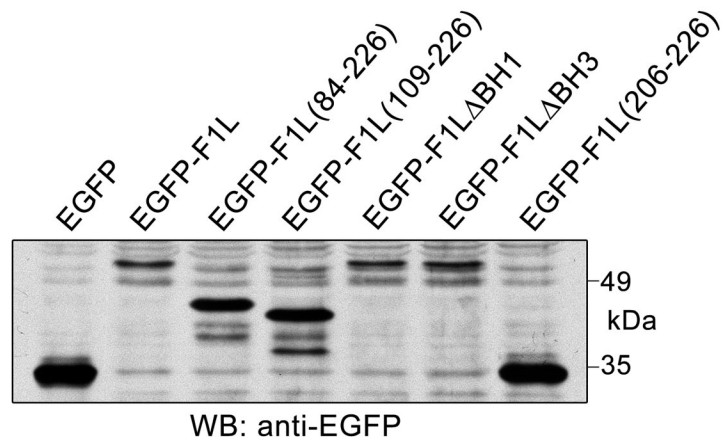
Figure 4.4 F1L BH mutants are unable to inhibit TNFα-induced apoptosis. A. The anti-apoptotic activity of F1L BH mutants was tested by transfecting HeLa cells with pEGFP, pEGFP-F1L, pEGFP-F1L(84-226), pEGFP-F1L(109-226), pEGFP-F1LΔ BH1, pEGFP-F1LΔBH3, and pEGFP-F1L(206-226). Eighteen hours post transfection, cells were treated with 10ng/mL TNFα and 5μg/mL cyclohexamide for 6 hours before staining with TMRE. EGFP and TMRE fluorescence were analyzed by flow cytometry and the percentage of killing following TNFα treatment from three independent experiments is represented. **B.** A duplicate experiment was set up as in (**A**). Following 6 hours with TNFα and cyclohexamide, cell lysates were harvested in SDS sample buffer and subject to SDS-PAGE. EGFP-tagged protein levels were resolved by western blotting with anti-EGFP.

expressing HeLa cells were sensitive to TNFα treatment and underwent apoptosis. In contrast, cells expressing EGFP-F1L were protected from TNFα-induced apoptosis; only 10% of EGFP-F1L-expressing cells were apoptotic (Fig 4.4A). Unlike wildtype EGFP-F1L, mutations in the N-terminal region of F1L or mutation of the BH1 or BH3 domain of F1L rendered the mutant sensitive to apoptosis induced by TNFα, indicated by mitochondrial depolarization in nearly 35-45% of transfected cells (Fig 4.4A). Not surprisingly, a mutant comprising only the C-terminal transmembrane of F1L, EGFP-F1L(206-226), did not prevent against TNFα-induced apoptosis due to the lack of cytoplasmic functional domains. The expression of each EGFP-tagged protein was confirmed by western blotting transfected cell lysates with anti-EGFP following SDS-PAGE (Fig 4.4B). Therefore, the inability of the F1L BH mutants to protect against TNFα-induced apoptosis was not due to lack of protein expression, since each mutant expressed to levels comparable with wildtype EGFP-F1L (Fig 4.4B). These data indicated that the BH1 and BH3 domains were required for the anti-apoptotic activity of F1L. Additionally, the sensitivity of EGFP-F1L(84-226) to TNFα-induced apoptosis suggested that the BH4 domain or other regions in the N-terminus of F1L were required for the protein to inhibit cell death.

4.5 F1L POSSESSES FUNCTIONAL BH DOMAINS REQUIRED FOR BAK INTERACTION

4.5.1 The interaction between F1L BH mutants and Bak is hindered during transfection.
Mutations in BH domains 1-3 of cellular anti-apoptotic proteins severely impair interactions with pro-apoptotic counterparts and thus overall protein function [260,634,635,636,637]. Although F1L mutants devoid of the BH1 or BH3 domain retained mitochondrial localization, they failed to prevent TNFα-induced apoptosis (Figs 4.3 and 4.4). Since Bak is a major interacting partner of F1L, we sought to determine whether the F1L BH domain mutants retained the ability to bind Bak by immunoprecipitation. HEK 293T cells were transfected with EGFP-tagged wildtype or mutant F1L constructs along with

pcDNA-HA-Bak and the interaction was assessed by immunoprecipitation with an anti-EGFP antibody. Western blotting with anti-Bak revealed that wildtype EGFP-F1L interacted strongly with HA-Bak, where as EGFP-F1L(84-226), EGFP-F1L(109-226), EGFP-F1LΔBH1, and EGFP-F1LΔBH3 displayed reduced Bak binding (Fig 4.5). HA-Bak did not interact with EGFP, as expected; however, some background binding to EGFP-F1L(206-226) was detected (Fig 4.5), suggesting potential binding abilities for the C-terminal transmembrane domain of F1L. Equal levels of immunoprecipitated EGFP-tagged proteins were confirmed using anti-EGFP, while expression levels of HA-Bak and EGFP-tagged proteins were observed in lysates (Fig 4.5). Interestingly, the interaction between EGFP-F1LΔBH3 and HA-Bak was greatly reduced compared to wildtype EGFP-F1L, while a more severe reduction in HA-Bak binding was observed with EGFP-F1LΔBH1 (Fig 4.5).   These data suggested that the BH1 domain, and likely the BH3 domain, of F1L played an important role in Bak interaction.

4.5.2 F1L BH mutants display reduced Bak binding during infection. To examine the interaction between F1L BH domain mutants with endogenously-expressed Bak during virus infection, HEK 293T cells were transfected with the empty vector pSC66, pSC66-FLAG-F1L, pSC66-FLAG-F1L(84-226), pSC66-FLAG-F1L(109-226), or pSC66-FLAG-F1LΔBH1. FLAG-tagged proteins in the pSC66 vector were controlled by a synthetic poxviral promoter; therefore, transfected cells were simultaneously infected with VV to drive expression of each transfected construct [564]. Fourteen hours post infection-transfection, immune complexes were isolated with anti-FLAG following lysis in 2% CHAPS buffer. Anti-Bak western blot revealed a strong interaction between Bak and wildtype FLAG-F1L, but no interaction with FLAG-F1L(84-226), FLAG-F1L(109-226), or FLAG-F1LΔBH1 (Fig 4.6). The loss of Bak interaction with F1L BH mutants was not due to a lack of the FLAG-tagged proteins in the immunoprecipitate or lysate, as demonstrated by anti-FLAG western blot (Fig 4.6). The infection-transfection data, along with transient transfection data in figure 4.5, revealed the
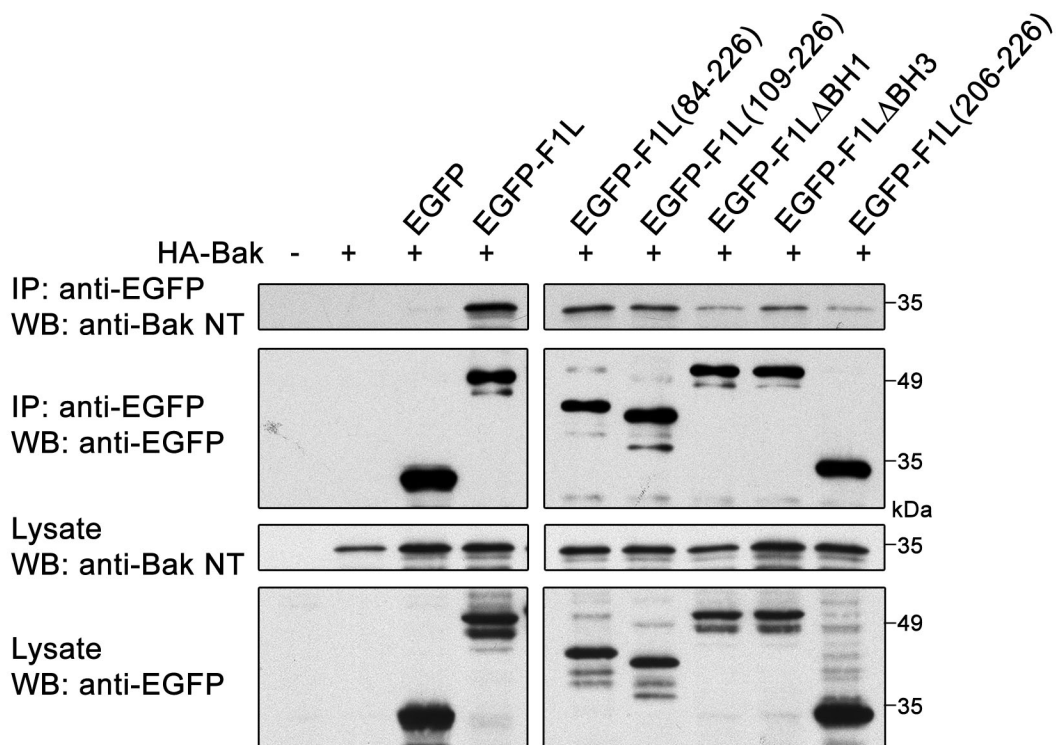
Figure 4.5 F1L BH mutants are defective in binding HA-Bak. HEK 293T cells were transiently transfected for 18 hours with pEGFP, pEGFP-F1L, pEGFP-F1L(84-226), pEGFP-F1L(109-226), pEGFP-F1LΔBH1, pEGFP-F1LΔBH3, or pEGFP-F1L(206-226) along with pcDNA-HA-Bak. Cells were lysed in 2% CHAPS lysis buffer and subjected to anti-EGFP immunoprecipitation. Immunoprecipitates and lysates were western blotted with anti-Bak NT to reveal HA-Bak protein levels or anti-EGFP to visualize EGFP-tagged proteins
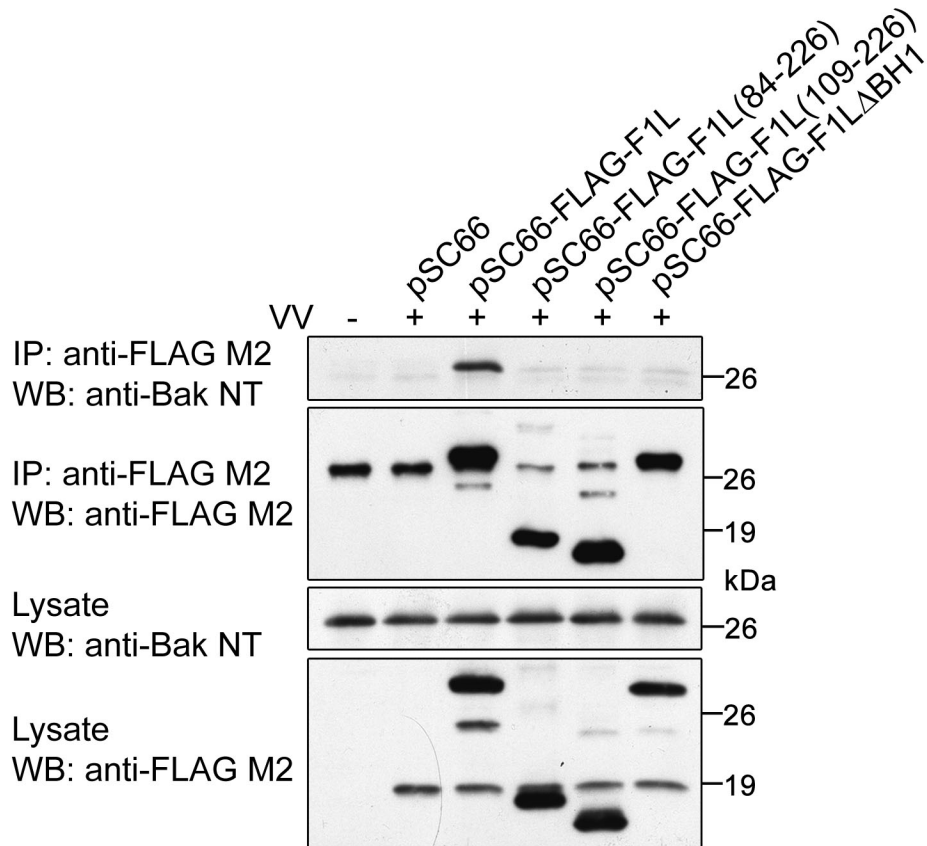
Figure 4.6 The interaction between Bak and F1L BH mutants is abrogated during infection. HEK 293T cells were infected at an MOI of 5 with VV and transfected with pSC66, pSC66-FLAG-F1L, pSC66-FLAG-F1L(84-226), pSC66-FLAG-F1L(109-226), and pSC66-FLAG-F1LΔBH1 for fourteen hours. Upon lysis in 2% CHAPS, FLAG-tagged proteins were immunoprecipitated with anti-FLAG M2. Both immunoprecipitates and lysates were western blotted with anti-Bak NT and anti-FLAG M2.

importance of the BH1 and BH3 domains of F1L for Bak interaction, as deletion of these domains decreased or fully abrogated binding to Bak. These data also suggested that the defect in Bak binding may have accounted for the inability of F1L BH mutants to inhibit TNFα-induced apoptosis (Fig 4.4).

4.6 POINT MUTATIONS IN THE BH1 AND BH3 DOMAINS OF F1L ALTER PROTEIN FUNCTION

4.6.1 Point mutations in the BH1 and BH3 domain of F1L abrogate interaction with Bak. To further elucidate the importance of the BH1 and BH3 domains of F1L in Bak binding, we generated point mutations using site-directed mutagenesis. Based on the crystal structure of F1L from MVA [555], we generated FLAG-F1L(G144F), which was mutated in the BH1 domain, and FLAG-F1L(V104A), which was mutated in the BH3 domain (Fig 2.1). Both of these residues fell within the binding groove of F1L and thus likely contacted the BH3 domain of Bak (Fig 4.7A); however, only G144 was conserved in cellular Bcl-2 proteins (Fig 4.7B). The corresponding mutations (G140F and V100A) in MVA F1L completely disrupts binding to the Bim BH3 peptide in *in vitro* binding assays [555]. Based on these data, we sought to determine if G144 in the BH1 domain and V104 in the BH3 domain of F1L were required for Bak binding. The contribution of the BH1 and BH3 domains in F1L for binding endogenous Bak during VV infection was assessed by placing these point mutants under control of a poxviral promoter to limit their expression to cells infected with VV. HEK 293T cells were transfected with pSC66-FLAG-F1L, pSC66-FLAG-F1L(V104A) or pSC66-FLAG-F1L(G144F) and simultaneously infected with VV. Following lysis in 2% CHAPS buffer, anti-FLAG complexes were immunoprecipitated. As shown in figure 4.8A, wildtype FLAG-F1L pulled down endogenous Bak in infected cells, whereas Bak binding to FLAG-F1L(V104A) and FLAG-F1L(G144F) was severely diminished. Each FLAG-tagged protein was efficiently immunoprecipitated and western blotting lysates with anti-Bak and anti-FLAG revealed expression of Bak and FLAG-tagged proteins, respectively (Fig 4.8A).

Figure 4.7 Point mutations in the F1L binding groove. A. Schematic diagram of F1L from MVA with the concave binding groove of F1L occupied by the BH3 peptide of Bak in magenta [677]. Highlighted regions indicate mutated residues in the binding groove of F1L, which include V104A, Y108E, M112W, M115W, A119W, I136F, G144F, V145F, L147F, and T149L. Residues have been re-numbered to represent VV(Cop) F1L. **B.** Alignment of BH1 and BH3 domains of VV(Cop) F1L with cellular Bcl-2 proteins. G144 in the BH1 domain was mutated to F144 and V104 in the BH3 domain was mutated to A104. Conserved residues are highlighted in black, similar residues in grey.
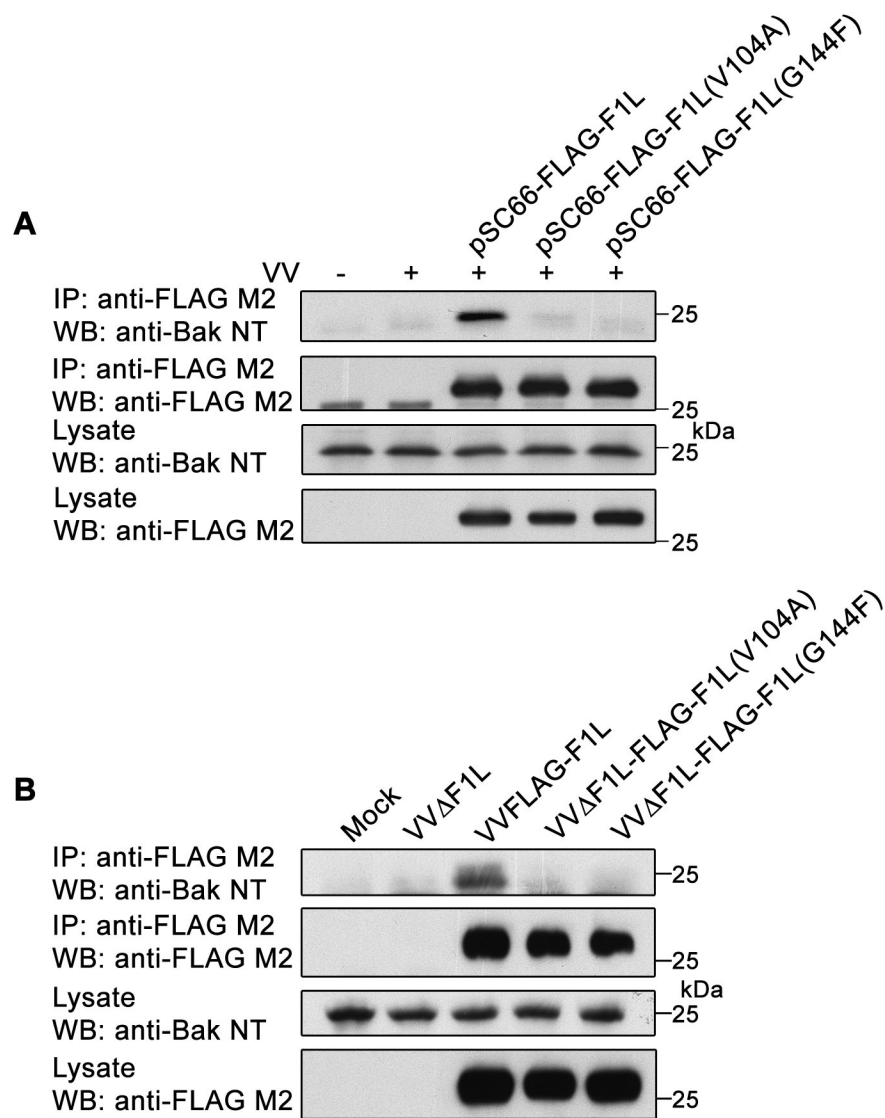
Figure 4.8 Point mutations in the BH1 and BH3 domains of F1L abrogate Bak binding. A. HEK 293T cells were mock-infected or infected with VV at an MOI of 5. Cells were simultaneously transfected with pSC66-FLAG-F1L, pSC66-FLAG-F1L(V104A), or pSC66-FLAG-F1L(G144F). Fourteen hours post infection/transfection, cells were subjected to anti-FLAG M2 immunoprecipitation following 2% CHAPS lysis. Both immunoprecipitates and lysates were western blotted with anti-Bak NT and anti-FLAG M2. **B.** HEK 293T cells were mock-infected or infected with VVΔF1L, VV-FLAG-F1L, VVΔF1L-FLAG-F1L(V104A), or VVΔF1L-FLAG-F1L(G144F) at an MOI of 5 for 12 hours. Lysis in 2% CHAPS was followed by anti-FLAG M2 immunoprecipitation and the immunoprecipitates and lysates were western blotted with anti-Bak NT and anti-FLAG M2.

To verify the requirement of both V104 and G144 for the interaction between F1L and Bak observed in the infection-transfection system of figure 4.8A, we generated recombinant vaccinia viruses expressing FLAG-F1L(V104A) and FLAG-F1L(G144F) in the absence of endogenous F1L. HEK 293T cells were either mock-infected, infected with the newly generated recombinant viruses, VVΔF1L-FLAG-F1L(V104A) or VVΔF1L-FLAG-F1L(G144F), or infected with VVΔF1L or VV-FLAG-F1L. Bak binding was assessed by anti-FLAG immunoprecipitation following lysis of infected cells in 2% CHAPS buffer. Western blotting immunoprecipitates with anti-Bak revealed that an interaction occurred between Bak and FLAG-F1L in VV-FLAG-F1L-infected cells, while no Bak was immunoprecipitated in mock-infected or VVΔF1L-infected cells (Fig 4.8B). Furthermore, FLAG-F1L(V104A) and FLAG-F1L(G144F), expressed from recombinant vaccinia viruses, were unable to co-immunoprecipitate endogenous Bak, despite equal FLAG-tagged protein levels in immunoprecipitates and lysates (Fig 4.8B). Together, the results indicated that despite a lack of obvious sequence identity to cellular Bcl-2 proteins, F1L contained divergent BH domains that were critical for interacting with Bak. Moreover, a single mutation in the BH1 domain or BH3 domain, which line the binding groove of F1L, completely abrogated binding to Bak.

4.6.2 The BH1 domain of F1L is critical for its anti-apoptotic activity during infection. Since mutation of both V104 and G144 of F1L drastically hampered binding to Bak, we assessed the contribution of these residues to the anti-apoptotic activity of F1L. Virus-induced apoptosis in infected Jurkat cells was assayed by monitoring Bak activation using the conformation specific antibody, anti-Bak AB-1 [177,184]. Additionally, virus-infected cells were treated with STS to determine the ability of the F1L mutants to protect against an external apoptotic stimulus. Jurkat cells were mock-infected or infected with VVEGFP, VVΔF1L, VVΔF1L-FLAG-F1L(V104A), or VVΔF1L-FLAG-F1L(G144F) for 4 hours before a 1.5 hour treatment with STS. Mock-infected cells treated with STS

demonstrated a dramatic increase in Bak activation (Fig 4.9 panel a). In contrast, Bak was not activated in cells infected with VVEGFP in the presence or absence of STS, indicating that wildtype VV fully prevented Bak activation (Fig 4.9 panel b). However, Bak activation occurred in VVΔF1L-infected cells and was even more pronounced during STS treatment (Fig 4.9 panel c). Interestingly, the F1L V104A mutation did not affect the anti-apoptotic function of the protein, as VVΔF1L-FLAG-F1L(V104A) prevented virus-induced and STS-induced Bak activation (Fig 4.9 panel d). In contrast, the G144F mutation in the BH1 domain of F1L did not affect the ability of VVΔF1L-FLAG-F1L(G144F) to prevent virus-induced apoptosis, but this mutation dramatically rendered the cells infected with this virus sensitive to STS-induced apoptosis (Fig 4.9 panel e). Therefore, while V104A and G144F mutations disrupted binding to Bak (Fig 4.8), only G144 played a critical role in the anti-apoptotic activity of F1L in response to STS treatment. Moreover, there appeared to be a Bak-independent anti-apoptotic mechanism for FLAG-F1L(V104A), since this mutant no longer interacted with Bak but remained protective against both virus- and STS-induced apoptosis.

4.7 CHARACTERIZATION OF THE F1L BINDING GROOVE

4.7.1 Identification of F1L binding pocket residues important for anti-apoptotic activity. Based on the solved crystal structure of MVA F1L, the binding groove of F1L is comprised of a number of residues that all make potential contacts with the Bak BH3 domain [555] (Fig 4.7A). Since mutation of G144 dramatically altered the pro-survival activity of F1L and mutation of both V104 and G144 hindered Bak binding (Figs 4.8 and 4.9), we sought to identify other binding groove residues of F1L that are important for anti-apoptotic activity. To this end, eight additional recombinant vaccinia viruses were generated using the parental virus, VVΔF1L: VVΔF1L-FLAG-F1L(Y108E), VVΔF1L-FLAG-F1L(M112W), VVΔF1L-FLAG-F1L(M115W), VVΔF1L-FLAG-F1L(A119W), VVΔF1L-FLAG-F1L(I136F), VVΔF1L-FLAG-F1L(V145F), VVΔF1L-FLAG-F1L(L147F), and VVΔF1L-FLAG-F1L(T149L) (Figs 2.1 and 4.7A). These viruses lacked endogenous F1L and were
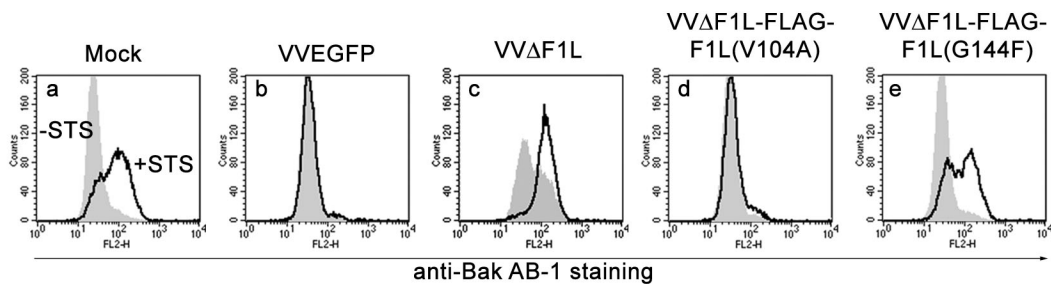
Figure 4.9 A point mutation in the BH1 domain of F1L hinders anti-apoptotic activity. Recombinant viruses expressing FLAG-F1L(V104A) or FLAG-F1L(G144F) were screened for ability to prevent apoptosis by mock-infecting (**a**) or infecting Jurkat cells with VVEGFP (**b**), VVΔF1L (**c**), VV ΔF1L-FLAG-F1L(V104A) (**d**), or VVΔF1L-FLAG-F1L(G144F) (**e**) at an MOI of 10. Four hours post infection, cells were treated with 250nM staurosporine (STS) for 1.5 hours to induce apoptosis. Bak N-terminal exposure was monitored by staining cells with the conformation-specific anti-Bak AB-1 antibody. Shaded histograms, untreated cells; open histograms, STS-treated cells.

therefore infected cells were inherently sensitive to virus-induced apoptosis, yet each recombinant virus expressed a FLAG-tagged point mutant of F1L, which if functional, could inhibit apoptosis triggered by virus infection. Wildtype Jurkat cells (Fig 4.10 panels a-l) and Jurkat cells deficient in Bak and Bax (Fig 4.10 panels m-w) were mock-infected, infected with the eight newly generated viruses, or infected with VVEGFP or VVΔF1L. To determine if viruses expressing point mutations in F1L could inhibit apoptosis induced by an external stimulus, infected cells were treated with STS. As observed previously, mock-infected cells were sensitive to STS treatment (Fig 4.10 panel a), VVEGFP-infected cells were completely protected against virus- and STS-induced apoptosis (Fig 4.10 panel b), while Bak was activated in cells infected with VVΔF1L and this was amplified upon STS treatment (Fig 4.10 panels c). Unlike VVΔF1L, the eight recombinant viruses prevented virus-induced apoptosis, since Bak activation was not detected during infection alone (Fig 4.10 panels d-k). This indicated that each F1L mutant was functional and able to replace the activity of endogenous F1L to inhibit cell death induced by virus infection. Some recombinant viruses, such as VVΔF1L-FLAG-F1L(M112W), VVΔF1L-FLAG-F1L(M115W), and VVΔF1L-FLAG-F1L(T149L), were equally protective against STS-induced apoptosis, demonstrating no increase in Bak activation (Fig 4.10 panels e, f, and k). Thus, mutation of M112, M115, or T149 did not interfere with the function of F1L. Jurkat cells infected with VVΔF1L-FLAG-F1L(Y108E), VVΔF1L-FLAG-F1L(V145F), and VVΔF1L-FLAG-F1L(L147F) were largely protective against STS-induced cell death, as only a small fraction of Bak was activated (Fig 4.10 panels d, i, and j). Intriguingly, however, recombinant viruses expressing FLAG-F1L(A119W) and FLAG-F1L(I136F) were much more sensitive to STS-induced apoptosis, as a large portion of Bak was activated in these cells, indicating that A119 and I136 play an important role in the anti-apoptotic activity of F1L (Fig 4.10 panels g and h). Staining mock-infected cells with anti-NK1.1, an isotype control antibody, confirmed the specificity of the results, as no Bak activation was observed following STS
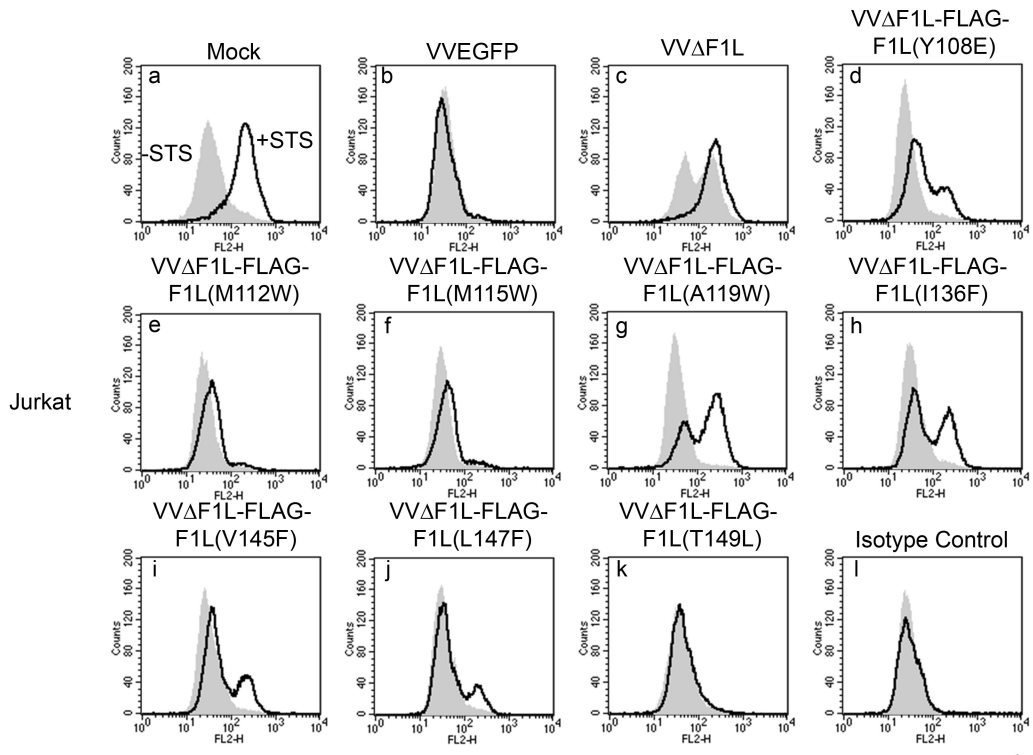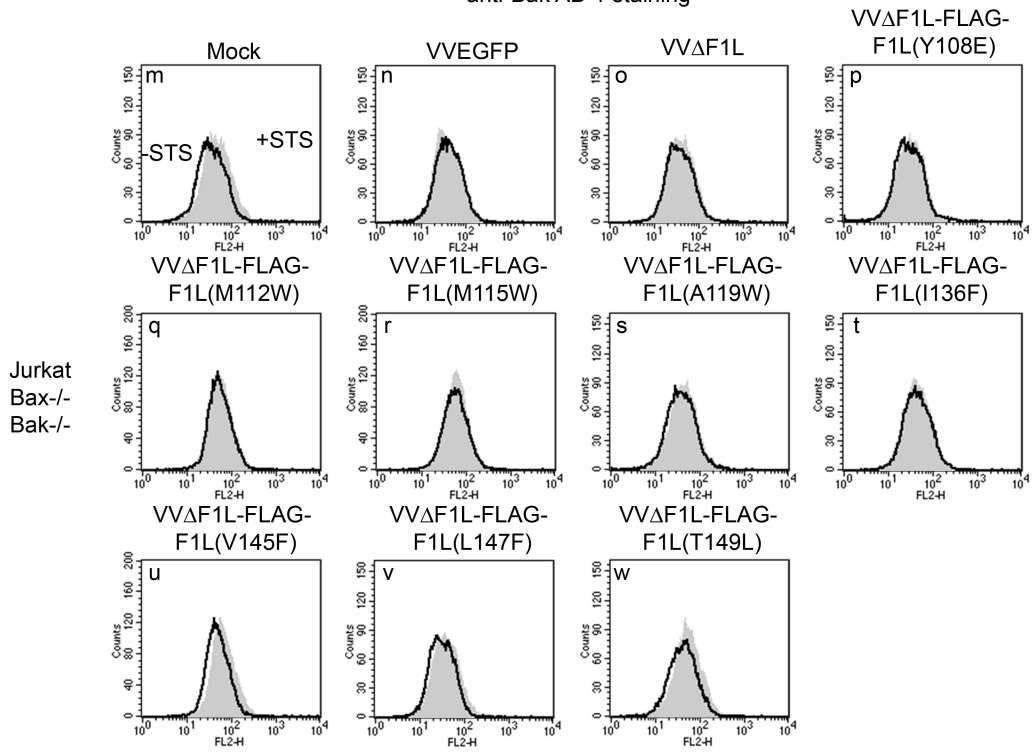
Figure 4.10 Characterizing residues in the binding groove of F1L important for anti-apoptotic function. Wildtype Jurkat cells (a-l) or Jurkat cells deficient in Bax and Bak (m-w) were mock-infected or infected with VVEGFP, VV ΔF1L, VVΔF1L-FLAG-F1L(Y108E), VVΔF1L-FLAG-F1L(M112W), VVΔF1L-FLAG-F1L(M115W), VVΔF1L-FLAG-F1L(A119W), VVΔF1L-FLAG-F1L(I136F), VVΔF1L-FLAG-F1L(V145F), VVΔF1L-FLAG-F1L(L147F), or VVΔF1L-FLAG-F1L(T149L) at an MOI of 10 for 4 hours. To induce apoptosis, cells were treated with 250nM staurosporine (STS) for 1.5 hours and Bak activation was detected with the conformation specific anti-Bak AB-1 antibody. Isotype control, wildtype Jurkat cells stained with anti-NK1.1; shaded histograms, untreated cells; open histograms, STS-treated cells.

treatment (Fig 4.10 panel l) [583]. Additionally, active Bak was not detected in Jurkat cells deficient in Bak and Bax during virus infection or STS treatment (Fig 4.10 panels m-w).

4.7.2 Identification of F1L binding pocket residues important for Bak binding.

Based on the data presented in figure 4.10, residues such as A119 and I136 appeared to be important for anti-apoptotic activity of F1L. M112, M115, and T149 were dispensable for this activity, while V145F, L147F, and Y108E were perhaps involved in inhibiting cell death in response to STS, but were not absolutely essential (Fig 4.10). To establish whether the anti-apoptotic ability of F1L point mutants correlated with the ability of each protein to interact with Bak, we infected HeLa cells with each recombinant virus tested in figure 4.10, along with VVΔF1L and VV-FLAG-F1L. Upon lysis in 2% CHAPS, FLAG-tagged complexes were immunoprecipitated with anti-FLAG. Western blotting with anti-Bak revealed a strong interaction between wildtype FLAG-F1L and Bak, as well as an equally strong interaction between FLAG-F1L(A119W) and Bak (Fig 4.11). The interaction between Bak and FLAG-F1L(M112W) was reduced, but still visible, while interactions between Bak and FLAG-tagged F1L mutants including Y108E, M115W, I136F, V145F, L147F, and T149L, were substantially reduced (Fig 4.11). In fact, the interaction with FLAG-F1L(Y108E) was barely detected. Each FLAG-tagged F1L construct was immunoprecipitated at equal amounts and expressed at comparable levels in the lysate, along with endogenous Bak (Fig 4.11). Together, the data in figures 4.10 and 4.11 revealed residues in F1L that did not significantly affect anti-apoptotic ability or Bak binding, such as M112, and residues that were required for inhibition of cell death and interaction with Bak, such as I136. Interestingly, some residues, such as A119, were required for anti-apoptotic ability and not Bak interaction, while other residues, such as M115, were essential for Bak binding but dispensable for inhibition of apoptosis. These data, which are summarized in Table 4.1, suggested that F1L is capable of inhibiting cell death in a Bak-independent manner and, therefore, further
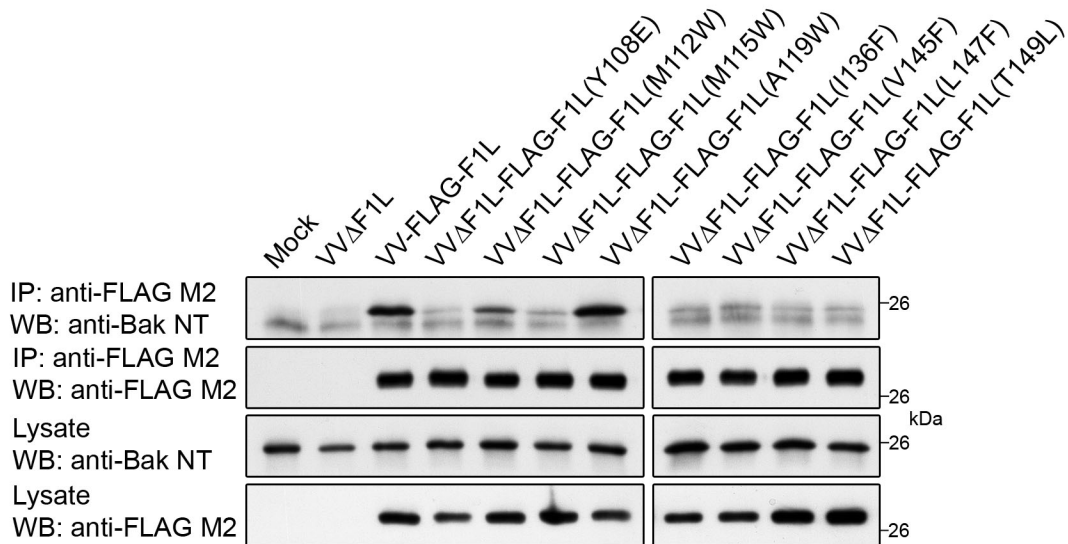
Figure 4.11 Characterizing residues in the binding groove of F1L important for Bak binding. HeLa cells were mock-infected or infected at an MOI of 5 with VVΔF1L, VV-FLAG-F1L, VVΔF1L-FLAG-F1L(Y108E), VVΔF1L-FLAG-F1L(M112W), VVΔF1L-FLAG-F1L(M115W), VVΔF1L-FLAG-F1L(A119W), VVΔF1L-FLAG-F1L(I136F), VVΔF1L-FLAG-F1L(V145F), VVΔF1L-FLAG-F1L(L147F), or VVΔF1L-FLAG-F1L(T149L) for 12 hours. Cells were lysed in 2% CHAPS and subject to anti-FLAG M2 immunoprecipitation and immunoprecipitates were western blotted with anti-Bak NT or anti-FLAG M2. Protein expression was confirmed in lysates western blotted with anti-Bak NT and anti-FLAG M2.

Table 4.1 Summary of Anti-apoptotic Activity and Bak Binding Ability for F1L Binding Groove Mutants

Protein	Anti-apoptotic activity	Interaction with Bak
F1L	+++	+++
F1L(V104A)	+++	-
F1L(Y108E)	++	-
F1L(M112W)	+++	++
F1L(M115W)	+++	-
F1L(A119W)	+	+++
F1L(I136F)	+	+
F1L(G144F)	+	-
F1L(V145F)	++	++
F1L(L147F)	++	+
F1L(T149L)	+++	+

investigation of these F1L point mutations should help clarify other mechanisms employed by F1L to inhibit apoptosis.

4.8 DISCUSSION

Based on the conservation of hydrophobic residues important for mediating interactions between cellular Bcl-2 proteins, we identified highly divergent BH domains in F1L (Figs 4.1 and 4.2). Importantly, these domains coincide with the proposed BH domains based on the recently solved crystal structure of F1L [555]. The BH1 and BH3 domains of F1L were not required for mitochondrial localization (Fig 4.3). These regions were, however, important for the anti-apoptotic activity of F1L (Fig 4.4). Similarly, the N-terminal 83 and 108 amino acids of F1L were not involved in mitochondrial targeting but were essential for the inhibition of TNFα induced apoptosis (Figs 4.3 and 4.4). Both the BH3 and BH4 domains were absent in F1L(109-226), while only the BH4 domain was absent in F1L(84-226); thus, similar to cellular anti-apoptotic proteins, the BH4 domain may play an important role in the anti-apoptotic function of F1L [210,634,637]. Or, alternatively, other residues in the N-terminus of F1L may be required for pro-survival activity.

The BH1 and BH3 domains of F1L display little sequence similarity to those of cellular Bcl-2 proteins (Fig 4.2), yet these domains were essential for binding to Bak (Figs 4.5 and 4.6). Additionally, mutating a single amino acid in either the BH1 or BH3 domain of F1L completely abrogated the interaction with endogenous Bak during VV infection (Fig 4.8). Likewise, mutations in the BH1 domain of KSHV Bcl-2, AdV E1B-19K, ASFV A179L, and EBV BHRF1 eliminate the anti-apoptotic function of these vBcl-2 proteins [504,518,522,646]. Although both V104A and G144F mutations in F1L disrupted binding to Bak (Fig 4.8), only G144F interfered with the anti-apoptotic activity of F1L in response to STS (Fig 4.9). G144 is the only conserved residue in F1L that resembles the NWGR sequence in both cellular and viral Bcl-2 homologues (Fig 4.7B) [175]. Mutating this glycine in Bcl-2 or KSHV Bcl-2 abrogates the pro-survival activity of these

proteins [260,504]; therefore, G144 likely plays an equally important role in the anti-apoptotic function of F1L. Interestingly, the V104A mutation in the BH3 domain of F1L prevented Bak binding but had no effect on the ability of F1L to prevent virus- or STS-induced apoptosis (Figs 4.8 and 4.9). This suggests that the anti-apoptotic function of F1L does not rely solely on binding and inhibiting Bak. F1L(V104A) does not have measurable affinity for a Bim BH3 peptide in binding assays [555], yet it remains to be determined if this mutant affects Bim binding in a cellular context. Although differential binding to Bim may explain the protection observed with F1L(V104A) and apoptosis sensitivity observed with F1L(G144F), we cannot exclude the possibility that F1L(V104A) may retain the ability to interact with other BH3-only proteins or proteins outside of the Bcl-2 family in order to inhibit apoptosis.

The majority of the residues that comprise the binding groove of F1L are hydrophobic (Fig 4.7A). We created a panel of point mutations in F1L to determine which residues within the binding pocket were important for interaction with Bak and anti-apoptotic activity. Importantly, all of the viruses bearing point mutations in F1L were resistant to VVΔF1L-induced apoptosis, in contrast to VVΔF1L (Fig 4.10). This implied that the mutant F1L constructs were indeed functional enough to inhibit cell death during early times of infection with VVΔF1L. Our mutational analysis, however, revealed residues, such as I136, that were critical for inhibiting STS-induced apoptosis and binding to Bak (Figs 4.10 and 4.11). The results for F1L(I136F) mirrored what was observed for F1L(G144F), suggesting that these residues inhibit apoptosis in a manner that depends on Bak binding. On the other hand, a Bak-independent anti-apoptotic mechanism appears to exist for F1L. Similar to F1L(V104A), F1L(M115W) was able to inhibit STS-induced apoptosis despite no longer interacting with Bak (Figs 4.10 and 4.11). Moreover, A119 was required for inhibition of STS-induced death but dispensable for interaction with Bak (Figs 4.10 and 4.11). Together, these data point to an alternative mechanism employed by F1L to inhibit

apoptosis. The F1L point mutations generated in this study will undoubtedly be useful in dissecting the contribution of BH3-only proteins or other mitochondrial apoptotic machinery to the anti-apoptotic function of F1L.

CHAPTER 5: F1L is Regulated by the Ubiquitin-Proteasome System

5.1 INTRODUCTION

The UPS regulates a number of cellular processes, including transcription, cell division, antigen processing, and apoptosis [371,372,373]. Although the conjugation of the 8kDa ubiquitin molecule involves three enzymes (E1, E2, and E3), it is the E3 ubiquitin ligase that transfers ubiquitin onto target proteins and ultimately confers substrate specificity (Fig 1.18) [371,372]. The human genome contains over 600 annotated genes predicted to encode ubiquitin ligases, many of which function as multi-protein complexes that require one of seven cullin family members [377]. The best studied cullin-based ubiquitin ligase is the SCF complex (Fig 1.19B). In this complex, Cul-1 acts as a molecular scaffold to interact with the catalytically active RING finger protein Roc1 and the E2 conjugating enzyme carrying ubiquitin [393,394]. Cul-1 also binds the linker protein Skp1, which recruits substrates through an adaptor protein that contains an F-box motif, such as β-TrCP [395,402,403,404,405]. Importantly, many SCF target proteins require prior phosphorylation in order to be recognized and ubiquitinated by the complex [402,404,405,647].

The conjugation of ubiquitin onto substrates involves the formation of an isopeptide bond between the C-terminal glycine of ubiquitin and a lysine residue within the substrate [371,372]. A protein can be monoubiquitinated on one lysine residue or multiple monoubiquitination events may occur on more than one lysine residue [379,380]. Proteins are singly or multiply monoubiquitinated to alter their function and this is important for various cellular functions including endosomal sorting and DNA repair [373]. Ubiquitin can also be attached to a lysine residue in the preceding ubiquitin molecule already attached to a protein [379,380]. Continuous cycles of ubiquitination result in polyubiquitinated chains and this is thought to be mediated by a fourth enzyme, the E4 [648,649]. Importantly, however, ubiquitin contains seven lysines and the specific lysine that partakes in polyubiquitin chain formation determines the fate of the target protein (Fig 1.19A) [379,380,381]. For example, polyubiquitin

chains formed on K63 of ubiquitin are associated with various signalling events, protein synthesis, and endocytosis [379,383]. In contrast, K48-linked polyubiquitin chains typically send a protein to the 26S proteasome for degradation [379,382]. The free amino group at the N-terminus of ubiquitin can also serve as a receptor for an incoming ubiquitin molecule [650,651]. Linear ubiquitin chains formed through the N-terminus of ubiquitin have recently been implicated in signalling pathways for NFκB activation [652,653]. Although most reports of ubiquitination involve lysine residues or the free amino group at the N-terminus, it has recently become evident that other residues, such as serine, threonine, and cysteine, can also serve as ubiquitin linkage sites [424,654,655,656].

The 26S proteasome is a large multi-protein complex responsible for the degradation of many cellular proteins tagged with polyubiquitin chains linked through K48 of ubiquitin [382,406,407]. In addition to its housekeeping role in turning over old or damaged proteins, the proteasome is also responsible for producing immunogenic peptides for presentation on MHC class I, an event particularly important during virus infection [406]. The β-catalytic subunits of the 20S core confer the enzymatic properties of the 26S proteasome and through the action of β1, β2, and β5 subunits, proteins are processively degraded into small peptides that diffuse out of the core (Fig 1.20) [382,406,407]. Various chemical inhibitors of the proteasome have been created, the first of which belonged to a class of peptide aldehydes [412,413]. One of these peptides, MG132, is a potent inhibitor of the chymotrypsin-like activity of the β5 subunits and commonly used in research [414,415].

The UPS plays a critical role in mediating events occurring at mitochondria, specifically the processes regulating mitochondrial morphology and apoptosis. The UPS primarily targets proteins integrated in the OMM or cytoplasmic factors that regulate mitochondrial function [657]. Although these proteins can be regulated by cytoplasmic E3 ligases, there is a growing list of

resident mitochondrial E3 ligases present in the OMM [657]. Intriguingly, some of the mitochondrial E3 ligases regulate mitochondrial dynamics. MARCH-V is a member of the membrane-associated RING-CH (MARCH) protein family that contain a RING domain and two or more transmembrane domains [658]. Mitochondrial-localized MARCH-V, or MITOL (mitochondrial ubiquitin ligase), ubiquitinates Drp1, the key mediator of fission [659,660]. Drp1 ubiquitination and degradation slows the process of fission and produces long fused mitochondria [659,660]. More recently, MARCH-V has been proposed to promote fission by ubiquitinating the fusion protein Mfn1 and cooperating with Drp1; thus, the exact role of MARCH-V in regulating mitochondrial morphology is somewhat contentious [661,662]. In addition to MARCH-V, the mitochondrial ubiquitin ligase activator of NFκB (MULAN) is a RING-containing ligase whose target proteins are currently unknown, yet expression of the protein causes extensive mitochondrial fragmentation [377]. Although first identified as an activator of NFκB signalling [663], evidence now exists that MULAN interferes with mitochondrial dynamics and induces apoptosis upon overexpression, providing further evidence for a link between mitochondrial morphology and the cell death machinery [664].

Many members of the Bcl-2 family are turned over by the UPS. Upon phosphorylation, BimEL is ubiquitinated by the SCF$^{\beta\text{-TrCP}}$ complex in order to prevent apoptosis, whereas ubiquitination of Bid is associated with degradation as well as activation to form tBid [422,423,424]. The SCF$^{\beta\text{-TrCP}}$ complex, along with the SCF^{FBW7} complex, is also involved in the ubiquitination and degradation of phosphorylated Mcl-1 in order to induce apoptosis during times of growth factor deprivation [439,440,441,442]. Furthermore, the BH3 domain-containing ubiquitin ligase Mule controls Mcl-1 levels in healthy cells and also during genotoxic stress [437,438]. Despite the identification of mitochondrial ubiquitin ligases that control mitochondrial dynamics, all ubiquitin ligases involved in

regulating apoptosis to date are cytoplasmic and it is currently unclear whether proteins in the OMM control the levels of Bcl-2 family members.

The UPS regulates numerous cellular processes, from housekeeping functions to immune-related functions, so not surprisingly, the UPS machinery is often targeted by viruses. Viruses have devised clever strategies to modulate cellular ubiquitination and degradation or co-op the UPS for their own benefit [665,666]. This is particularly true for poxviruses [667,668]. Entomopoxviruses encode proteins with strong homology to cellular RING-containing IAPs [483,484]. AMV-IAP from Amsacta moorei targets caspases and inhibits apoptosis, although whether this occurs by ubiquitination and degradation of caspases, similar to cellular IAPs, has not yet been established [487,488]. Myxoma virus M153R is a RING finger ubiquitin ligase that bears strong homology with the human MARCH protein family [447,448,658]. M153R is a membrane bound ubiquitin ligase that stimulates the ubiquitination and degradation of MHC class I and CD4 in infected cells to prevent detection by the host immune system [447,448]. Many orthopoxviruses encode the RING-containing ubiquitin ligase, p28 [668]. In addition to a RING domain that is required for ubiquitin ligase activity, p28 also contains a KilA-N DNA binding domain required for localization to DNA-rich viral factories [492,493]. Although the substrates of p28 have yet to be identified, p28 inhibits UV-induced apoptosis and plays as essential role in ectromelia virus pathogenesis [489,491].

Poxviruses also produce a number of proteins to modulate cullin-based ubiquitin ligases [667,668,669]. The SCF complex is targeted by viral F-box-like proteins, many of which contain ankyrin domain repeats likely involved in substrate recognition [670]. A number of poxviruses encode multiple F-box/ankyrin proteins [668,670]. Myxoma virus MT-5 interacts with Cul-1 and regulates cells cycle, while all five Orf virus F-box/ankyrin proteins interact with the SCF but the role of these proteins has not been resolved [671,672,673]. F-box/ankyrin proteins from a variety of orthopoxviruses have been implicated in

impeding NFκB signalling mainly through interactions with the SCF and components of the NFκB pathway [571,674,675,676]. Poxviruses also target the related ubiquitin ligase complex consisting of Cul-3. Most poxvirus family members encode proteins containing Bric-a-Brac, Tramtrack, or Broad-complex (BTB) domains and kelch domains [668]. Ectromelia virus proteins EVM150 and EVM167 interact with Cul-3 to produce functional ubiquitin ligases [572]. However, the identification of substrates is anxiously anticipated for poxviral F-box/ankyrin and BTB/kelch proteins in order to understand what cellular pathways or perhaps viral proteins are targeted by the UPS. Moreover, the genomes of canarypox virus and an entomopoxvirus contain genes with homology to cellular ubiquitin, although the role these proteins play during infection has yet to be established [484,532].

Poxviruses encode a number of proteins to interfere with and modulate the cellular ubiquitination machinery, suggesting this pathway is active during infection [667,668]. Given that the activity and protein levels of many Bcl-2 family members are controlled by ubiquitination and degradation, we sought to determine if F1L, the anti-apoptotic protein in VV, was regulated by ubiquitination, an event previously undescribed for viral inhibitors of apoptosis. Ubiquitination most commonly occurs on one or several lysines in a target protein [379,380]. F1L contains eleven lysines, nine of which reside in the cytoplasmic domain (Fig 5.1). The transmembrane domain of F1L is flanked by K206 in the cytoplasm and K219 in mitochondria, while K222 is located within the hydrophilic tail (Fig 5.1) [548]. The crystal structure of F1L revealed that the cytoplasmic lysines are all solvent exposed and thus accessible to cytosolic ubiquitination machinery (Fig 5.2) [677]. As the C-terminal region of F1L was deleted in order to solubilize the protein for crystallization, no data is available for the accessibility of K206, K219, or K222 [555]. However, since all lysines present in the crystal structure of F1L are surface exposed, each one is a potential target for ubiquitination.
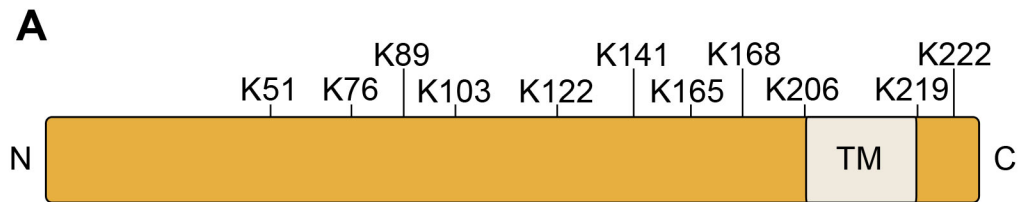
A

K51 K76 K89 K103 K122 K141 K165 K168 K206 K219 K222

N TM C

B

```
1                                                 50
MLSMFMCNNIVDYVDDIDNGIVQDIEDEASNNVDHDYVYPLPENMVYRFD

51                                               100
KSTNILDYLSTERDHVMMAVRYYMSKQRLDDLYRQLPTKTRSYIDIINIY

101                                              150
CDKVSNDYNRDMNIMYDMASTKSFTVYDINNEVNTILMDNKGLGVRLATI

151                                              200
SFITELGRRCMNPVKTIKMFTLLSHTICDDCFVDYITDISPPDNTIPNTS

201                     226
TREYLKLIGITAIMFATYKTLKYMIG
```

Figure 5.1 F1L contains eleven lysine residues. A. Schematic diagram of F1L encoded by VV(Cop). F1L contains 11 lysines: K51, K76, K89, K103, K122, K141, K165, K168, and K206 are in the cytoplasmic domain, while K219 and K222 are inserted into mitochondria. N, N-terminus; C, C-terminus; TM, transmembrane domain. **B.** Amino acid sequence of VV(Cop) F1L. Of the 226 amino acids present in F1L, 11 are lysine residues (highlighted in blue). Lysines 206 and 219 flank the transmembrane domain (boxed residues) and, along with lysine 222, are important for mitochondrial localization.
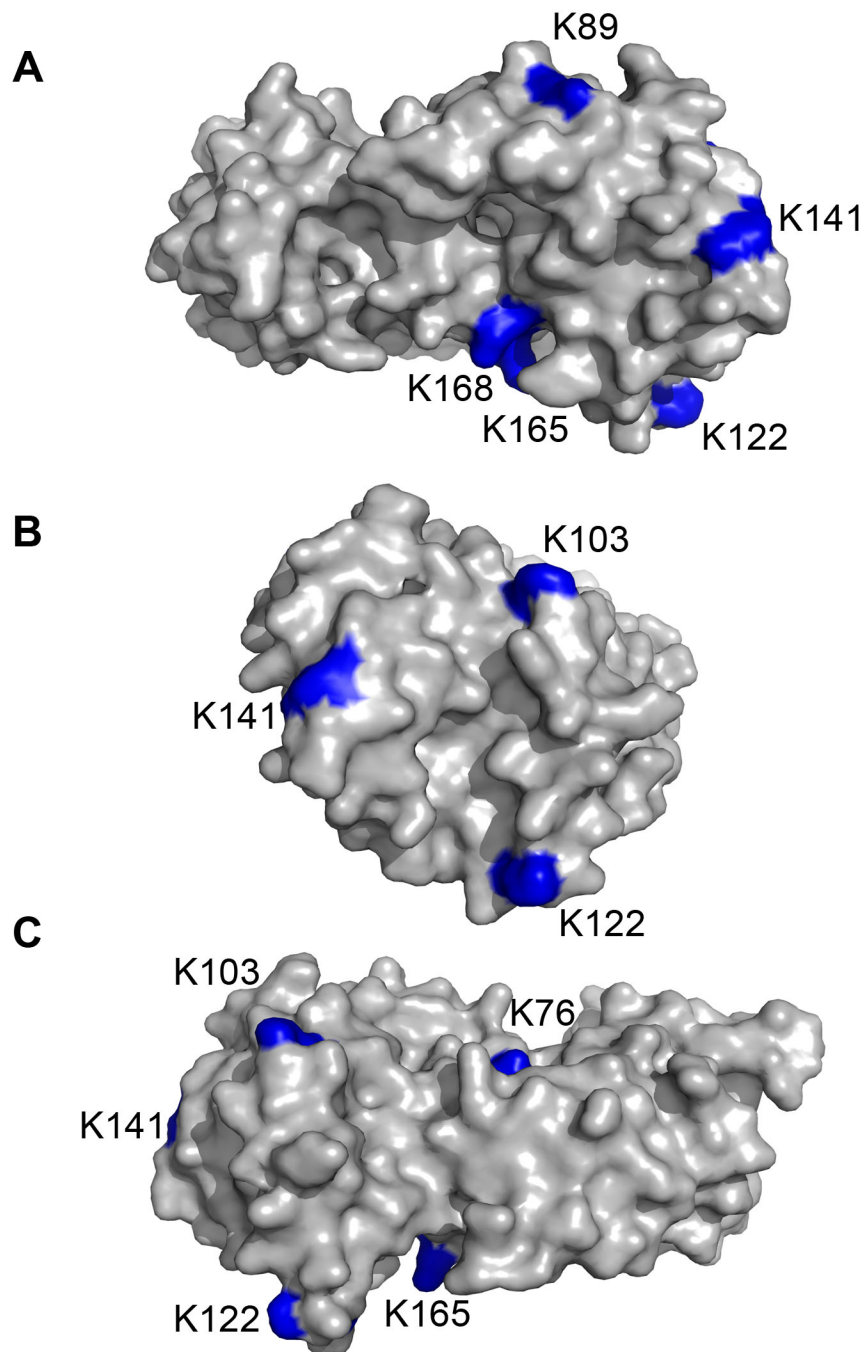
Figure 5.2 The lysine residues in F1L are surface exposed. A. Space filling model of F1L encoded by MVA, which shares 98% nucleic acid identity with F1L from VV(Cop). Lysine resides (blue) are numbered according to VV(Cop). Model was rotated 90° (**B**) or 180° (**C**) relative to (**A**). K51 is present in α-helix α0, which is not present in the main Bcl-2 like fold of F1L and thus absent from the model. K206, K219, and K222 are not present due to the deletion of the F1L C-terminus in the crystal structure [677].

5.2 F1L ASSOCIATES WITH UBIQUITIN

5.2.1 F1L is present in high molecular weight species with ubiquitin. The addition of ubiquitin onto target substrates occurs in a sequential manner [371,372]. As such, the addition of each consecutive ubiquitin molecule can be observed as 8kDa increments by SDS-PAGE and polyubiquitinated proteins form high molecular weight adducts often observed as a ubiquitin "smear" [375,376]. Indeed, the high molecular weight laddering characteristic of ubiquitination was observed in HeLa cells infected with VV-FLAG-F1L (Fig 5.3A). Western blotting with anti-FLAG revealed that the unmodified form of FLAG-F1L, which has a molecular weight of 28kDa, increased dramatically over 12 hours of infection, which is expected since this open reading frame is under the control of a powerful synthetic promoter (Fig 5.3A). Additionally, a slower migrating species with a molecular weight of 36kDa appeared at 8 hours and more prominently at 12 hours post infection. The 8kDa increase in molecular weight suggested the 36kDa form of FLAG-F1L may represent a monoubiquitinated species. Moreover, the presence of high molecular weight FLAG-F1L products at 12 hours post infection implied that polyubiquitin chains or multiple monoubiquitin chains were forming (Fig 5.3A). To confirm that F1L was indeed present in these high molecular weight adducts, the samples were western blotted with an anti-F1L antibody, which revealed an almost identical protein profile to figure 5.3A (Fig 5.3B). To further support the observation that F1L and ubiquitin were present in these slower migrating species, HeLa cells were mock-infected or infected with wildtype VV or VV-FLAG-F1L and subjected to anti-FLAG immunoprecipitation. Products were separated by SDS-PAGE and silver stained before excising unique bands from VV-FLAG-F1L-infected cells. Mass spectrometric analysis of these bands revealed the presence of F1L at 28kDa and also at higher molecular weights (Fig 5.3C). Importantly, ubiquitin was detected with F1L in high molecular weight complexes, suggesting that F1L was ubiquitinated during infection, resulting in the formation of high molecular weight products. Notably,
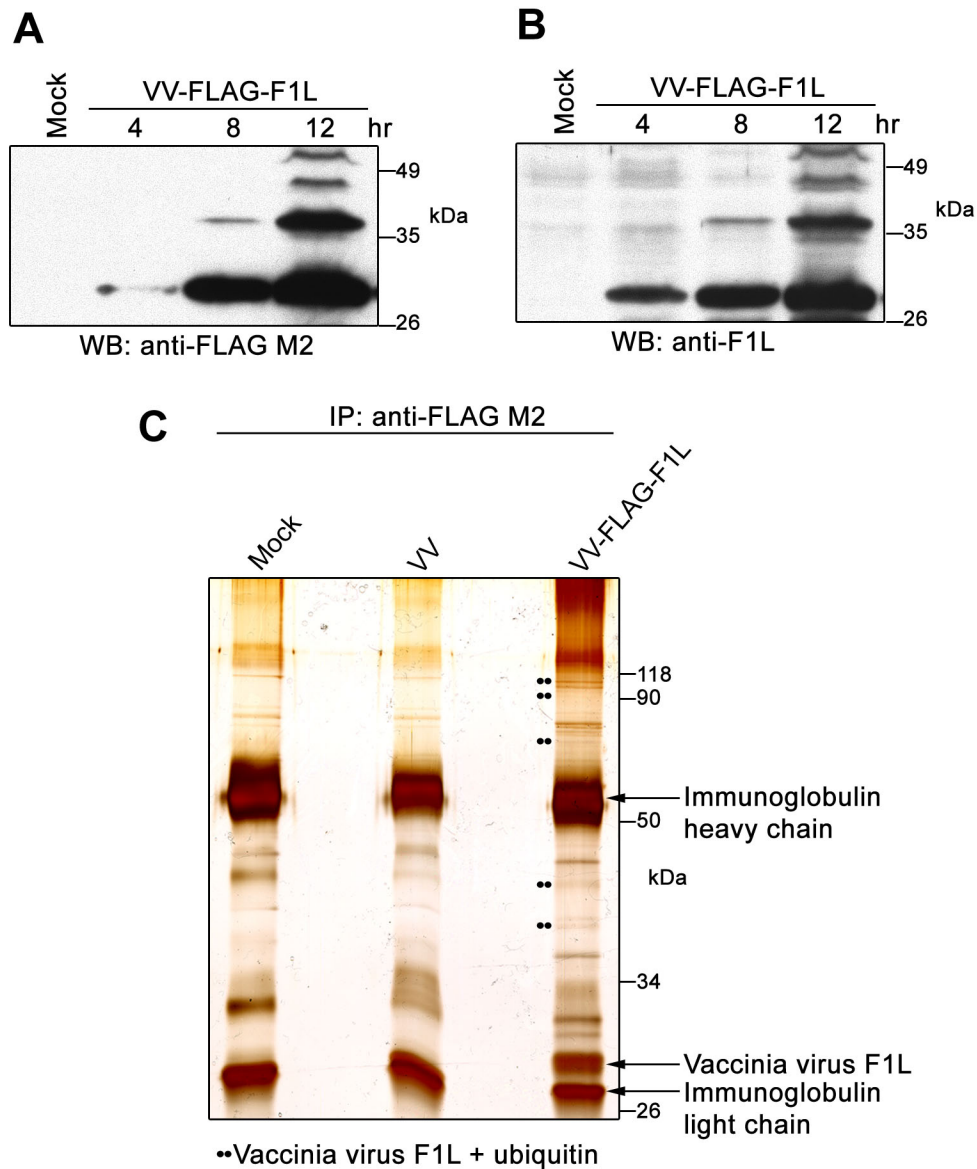
Figure 5.3 F1L forms high molecular weight adducts containing ubiquitin. HeLa cells were mock-infected or infected with VV-FLAG-F1L at an MOI of 5. Whole cell lysates were harvested at 4, 8, or 12 hours post infection and western blotted with anti-FLAG M2 (**A**) or anti-F1L (**B**) to demonstrate high molecular weight laddering of FLAG-F1L. **C**. Mock-infected HeLa cells or HeLa cells infected with VV or VV-FLAG-F1L at an MOI of 5 were lysed 12 hours post infection in 1% NP-40 lysis buffer and subject to anti-FLAG M2 immunoprecipitation. Samples were resolved by SDS-PAGE and visualized by silver staining. Unique bands in VV-FLAG-F1L immunoprecipitates were excised and analyzed by mass spectrometry, revealing the presence of F1L and ubiquitin at high molecular weights (filled circles).

the presence of FLAG-F1L and ubiquitin was specific to cells infected with VV-FLAG-F1L, as they were not detected in mock-infected or VV-infected samples (Fig 5.3C).

5.2.2 F1L associates with conjugated ubiquitin. Since both F1L and ubiquitin were detected in high molecular weight adducts, we next examined whether F1L associated with conjugated ubiquitin. HeLa cells were infected with a VV overexpressing HA-tagged ubiquitin, VV-HA-ubiquitin. Cells were co-infected with VV-FLAG-F1L, or as controls, VV-FLAG-EVM004, which expresses the 33kDa BTB domain-containing protein from ectromelia virus, or VV-FLAG-EVM150, which expresses an 88kDa BTB/kelch protein from ectromelia virus [572]. Additionally, cells were infected with viruses expressing two other poxviral anti-apoptotic proteins to determine if ubiquitination was specific to F1L or common to other mitochondrial inhibitors of apoptosis. The first, VVΔF1L-FLAG-EVM025(E255), expresses the 26kDa C-terminus (aa255-456) of the F1L orthologue from ectromelia virus, EVM025, which shares approximately 95% identity with F1L [570]. The second virus, VVΔF1L-FLAG-FPV039, expresses the 20kDa anti-apoptotic Bcl-2 homologue from fowlpox virus [533]. Infected cells were lysed in 1% NP-40 lysis buffer and subject to anti-FLAG immunoprecipitation. Western blotting with an anti-HA antibody revealed high molecular weight HA-ubiquitin smears that co-immunoprecipitated with the positive control, FLAG-EVM150, which associates active Cul-3 ubiquitin ligases (Fig 5.4) [572]. In contrast, no HA-ubiquitin was detected in mock-infected cells or cells expressing the negative control FLAG-EVM004, which does not associate with ubiquitin or ubiquitination machinery (Fig 5.4) [572]. HA-ubiquitin did, however, co-immunoprecipitate with FLAG-F1L and also the fowlpox virus anti-apoptotic protein FLAG-FPV039 (Fig 5.4). While both anti-apoptotic proteins associated with HA-ubiquitin, FLAG-FPV039 was highly ubiquitinated, far more than the positive control FLAG-EVM150. Faint HA-ubiquitin staining was detected with FLAG-EVM025(E255) in comparison with FLAG-F1L, despite the high
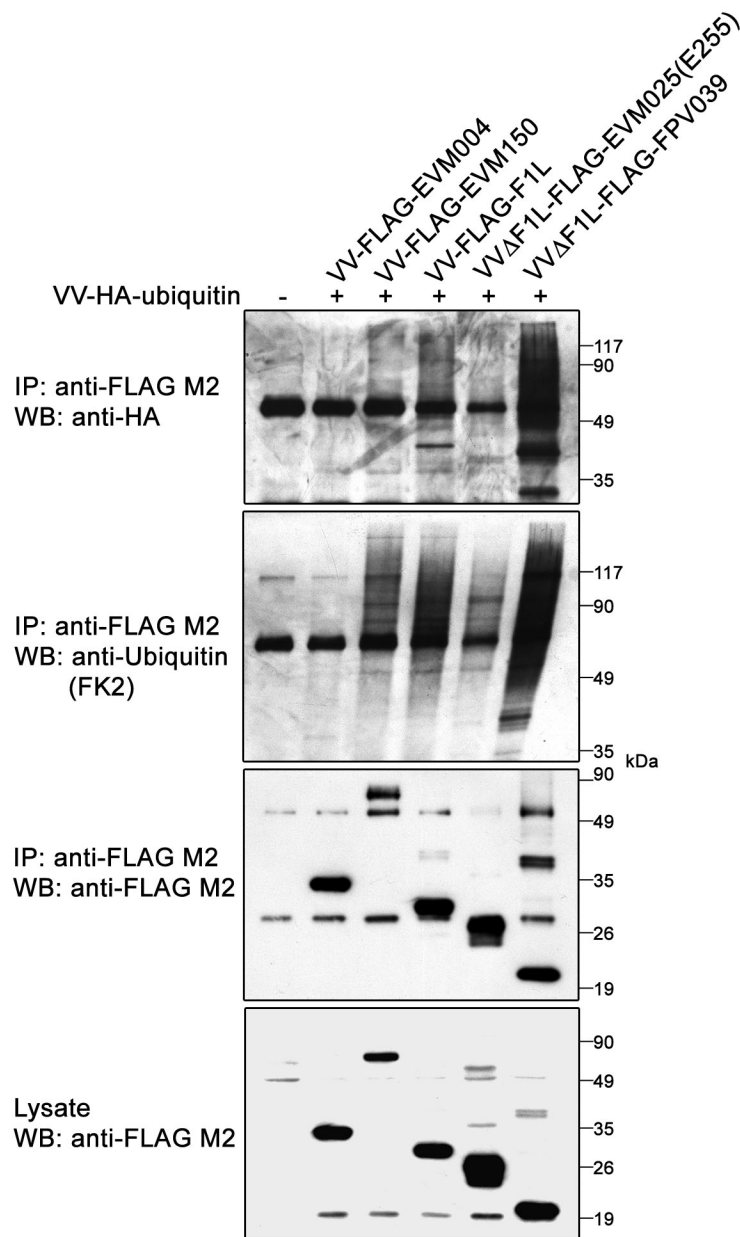
Figure 5.4 F1L associates with exogenously expressed ubiquitin. The association between F1L and exogenous ubiquitin was assessed in HeLa cells that were mock-infected or infected at an MOI of 5 with VV-FLAG-EVM004, VV-FLAG-EVM150, VV-FLAG-F1L, VVΔF1L-FLAG-EVM025(E255), or VVΔ F1L-FLAG-FPV039. Cells were co-infected with VV-HA-ubiquitin at an MOI of 5 and cells were lysed in 1% NP-40 buffer 12 hours post infection. Anti-FLAG M2 immunoprecipitates were western blotted with anti-HA, anti-ubiquitin (FK2), or anti-FLAG M2 to detect HA-ubiquitin, conjugated ubiquitin, or FLAG-tagged proteins, respectively. Expression of FLAG-tagged proteins was confirmed by western blotting lysates with anti-FLAG M2.

similarity between the two proteins (Fig 5.4). Ubiquitin was also detected in the anti-FLAG immunoprecipitates using an anti-ubiquitin (FK2) antibody that detects only conjugated ubiquitin in the form of monoubiquitin and polyubiquitin chains [577]. Western blotting with the anti-ubiquitin (FK2) antibody revealed conjugated ubiquitin associated with FLAG-EVM150, FLAG-F1L, FLAG-FPV039, and to a lesser extent, FLAG-EVM025(E255) (Fig 5.4). Both immunoprecipitates and lysates western blotted with anti-FLAG demonstrated comparable levels of FLAG-tagged proteins pulled down and expressed, respectively (Fig 5.4).

The previous data exhibited an association between F1L and exogenously expressed HA-ubiquitin. To examine the association between F1L and endogenous ubiquitin, HeLa cells were mock-infected or infected with VV-FLAG-F1L, VV-FLAG-EVM004, VV-FLAG-EVM150, VVΔF1L-FLAG-EVM025(E255), or VVΔF1L-FLAG-FPV039. Cells were lysed in 1% NP-40 buffer and immunoprecipitated with anti-FLAG. Similar to the results in figure 5.4, immunoprecipitated FLAG-EVM150, FLAG-F1L, FLAG-FPV039, and to a lesser extent FLAG-EVM025(E255), produced ubiquitin smears on the anti-ubiquitin (FK2) western blot, indicating an association with endogenously expressed conjugated ubiquitin (Fig 5.5). In contrast, conjugated ubiquitin was not present in anti-FLAG immunoprecipitates from mock-infected cells or cells expressing FLAG-EVM004. Immunoprecipitates were western blotted with anti-FLAG to reveal comparable pull down of all FLAG-tagged proteins (Fig 5.5). Furthermore, higher molecular weight species of FLAG-F1L, FLAG-EVM025(E255), and FLAG-FPV039 were evident in immunoprecipitates probed with anti-FLAG, suggestive of monoubiquitination and polyubiquitination (Fig 5.5). The approximate 8kDa increase in molecular weight for each of these three proteins suggested that the modified species represented monoubiquitinated protein, which for FLAG-F1L was 36kDa, whereas the high molecular weight products observed for FLAG-F1L and FLAG-FPV039 were potentially polyubiquitinated species (Fig 5.5). Similar results were observed when lysates were western blotted with anti-FLAG (Fig
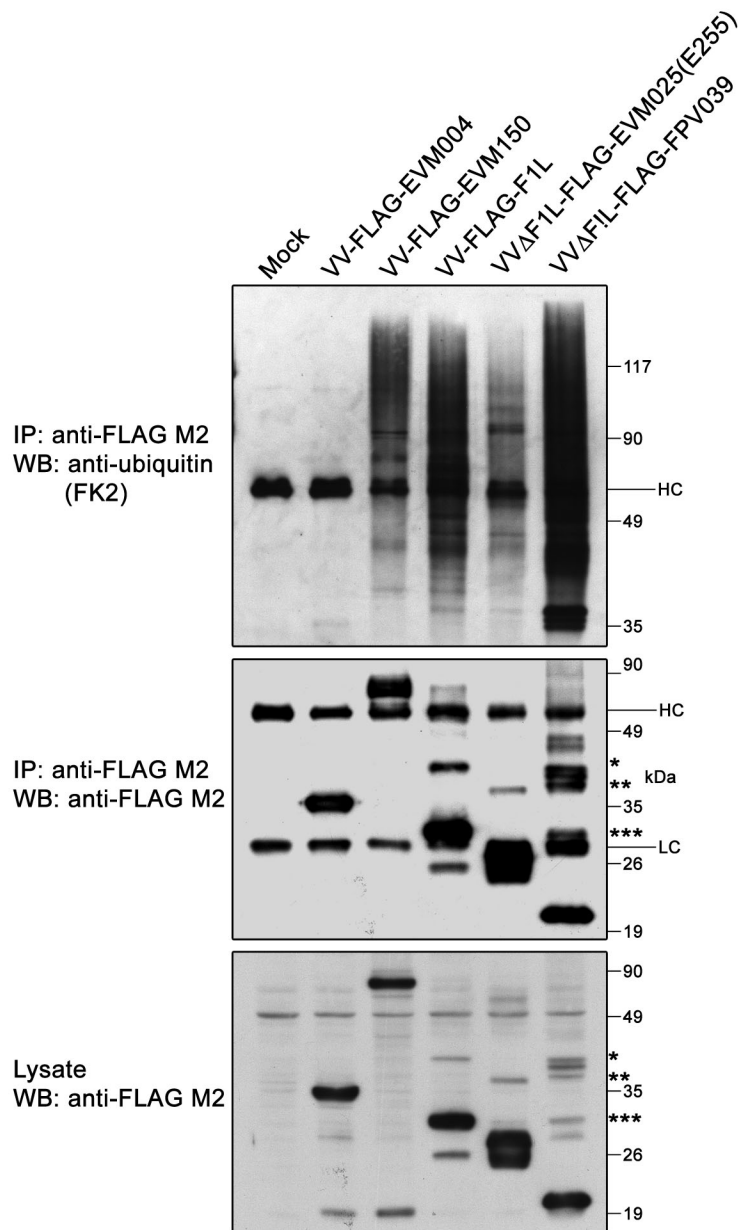
Figure 5.5 F1L associates with endogenous conjugated ubiquitin. Mock-infected HeLa cells or HeLa cells infected with VV-FLAG-EVM004, VV-FLAG-EVM150, VV-FLAG-F1L, VVΔF1L-FLAG-EVM025(E255), or VVΔF1L-FLAG-FPV039 for 12 hours and lysed in 1% NP-40 buffer. Anti-FLAG M2 immunoprecipitates were western blotted with anti-ubiquitin (FK2) to reveal endogenous conjugated ubiquitin. Immunoprecipitates and lysates were western blotted with anti-FLAG M2. Asterisks mark the predicted mono-ubiquitinated species of FLAG-F1L (*), FLAG-EVM025(E255) (**), and FLAG-FPV039 (***). HC, heavy chain; LC, light chain.

5.5). Although high molecular weight species for FLAG-EVM150 were not observed in immunoprecipitates or lysates western blotted with anti-FLAG, this protein associated with conjugated ubiquitin, suggesting that FLAG-EVM150 was turned over rapidly, or, alternatively, larger forms of the protein were difficult to detect given its high molecular weight (Fig 5.5). The ubiquitination of F1L was likely not a result of ubiquitinated proteins bound to F1L since similar results were observed when cells were lysed in RIPA lysis buffer, a more stringent detergent that disrupts most protein-protein interactions while preserving covalent bonds, such as isopeptide bonds between ubiquitin and a substrate (Fig A.2) [678,679]. Together, these data revealed that F1L and other poxviral anti-apoptotic proteins were regulated by cellular ubiquitination machinery. However, the outcome of F1L ubiquitination and the effect of ubiquitination on the anti-apoptotic activity of F1L have yet to be elucidated.

5.2.3 F1L and ubiquitin colocalize at mitochondria. The conjugation of ubiquitin onto target proteins is a continual process that occurs throughout a cell [371,372]. Given that F1L is exclusively found at mitochondria [547,548] and F1L associated with conjugated ubiquitin, we sought to determine whether ubiquitin could be detected at mitochondria in the presence of F1L. HeLa cells were mock-infected or infected with VV, VV-FLAG-EVM004, or VV-FLAG-F1L. Twelve hours post infection, cells were fixed and permeabilized before staining with anti-ubiquitin (FK2) and anti-FLAG for visualization by confocal microscopy. The DNA-binding fluorescent stain, DAPI, was used to stain both the nucleus and the perinuclear virus factories in infected cells. Conjugated ubiquitin was found diffuse throughout mock-infected cells, occupying both the cytoplasm and the nucleus (Fig 5.6 panels a-d). In VV-infected cells, conjugated ubiquitin remained largely diffuse with a few areas of enrichment or "speckles" in the cytoplasm (Fig 5.6 panels e-h). Similarly, the pattern of conjugated ubiquitin in VV-FLAG-EVM004-infected cells resembled VV-infected cells, as it was spread throughout the cell with several enriched areas (Fig 5.6 panels i-l). The concentrated areas
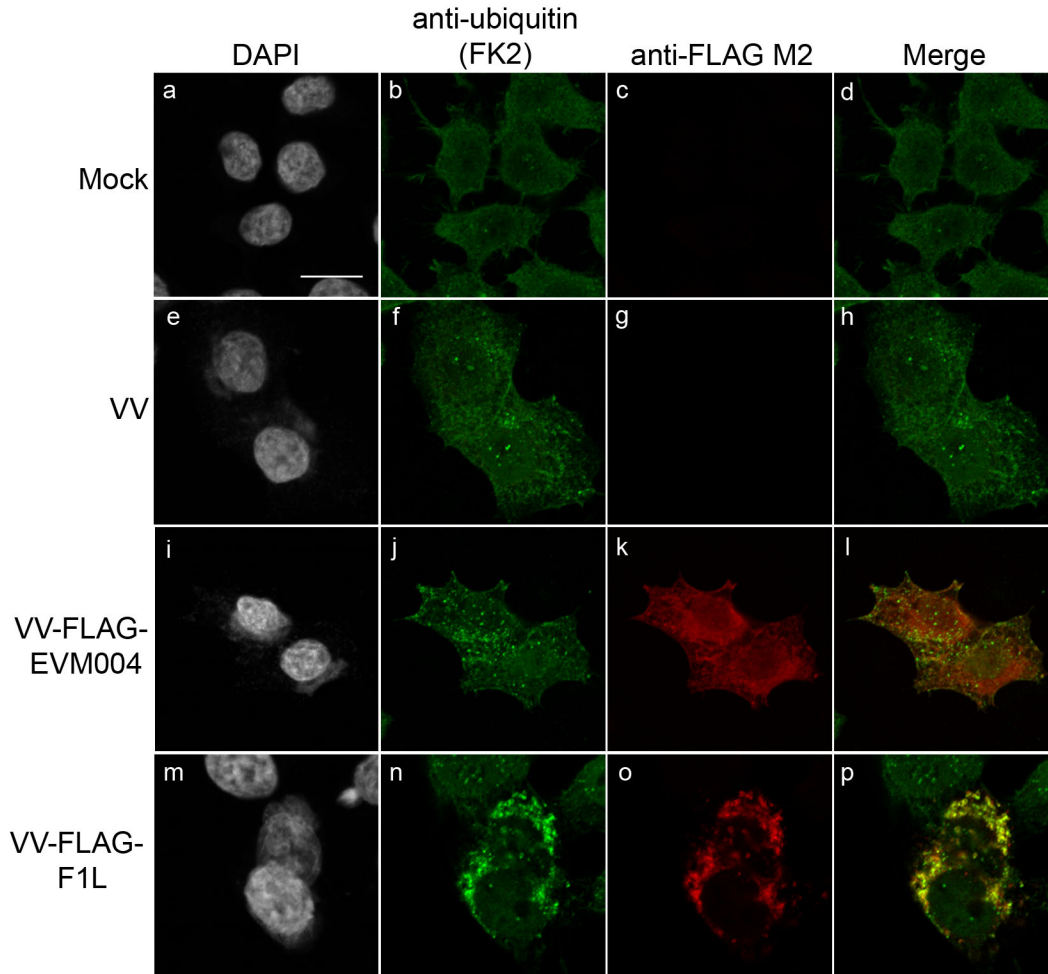
Figure 5.6 Conjugated ubiquitin colocalizes with F1L at mitochondria. The localization of conjugated ubiquitin was assessed by mock-infecting HeLa cells or infecting with VV, VV-FLAG-EVM004, or VV-FLAG-F1L for 12 hours. Cells were fixed, permeabilized, and stained with DAPI, anti-ubiquitin (FK2), or anti-FLAG M2 prior to visualization by confocal microscopy. Conjugated ubiquitin was detected in the nucleus and cytoplasm in mock-infected cells (**a-d**) and cells infected with VV (**e-h**) and VV-FLAG-EVM004 (**i-l**). In contrast, conjugated ubiquitin colocalized with FLAG-F1L at mitochondria in VV-FLAG-F1L-infected cells (**m-p**). Bar=15μm.

of conjugated ubiquitin were not enriched with FLAG-EVM004, suggesting that FLAG-EVM004 did not colocalize with ubiquitin (Fig 5.6 panels i-l). Interestingly, in cells infected with VV-FLAG-F1L, conjugated ubiquitin was found almost exclusively at mitochondria where FLAG-F1L was located (Fig 5.6 panels m-p). This suggested that overexpression of F1L during infection caused a drastic redistribution of conjugated ubiquitin to mitochondria where it colocalized with FLAG-F1L.

Ubiquitin chains can form on one of seven lysines within ubiquitin [379,380]. Most commonly, polyubiquitin chains linked through K48 lead to proteasomal degradation of the protein; whereas monoubiquitin or polyubiquitin chains formed on K63 can alter protein function [379,382,383]. To better understand the type of ubiquitin chain formed on F1L, we performed colocalization studies using an HA-tagged wildtype ubiquitin or a mutant ubiquitin that is only capable of forming chains through K48, HA-K48-ubiquitin. In this mutant, all lysines except K48 have been mutated forcing ubiquitin chains containing this mutant to form on K48, and thus on proteins to be degraded by the proteasome. HeLa cells were infected with VV or VV-FLAG-F1L and transfected with pcDNA-HA-ubiquitin or pBluescript-HA-K48-ubiquitin. Since both ubiquitin constructs are under the control of a T7 promoter, infected cells were co-infected at a low MOI with VVT7, a recombinant VV that expresses T7 polymerase, to drive the expression of ubiquitin [568,569]. In mock cells no ubiquitin or F1L was detected with anti-HA or anti-FLAG M2, respectively (Fig 5.7 panels a-d). During infection with VV, staining with anti-HA demonstrated that wildtype HA-ubiquitin was distributed throughout the cell (Fig 5.7 panels e-h). Likewise, HA-K48-ubiquitin was localized throughout the cell during VV infection (Fig 5.7 panels i-l). Infection with VV-FLAG-F1L demonstrated a reticular mitochondrial pattern for FLAG-F1L (Fig 5.7 panels m-p). In VV-FLAG-F1L-infected cells transfected with wildtype HA-ubiquitin, HA-staining was no longer observed throughout the cell (Fig 5.7 panels q-t). Instead, HA-ubiquitin

	DAPI	anti-HA	anti-FLAG M2	Merge

Mock — a, b, c, d

VV + HA-WT-Ub — e, f, g, h

VV + HA-K48-Ub — i, j, k, l

VV-FLAG-F1L — m, n, o, p

VV-FLAG-F1L + HA-WT-Ub — q, r, s, t

VV-FLAG-F1L + HA-K48-Ub — u, v, w, x
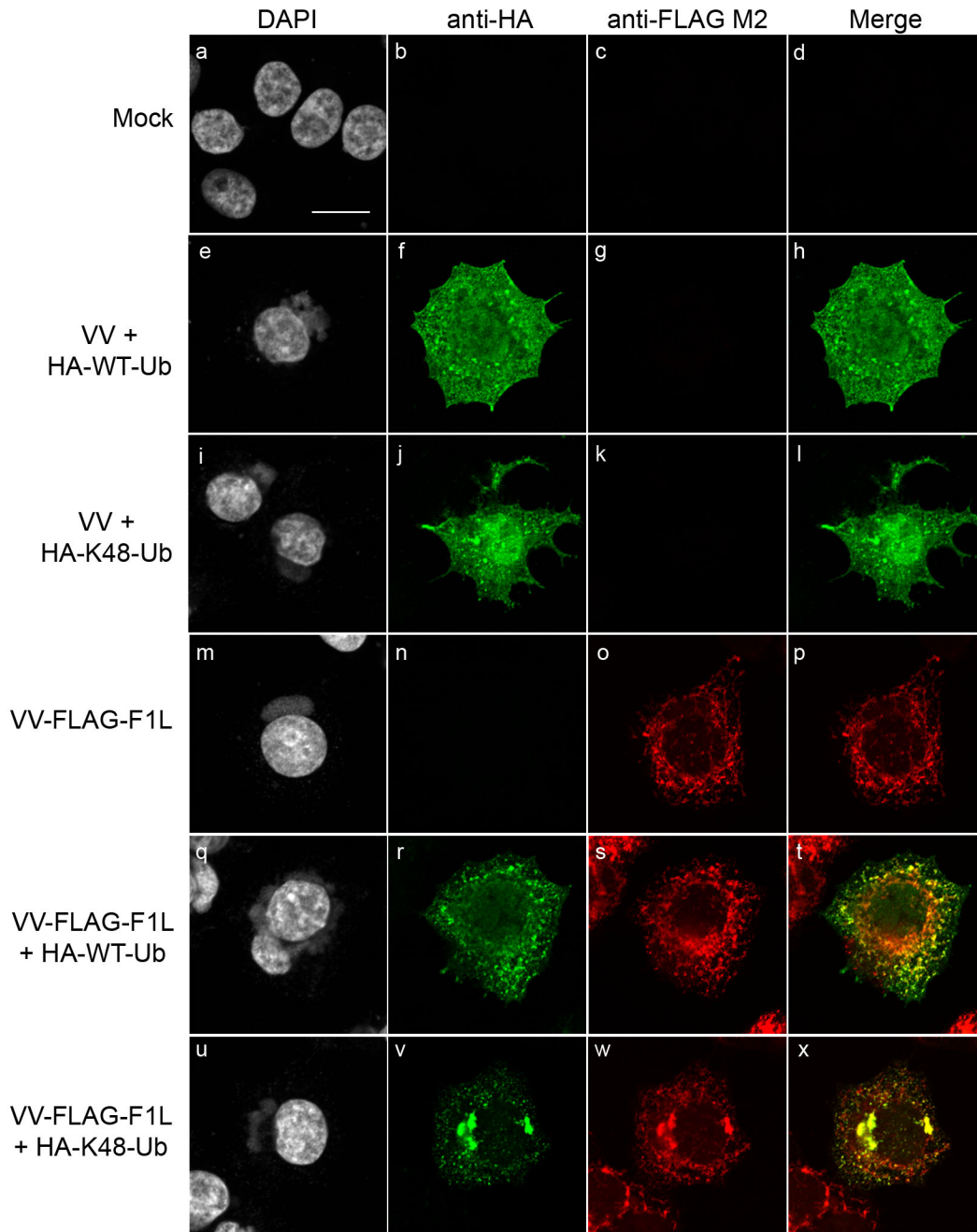
Figure 5.7 F1L colocalizes at mitochondria with wildtype ubiquitin and K48-ubiquitin. HeLa cells were mock-infected or infected with VV or VV-FLAG-F1L at an MOI of 4. Cells were simultaneously transfected with pcDNA-HA-ubiquitin (HA-WT-Ub) or pBluescript-HA-K48-ubiquitin (HA-K48-Ub). To drive expression of ubiquitin constructs during infection, cells were co-infected with VVT7 at an MOI of 1. Fourteen hours post infection-transfection, cells were fixed and stained with DAPI, anti-HA, or anti-FLAG M2 before analysis by confocal microscopy. **a-d**, mock-infected and mock-transfected; **e-h**, VV-infected and HA-WT-Ub-transfected; **i-l**, VV-infected and HA-K48-Ub-transfected; **m-p**, VV-FLAG-F1L-infected; **q-t**, VV-FLAG-F1L-infected and HA-WT-Ub-transfected; **u-x**, VV-FLAG-F1L-infected and HA-K48-Ub transfected. Bar=15μm.

colocalized at mitochondria with FLAG-F1L (Fig 5.7 panels q-t). Ubiquitin redistribution to mitochondria was also seen in VV-FLAG-F1L-infected cells expressing HA-K48-ubiquitin (Fig 5.7 panels u-x). Curiously, in cells that demonstrated colocalization between FLAG-F1L and either HA-WT-Ub or HA-K48-Ub, mitochondria were slightly were punctate than reticular (Fig 5.7 panels q-x). We noted that the colocalization between FLAG-F1L and HA-ubiquitin was much stronger when mitochondria adopted a condensed and punctate morphology, as opposed to a reticular pattern (Fig A.3). While the reason for this observation is not clear, it is obvious that the overexpression of FLAG-F1L is able to induce the relocalization of ubiquitin from the cytoplasm and nucleus to mitochondria. Moreover, the colocalization of FLAG-F1L and HA-K48-ubiquitin suggested that the ubiquitin chains formed on F1L may result in proteasomal degradation of the protein.

5.3 F1L IS DEGRADED BY THE 26S PROTEASOME

5.3.1 F1L protein levels are stabilized by proteasome inhibition during transfection.
Polyubiquitin chains formed through K48 of ubiquitin typically target a protein for degradation by the 26S proteasome, an event mediated by the catalytic β-subunits in the 20S proteolytic core [382,406]. F1L colocalized with HA-K48-ubiquitin, suggesting that K48-mediated chains form on F1L (Fig 5.7). To determine if ubiquitinated F1L was degraded by the proteasome in the absence of virus infection, HeLa cells were transfected with pEGFP, pEGFP-F1L, or pEGFP-p28, the ubiquitin ligase from VV(IHDW) that is potentially regulated by the UPS [492,493,566]. Following transfection, the 26S proteasome was inhibited by treating cells with the cell-permeable peptide aldehyde, MG132, for 6 hours. To measure cell viability, cells were stained with the mitochondrial-specific fluorophore TMRE since prolonged treatment with proteasome inhibitors can have cytotoxic effects [680,681]. TMRE and EGFP fluorescence were measured by flow cytometry and protein stabilization was assessed by EGFP fluorescence. While MG132 treatment did not significantly enhance EGFP

protein levels (Fig 5.8A panels a and b), the level of EGFP fluorescence in the TMRE-positive, or healthy, population increased from 10.8% to 41.7% in EGFP-p28 expressing cells in the presence of MG132 (Fig 5.8A panels c and d). Thus, EGFP-p28, but not EGFP, was regulated by proteasomal degradation. In addition, 25.1% of TMRE-positive cells expressed EGFP-F1L and this increased to 48.1% during MG132 treatment, indicating protein stabilization during proteasomal inhibition (Fig 5.8A panels e and f).   Data from three independent experiments were quantified and represented in Fig 5.8B. Again, EGFP was not stabilized by MG132, whereas proteasomal inhibition resulted in a fourfold increase of EGFP-p28 and a twofold increase of EGFP-F1L (Fig 5.8B). Stabilization of EGFP-F1L during proteasomal inhibition was further reinforced by harvesting transfected whole cell lysates following 6 hours of MG132 treatment and resolving with SDS-PAGE. Western blotting with an anti-EGFP antibody revealed that in agreement with the flow cytometry results in figure 5.8A and B, EGFP-p28 protein levels, but not EGFP, increased dramatically with MG132 (Fig 5.8C). Importantly, upon MG132 treatment, protein levels of EGFP-F1L were enhanced, indicating that F1L was indeed regulated by the 26S proteasome (Fig 5.8C).

5.3.2 F1L protein levels are stabilized by proteasome inhibition during infection. In order to assess the effect of proteasomal inhibition on F1L during infection, HeLa cells were infected with VV or VVEGFP, both of which express endogenous F1L, or VVΔF1L as a negative control. Cells were pretreated with MG132 before infection and the proteasome inhibitor was added to infected cells one hour after infection. Whole cells lysates harvested at 4, 8, or 12 hours post infection were western blotted with an anti-F1L antibody and revealed that F1L was produced during infection with VV and VVEGFP, but not in VVΔF1L-infected cells (Fig 5.9). In the presence of MG132, F1L protein levels greatly increased during VV and VVEGFP infection, indicating that inhibition of the proteasome stabilized endogenous F1L. Additionally, treatment with MG132 yielded a higher molecular weight product at 8 and 12 hours post infection that
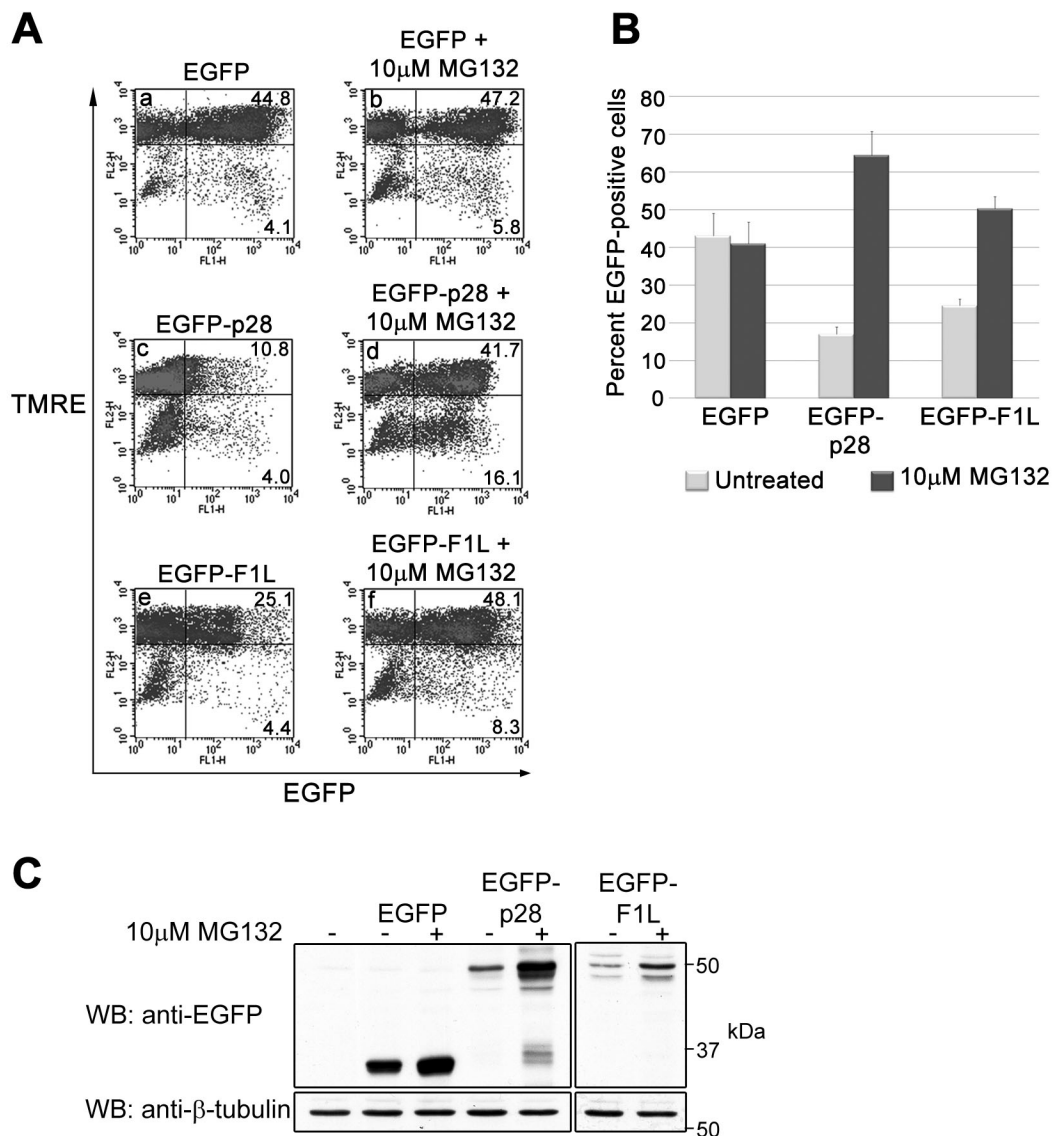
Figure 5.8 F1L is degraded by the proteasome during transfection. A. To analyze the stability of F1L during proteasomal inhibition, HeLa cells were transfected with pEGFP (**a,b**), pEGFP-p28 (**c,d**), or pEGFP-F1L (**e,f**) for 16 hours prior to the addition of 10µM MG132 for 6 hours. Live cells were stained with the cell-permeable fluorescent dye, TMRE, and TMRE-positive and EGFP-positive cells were analyzed by flow cytometry. **B.** The experiment in (**A**) was performed in triplicate and graphed with standard deviations. **C.** Whole cell lysates were harvested from HeLa cells that were transfected and treated with MG132 as described in (**A**). Samples were resolved by SDS-PAGE and western blotted with anti-EGFP and, as a loading control, anti-β-tubulin.
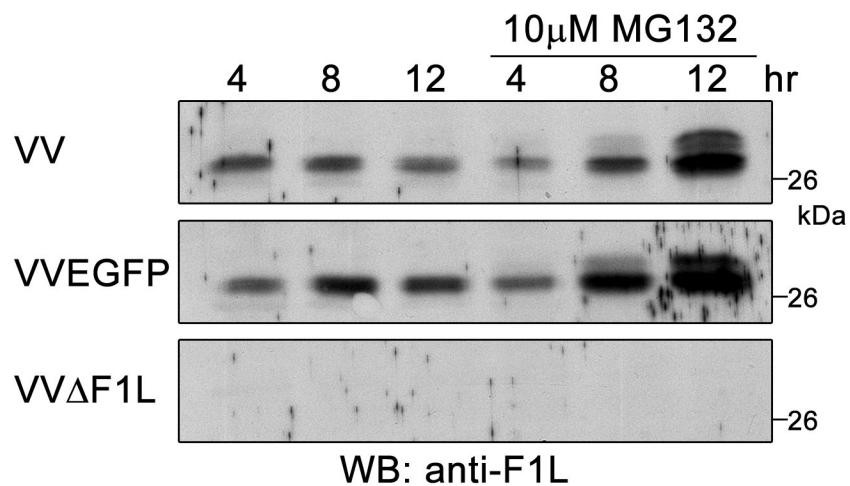
Figure 5.9 Endogenous F1L is degraded by the proteasome during infection. F1L stability during infection was assessed by infecting HeLa cells with VV, VVEGFP, or VVΔF1L at an MOI of 10 for 4, 8, or 12 hours. Cells were infected in the absence or presence of 10μM MG132. Whole cell lysates were harvested and western blotted with anti-F1L to examine endogenous F1L protein levels.

was detected by the anti-F1L antibody (Fig 5.9). The modest increase in molecular weight compared to F1L suggested this species may represent a post-translationally modified form of F1L, such as a phosphoprotein. Unfortunately, attempts to confirm the possible phosphorylation of F1L during calf intestinal phosphatase treatment were unsuccessful due to the unexplained insolubility of F1L in the presence of MG132. From these data, it was evident that ubiquitination of F1L resulted in proteasomal degradation, and additionally, F1L may be modified prior to degradation based on the presence of a slower migrating F1L species upon proteasomal inhibition.

We have observed the stabilization of F1L by proteasome inhibition upon transfection and VV infection. To determine whether inhibition of the proteasome could prolong the half-life of F1L during infection, HeLa cells were infected with VV-FLAG-F1L for 12 hours. Cells were starved of methionine and cysteine prior to incubation with ^{35}S methionine and cysteine. After 30 minutes of radiolabelling, fresh media or media containing MG132 was added to the cells. At various times post radiolabelling, cells were lysed in 1% NP-40 lysis buffer and immunoprecipitated with anti-FLAG before visualizing radiolabelled anti-FLAG immunoprecipitates by autoradiography. In the absence of MG132, FLAG-F1L protein levels were significantly decreased after 4 hours and barely detectable at 8 and 12 hours (Fig 5.10). Thus, FLAG-F1L was fully turned over within 4-8 hours of being produced. Treating cells with MG132, however, dramatically stabilized FLAG-F1L and the protein was still present at 12 hours (Fig 5.10). No radiolabelled proteins were observed in mock-infected cells following anti-FLAG immunoprecipitation, confirming the specificity for FLAG-F1L. Together, these data suggested that F1L was targeted to the 26S proteasome in the absence and presence of infection and proteasomal inhibition prolonged the half-life of the protein.

5.4 CULLIN-1 IS A POTENTIAL UBIQUITIN LIGASE THAT UBIQUITINATES F1L
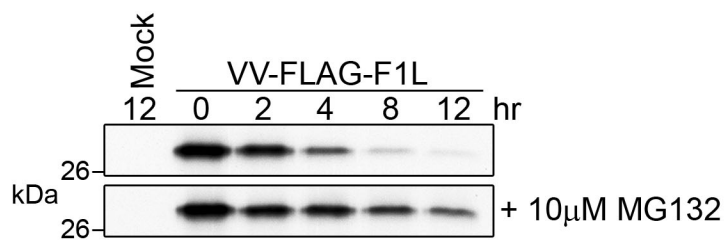
Figure 5.10 Proteasomal inhibition extends the half-life of F1L during infection. HeLa cells were mock-infected or infected with VV-FLAG-F1L at an MOI of 5 for 12 hours. Cells were starved of methionine and cysteine for 30 minutes before radiolabelling with 45µCi of ^{35}S-containing methionine and cysteine for 30 minutes. Fresh media or media containing 10µM MG132 was added to the cells and cells were harvested at 0, 2, 4, 8, or 12 hours post labelling. Cells were lysed in 1% NP-40 buffer and FLAG-F1L was immunoprecipitated with anti-FLAG M2. Radiolabelled FLAG-F1L was visualized by autoradiography.

The human genome contains over 600 predicted ubiquitin ligases that are capable of transferring ubiquitin onto target substrates and it is common for multiple ubiquitin ligases to ubiquitinate one cellular protein [377,437,438,439,440]. The stabilization of transiently-transfected EGFP-F1L during proteasome inhibition (Fig 5.8) suggested that F1L can be ubiquitinated and degraded in the absence of other viral proteins. Thus, one or more cellular ubiquitin ligases are likely responsible for conjugating ubiquitin onto F1L. Although speculative, the potential phosphorylated species of F1L that accumulated during MG132 treatment implied that F1L may be phosphorylated before being ubiquitinated and degraded (Fig 5.9). Importantly, phosphorylation plays a key role in targeting proteins to ubiquitin ligases for ubiquitination and this is particularly true for the SCF complex [402,404,405,647].

To determine if the SCF machinery was involved in the ubiquitination of F1L, HEK 293T cells were infected with VV or VV-HA-Cul1ΔRoc1. VV-HA-CulΔRoc1 is a recombinant VV expressing a mutant form of HA-tagged Cul-1 devoid of the Roc1-binding domain [682]. The inability of Roc1 to bind Cul-1 ceases catalytic activity of the E3 ligase complex, but the mutant form of Cul-1 can bind substrates and serves as a dominant negative mutant [682]. Cells were co-infected with VV-FLAG-EVM004, VV-FLAG-F1L, or VVΔF1L-FLAG-FPV039. Twelve hours post infection cells were lysed in 1% NP-40 buffer and anti-FLAG was used to immunoprecipitate the FLAG-tagged proteins. Western blotting the immunoprecipitates with anti-ubiquitin (FK2) indicated that ubiquitination was not detected in mock-infected cells and FLAG-EVM004 was not ubiquitinated in the presence of either VV or VV-HA-Cul1ΔRoc1 (Fig 5.11). In cells co-infected with VV and VV-FLAG-F1L, FLAG-F1L associated with conjugated ubiquitin (Fig 5.11). In comparison, substantially less conjugated ubiquitin was associated with FLAG-F1L in the presence of the dominant negative Cul-1 (Fig 5.11). These data suggest that the SCF machinery was involved in the conjugation of ubiquitin onto F1L. However, FLAG-F1L still associated with an appreciable level of conjugated
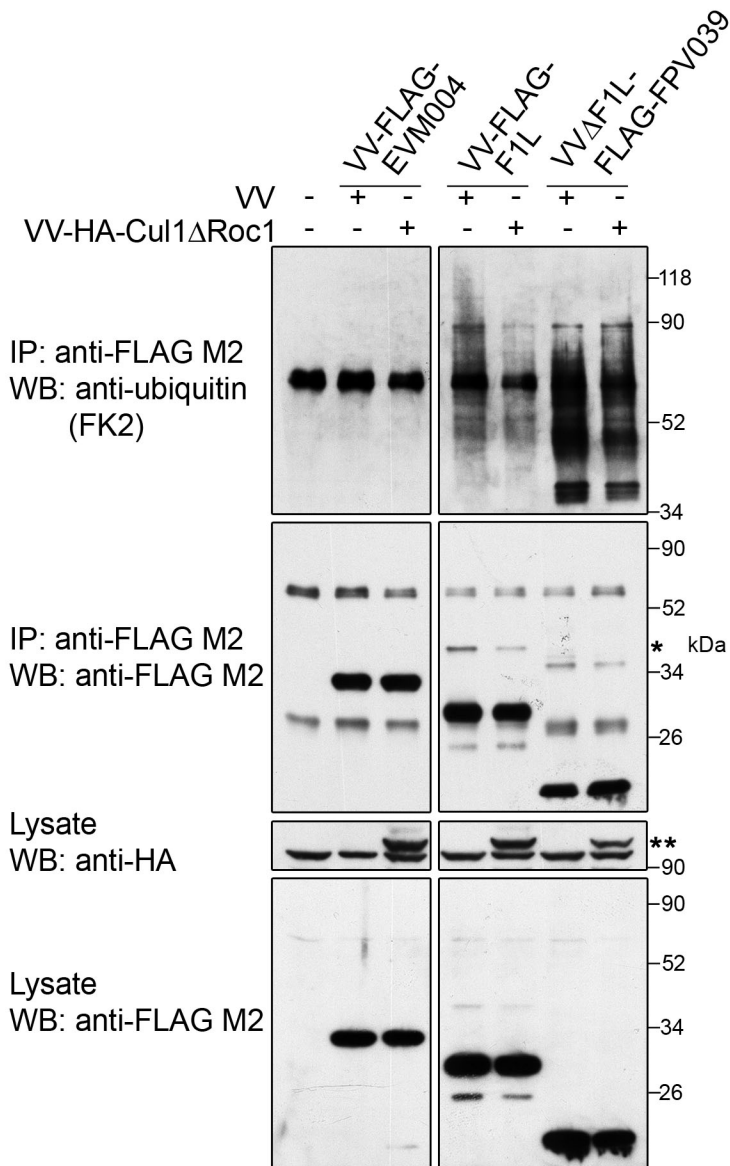
Figure 5.11 F1L is ubiquitinated by the SCF complex during infection. HEK 293T cells were mock-infected or infected at an MOI of 5 with VV-FLAG-EVM004, VV-FLAG-F1L, or VVΔF1L-FLAG-FPV039 and co-infected with VV or VV-HA-Cul1Δ Roc1 at an MOI of 5. Twelve hours post infection, cells were lysed in 1% NP-40 buffer and immunoprecipitated with anti-FLAG M2. Immunoprecipitates were western blotted with anti-ubiquitin (FK2) and anti-FLAG M2, and lysates were western blotted with anti-HA and anti-FLAG M2. The suspected monoubiquitinated FLAG-F1L was indicated by a single asterisk in the anti-FLAG immunoprecipitate, while HA-Cul1ΔRoc1 was marked by a double asterisk in lysates probed with anti-HA.

ubiquitin in cells infected with VV-HA-Cul1ΔRoc1, implying that Cul-1 was likely not the sole ubiquitin ligase targeting F1L. In contrast to FLAG-F1L, western blotting immunoprecipitates with anti-ubiquitin (FK2) revealed that ubiquitination of FLAG-FPV039 was not altered by dominant negative Cul-1 (Fig 5.11). Immunoprecipitates western blotted with anti-FLAG demonstrated that the dominant negative Cul-1 had no significant effect on the immunoprecipitated protein levels of FLAG-F1L or any other FLAG-tagged protein (Fig 5.11). However, the 36kDa species of FLAG-F1L, suspected to be monoubiquitinated F1L, was slightly reduced in VV-HA-Cul1ΔRoc1-infected cells, compared to VV-infected cells, further indicating a decrease in the ubiquitination of F1L when the SCF was impaired (Fig 5.11). Lastly, the expression of the HA-Cul1ΔRoc1 was confirmed by western blotting lysates with anti-HA and lysates were western blotted with anti-FLAG to examine expression of FLAG-tagged proteins (Fig 5.11). The ability of the SCF to conjugate ubiquitin onto F1L did not extend to other cullin family members, since a dominant negative Cul-3 had no effect on the association of ubiquitin with F1L (Fig A.4). However, other ubiquitin ligases were likely involved in regulating F1L, since the dominant negative Cul-1 was unable to completely inhibit F1L ubiquitination (Fig 5.11).

5.5 MAPPING RESIDUES IN F1L REQUIRED FOR UBIQUITINATION

5.5.1 Identifying F1L lysine residues targeted for ubiquitination. F1L contains eleven lysine residues, nine of which reside in the cytoplasmic domain (Figs 5.1 and 5.2), leading us to hypothesize that ubiquitination of F1L likely occurs on one or more of the cytoplasmically accessible lysines. In order to begin identifying lysines in F1L that are targeted for ubiquitination, site directed mutagenesis was employed to mutate the cytoplasmic lysines and determine whether the association between F1L and conjugated ubiquitin was affected. A panel of FLAG-F1L mutants were generated whereby lysine to arginine mutations were introduced sequentially (Table 5.1). Mutations were added to a triple lysine mutant, pSC66-FLAG-F1L(3K-R), which contains K122R, K165R, and K168R.

Table 5.1 F1L Lysine to Arginine Mutations.

Construct	Mutations
pSC66-FLAG-F1L(K122R)	K122R
pSC66-FLAG-F1L(K206R)	K206R
pSC66-FLAG-F1L(K122/103R)	K122R, K103R
pSC66-FLAG-F1L(K122/89R)	K122R, K89R
pSC66-FLAG-F1L(3K-R)	K122R, K165R, K168R
pSC66-FLAG-F1L(4K-R)	K122R, K165R, K168R, K103R
pSC66-FLAG-F1L(5K-R)	K122R, K165R, K168R, K103R, K89R
pSC66-FLAG-F1L(6K-R)	K122R, K165R, K168R, K103R, K89R, K51R
pSC66-FLAG-F1L(7K-R)	K122R, K165R, K168R, K103R, K89R, K51R, K76R
pSC66-FLAG-F1L(8K-R)	K122R, K165R, K168R, K103R, K89R, K51R, K76R, K141R
pSC66-FLAG-F1L(9K-R)	K122R, K165R, K168R, K103R, K89R, K51R, K76R, K141R, K206R

Ultimately, all nine cytoplasm-facing lysines in F1L were mutated to generate pSC66-FLAG-F1L(9K-R) (Fig 2.1) and the panel of lysine-deficient F1L constructs was analyzed for ubiquitination. HEK 293T cells were infected with VV and transfected with pSC66-FLAG-F1L or pSC66-FLAG-F1L constructs carrying lysine mutations from 3K-R to 9K-R. Following lysis in 1% NP-40 buffer, proteins were immunoprecipitated with anti-FLAG and the association with ubiquitin was resolved with SDS-PAGE and western blotting with anti-ubiquitin (FK2). Comparable to wildtype FLAG-F1L, all F1L lysine-deficient mutants unexpectedly associated with conjugated ubiquitin, including FLAG-F1L(9K-R), which lacks all nine cytoplasmic lysines (Fig 5.12). Immunoprecipitates were western blotted with anti-FLAG to demonstrate equal levels of each FLAG-F1L construct with a molecular weight of 28kDa (Fig 5.12). A longer exposure of the anti-FLAG western blot revealed that the 36kDa monoubiquitinated product of F1L was no longer present in immunoprecipitates as more lysine mutations were introduced (Fig 5.12). This higher molecular weight F1L species was present in wildtype FLAG-F1L, FLAG-F1L(3K-R), FLAG-F1L(4K-R), and FLAG-F1L(5K-R), but was barely detected in FLAG-F1L(6K-R) to FLAG-F1L(9K-R). All lysine-deficient F1L mutants were expressed at comparable levels, evident in lysates western blotted with anti-FLAG and loss of the 36kDa F1L species was again observed in FLAG-F1L(6K-R), FLAG-F1L(7K-R), FLAG-F1L(8K-R), and FLAG-F1L(9K-R) lysates upon longer exposure of the anti-FLAG western blot (Fig 5.12). To ensure that the disappearance of the 36kDa F1L product was not due to improper loading, lysates were western blotted with anti-β-tubulin as a control (Fig 5.12). Therefore, although the accumulation of lysine to arginine mutations did not appear to influence the association between F1L and conjugated ubiquitin, the post-translationally modified species of F1L were altered; yet the cause of this observation remains uncertain.

To further examine the ubiquitination of lysine-deficient F1L mutants, ubiquitin association with FLAG-F1L(8K-R) and FLAG-F1L(9K-R) was assessed in
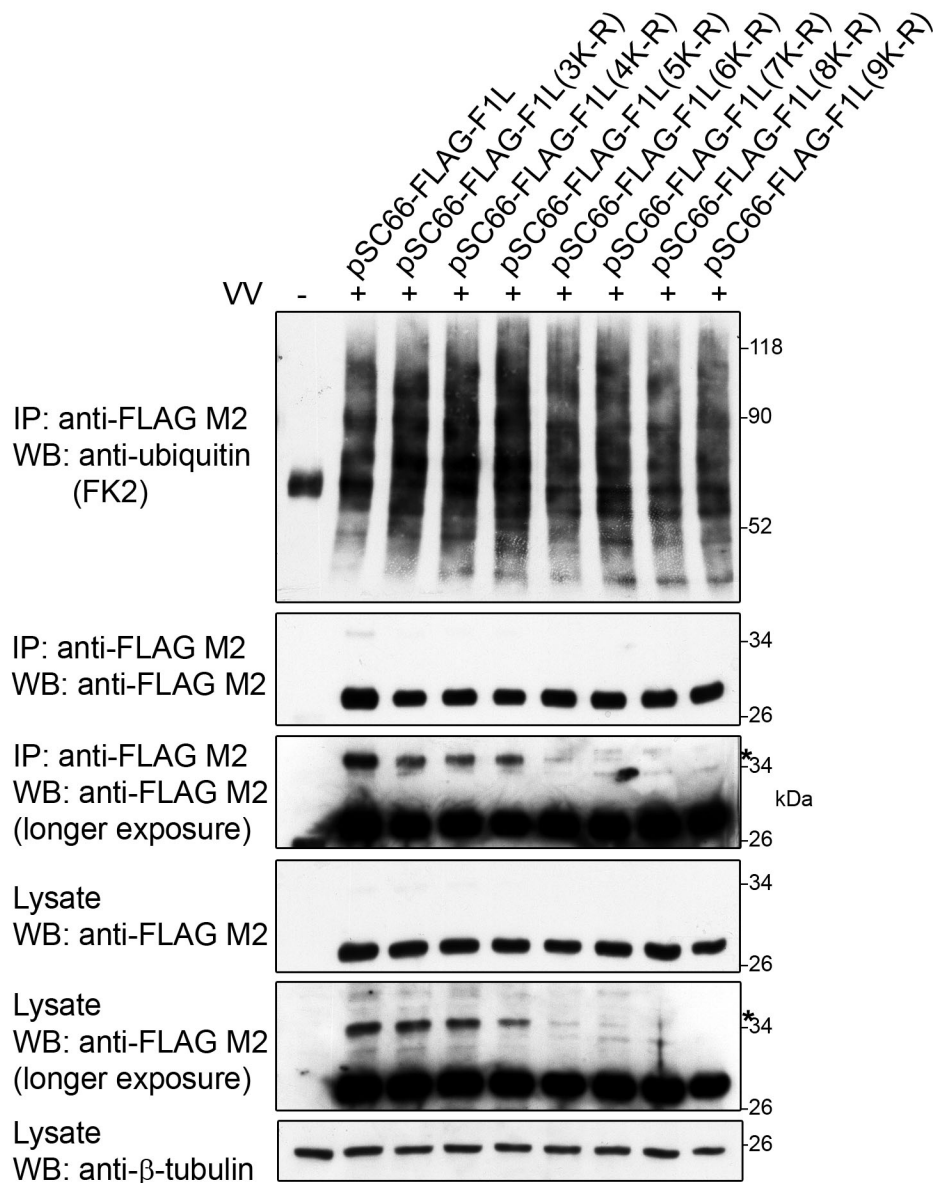
Figure 5.12 Lysine-deficient F1L mutants associate with conjugated ubiquitin but display altered post-translational modifications. HEK 293T cells were mock-infected or infected at an MOI of 5 with VV. Cells were simultaneously transfected with pSC66-FLAG-F1L, pSC66-FLAG-F1L(3K-R), pSC66-FLAG-F1L(4K-R), pSC66-FLAG-F1L(5K-R), pSC66-FLAG-F1L(6K-R), pSC66-FLAG-F1L(7K-R), pSC66-FLAG-F1L(8K-R), or pSC66-FLAG-F1L(9K-R) for fourteen hours. Cells were lysed in 1% NP-40 buffer and subject to anti-FLAG M2 immunoprecipitation. Immunoprecipitates were western blotted with anti-ubiquitin (FK2) or anti-FLAG M2 and lysates were western blotted with anti-FLAG M2 or anti-β-tubulin. Longer exposures of anti-FLAG M2 western blots were included for immunoprecipitates and lysates. The 36kDa suspected monoubiquitinated form of FLAG-F1L was indicated by an asterisk.

both NP-40 and RIPA lysis buffers. HEK 293T cells were infected with VV and transfected with pSC66-FLAG-F1L, pSC66-FLAG-F1L(8K-R), pSC66-FLAG-F1L(9K-R), or pSC66-FLAG-F1L(K206R). In order to generate pSC66-FLAG-F1L(9K-R) from pSC66-FLAG-F1L(8K-R), K206 was mutated to arginine (Table 5.1). This lysine flanks the N-terminal side of the transmembrane domain in F1L, which is important for mitochondrial localization (Fig 5.1) [548]. Thus, the K206R mutation was tested alone to ascertain whether the absence of K206 altered any functional aspect of F1L. Fourteen hours after infection, each sample was divided and lysed in either 1% NP-40 buffer or RIPA buffer prior to anti-FLAG immunoprecipitation. In a more stringent detergent, such as RIPA, FLAG-F1L mutants lacking 8 or 9 lysine residues, as well as FLAG-F1L bearing the single K206R mutation, were ubiquitinated at levels comparable to wildtype FLAG-F1L (Fig 5.13A). Upon lysis in 1% NP-40 buffer, it appeared as though FLAG-F1L(8K-R) and FLAG-F1L(9K-R) were associated with slightly more conjugated ubiquitin than wildtype FLAG-F1L or FLAG-F1L(K206R) (Fig 5.13B). FLAG-F1L, FLAG-F1L(8K-R), FLAG-F1L(9K-R), and FLAG-F1L(K206R) were all immunoprecipitated with anti-FLAG equally in RIPA (Fig 5.13A) and 1% NP-40 (Fig 5.13B). Once again, lysates western blotted with anti-FLAG revealed a loss of the 36kDa monoubiquitinated species of F1L in cells expressing FLAG-F1L(8K-R) and FLAG-F1L(9K-R) (Fig 5.13A and B). The K206R-bearing F1L mutant resembled wildtype FLAG-F1L as the 36kDa species was present, indicating that mutation of K206 alone did not alter the post-translational modification of F1L (Fig 5.13A and B). Interestingly, a longer exposure of the lysates not only demonstrated a loss of the 36kDa product in FLAG-F1L(8K-R)- and FLAG-F1L(9K-R)-expressing cells, but the appearance of a 34kDa and 38kDa F1L species in both RIPA and NP-40 buffers (Fig 5.13A and B). The 34kDa and 38kDa F1L species were not detected in cells expressing FLAG-F1L or FLAG-F1L(K206R), indicating unique post-translational modifications of FLAG-F1L(8K-R) and FLAG-F1L(9K-R). Thus, depleting lysine residues in F1L affected the formation of high molecular weight species of the
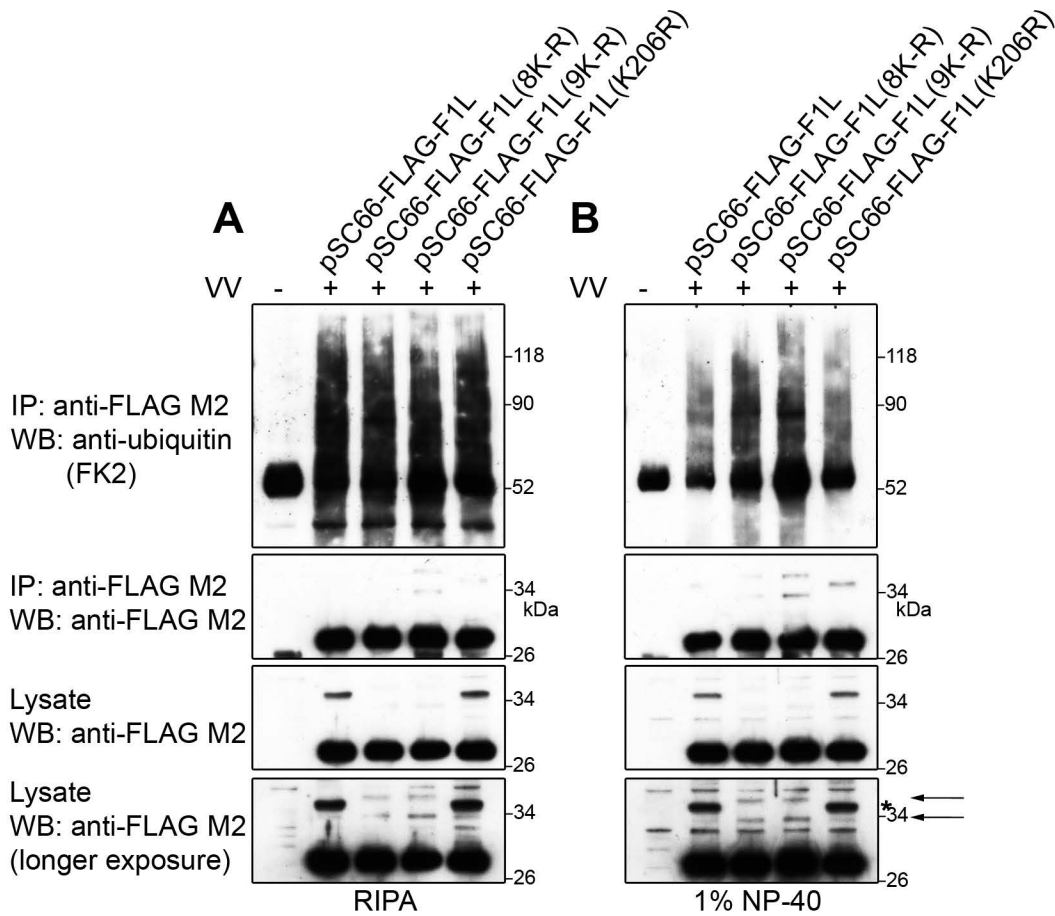
Figure 5.13 Lysine-deficient F1L mutants are directly conjugated to ubiquitin.
HEK 293T cells were mock-infected or infected at an MOI of 5 with VV and
transfected with pSC66-FLAG-F1L, pSC66-FLAG-F1L(8K-R),
pSC66-FLAG-F1L(9K-R), or pSC66-FLAG-F1L(K206R). Fourteen hours post
infection-transfection, samples were divided and cells were lysed in RIPA buffer
(**A**) or 1% NP-40 buffer (**B**) before anti-FLAG M2 immunoprecipitation.
Immunoprecipitates were western blotted with anti-ubiquitin (FK2) or anti-FLAG
M2 and lysates were western blotted with anti-FLAG M2. Longer exposures of
lysates western blotted with anti-FLAG M2 revealed loss of the 36kDa FLAG-F1L
species (*) in FLAG-F1L(8K-R) and FLAG-F1L(9K-R) and appearance of 34kDa and
38kDa products (arrows).

protein, suspected to be ubiquitinated forms, yet the association of FLAG-F1L(8K-R) and FLAG-F1L(9K-R) with conjugated ubiquitin was not visibly altered. The association between conjugated ubiquitin and FLAG-F1L(8K-R) and FLAG-F1L(9K-R) was not an artifact of the anti-ubiquitin (FK2) antibody, since similar results were observed using an antibody specific for ubiquitin and not the isopeptide linkages between ubiquitin that are detected by anti-ubiquitin (FK2) (Fig A.5).

To determine whether the altered post-translational modifications of FLAG-F1L(8K-R) and FLAG-F1L(9K-R) were specific to transient transfection conditions, recombinant viruses were constructed. FLAG-F1L(8K-R) and FLAG-F1L(9K-R) were recombined into VVΔF1L, which lacks endogenous F1L. VVΔF1L-FLAG-F1L(8K-R) and VVΔF1L-FLAG-F1L(9K-R) do not produce endogenous F1L, but express FLAG-F1L(8K-R) and FLAG-F1L(9K-R), respectively. To investigate the post-translational modifications of both FLAG-F1L and FLAG-F1L lysine-deficient mutants, particularly the presence or absence of the 36kDa species, infected HeLa cell lysates were harvested at 16 hours post infection and western blotted with anti-FLAG. Similar to the infection-transfection results in figures 5.12 and 5.13, FLAG-F1L was visible with a molecular weight of 28kDa in VV-FLAG-F1L-infected cells (Fig 5.14). Additionally, numerous high molecular weight species were observed for FLAG-F1L, with the suspected monoubiquitinated form being the most prominent modified form with a molecular weight of 36kDa. Interestingly, the 36kDa F1L species and higher molecular weight forms of F1L were clearly absent in cells infected with VVΔF1L-FLAG-F1L(8K-R) and VVΔF1L-FLAG-F1L(9K-R) (Fig 5.14). The unmodified 28kDa forms of FLAG-F1L(8K-R) and FLAG-F1L(9K-R) were unaffected; however, two higher molecular weight forms were still present. The 34kDa and 38kDa forms of FLAG-F1L(8K-R) and FLAG-F1L(9K-R) resembled what was observed previously in figure 5.13, reinforcing the idea that depleting lysine residues severely altered the post-translational modification of F1L. Not surprisingly, mock-infected cells and VVΔF1L-infected cells were negative for the expression of FLAG-tagged proteins (Fig 5.14). As a
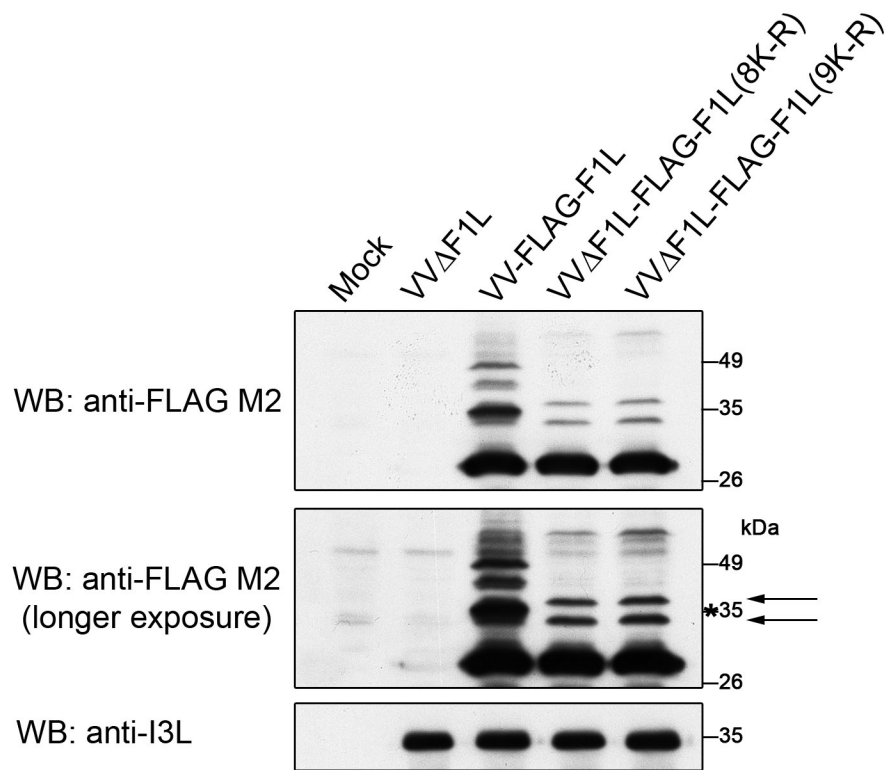
Figure 5.14 Recombinant viruses expressing FLAG-F1L(8K-R) and FLAG-F1L(9K-R) exhibit altered post-translational modifications. HeLa cells were mock-infected or infected with VVΔF1L, VV-FLAG-F1L, VVΔF1L-FLAG-F1L(8K-R), or VVΔF1L-FLAG-F1L(9K-R) at an MOI of 5 for 16 hours. Whole cell lysates were harvested and subject to SDS-PAGE. Anti-FLAG M2 and anti-I3L were used for western blotting. A longer exposure of the anti-FLAG M2 western blot was included to demonstrate the 36kDa FLAG-F1L product (*) and the 34kDa and 38kDa products (arrows).

control for infection, whole cell lysates were western blotted with anti-I3L to detect the viral single-stranded DNA binding protein [683,684].

5.5.2 Both the cytoplasmic and transmembrane domains of F1L are ubiquitinated. Although the presence of high molecular weight FLAG-F1L products was altered upon lysine mutation, the association with conjugated ubiquitin in figures 5.12 and 5.13 suggested that F1L lysine-deficient mutants were still ubiquitinated. While lysine residues are the most common targets for ubiquitination machinery, other residues such as cysteine, serine, and threonine are capable of forming covalent bonds with ubiquitin [424,654,655,656]; therefore, non-lysine residues in the cytoplasmic domain of F1L may account for the association of ubiquitin with FLAG-F1L(9K-R). Alternatively, the two remaining lysines within the mitochondrially-inserted tail of F1L may account for ubiquitination of FLAG-F1L(9K-R) (Fig 5.1). To test the possibility that the C-terminal tail of F1L could be ubiquitinated, HEK 293T cells were infected with VV and transfected with F1L constructs bearing N-terminal EGFP tags. Along with wildtype pSC66-EGFP-F1L, these included a fusion protein containing amino acids 1-198 of F1L and 143-174 of a VV protein B6R (pSC66-EGFP-F1L/B6R), an F1L mutant lacking the transmembrane domain (pSC66-EGFP-F1L(1-206)), and an F1L mutant consisting of only the transmembrane domain (pSC66-EGFP-F1L(206-226)). As a control, pSC66-EGFP-EVM004 was used. Anti-EGFP immunoprecipitation and anti-ubiquitin (FK2) western blotting revealed no ubiquitination in mock-infected or EGFP-EVM004-expressing cells (Fig 5.15). In comparison, strong ubiquitin association was evident with wildtype EGFP-F1L, while all three mutated versions of F1L remained associated with ubiquitin, albeit to lower levels (Fig 5.15). As controls, immunoprecipitates and lysates were western blotted with anti-EGFP to ensure sufficient levels of each EGFP-tagged protein (Fig 5.15). EGFP-F1L/B6R localizes to the ER due to the B6R transmembrane domain [576], indicating that ubiquitination of the first 198 amino acids of F1L, which contains 8 lysines, did not specifically require
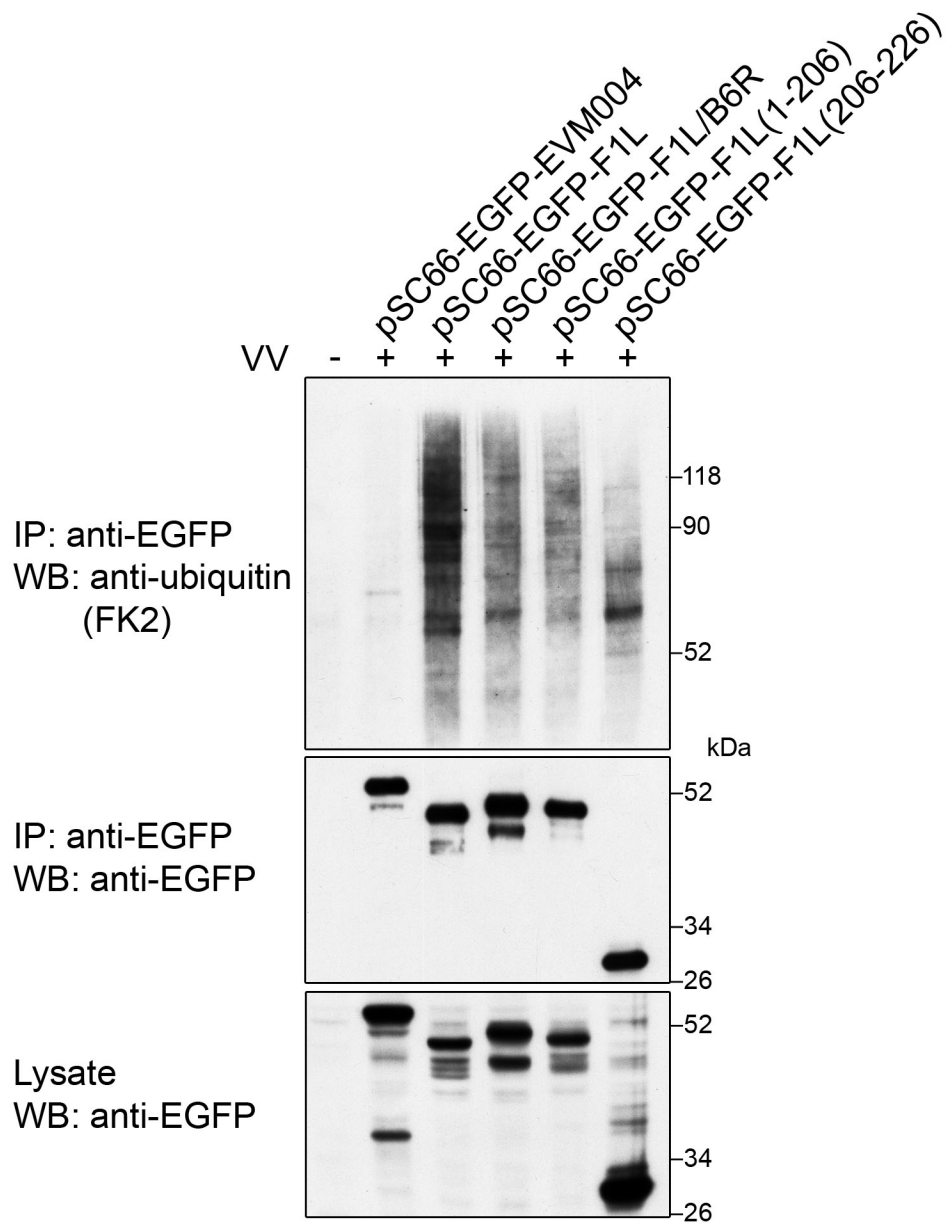
Figure 5.15 The cytoplasmic and transmembrane domains of F1L are ubiquitinated. HEK 293T cells were mock-infected or infected with VV at an MOI of 5 and transfected with pSC66-EGFP-EVM004, pSC66-EGFP-F1L, pSC66-EGFP-F1L/B6R, pSC66-EGFP-F1L(1-206), or pSC66-EGFP-F1L(206-226). Fourteen hours post infection-transfection, cells were lysed in 1% NP-40 and subject to anti-EGFP immunoprecipitation. Anti-ubiquitin (FK2) was used to western blot the immuno-precipitates, while anti-EGFP was used to western blot immunoprecipitates and lysates.

mitochondrial localization. However, ubiquitination of EGFP-F1L/B6R was slightly reduced compared to wildtype EGFP-F1L, suggesting that either mitochondrial localization or the C-terminal 28 amino acids of F1L were required for efficient ubiquitination of the protein (Fig 5.15). The reduced ubiquitination of EGFP-F1L(1-206) and EGFP-(206-226) implied that neither the cytoplasmic domain nor the mitochondrial-inserted transmembrane domain were sufficient to fully restore ubiquitination of F1L, yet each portion of the protein associated with a appreciable amount of conjugated ubiquitin (Fig 5.15). In fact, high molecular weight adducts of EGFP-F1L(206-226) were observed in lysates probed with anti-EGFP, implying that the last 20 amino acids of F1L, comprising the transmembrane domain and hydrophilic tail, were targeted for ubiquitination (Fig 5.15). These results suggested that the association of FLAG-F1L(9K-R) with conjugated ubiquitin may be due, at least in part, to the presence of K219 and K222 in the transmembrane region of F1L.

5.6 CHARACTERIZATION OF LYSINE-DEFICIENT MUTANTS F1L(8K-R) AND F1L(9K-R)

5.6.1 F1L lysine mutants retain mitochondrial localization. In addition to serving as ubiquitin conjugation sites, lysine residues are critically important for targeting proteins to intracellular membranes [220]. Mitochondrial localization is essential for the anti-apoptotic activity of F1L, as mutants that no longer insert into the OMM are unable to inhibit apoptosis [548]. The C-terminal transmembrane domain of F1L, which is flanked by K206 and K219, is required for localization to mitochondria [548]. Along with K222 in the hydrophilic tail of F1L, these C-terminal lysine residues have all been shown to have a role in mitochondrial targeting [548]. To ensure that accumulating lysine to arginine mutations, particularly K206R, did not alter the subcellular localization of F1L, confocal microscopy was used to assess mitochondrial targeting. HeLa cells were infected with VVT7 and transfected with pSC66-FLAG-F1L, pSC66-FLAG-F1L(8K-R), pSC66-FLAG-F1L(9K-R), or pSC66-FLAG-F1L(K206R) for 14 hours before

fixation. While FLAG-tagged proteins were visualized by anti-FLAG staining, mitochondria were detected using the mitochondrial marker cytochrome *c*. Staining with anti-cytochrome *c* illustrated a diffuse and reticular mitochondrial network in VVT7-infected cells in the absence of FLAG-tagged proteins (Fig 5.16 panels a-d). Likewise, FLAG-F1L was reticular and colocalized with the mitochondrial marker cytochrome *c* (Fig 5.16 panels e-h). Mutation of 8 or 9 lysines did not affect mitochondrial localization of F1L, as both FLAG-F1L(8K-R) and FLAG-F1L(9K-R) colocalized with cytochrome *c* (Fig 5.16 panels i-p). However, mitochondria containing FLAG-F1L(8K-R) and FLAG-F1L(9K-R) appeared slightly more punctate and less reticular than mitochondria containing wildtype FLAG-F1L (Fig 5.16 panels e-p). Mitochondria expressing FLAG-F1L(K206R) were diffuse and reticular, mirroring the morphology observed with wildtype FLAG-F1L, despite lacking K206 (Fig 5.16 panels q-t). Thus, mutation of all the cytoplasmic lysines in F1L, including K206, did not disturb mitochondrial localization of the protein. However, in cells expressing FLAG-F1L(8K-R) and FLAG-F1L(9K-R), the mitochondrial network was less tubular and more condensed compared to cells expressing wildtype FLAG-F1L.

5.6.2 Expression of FLAG-F1L(8K-R) and FLAG-F1L(9K-R) disrupts the mitochondrial ultrastructure. While FLAG-F1L(8K-R) and FLAG-F1L(9K-R) maintained mitochondrial localization, their expression during infection-transfection studies appeared to alter mitochondrial morphology (Fig 5.16). To further investigate this observation, mitochondrial architecture was examined during infection with recombinant viruses expressing FLAG-F1L(8K-R) and FLAG-F1L(9K-R). HeLa cells were infected with VVΔF1L, VV-FLAG-F1L, VVΔF1L-FLAG-F1L(8K-R), or VVΔF1L-FLAG-F1L(9K-R) for 12 hours before analyzing DAPI and anti-FLAG-stained cells by confocal microscopy. In VVΔF1L, the F1L open reading frame is disrupted by the insertion of an EGFP cassette [550]; therefore, VVΔF1L, VVΔF1L-FLAG-F1L(8K-R), and VVΔF1L-FLAG-F1L(9K-R), lack endogenous F1L and express EGFP, which can be used as a fluorescent marker for infection. As

	DAPI	anti-Cyt c	anti-FLAG M2	Merge
VVT7	a	b	c	d
VVT7 + pSC66-FLAG-F1L	e	f	g	h
VVT7 + pSC66-FLAG-F1L(8K-R)	i	j	k	l
VVT7 + pSC66-FLAG-F1L(9K-R)	m	n	o	p
VVT7 + pSC66-FLAG-F1L(K206R)	q	r	s	t
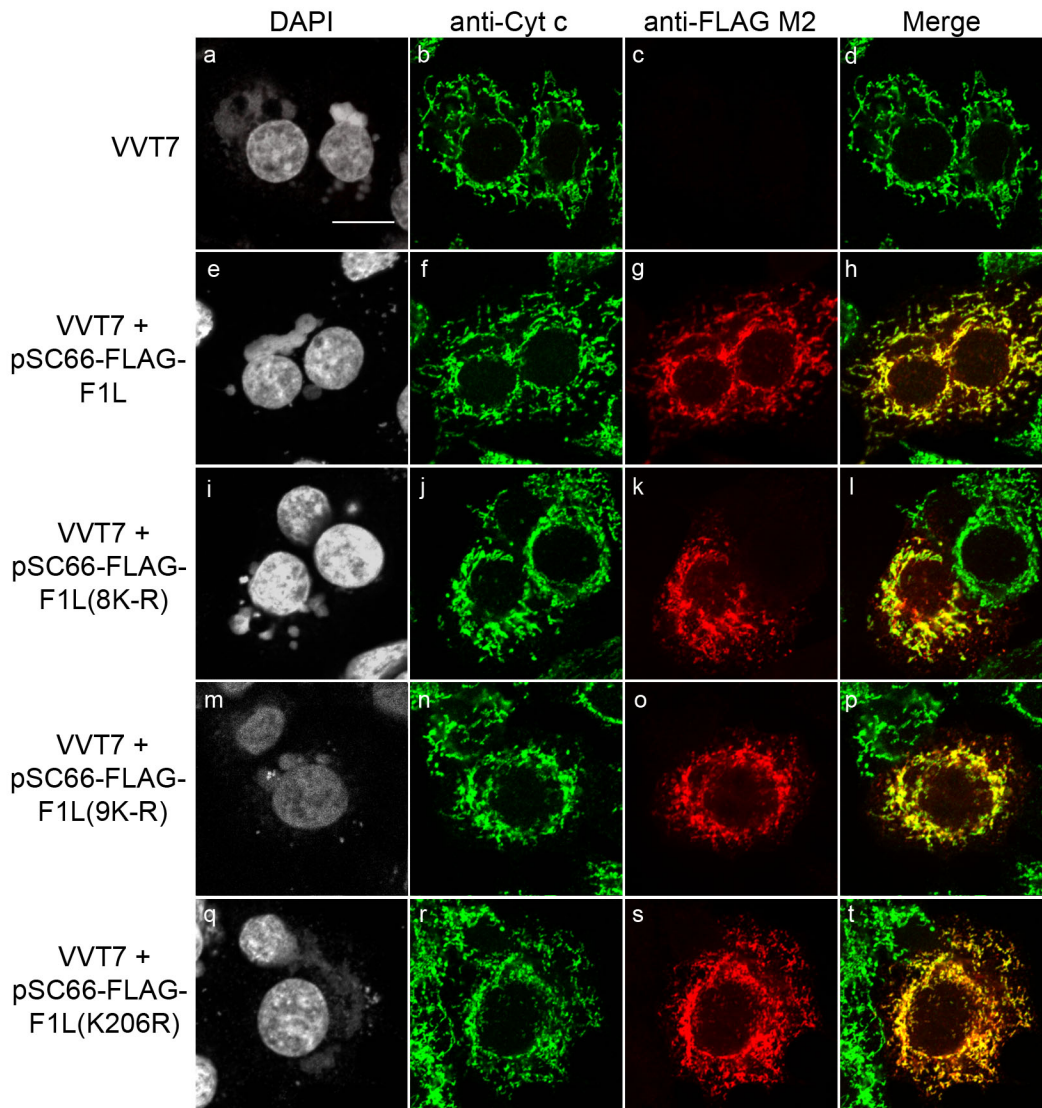
Figure 5.16 FLAG-F1L(8K-R) and FLAG-F1L(9K-R) localize to mitochondria during infection-transfection. The subcellular localization of lysine-deficient F1L mutants was determined by infecting HeLa cells with VVT7 at an MOI of 5 and transfecting pSC66-FLAG-F1L, pSC66-FLAG-F1L(8K-R), pSC66-FLAG-F1L(9K-R), or pSC66-FLAG-F1L(K206R) for 14 hours. Fixed cells were stained with DAPI, anti-cytochrome c, or anti-FLAG M2 and analyzed by confocal microscopy. **a-d**, VVT7-infected cells; **e-h**, VVT7-infected and pSC66-FLAG-F1L-transfected cells; **i-l**, VVT7-infected and pSC66-FLAG-F1L(8K-R)-transfected cells; **m-p**, VVT7-infected and pSC66-FLAG-F1L(9K-R)-transfected cells; **q-t**, VVT7-infected and pSC66-FLAG-F1L(K206R)-transfected cells. Bar=15μm.

expected, mock-infected cells lacked viral factories and did not contain EGFP or FLAG-tagged proteins (Fig 5.17 panels a-d). In contrast, both DAPI-positive viral factories and EGFP fluorescence were detected in VVΔF1L-infected cells (Fig 5.17 panels e-h). In cells infected with VV-FLAG-F1L, anti-FLAG staining revealed that FLAG-F1L adopted a reticular pattern with tubular structures, characteristic of mitochondria (Fig 5.17 panels i-l). However, EGFP fluorescence was not observed due to an intact F1L open reading frame. In comparison to VV-FLAG-F1L-infected cells, cells infected with VVΔF1L-FLAG-F1L(8K-R) and VVΔF1L-FLAG-F1L(9K-R) expressed EGFP, and furthermore, anti-FLAG staining revealed punctuate and aggregated structures reminiscent of mitochondria with defects in fission and fusion (Fig 5.17 panels m-t). Magnifications of the anti-FLAG images revealed that unlike mitochondria containing FLAG-F1L, which formed tubular structures characteristic of healthy mitochondria, the majority of FLAG-F1L(8K-R)- and FLAG-F1L(9K-R)-containing mitochondria lacked tubular structures and were severely fragmented and aggregated (Fig 5.17 panels l, p, and t). Localization patterns of FLAG-F1L, FLAG-F1L(8K-R) and FLAG-F1L(9K-R) were quantified in figure A.6. Together, the data indicate that although still present at mitochondria, both FLAG-F1L(8K-R) and FLAG-F1L(9K-R) severely altered the mitochondrial ultrastructure, suggesting that the post-translational modifications of F1L might somehow be important for mitochondrial integrity.

5.6.3 Conjugated ubiquitin is recruited to mitochondria during VVΔF1L-FLAG-F1L(8K-R) and VVΔF1L-FLAG-F1L(9K-R) infection. Despite the loss of all nine cytoplasmic lysines, FLAG-F1L(9K-R) was capable of associating with conjugated ubiquitin and also localizing to mitochondria, albeit morphologically-disrupted mitochondria (Figs 5.12, 5.13, 5.16, and 5.17). Given the extensive rearrangement of mitochondrial ultrastructure upon expression of FLAG-F1L(8K-R) and FLAG-F1L(9K-R), we sought to determine if the lysine-deficient mutants recruited ubiquitin to fragmented and aggregated mitochondria. To this end, confocal microscopy was employed to assess colocalization with conjugated
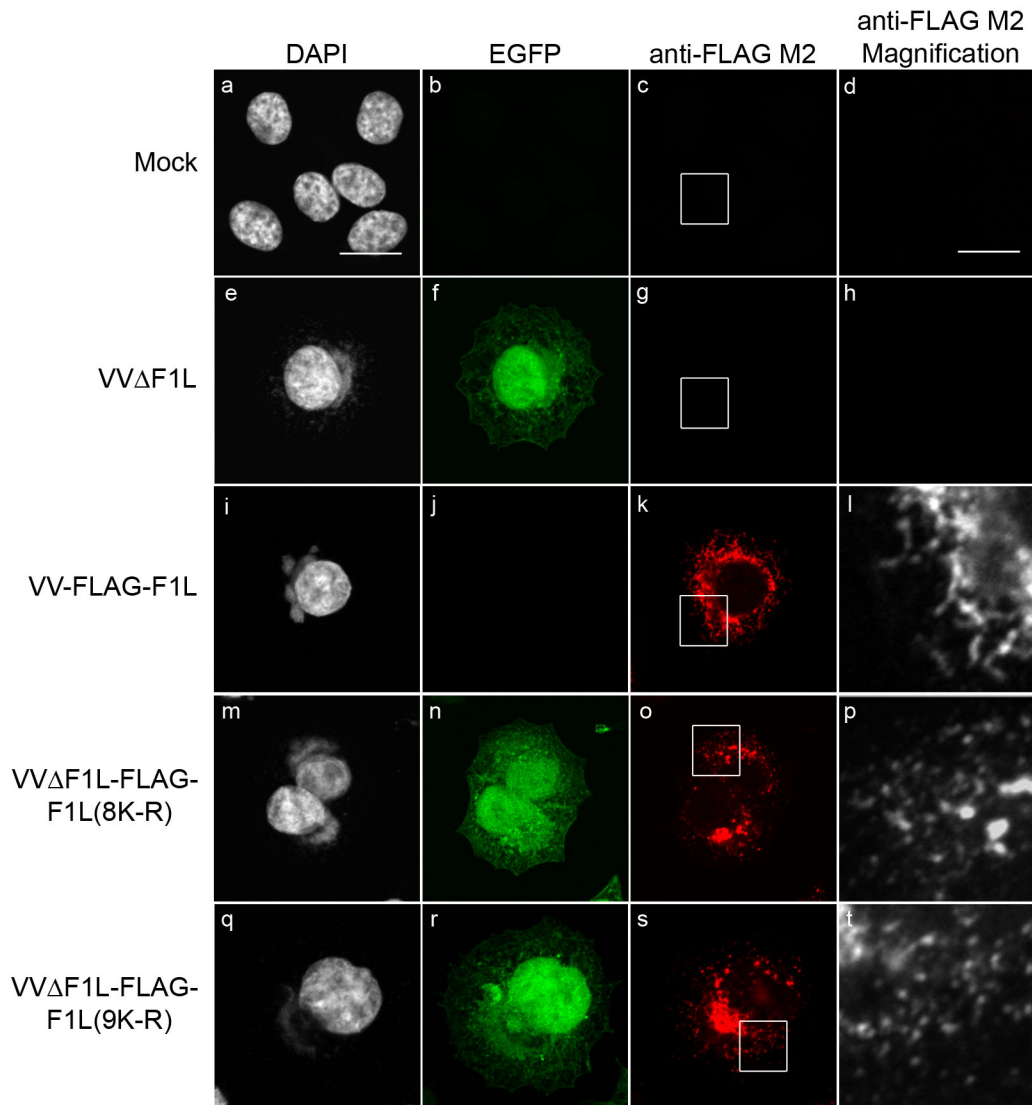
Figure 5.17 VVΔF1L-FLAG-F1L(8K-R) and VVΔF1L-FLAG-F1L(9K-R) disrupt mitochondrial ultrastructure. HeLa cells were mock-infected or infected with VV ΔF1L, VV-FLAG-F1L, VVΔF1L-FLAG-F1L(8K-R), or VVΔF1L-FLAG-F1L(9K-R) for 12 hours at an MOI of 5. Confocal microscopy was used to visualize fixed cells expressing EGFP or stained with DAPI and anti-FLAG M2. **a-d**, mock-infected cells; **e-h**, VVΔF1L-infected cells; **i-l**, VV-FLAG-F1L-infected cells; **m-p**, VVΔ F1L-FLAG-F1L(8K-R)-infected cells; **q-t**, VVΔF1L-FLAG-F1L(9K-R)-infected cells. The boxed areas in **c,g,k,o**, and **s** are magnified in **d,h,l,p**, and **t**, respectively. Bar in **a**=15μm. Bar in **d**=3μm.

ubiquitin during virus infection. HeLa cells were infected with VV and transfected with pSC66-FLAG-F1L, pSC66-FLAG-F1L(8K-R), or pSC66-FLAG-F1L(9K-R). Anti-ubiquitin (FK2) was used to visualize the subcellular localization of conjugated ubiquitin, while anti-FLAG displayed the localization of FLAG-tagged proteins. In mock cells, conjugated ubiquitin was found disperse throughout in the cell, in both the cytoplasm and the nucleus (Fig 5.18 panels a-d). In VV-infected cells, ubiquitin remained throughout the cell but formed several enriched areas, or speckles (Fig 5.18 panels e-h). Cells infected with VV and transfected with pSC66-FLAG-F1L demonstrated one of two localization patterns. In some cells, no significant colocalization between ubiquitin and F1L was observed. Instead, conjugated ubiquitin remained speckled throughout the cytoplasm and FLAG-F1L was reticular (Fig 5.18 panels i-l). However, in other cells, conjugated ubiquitin and FLAG-F1L colocalized in perinuclear aggregates and punctuate structures, suggestive of disturbed mitochondria (Fig 5.18 panels m-p). Similar to the latter phenotype, VV-infected cells transfected with pSC66-FLAG-F1L(8K-R) or pSC66-FLAG-F1L(9K-R), exhibited conjugated ubiquitin in compact, aggregated structures in the cytoplasm that colocalized with aggregates containing FLAG-F1L(8K-R) and FLAG-F1L(9K-R) (Fig 5.18 panels q-x). Although FLAG-F1L-expressing cells revealed two distinct phenotypes, the majority of cells expressing FLAG-F1L(8K-R) and FLAG-F1L(9K-R) demonstrated complete colocalization with ubiquitin in cytoplasmic aggregates (Fig A.7).

5.6.4 Investigating the protein stability of FLAG-F1L(9K-R). FLAG-F1L(9K-R) lacks all nine cytoplasmic lysines with the two remaining lysines in the C-terminal tail of the protein, which is inserted into mitochondria. Unlike wildtype F1L, this mutant no longer formed high molecular weight complexes but, intriguingly, the loss of nine cytoplasm-exposed lysines had no visible effect on the association with ubiquitin (Figs 5.12 and 5.13). To directly compare the stability of wildtype FLAG-F1L and FLAG-F1L(9K-R), we infected HeLa cells with VV-FLAG-F1L or VVΔF1L-FLAG-F1L(9K-R) and performed half-life studies. After 12 hours of

	DAPI	anti-ubiquitin (FK2)	anti-FLAG M2	Merge
Mock	a	b	c	d
VV	e	f	g	h
VV + pSC66-FLAG-F1L	i	j	k	l
VV + pSC66-FLAG-F1L	m	n	o	p
VV + pSC66-FLAG-F1L(8K-R)	q	r	s	t
VV + pSC66-FLAG-F1L(9K-R)	u	v	w	x
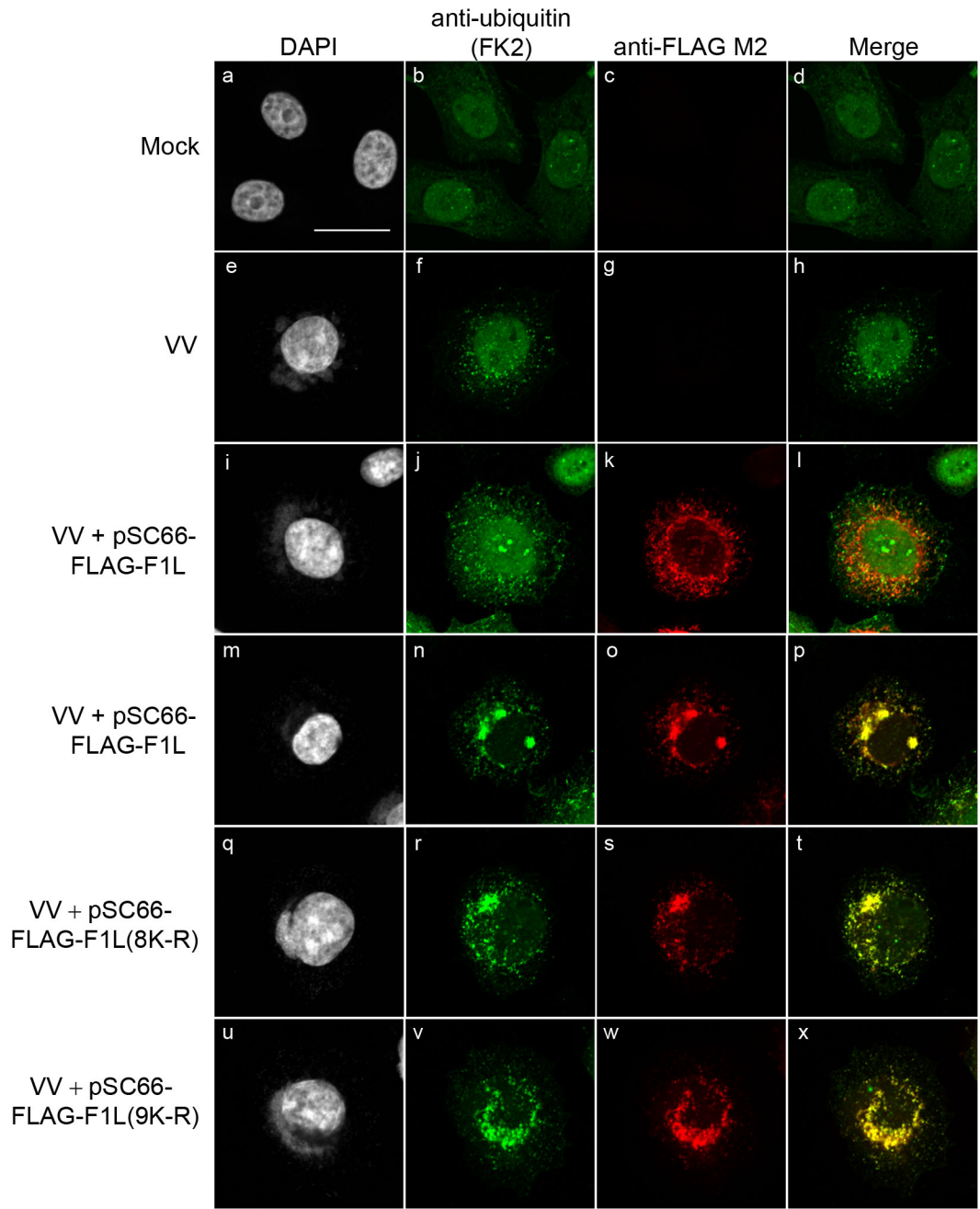
Figure 5.18 FLAG-F1L(8K-R) and FLAG-F1L(9K-R) recruit conjugated ubiquitin to mitochondria. HeLa cells were mock-infected or infected at an MOI of 5 with VV and simultaneously transfected with pSC66-FLAG-F1L, pSC66-FLAG-F1L(8K-R), or pSC66-FLAG-F1L(9K-R) for fourteen hours. Fixed cells were stained with DAPI, anti-ubiquitin (FK2), and anti-FLAG M2. Colocalization between conjugated ubiquitin and FLAG-tagged proteins was assessed in the merged images. **a-d**, mock-infected cells; **e-h**, VV-infected cells; **i-p**, VV-infected and pSC66-FLAG-F1L-transfected cells; **q-t**, VV-infected and pSC66-FLAG-F1L(8K-R)-transfected cells; **u-x**, VV-infected and pSC66-FLAG-F1L(9K-R)-transfected cells. Bar=15μm.

infection, cells were labelled with radioactive ^{35}S-containing cysteine and methionine for 30 minutes. Fresh media was added to the cells and cell lysates were harvested up to 12 hours post labelling and subject to anti-FLAG immunoprecipitation. The autoradiograph revealed that FLAG-F1L was present at 2 and 4 hours and barely detectable at 8 hours, while FLAG-F1L(9K-R) was turned over slightly faster, with less protein visible by 4 hours post radiolabelling (Fig 5.19). Thus, despite the loss of nine lysines in FLAG-F1L(9K-R), the mutant construct is slightly less stable than wildtype FLAG-F1L, suggesting other major targets for ubiquitination may exist in FLAG-F1L(9K-R).

5.7 VACCINIA VIRUSES EXPRESSING LYSINE-DEFICIENT F1L MUTANTS DISPLAY DEFECTS IN ANTI-APOPTOTIC FUNCTION AND GROWTH

5.7.1 Lysine-deficient F1L mutants prevent early virus-induced apoptosis. To determine if accumulating lysine to arginine mutations affected the function of F1L, the ability of FLAG-F1L(8K-R) and FLAG-F1L(9K-R) to inhibit apoptosis was examined. Jurkat cells were mock-infected or infected with VVEGFP, VVΔF1L, VVΔF1L-FLAG-F1L(8K-R), or VVΔF1L-FLAG-F1L(9K-R) in duplicate. Four hours post infection, half of the samples were treated with STS for an additional two hours. Bak activation was examined by flow cytometry using the conformation-specific antibody, Bak AB-1 [177,184]. Bak activation was not detected in mock-infected cells until the addition of STS (Fig 5.20 panel a). While VVEGFP completely prevented the activation of Bak in response to virus infection and STS treatment (Fig 5.20 panel b), Bak was partially activated in VVΔF1L-infected cells and this activation was augmented in response to STS treatment (Fig 5.20 panel c). In contrast to VVΔF1L, Jurkat cells infected with VVΔF1L-FLAG-F1L(8K-R) or VVΔF1L-FLAG-F1L(9K-R) were completely resistant to apoptosis during infection as no Bak activation was detected (Fig 5.20 panels d and e). These viruses, however, were unable to prevent the activation of Bak in response to STS treatment. Thus, early during infection, FLAG-F1L(8K-R) and FLAG-F1L(9K-R) compensated for the loss of endogenous F1L and completely inhibited VVΔF1L-
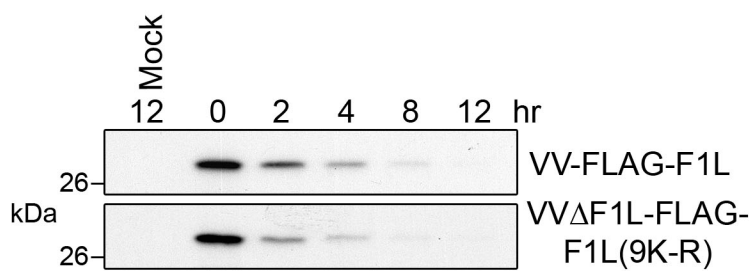
Figure 5.19 Loss of the nine cytoplasmic lysines in F1L does not prolong protein half-life. To compare the half-lives of FLAG-F1L and FLAG-F1L(9K-R), HeLa cells were mock-infected or infected at an MOI of 5 with VV-FLAG-F1L or VVΔ F1L-FLAG-F1L(9K-R) for 12 hours. Cells were subsequently starved of methionine and cysteine for 30 minutes and pulsed with 45μCi of ^{35}S-containing methionine and cysteine for 30 minutes. Following the addition of fresh media, cells were harvested up to 12 hours post radiolabelling, subject to anti-FLAG M2 immunoprecipitation, and resolved by SDS-PAGE and autoradiography.
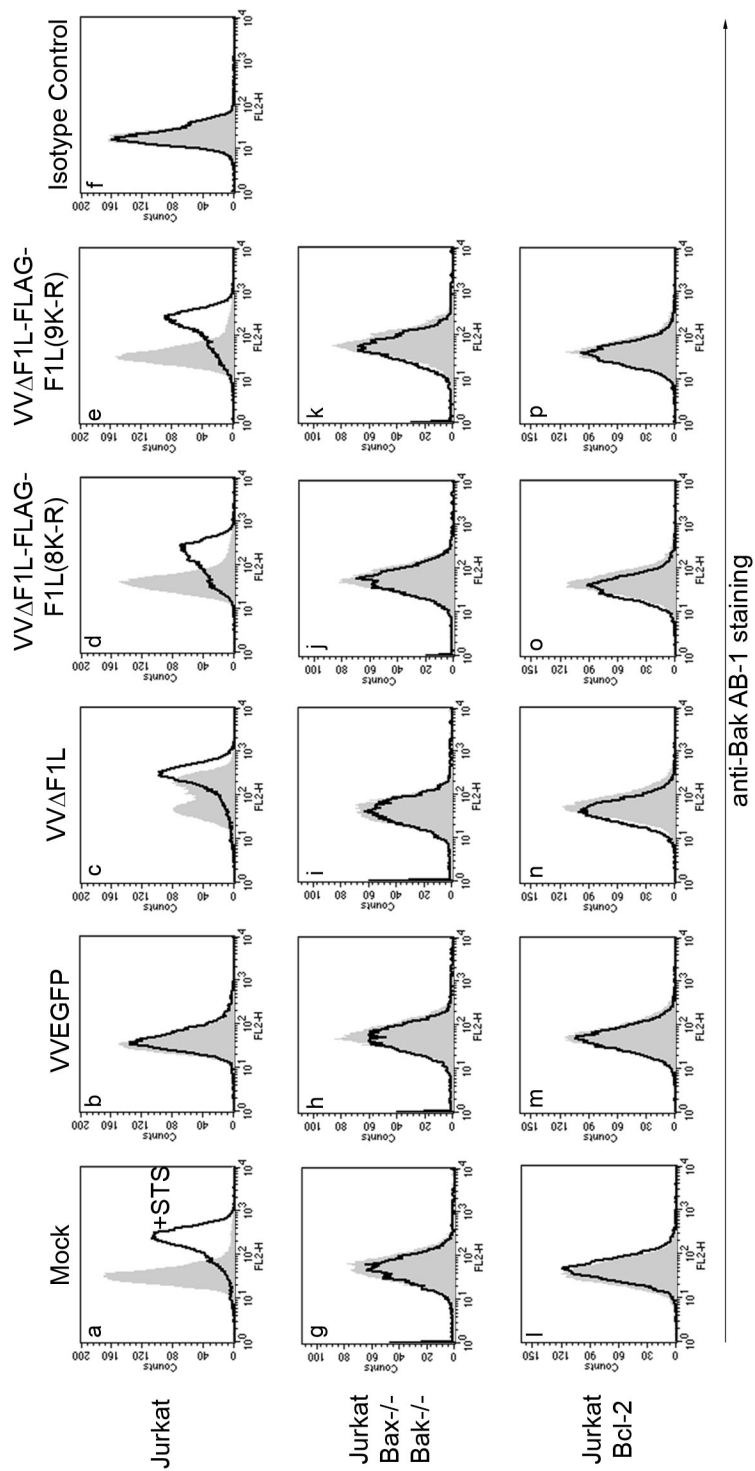
Figure 5.20 VVΔF1L-FLAG-F1L(8K-R) and VVΔF1L-FLAG-F1L(9K-R) inhibit early virus-induced apoptosis. To examine anti-apoptotic abilities of FLAG-F1L(8K-R) and FLAG-F1L(9K-R), Jurkat cells were mock-infected or infected with VVEGFP, VVΔ F1L, VVΔF1L-FLAG-F1L(8K-R), or VVΔF1L-FLAG-F1L(9K-R) at an MOI of 10 for 4 hours. Cells were left untreated or treated with 250nM staurosporine (STS) for 2 hours. Activated Bak was detected with anti-Bak AB-1 by flow cytometry. **a-f**, wildtype Jurkat cells; **g-k**, Bax- and Bak-deficient Jurkat cells; **l-p**, Jurkat cells overexpressing Bcl-2. Grey histograms represent mock- or virus-infected cells, while open histograms represent mock- or virus-infected cells treated with STS. Anti-NK1.1 was used as an isotype control (**f**).

237

induced apoptosis. Despite mitochondrial localization and ability to prevent early virus-induced apoptosis, cells infected with the lysine-deficient F1L mutant viruses were sensitive to external stimuli, such as STS, suggesting a functional defect in the ability of these mutants to inhibit Bak activation. As a control, mock-infected Jurkat cells were stained with an isotype control antibody, anti-NK1.1, which did not detect Bak activation in response to STS (Fig 5.20 panel f). The specificity of the anti-Bak AB-1 antibody was assessed by infecting Bak- and Bax-deficient Jurkat cells with the above viruses (Fig 5.20 panels g-k). Additionally, Jurkat cells overexpressing Bcl-2 were refractory to Bak activation induced by all viruses tested (Fig 5.20 panels l-p), indicating that the apoptosis induced by STS in VVΔF1L-FLAG-F1L(8K-R)- and VVΔF1L-FLAG-F1L(9K-R)-infected cells was mediated through the mitochondrial pathway.

5.7.2 Lysine-deficient F1L mutants fail to prevent late virus-induced apoptosis.

FLAG-F1L(8K-R) and FLAG-F1L(9K-R) inhibited apoptosis induced by VVΔF1L at 6 hours post infection (Fig 5.20); however, by 12 hours post infection, mitochondria expressing the lysine-deficient F1L mutants were severely fragmented (Fig 5.17). To examine whether F1L lysine-deficient mutants could inhibit apoptosis late during infection, Jurkat cells were infected with VVEGFP, VVΔF1L, VVΔF1L-FLAG-F1L(8K-R), or VVΔF1L-FLAG-F1L(9K-R), and whole cell lysates were harvested up to 20 hours post infection. Western blotting with anti-PARP demonstrated maintenance of full-length PARP in VVEGFP-infected cells (Fig 5.21). However, infection with VVΔF1L resulted in a minor loss of full-length PARP at 15 and 20 hours post infection and the slight appearance of cleaved PARP (Fig 5.21). Interestingly, Jurkat cells infected with VVΔF1L-FLAG-F1L(8K-R) or VVΔF1L-FLAG-F1L(9K-R) did not show signs of apoptosis by 10 hours post infection, yet at 15 and 20 hours post infection, full-length PARP was slightly decreased and a significant amount of cleaved PARP was present (Fig 5.21). The expression of FLAG-F1L(8K-R) and FLAG-F1L(9K-R) was determined by western blotting with anti-FLAG and infection efficiency was evaluated by probing for the
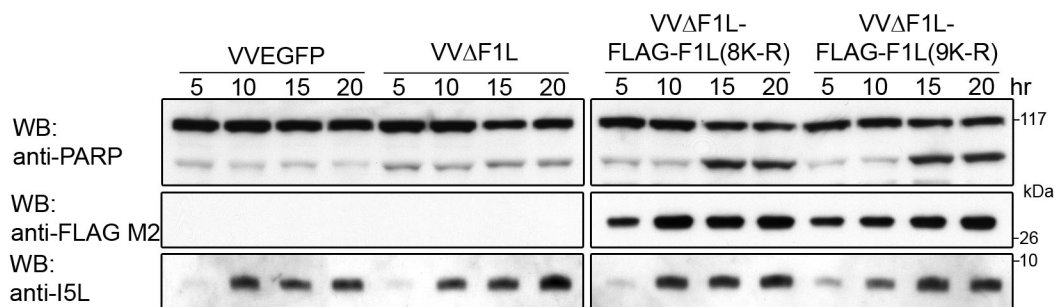
Figure 5.21 VVΔF1L-FLAG-F1L(8K-R) and VVΔF1L-FLAG-F1L(9K-R) induce apoptosis late during infection. Whole cell lysates were harvested from Jurkat cells infected with VVEGFP, VVΔF1L, VVΔF1L-FLAG-F1L(8K-R), or VVΔF1L-FLAG-F1L(9K-R) at an MOI of 10. Lysates were resolved by SDS-PAGE and western blotted with anti-PARP, anti-FLAG M2, or anti-I5L.

viral late protein I5L (Fig 5.21). Thus, while the lysine-deficient mutants of F1L prevented virus-induced apoptosis at early times during infection, the mutants were unable to inhibit apoptotic events that occurred later during infection. While the reason for early resistance and late sensitivity to apoptosis has not yet been elucidated, it is potentially related to changes that occur in the mitochondrial ultrastructure upon accumulation of FLAG-F1L(8K-R) and FLAG-F1L(9K-R).

5.7.3 Lysine-deficient F1L mutants are defective in Bak binding late during virus infection. To better understand the mechanism of apoptosis induction in VVΔF1L-FLAG-F1L(8K-R)- and VVΔF1L-FLAG-F1L(9K-R)-infected cells between 10-15 hours post infection, both lysine-deficient mutants were analyzed for Bak binding. HeLa cells were mock-infected or infected with each virus bearing 8 or 9 lysine mutations, along with VV-FLAG-F1L. Twelve hours post infection, cells were lysed in 2% CHAPS lysis buffer and subject to anti-FLAG immunoprecipitation. Western blotting with anti-Bak NT revealed a strong interaction between Bak and FLAG-F1L; however, Bak binding to FLAG-F1L(8K-R) and FLAG-F1L(9K-R) was severely hindered (Fig 5.22). The decreased Bak binding observed with FLAG-F1L(8K-R) and FLAG-F1L(9K-R) was not due to unequal levels of immunoprecipitated FLAG-tagged protein or unequal expression levels of endogenous Bak or FLAG-tagged constructs (Fig 5.22). The inability of FLAG-F1L(8K-R) and FLAG-F1L(9K-R) to bind Bak at 12 hours post infection may explain the initiation of cell death that occurs late during infection. Additionally, the loss of Bak interaction may be connected to the changes occurring in the mitochondrial network upon expression of the lysine-deficient F1L mutants, since fission and fusion events are tightly linked to apoptosis [139,159,160,161].

5.7.4 Vaccinia viruses expressing lysine-deficient F1L mutants exhibit growth defects. The loss of Bak binding and the initiation of apoptosis late during infection with VVΔF1L-FLAG-F1L(8K-R) and VVΔF1L-FLAGF1L(9K-R) suggested that release of progeny virus from infected cells might be impaired. To address
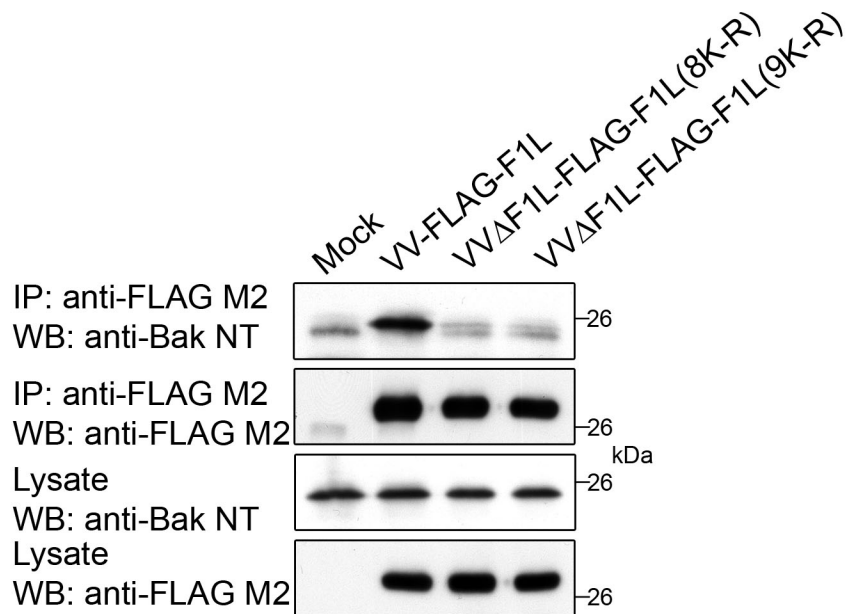
Figure 5.22 FLAG-F1L(8K-R) and FLAG-F1L(9K-R) display reduced binding to Bak late during infection. HeLa cells were mock-infected or infected with VV-FLAG-F1L, VVΔF1L-FLAG-F1L(8K-R), or VVΔF1L-FLAG-F1L(9K-R) at an MOI of 5 for 12 hours. Cells were lysed in 2% CHAPS and subject to anti-FLAG M2 immunoprecipitation. Immunoprecipitates and lysates were western blotted with anti-Bak NT or anti-FLAG M2.

this, BGMK cells were infected with VV, VVΔF1L, VVΔF1L-FLAG-F1L(8K-R), or VVΔF1L-FLAG-F1L(9K-R) for 42 hours. Cells were fixed and stained with crystal violet and plaque formation was assessed. While there was no difference in plaque size between VV and VVΔF1L (Fig 5.23A panels a-d), the plaques generated by VVΔF1L-FLAG-F1L(8K-R) and VVΔF1L-FLAG-F1L(9K-R) were visibly smaller (Fig 5.23A panels e-h). Measuring plaque area revealed that VVΔF1L-FLAG-F1L(8K-R) and VVΔF1L-FLAG-F1L(9K-R) plaques were two-fold smaller than plaques formed by VV and VVΔF1L (Fig 5.23B). Notably, while VVΔF1L has an apoptotic phenotype [550], plaques generated by this virus were similar in size to VV (Fig 5.23B). These data indicated that while the loss of F1L did not alter plaque formation in VVΔF1L, the presence of lysine-deficient F1L mutants significantly hampered virus release or virus spread, suggesting these mutants have a significant effect in infected cells. However, how exactly the loss of up to 9 lysines in F1L resulted in late virus-induced apoptosis and reduced viral growth is currently unclear but is perhaps linked to the severe changes occurring at mitochondria.

5.8 DISCUSSION

The data presented here are the first to examine the role of the UPS in the regulation of a viral apoptotic inhibitor. VV-FLAG-F1L-infected cells demonstrated high molecular weight laddering characteristic of ubiquitination and both F1L and ubiquitin were identified in high molecular weight adducts by mass spectrometry (Fig 5.3). Immunoprecipitation of the 28kDa FLAG-F1L protein revealed an association with conjugated ubiquitin, as well as the presence of higher molecular weight species of F1L, the most prominent of which was 36kDa (Figs 5.4 and 5.5). Based on the 8kDa increase compared to FLAG-F1L, this 36kDa product was assumed to be monoubiquitinated FLAG-F1L. The localization of conjugated ubiquitin was altered drastically in VV-FLAG-F1L-infected cells, in which ubiquitin accumulated at mitochondria with FLAG-F1L (Fig 5.6). In addition, FLAG-F1L colocalized with both HA-ubiquitin and HA-K48-
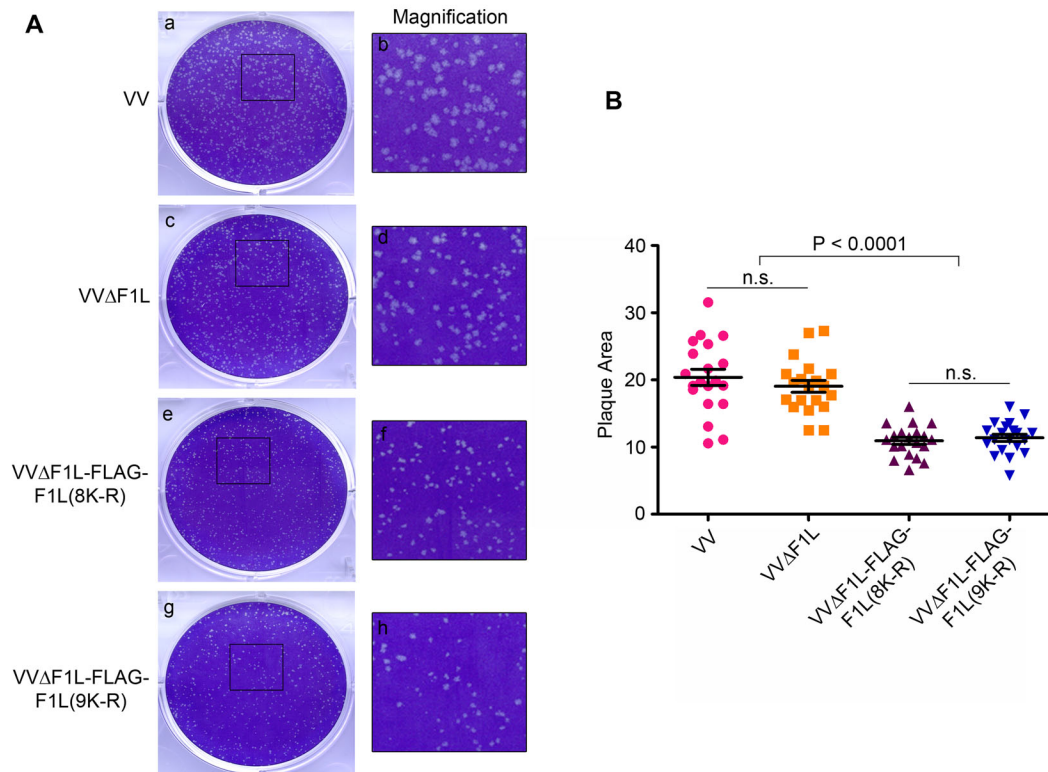
Figure 5.23 VVΔF1L-FLAG-F1L(8K-R) and VVΔF1L-FLAG-F1L(9K-R) exhibit a small plaque phenotype. A. BGMK cells were infected with serial dilutions of VV, VVΔF1L, VVΔF1L-FLAG-F1L(8K-R), or VVΔF1L-FLAG-F1L(9K-R) for 42 hours. Infected cell monolayers were fixed and stained with crystal violet solution to visualize plaques (**a-h**). **B.** The area of plaques shown in (**A**) were measured and graphed with standard deviations. P, probability value; n.s., not significant.

ubiquitin (Fig 5.7). The stabilization of endogenous F1L, along with the prolonged half-life of FLAG-F1L in VV-FLAG-F1L-infected cells during MG132 treatment demonstrated that F1L protein levels were tightly regulated by the 26S proteasome (Figs 5.9 and 5.10). Moreover, MG132-induced stability of EGFP-F1L in the absence of virus infection suggested that the ubiquitination and degradation of F1L was independent of other viral proteins (Fig 5.8).

Based on the obvious ubiquitination and degradation of F1L, we sought to define the ubiquitin ligase(s) responsible. The degradation of EGFP-F1L in the absence of virus infection (Fig 5.8) suggested a cellular ubiquitin ligase was responsible. Interestingly, a virus expressing dominant negative Cul-1, a component of the SCF ubiquitin ligase, decreased the ubiquitination observed for FLAG-F1L (Fig 5.11). The SCF plays a major role in the turnover of the Bcl-2 family members Mcl-1 and BimEL, both of which are phosphorylated prior to ubiquitination [422,439,440,441]. Although we were unable to determine whether MG132 treatment stabilized a phosphorylated version of F1L (Fig 5.9), it remains possible that F1L, like other SCF substrates, was phosphorylated prior to its ubiquitination. Further investigation is required to determine if a phosphorylated species of F1L exists and whether the SCF has a pronounced effect on the stability of F1L.

Mutation of all nine cytoplasmic lysine residues in F1L did not appear to affect the ability of the protein to associate with conjugated ubiquitin (Figs 5.12 and 5.13). FLAG-F1L(9K-R) associated with high molecular weight ubiquitin species even in the presence of RIPA lysis buffer, which destabilizes interactions among proteins (Fig 5.13) [678,679]. Additionally, the half-life of FLAG-F1L(9K-R) was not drastically altered compared to FLAG-F1L, suggesting it was ubiquitinated and degraded at a similar, albeit slightly faster, rate (Fig 5.19). K219 and K222, the two remaining lysines in F1L(9K-R), are located within the tail anchor of the protein and may be responsible for the observed association with ubiquitin. Indeed, using a panel of EGFP-F1L mutants, we demonstrated that the

last 20 amino acids of F1L comprising the transmembrane domain associated with a detectable amount of ubiquitin (Fig 5.15). While it remains possible that ubiquitination of F1L(9K-R) was attributed to K219 and K222, the ubiquitination of EGFP-F1L/B6R, which lacks the transmembrane domain of F1L and localizes to ER, implies that the C-terminal amino acids and mitochondrial localization of F1L were not absolutely required for ubiquitination (Fig 5.15). This was supported by the ubiquitination of EGFP-F1L(1-206), a cytoplasmic mutant that lacks the tail anchor (Fig 5.15).

A lysine-independent mode of ubiquitination has been previously documented for regulation of Baxβ, the constitutively active form of Bax [430]. A growing body of evidence now supports a role for non-lysine residues as ubiquitin conjugation sites [424,650,654,655,656]. The free amino group at the N-terminus of proteins can serve as a ubiquitin receptor site [650,651]; however, due to the presence of N-terminal EGFP or FLAG epitope tags on F1L, this is likely not the case since the N-terminal amino group of F1L is not available. Serine and threonine residues can be linked to ubiquitin to form hydroxyl ester bonds, and moreover, thioester bonds between ubiquitin and cysteine residues have been reported [424,654,655,656]. Interestingly, ubiquitination of non-lysine residues appears to be an important mechanism for ubiquitin ligases within the *Herpesviridae* family, yet whether the cellular homologues of these proteins function in a similar manner has yet to be resolved [654,655]. The ubiquitination of non-lysine residues has also been implicated in apoptosis: the generation of tBid requires ubiquitination of the N-terminal fragment after cleavage and this occurs on serine, threonine, and cysteine residues [424]. The role of serine, threonine, or cysteine residues in F1L ubiquitination has yet to be elucidated but may offer a possible explanation for the observed association between conjugated ubiquitin and FLAG-F1L(9K-R).

Although mutating the cytoplasmic lysines in F1L did not affect the association with conjugated ubiquitin, we observed significant differences in the

post-translational modifications of FLAG-F1L(8K-R) and FLAG-F1L(9K-R) (Figs 5.12-5.14). The 36kDa form of FLAG-F1L was no longer observed with FLAG-F1L(8K-R) and FLAG-F1L(9K-R) and these mutant proteins did not form high molecular weight products that are believed to represent polyubiquitinated species (Fig 5.14). Instead, only two slower migrating species, with molecular weights of 34kDa and 38kDa, were observed for FLAG-F1L(8K-R) and FLAG-F1L(9K-R) (Figs 5.13 and 5.14). The two species do not appear to be a result of ubiquitination since the modifications increase the size of the FLAG-F1L mutants by 6kDa and 10kDa. Therefore, these products likely represent a different type of post-translational modification, although the residues targeted and the nature of the modification require further study. One possibility is that the removal of all cytoplasmic lysines promoted alterations on other residues within F1L(9K-R). Although SUMOylation, the conjugation of a ubiquitin-like molecule SUMO, would yield an 11kDa increase in the molecular weight of a protein, the lysines required for this process are absent in F1L(9K-R) [685]. Thus, it is likely that other protein or lipid modifications occur on residues other than lysine in F1L(9K-R), yet curiously, these modifications do not appear to alter the association between the mutant protein and ubiquitin.

Mitochondrial targeting was not affected by the loss of all nine cytoplasmic lysines, including K219, which flanks the N-terminal side of the transmembrane domain (Fig 5.16). However, the lysine-deficient F1L mutants caused drastic alterations in mitochondrial morphology (Fig 5.17). Since changes in the mitochondrial architecture reflect health of both the organelle and the cell, the fragmentation of mitochondria observed during infection with VVΔF1L-FLAG-F1L(8K-R) and VVΔF1L-FLAG-F1L(9K-R) suggested these viruses had adverse affects on mitochondrial integrity. Compared to wildtype FLAG-F1L, almost all cells expressing FLAG-F1L(8K-R) or FLAG-F1L(9K-R) recruited conjugated ubiquitin to these morphologically-altered mitochondria (Fig 5.18). This suggested that the ubiquitination of the lysine-deficient F1L mutants, or alternatively other

mitochondrial proteins, was involved in changes to the mitochondrial ultrastructure. The UPS is intrinsically involved in mitochondrial fission and fusion events [377,659,660,661,662], but it is not clear if the accumulation of ubiquitin at mitochondria by the lysine-deficient F1L mutants is a cause or effect of the extensive changes in mitochondrial architecture. Infection with VVΔF1L-FLAG-F1L(8K-R) and VVΔF1L-FLAG-F1L(9K-R) may have resulted in changes to mitochondrial morphology that either required ubiquitination of mitochondrial proteins or stimulated the ubiquitination of proteins at mitochondria, leading to the recruitment of conjugated ubiquitin. Ultimately, these data point to a previously undefined role for F1L in regulating mitochondrial dynamics and this function appears to be tightly linked to the ubiquitination status of the protein.

The accumulation of lysine mutations raises the issue of protein misfolding, which could account for the ubiquitination of FLAG-F1L(8K-R) and FLAG-F1L(9K-R) [657]. However, at early times during infection, cells infected with VVΔF1L-FLAG-F1L(8K-R) and VVΔF1L-FLAG-F1L(9K-R) were completely refractory to virus-induced apoptosis, which suggested proper folding of the proteins (Fig 5.20). Based on these data, the lysine-deficient F1L mutants seemingly retained anti-apoptotic function and inhibited virus-induced death to levels comparable to wildtype F1L in VVEGFP. Both VVΔF1L-FLAG-F1L(8K-R) and VVΔF1L-FLAG-F1L(9K-R) were not as potent in preventing Bak activation in response to STS, particularly compared to VVEGFP; therefore, the mutants were effective inhibitors of virus-induced apoptosis but defective in curbing additional apoptotic insults (Fig 5.20). Although viruses expressing FLAG-F1L(8K-R) and FLAG-F1L(9K-R) inhibited virus-induced apoptosis early during infection, at later times apoptosis occurred (Fig 5.21). Interestingly, at 12 hours post infection, mitochondria expressing the lysine-deficient F1L mutants were severely punctate (Fig 5.17) and this coincided with a lack of Bak binding to both FLAG-F1L(8K-R) and FLAG-F1L(9K-R) (Fig 5.22). Thus, despite preventing virus-induced apoptosis early during infection, VVΔF1L-FLAG-F1L(8K-R) and VVΔF1L-FLAG-F1L(9K-R)

promoted massive rearrangements to the mitochondrial network at late times post infection and activated the cell death machinery. We cannot discern from the data whether the loss of Bak binding was a cause or result of the mitochondrial changes and subsequent apoptosis that occurs during VVΔF1L-FLAG-F1L(8K-R) and VVΔF1L-FLAG-F1L(9K-R) infection.   However, since the viruses were able to inhibit apoptosis, albeit only at early times, we speculate that the accumulation of the lysine-deficient mutants in the mitochondria interfered with the architecture of the organelle resulting in apoptosis.   The apoptosis initiated by VVΔF1L-FLAG-F1L(8K-R) and VVΔF1L-FLAG-F1L(9K-R) is so potent, in fact, that it occurs much faster than apoptosis induced by VVΔF1L, which completely lacks F1L (Fig 5.21).   Moreover, the apoptosis observed with the mutant viruses probably accounted for the small plaque phenotype, suggesting that pre-mature cell death may interfere with virus release from infected cells (Fig 5.23). This is supported by the fact that VVΔF1L-FLAG-F1L(8K-R) and VVΔF1L-FLAG-F1L(9K-R) exhibited slightly delayed growth *in vitro* in subsequent rounds of infection (Fig A.8). From these data, it appeared that the expression of FLAG-F1L(8K-R) and FLAG-F1L(9K-R) caused ubiquitin accumulation at mitochondria and vast changes in mitochondrial ultrastructure. Additionally, viruses expressing these proteins activated the apoptotic machinery late during infection and this had severe consequences on virus growth.   Future studies aimed at discerning the cause of the mitochondrial disruption and the initiation of apoptosis during VVΔF1L-FLAG-F1L(8K-R) and VVΔF1L-FLAG-F1L(9K-R) infection will help to better understand both the phenotypes of these viruses and the relationship between F1L, ubiquitination, and mitochondrial dynamics.

CHAPTER 6: Discussion

6.1 VACCINIA VIRUS F1L INHIBITS APOPTOSIS AT MITOCHONDRIA

Apoptosis is a powerful antiviral barrier; thus, many viruses have evolved strategies that overcome cell death to ensure viral replication and propagation [52,54,443]. Many DNA viruses encode vBcl-2 homologues that inhibit the mitochondrial checkpoint [495,496], yet several poxviruses encode novel inhibitors of apoptosis that do not display apparent sequence similarity to members of the Bcl-2 family [63,444]. VV F1L is expressed early during infection, localizes exclusively to mitochondria, and inhibits the activation of Bak and Bax [548,549,550]. F1L accomplishes this by interacting with Bak and the BH3-only protein BimL to prevent mitochondrial depolarization and cytochrome *c* release (Fig 1.22B) [547,550,551,552]. Based on functional similarities between F1L and cellular anti-apoptotic proteins, such as Mcl-1, we speculated that F1L either cooperates with or replaces these proteins during VV infection. Prior to this study, however, the mechanism by which F1L interacts with Bak was unknown, given its lack of sequence identity to cellular Bcl-2 proteins. Moreover, it was not known whether F1L was subject to cellular regulatory mechanisms in a manner similar to various Bcl-2 family members.

6.2 F1L AND MCL-1 HAVE SIMILAR ANTI-APOPTOTIC FUNCTIONS

Mcl-1 is a critical negative regulator of Bak activity and the Bak-Mcl-1 complex must be disrupted prior to Bak activation [266,289,354]. Mcl-1 is a unique member of the cellular anti-apoptotic proteins with a binding profile distinct from Bcl-2 and Bcl-xL [287,288,432]. The importance of Mcl-1 as an inhibitor of Bak activation was recently highlighted in Mcl-1-deficient thymocytes that die in a Bak-specific manner [686]. In fact, the anti-apoptotic functions of Bcl-2 and Mcl-1 are not redundant in thymocytes and Bcl-2 cannot compensate for the loss of Mcl-1 [686]. The integral role of Mcl-1 in maintaining Bak in an inactive state is highlighted by viruses that target Mcl-1 to promote Bak activation and apoptosis. In addition to AdV E1a, which induces a DNA damage response that stimulates disruption of the Bak-Mcl-1 complex and proteasomal

degradation of Mcl-1 [354], vesicular stomatitis virus promotes Bak-dependent cell death by releasing Bak from both Mcl-1 and Bcl-xL and promoting the degradation of Mcl-1 [687,688]. Moreover, the core protein in hepatitis C virus contains a BH3-like domain that specifically interacts with Mcl-1, in a manner similar to Noxa, and contributes to virus-induced apoptosis [689].

We have not discerned whether the VV-induced dissociation of Mcl-1 from Bak was a cellular response to VV infection or a direct result of F1L outcompeting Mcl-1 for the Bak BH3 domain, although the latter would suggest that F1L has a stronger affinity for Bak compared to Mcl-1. However, we have determined that Mcl-1 was not required to inhibit Bak during infection with VV due to the presence of F1L (Fig 6.1). Although Mcl-1 was displaced from Bak, we found that Mcl-1 remained at mitochondria during infection, suggesting that it may contribute to cell survival during VV infection (Figs 3.5 and 3.8). Interestingly, *mcl-1* is upregulated upon infection with VV and the apoptosis-inducing VV lacking E3L, supporting a possible role for Mcl-1 during infection [690]. In addition to binding Bak, Mcl-1 binds a variety of BH3-only proteins, including Bim, Puma, Noxa, tBid, and Bik [266,567,588,590,592,613]. Mcl-1 may, therefore, bind one or more of these BH3-only proteins to prevent apoptosis during VV infection. Unfortunately, the BH3-only proteins that are activated in response to VV infection have yet to be identified. Notably, both F1L and Mcl-1 interact with Bim [549,567,592]. The fate of the Bim-Mcl-1 complex has not been investigated during infection so it is not clear if Mcl-1 is required to prevent Bim activity or if F1L replaces Mcl-1 by binding Bim. Alternatively, Mcl-1 may be completely dispensable during VV infection and not required to inhibit cell death in the presence of F1L since the two proteins have overlapping anti-apoptotic activities.

The rapid degradation of Mcl-1 following genotoxic insults or growth factor deprivation is not observed with other cellular anti-apoptotic proteins [287,288,432]. It remains to be determined if the degradation of Mcl-1 is solely
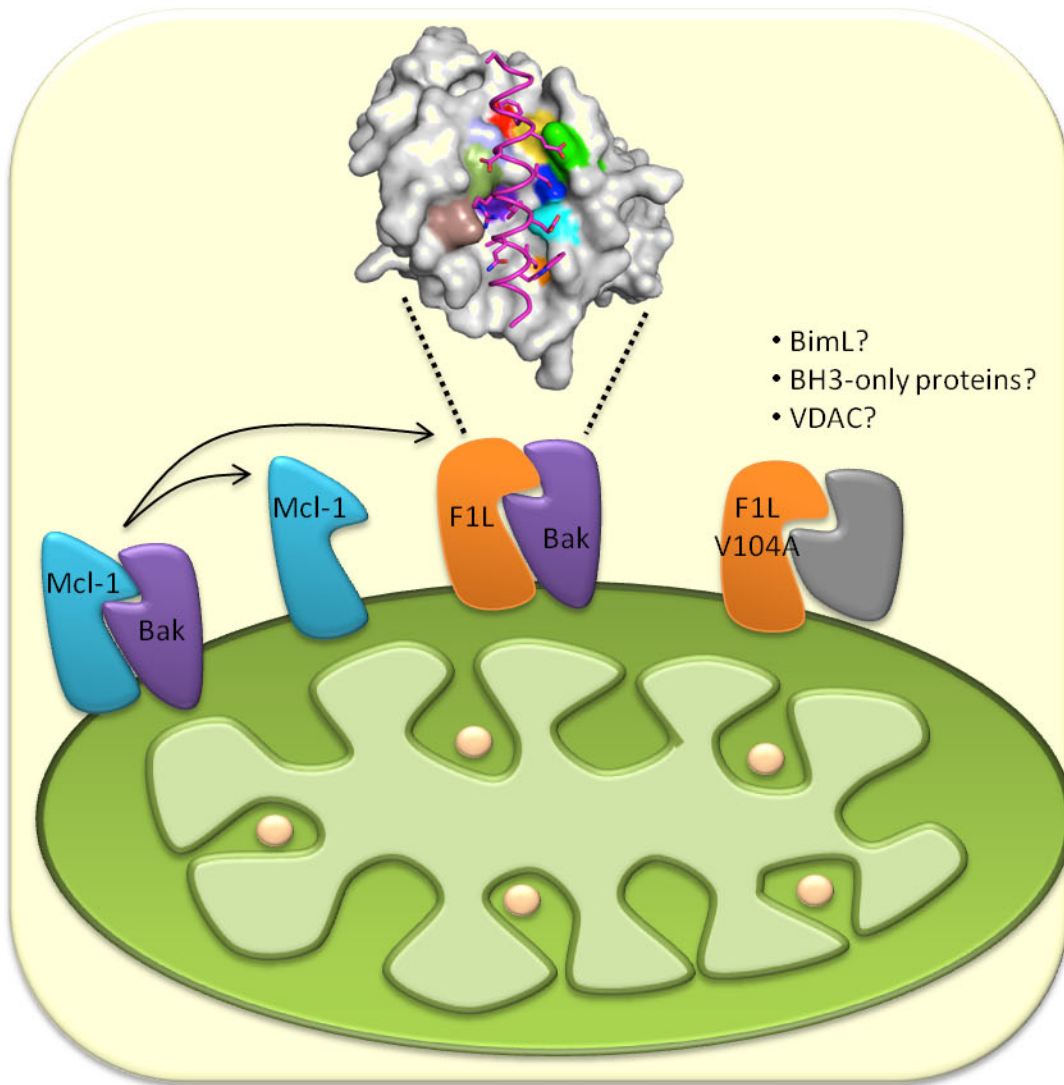
Figure 6.1 F1L interacts with Bak using divergent BH domains and replaces Mcl-1. During VV infection, the Bak-Mcl-1 complex is disrupted and F1L binds and inhibits Bak. Mcl-1 is relatively stable and remains at mitochondria but whether it plays a significant anti-apoptotic role during infection is not known. The interaction between F1L and Bak is mediated by the BH3 domain of Bak and the hydrophobic binding groove of F1L composed of divergent BH domains 1-3 [677]. F1L(V104A), which is mutated in the BH1 domain of F1L, no longer interacts with Bak but prevents against virus-induced and STS-induced apoptosis. This mutant may therefore interact with one or more proteins to inhibit apoptosis in a Bak-independent manner.

to promote the full activation of Bak and various BH3-only proteins in response to specific stimuli. Based on the embryonic lethality of Mcl-1-deficient cells and the unique N-terminus of Mcl-1, it is also possible that Mcl-1 has roles aside from regulating apoptosis that set it apart from other cellular anti-apoptotic proteins [350,597]. Further investigation into new potential roles of Mcl-1 in preventing apoptosis may shed light on other possible mechanisms employed by F1L to inhibit death or other roles Mcl-1 may play during VV infection.

6.3 F1L INTERACTS WITH BAK USING DIVERGENT BH DOMAINS

Although F1L lacks sequence homology to the Bcl-2 family of proteins, we and others have identified Bak as a major target of F1L [550,551]. Here, we show that the association between F1L and Bak was conserved in human, murine, and chicken cells (Fig 3.1). The ability of F1L to bind Bak in a cellular context contrasts with the low affinity of MVA F1L for a Bak BH3 peptide in binding assays [555,644], suggesting that the interaction may require the presence of a membrane since these proteins are normally anchored in the OMM [177,548]. Alternatively, the conformation of full-length Bak may be important for binding to F1L. The discrepancy between immunoprecipitation data and *in vitro* binding assays using BH3 peptides has been observed previously for Bak, underscoring the importance of examining interactions between Bcl-2 family members in a physiologically relevant system [691]. This issue is further highlighted by the fact that F1L is able to bind detergent-activated Bax but F1L prevents Bax activation from occurring in the first place [549]. Therefore, although F1L can bind activated Bax, the interaction does not likely occur during infection, since Bax does not become activated in the presence of F1L [549].

We have identified degenerate BH domains within F1L based on the conservation of hydrophobic residues that mediate protein interactions within the cellular Bcl-2 family (Figs 4.1 and 4.2). The BH1 and BH3 domains were important for mediating Bak binding and preventing TNFα-induced apoptosis (Figs 4.4 and 4.5). Furthermore, point mutations in the BH1 (G144F) and BH3

(V104A) domains of F1L abrogated binding to endogenous Bak during VV infection (Fig 4.8). Although both F1L(V104A) and F1L(G144F) were impaired with respect to Bak binding, only F1L(G144F) displayed a defect in pro-survival activity (Fig 4.9). Therefore, we believe that F1L(V104A), but not F1L(G144F), interacts with a protein other than Bak in order to prevent virus-induced and STS-induced apoptosis (Fig 6.1). A potential candidate is BimL, a known interacting partner of F1L [549]. Although the affinity of F1L(V104A) and F1L(G144F) for a Bim BH3 peptide was undetectable in *in vitro* binding assays [555], it has yet to be determined if the F1L mutant proteins interact with BimL in a cellular context. Additionally, F1L(V104A) may interact with one or more members of the BH3-only protein family, aside from BimL, in order to inhibit apoptosis. Further investigation into the BH3-only protein binding profiles of F1L(V104A), F1L(G144F), and other F1L binding pocket mutants may reveal new interacting partners and thus new ways in which F1L targets the Bcl-2 family.

In addition to binding BimL or other BH3-only proteins, a third explanation for the protective phenotype of F1L(V104A) is binding to apoptosis-regulating proteins outside of the Bcl-2 family. Interestingly, mass spectrometric analysis of VV-FLAG-F1L-infected cells revealed co-immunoprecipitation of VDAC and ANT with FLAG-F1L (Fig A.9). Although preliminary, the data suggest that F1L interacted with components of the PTP (Fig 1.9). It remains to be determined, however, whether this interaction can be further substantiated and how exactly these proteins interact with F1L. In support of an interaction between F1L and the PTP, various other viral anti-apoptotic proteins interact with one or more PTP components. HCMV vMIA was first described to interact with ANT in order to prevent MOMP and apoptosis, perhaps by preventing ANT association with pro-apoptotic Bcl-2 family members [643,692] and myxoma virus M11L interacts with the OMM protein PBR [536]. Additionally, the pro-apoptotic protein PB1-F2 from influenza virus interacts with ANT and VDAC to induce apoptosis [693,694]. Although components of the PTP are targeted by

various viral proteins, it is unclear why proteins such as vMIA, M11L, and perhaps F1L, interact with both PTP proteins and Bcl-2 family members and how these proteins physically interact with ANT and VDAC. The membrane-inserted α-helices 5 and 6 of Bcl-xL interact with VDAC, although it is not known yet if these α-helices in F1L insert into the OMM or interact with VDAC [294]. F1L could interact with VDAC via the binding pocket comprised of BH domains 1-3, which would suggest a cryptic BH3-like domain in VDAC. Indeed, it has been reported that VDAC2 binds the hydrophobic binding cleft of Bak [290]. Therefore, the point mutations we have generated in the binding groove of F1L may alter binding to VDAC and perhaps ANT, although the IMM localization of the latter protein makes this type of interaction unlikely. This may be particularly important in dissecting the functional differences between F1L(V104A) and F1L(G144F); that is, F1L(V104A) may maintain the interaction with VDAC, while F1L(G144F) may no longer bind this protein (Fig 6.1). If an interaction between F1L, VDAC, and ANT does indeed occur, the outcome of the interaction remains elusive. Although it has been reported that Bcl-xL inhibits PTP opening to prevent apoptosis [306], the binding of VDAC to Bcl-xL has also been suggested to prevent Bcl-xL from binding to Bak and Bax [695]. Thus, it will be important to determine whether the interaction with F1L inhibits the activity of the pro-apoptotic PTP or whether VDAC binding inhibits the anti-apoptotic activity of F1L. Lastly, the significance of F1L binding components of the PTP, in addition to Bcl-2 family members, is unclear, since apoptosis occurs following Bak and Bax activation without a requirement for PTP opening [294,318,319].

In an attempt to characterize residues that mediate the interactions of F1L, we have mutated numerous residues in the binding groove of F1L. These mutants will likely prove useful in dissecting the interactions between F1L and the pro-apoptotic proteins Bak and BimL and in assessing the contribution of each protein to apoptosis induction in response to VV infection. In addition, these mutants may establish the importance of other cellular proteins involved

in the anti-apoptotic mechanism of F1L. Our data revealed that mutating a single amino acid in the binding groove of F1L could severely hinder Bak binding (Figs 4.8 and 4.11). We have yet to determine whether mutating single amino acids in the BH3 domain of Bak would also be sufficient to disrupt the interaction, although *in vitro* binding assays with Bim BH3 peptides suggest this is likely [555]. The loss of Bak binding upon mutation of a single amino acid in F1L contrasts with the flexibility observed with Mcl-1 [243,632]. Minor structural changes in the binding cleft of Mcl-1 accommodate mutations in the BH3 domains of Bim and Noxa [243,632]. Although the ability of Mcl-1 to accommodate mutations in the Bak BH3 domain is not known, the relative rigidity of the F1L binding groove may explain the more selective binding profile of F1L in comparison to Mcl-1. It will be interesting to ascertain whether the BH domains we have characterized and the essential residues we have identified in VV F1L function similarly in F1L orthologues of other Orthopoxviruses, as well as the F1L homologue in the most recently sequenced but unclassified Yoka poxvirus [696].

6.4 THE BCL-2 CORE FOLD HAS BEEN EVOLUTIONARILY CONSERVED

vBcl-2 proteins were originally characterized as proteins that share significant sequence homology with the cellular Bcl-2 family, particularly within BH regions [497,498]. The first described vBcl-2 proteins, such as KSHV Bcl-2 and EBV BHRF-1, also resemble cellular Bcl-2 proteins at a structural level with the conserved BH domains forming the BH3 binding pocket [504,509]. It is now apparent, however, that many viral anti-apoptotic proteins adopt Bcl-2-like folds despite lacking sequence homology (Fig 6.2). F1L and M11L are excellent examples of viral proteins that adopt overall folds resembling Bcl-2 family members despite changes at the sequence level [539,540,555]. Additionally, secondary structure analysis predicts folds similar to Bcl-xL and Bcl-w for vMIA and ORFV125, respectively [526,544]. Therefore, the classification of vBcl-2 proteins ought to be based on structural homology, since conservation of the
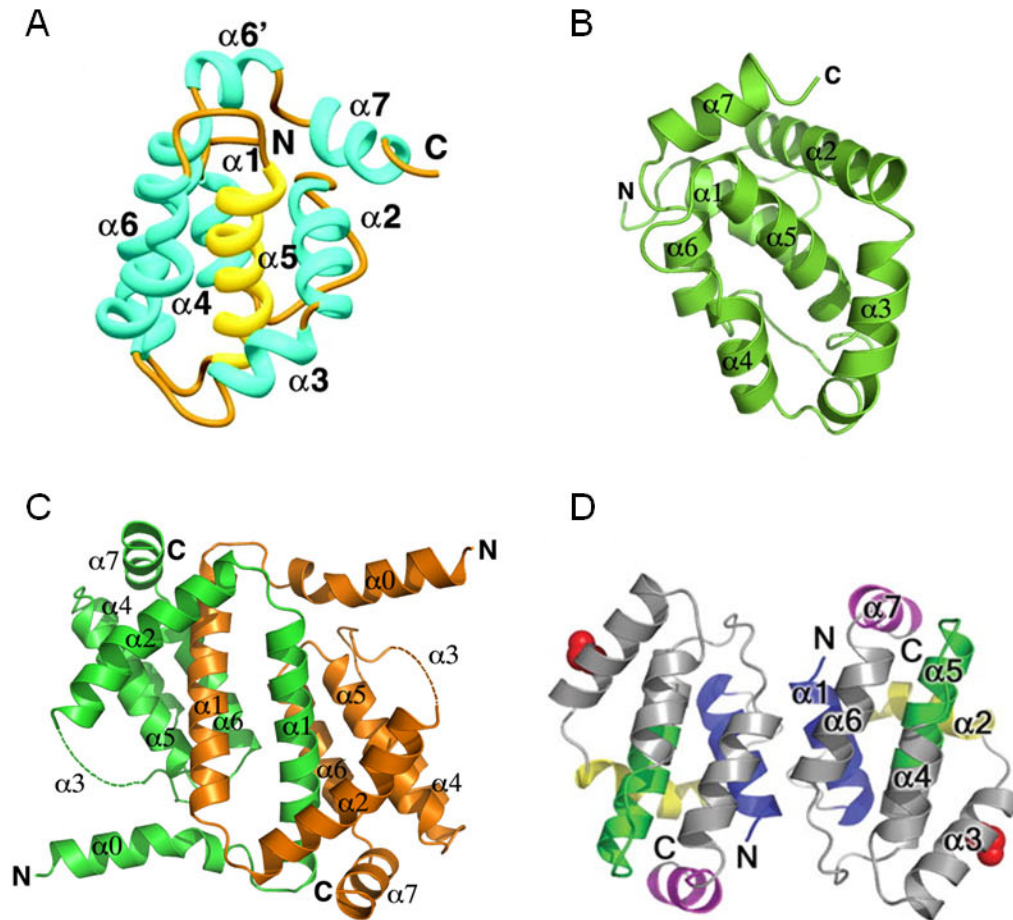
Figure 6.2 Conservation of the Bcl-2 Fold. Helical representations of KSHV Bcl-2 (**A**), myxoma virus M11L (**B**), MVA F1L (**C**), and VV(WR) N1L (**D**). While KSHV Bcl-2 contains highly conserved BH domains, M11L, F1L, and N1L all adopt Bcl-2-like folds despite lacking strong amino acid similarity with cellular Bcl-2 proteins. Both F1L and N1L forms dimers but only F1L forms a domain-swapped homodimer. α-helices are numbered and N- and C-termini are labelled. Adapted from [504,539,555,699].

Bcl-2-like fold can occur in spite of divergence at a sequence level. In support of this, the BH3-only protein Bid contains a single BH3 domain and yet structurally resembles multi-domain Bcl-2 family members [240], indicating that sequence motifs are not absolutely essential for structure. In addition, the presence of a BH4 domain as the defining feature of anti-apoptotic Bcl-2 family members has been met with challenge. The BH4 domain is by far the least conserved BH domain and its presence in Mcl-1 and A1 is controversial [350,697]. Moreover, it has been recently proposed that cyptic BH4 domains are present in members other than anti-apoptotic proteins, such as Bak and Bax [555]. Thus, it is increasingly apparent that vBcl-2 proteins in poxviruses and other DNA viruses share the evolutionarily conserved Bcl-2 fold in spite of massive changes in their protein sequence.

Unlike previously described vBcl-2 proteins and their cellular counterparts, F1L forms a domain-swapped homodimer that is unique among apoptotic inhibitors [555]. It remains to be established whether the interaction with Bak or BimL requires F1L in a dimer conformation and whether this conformation has a role in the ability of F1L to inhibit apoptosis. Intriguingly, mutation of a region in MVA F1L that corresponds to residues 68-88 in VV(Cop) F1L was shown to abrogate Bak binding and the apoptotic activity of F1L [551]. However, this region comprises the BH4 domain that we have identified in F1L and takes part in homodimerization; therefore, deleting this region likely disrupts the structure of F1L and is not in fact responsible for Bak binding [555]. Indeed, we have found that F1L(84-226), which lacks the unique N-terminus and BH4 domain of F1L, no longer interacted with Bak or prevented TNFα-induced apoptosis (Figs 4.4-4.6). Interestingly, in addition to F1L, VV contains several other proteins that adopt Bcl-2-like folds and one of these proteins also forms a dimer [22,698]. N1L adopts an overall fold that resembles cellular Bcl-2 family members, yet α-helices 1 and 6 interact with the equivalent helices in a neighbouring molecule to form a dimer (Fig 6.2) [699,700,701]. Although an

anti-apoptotic role for N1L has been proposed, it is more likely that the protein inhibits NFκB signalling and not the apoptotic pathway [699,702,703]. Two additional VV proteins, A52R and B14R, inhibit the pro-inflammatory NFκB pathway and each adopt a Bcl-2-like fold as well [704]. The identification of VV proteins that adopt folds reminiscent of cellular Bcl-2 proteins but function outside of apoptosis strongly suggests that the Bcl-2-like fold represents an evolutionarily favoured structure that extends beyond the mitochondrial death machinery [22].

6.5 F1L IS REGULATED BY THE UBIQUITIN-PROTEASOME SYSTEM

VV and many other members of the *Poxviridae* family encode a plethora of proteins aimed at modulating the cellular UPS [667,668]. These include ubiquitin ligases, such as M153R and p28, and adaptor proteins that function in complexes with cellular ubiquitin ligases, such as BTB/kelch proteins and F-box/ankyrin proteins [667,668]. Furthermore, we and others have demonstrated that a functional UPS is integral for *Orthopoxvirus* infections at the level of core uncoating or DNA replication and thus general shutdown of the UPS is detrimental early during VV infection [705,706]. Here we have characterized a novel relationship between poxviruses and the UPS: the ubiquitination and degradation of the VV anti-apoptotic protein F1L (Fig 6.3).

We have implicated the SCF as a putative ubiquitin ligase that mediates the ubiquitination of F1L although the adaptor protein involved is unknown (Fig 5.11). VV contains two F-box/ankyrin proteins; the 68k ankyrin-like protein from MVA interacts with Cul-1 and the ectromelia virus orthologue of the remaining protein also functions as part of the SCF complex [571,675]. It is therefore possible that VV F-box/ankyrin proteins or cellular F-box proteins interact with Cul-1 to recruit and ubiquitinate F1L during infection. The SCF complex did not appear to be solely responsible for F1L ubiquitination, indicating other ubiquitin ligases are involved in regulating F1L (Fig 6.3). Whether these ligases are cytoplasmic or mitochondrial is a question that has not yet been addressed;
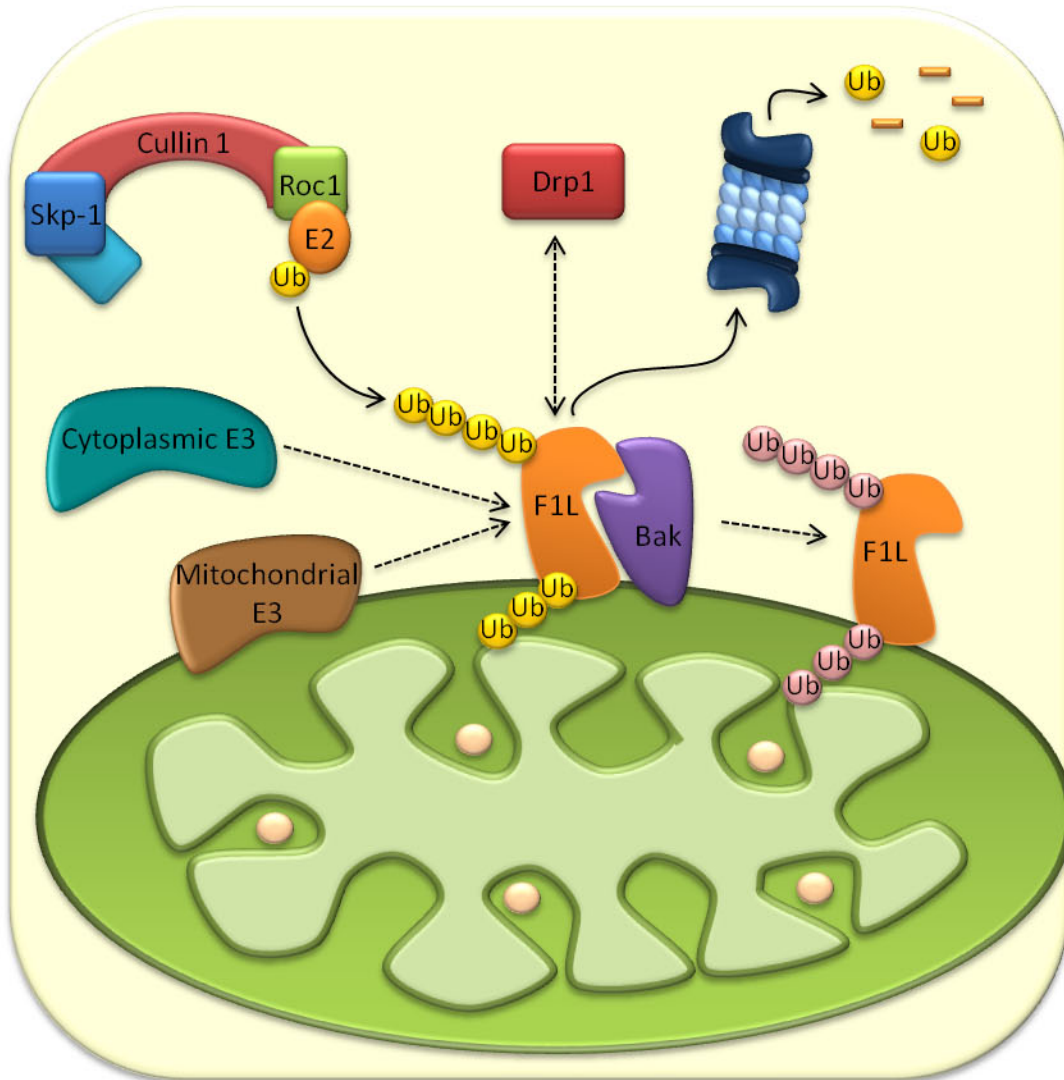
Figure 6.3 F1L is ubiquitinated and degraded. F1L is ubiquitinated by the SCF complex and potentially one or more ubiquitin ligases, either cytoplasmic or mitochondrial. Ubiquitination may occur on cytoplasmic residues other than lysine and/or in the mitochondria-inserted domain of F1L. Polyubiquitination of F1L targets the protein to the 26S proteasome for degradation, although it is unclear whether the interacting partners of F1L are degraded as well. The ubiquitination of F1L appears to be linked to mitochondrial morphology, suggesting F1L may influence the activity of proteins involved in fission or fusion, such as Drp1. In addition to proteasomal degradation, the ubiquitination of F1L may occur on K63 or other lysines (represented by pink ubiquitin chains) in ubiquitin to alter the activity of the protein.

however, the ubiquitination of F1L in the absence of virus infection suggests the involvement of cellular ubiquitin ligases (Fig 5.8). Potential candidates include the cytoplasmic BH3 domain-containing E3 ligase Mule, which is involved in mediating the turnover of Mcl-1 [437,438]. More recently, cytoplasmic ubiquitin ligases that target Bax and Bcl-2 have been identified. Bax is ubiquitinated by the "in between ring"-type RING finger ubiquitin ligase IBRDC2 that resides in the cytoplasm until Bax becomes activated and translocates to mitochondria [707]. Once at mitochondria, IBRDC2 ubiquitinates Bax to prevent unwanted apoptosis [707]. Moreover, Bcl-2 protein levels are regulated by the Cul-3 ubiquitin ligase in conjunction with the BTB/kelch protein Keap1 to promote apoptosis [708]. We have found no evidence supporting a role of the Cul-3-based machinery in the ubiquitination of F1L but we have not yet assessed IBRDC2 as a potential ubiquitin ligase for F1L. In addition to the cytoplasmic ubiquitin ligases that target members of the Bcl-2 family, it remains possible that F1L may be targeted by mitochondrial ligases, such as MARCH-V or MULAN. These ubiquitin ligases have important roles in regulating mitochondrial dynamics, but to date, no evidence exists for a role in regulating the Bcl-2 family of proteins [377,659,660,661,662]. In addition to cytoplasmic and mitochondrial ubiquitin ligases, it is also possible that F1L ubiquitination may be counteracted by the activity of cytoplasmic DUBs or a recently identified DUB residing in the OMM [709].

The identification of ubiquitin ligases responsible for the degradation of F1L will hopefully also shed light on the mechanism and timing of F1L ubiquitination. The majority of F1L is exposed to the cytoplasm and thus accessible to the UPS machinery [548]. This is presumably how the protein could be targeted by ubiquitin ligases embedded in the OMM or by cytoplasmic ubiquitin ligases following their recruitment to mitochondria. Whether F1L is constitutively ubiquitinated or requires a specific signal to initiate the process remains unknown. It is possible that F1L is ubiquitinated following translation of

the protein prior to mitochondrial insertion. Alternatively, F1L may be extruded from the OMM into the cytoplasm prior to ubiquitination, in a similar manner to ER proteins [710]. This could be particularly important for the ubiquitination of the tail anchor, which is inaccessible to the UPS when F1L is inserted in the OMM.

If the nine cytoplasmic lysines play a role in the ubiquitination of F1L, they do not appear to be the sole targets since FLAG-F1L(9K-R) associated with levels of conjugated ubiquitin comparable to FLAG-F1L (Figs 5.12 and 5.13). Deletion of the cytoplasmic lysines in F1L did, however, alter the post-translational modifications of the protein (Figs 5.13 and 5.14). We have not determined whether the presence of high molecular weight species in lysine-deficient F1L mutants was altered due to accumulating lysine to arginine mutations, or alternatively, if the mutation of a specific lysine was responsible. The suspected monoubiquitinated form of F1L, with a molecular weight of 34kDa, was notably absent in cells expressing FLAG-F1L(8K-R) and FLAG-F1L(9K-R), perhaps due to accumulating mutations (Figs 5.13 and 5.14). Instead, it is possible that the K51R mutation, which distinguishes FLAG-F1L(5K-R) and FLAG-F1L(6K-R), is responsible for the decreased monoubiquitination of FLAG-F1L(6K-R) (Fig 5.12). Until single lysine mutants are generated, we cannot discern between the two possibilities. Intriguingly, it has been recently reported that both Mcl-1 and BimEL can be degraded by the proteasome in a ubiquitin-independent manner [711,712]. It is therefore interesting to speculate that proteasomal degradation of F1L could also be regulated by a ubiquitin-independent mechanism.

In addition to serving as ubiquitin conjugation sites, the lysine residues in F1L may be involved in functions that are independent of ubiquitination and degradation. FLAG-F1L(6K-R), FLAG-F1L(7K-R), FLAG-F1L(8K-R), and FLAG-F1L(9K-R) all contain the K76R mutation (Table 5.1). K76 resides in the predicted BH4 domain of F1L and represents the only conserved amino acid within the domain

(Fig 4.2). Mutation of K76 may therefore alter the anti-apoptotic activity of F1L and account for the apoptosis observed in cells infected with VVΔF1L-FLAG-F1L(8K-R) and VVΔF1L-FLAG-F1L(9K-R) (Figs 5.20 and 5.21). Additionally, the K51R mutation in FLAG-F1L(7K-R), FLAG-F1L(8K-R), and FLAG-F1L(9K-R) is located in the unique N-terminal region of F1L that is important for protein dimerization [555]. Although the importance of dimerization has yet to be determined, K51R may interfere with the formation of dimers and may thus affect F1L function. Moreover, K103R, which was introduced into FLAG-F1L(4K-R), and K141R, which was introduced into FLAG-F1L(8K-R), represent mutations in the BH3 domain and BH1 domain, respectively (Fig 2.1). Therefore, these mutations may interefere with Bak binding or the anti-apoptotic activity of F1L, similar to the G144F mutation in the BH1 domain. It also remains possible that other regions of F1L are involved in mediating protein interactions and therefore may require one or more of the surface-exposed lysine residues. Indeed, the area opposite of the hydrophobic binding groove in Bax, composed of α-helices 1 and 6, has been implicated in binding a chemically stabilized Bim BH3 peptide [279]. This interaction requires a Bax lysine residue and mutation of this residue abrogates both the interaction with the Bim BH3 peptide and the pro-apoptotic activity of Bax [279]. Moreover, K128, which is located downstream of the BH1 domain in Bax, has been implicated in the pro-apoptotic activity of the protein [713,714]. However, we have yet to determine whether specific lysine residues of F1L play a role in mediating interactions with cellular proteins. Although we have not discerned whether the "back" of F1L engages in protein interactions, we believe this is unlikely since this region is the dimer interface and α-helix 1 interacts with the second F1L monomer [555].

Perhaps one of the most unexpected findings in this study was the extensive changes to mitochondrial ultrastructure upon expression of lysine-deficient F1L mutants (Fig 5.17). Although the connection between F1L lysine residues and mitochondrial architecture remains elusive, the data suggest that

F1L influences mitochondrial fission and fusion machinery (Fig 6.3). We have yet to establish a role for F1L in mitochondrial dynamics, although we have observed changes in mitochondrial morphology and recruitment of ubiquitin to mitochondria expressing wildtype FLAG-F1L, albeit less frequently compared to lysine-deficient F1L constructs (Figs 5.17 and 5.18). Given the extensive cross-talk between apoptosis and mitochondrial dynamics [139,159,160,161], it may not be extremely surprising that viral anti-apoptotic proteins influence both processes. Interestingly, expression of HCMV vMIA potently inhibits Bax, yet results in extensive fragmentation of mitochondria [715,716]. The mitochondrial fragmentation induced by vMIA is independent of its ability to bind Bax but both the cause and outcome of the mitochondrial changes await further investigation [526]. Additionally, it is unclear whether mitochondrial fragmentation is indeed caused by vMIA, and perhaps F1L, or whether the fragmentation signifies the initiation of apoptosis that is subsequently inhibited by the viral proteins.

Although we have implicated the UPS in regulating F1L, we are left with an important unanswered question: why is F1L ubiquitinated? Perhaps the ubiquitination is part of the cellular antiviral response to induce F1L degradation and promote apoptosis. However, the ubiquitination of F1L does not appear to dampen the protective function of the protein, although this cannot be fully addressed until anti-apoptotic activity is assessed in an F1L mutant that is no longer regulated by the UPS. Alternatively, F1L ubiquitination could occur late during VV infection to promote apoptosis and virus dissemination. While this is a possibility, FLAG-F1L was ubiquitinated by 12 hours post infection in VV-FLAG-F1L-infected cells (Figs 5.3-5.5) and the stabilization of endogenous F1L during MG132 treatment was observed by 8 hours post infection in cells infected with VV and VVEGFP (Fig 5.9). Apoptosis was not detected in cells expressing F1L at 20 hours post infection (Fig 5.21), suggesting that the ubiquitination of F1L was not solely a mechanism for virus release since F1L protects cells late during infection despite ubiquitination early on. Additionally, F1L degradation may be

coupled to the degradation of Bak and BimL. In this way, F1L may serve as a vehicle to promote the proteasomal degradation of its pro-apoptotic interacting partners in order to prevent oligomerization of Bak and Bax in the OMM. Conversely, the ubiquitination of F1L could also have non-degradative functions. We have not excluded the possibility that the ubiquitin linkages formed on F1L could form on lysines other than K48 in ubiquitin. Perhaps K63-linked chains form on F1L to somehow alter its activity or protein interactions at mitochondria (Fig 6.3)

Given that the levels of proteins embedded in the OMM are highly regulated by the UPS, it is possible that F1L is ubiquitinated and degraded to prevent a build up of protein in the OMM [95,657]. We have not ruled out this theory, although based on the level of endogenous F1L produced during VV infection, it does not seem necessary to regulate the protein level (Fig 5.9). While the precise mechanism governing F1L ubiquitination and degradation remains elusive, our data suggest that other vBcl-2 proteins may be subjected to the same regulation. Indeed, we have demonstrated that the F1L orthologue EVM025 and the distantly related avipoxvirus protein FPV039 also associated with conjugated ubiquitin (Figs 5.4 and 5.5). It is therefore of interest to determine whether these proteins are also targeted for proteasomal degradation and whether the ubiquitination status of these proteins affects their ability to inhibit apoptosis. Further investigation is also required to determine if the regulation of mitochondria-localized anti-apoptotic proteins by the UPS is specific to poxviruses or something that is shared with other DNA viruses that manipulate the mitochondrial machinery.

6.6 CONCLUSION

Numerous members of the *Poxviridae* family contain predicted mitochondrial anti-apoptotic proteins, highlighting the importance of inhibiting the mitochondrial machinery during infection [533,535,541,543,547]. F1L is only found within members of the *Orthopoxvirus* genus where it is highly conserved

[547]. Since the identification of VV F1L as a mitochondrial apoptosis inhibitor in 2003, the mechanism of this unique protein has been extensively studied [547,548,549,550,551,553,554,555,644]. F1L replaces the function of Mcl-1 and acts as a guardian of the mitochondrial death machinery by targeting Bak and BimL, a binding profile that differs from cellular and viral anti-apoptotic proteins [549,550]. The way in which F1L binds these proteins was once a puzzling question based on the minimal sequence conservation compared to cellular Bcl-2 proteins. Although lacking conserved amino acid signatures, F1L retains a typical pattern of hydrophobic residues common in Bcl-2 family members. Moreover, the structural similarities between F1L and Bcl-2 proteins highlight the fact that specific sequence elements of cellular Bcl-2 proteins and vBcl-2 proteins do not necessarily dictate protein function [555]. Instead, classification of vBcl-2 proteins should be based on conservation of structural motifs. The divergence of F1L, as well as other poxviral proteins, such as M11L and ORFV125, from cellular Bcl-2 proteins suggests that these proteins have maintained only the minimal sequence requirements [539,540,544,555]. These proteins therefore serve as useful tools not only for dissection of the mitochondrial apoptotic pathway, but also for characterizing the minimal functional elements of the Bcl-2 family. In addition to functional conservation between F1L and cellular Bcl-2 proteins, the cellular mechanisms regulating F1L are also shared with Bcl-2 family members. This spurs the question of whether or not the UPS is involved in regulating other vBcl-2 proteins present in and outside the poxvirus family. Furthermore, the finding that F1L is involved in mitochondrial dynamics suggests the function of F1L may extend beyond apoptosis. Future studies may establish a clearer link between the two functions of F1L and also between the cellular processes of mitochondrial morphology and apoptosis. In studying the anti-apoptotic function and regulation of vBcl-2 proteins, such as F1L, we hope to better understand the apoptotic pathway and cellular mechanisms governing the process. Additionally, we also hope to provide insight into the mechanism and

regulation of F1L, since the viral protein has potential therapeutic uses in the development of new vaccines and the prevention of apoptosis-related diseases.

CHAPTER 7: References

1. Damon IK (2007) Poxviruses. In: Knipe DM, Howley PM, editors. Fields Virology. Philadelphia: Lippincott Williams & Wilkins. pp. 2947-2975.
2. Moss B (2007) Poxviridae: The Viruses and Their Replication. In: Knipe DM, Howley PM, editors. Fields Virology. Philadelphia: Lippincott Williams & Wilkins. pp. 2905-2946.
3. Esposito JJ, Fenner F (2001) Poxviruses. In: Knipe DM, Howley PM, editors. Fields Virology. Philadelphia: Lippincott, Williams & Wilkins. pp. 2885-2921.
4. Moore ZS, Seward JF, Lane JM (2006) Smallpox. Lancet 367: 425-435.
5. Bollet AJ (2004) The small pox. Plagues and poxes: The impact of human history on epidemic disease New York: Demos Medical Publishing, Incorporated. pp. 75-89.
6. Hopkins DR (2002) The greatest killer: smallpox in history. Chicago: University of Chicago Press.
7. McFadden G (2005) Poxvirus tropism. Nat Rev Microbiol 3: 201-213.
8. Fenner F, Wittek R, Dumbell KR (1989) The orthopoxviruses. San Diego: Academic Press.
9. Fenner F (2000) Adventures with poxviruses of vertebrates. FEMS Microbiol Rev 24: 123-133.
10. Fenner F, Buller ML (1997) Mousepox. In: Nathanson N, editor. Viral Pathogensis. Philadelphia: Lippincott-Raven Publishers. pp. 535-553.
11. Parker S, Nuara A, Buller RM, Schultz DA (2007) Human monkeypox: an emerging zoonotic disease. Future Microbiol 2: 17-34.
12. Baxby D (1977) The origins of vaccinia virus. J Infect Dis 136: 453-455.
13. Fenner F (1982) A successful eradication campaign. Global eradication of smallpox. Rev Infect Dis 4: 916-930.
14. Baxby D (1979) Edward Jenner, William Woodville, and the origins of vaccinia virus. J Hist Med Allied Sci 34: 134-162.
15. Organisation WH. 1980; Geneva. World Health Organisaion.
16. Guo ZS, Bartlett DL (2004) Vaccinia as a vector for gene delivery. Expert Opin Biol Ther 4: 901-917.
17. Thorne SH (2008) Oncolytic vaccinia virus: from bedside to benchtop and back. Curr Opin Mol Ther 10: 387-392.
18. Moss B (1996) Genetically engineered poxviruses for recombinant gene expression, vaccination, and safety. Proc Natl Acad Sci U S A 93: 11341-11348.
19. Haga IR, Bowie AG (2005) Evasion of innate immunity by vaccinia virus. Parasitology 130 Suppl: S11-25.
20. Seet BT, Johnston JB, Brunetti CR, Barrett JW, Everett H, Cameron C, Sypula J, Nazarian SH, Lucas A, McFadden G (2003) Poxviruses and immune evasion. Annu Rev Immunol 21: 377-423.
21. Perdiguero B, Esteban M (2009) The interferon system and vaccinia virus evasion mechanisms. J Interferon Cytokine Res 29: 581-598.
22. Bahar MW, Graham SC, Chen RA, Cooray S, Smith GL, Stuart DI, Grimes JM (2011) How vaccinia virus has evolved to subvert the host immune response. J Struct Biol 175: 127-134.
23. Gubser C, Hue S, Kellam P, Smith GL (2004) Poxvirus genomes: a phylogenetic analysis. J Gen Virol 85: 105-117.
24. Upton C, Slack S, Hunter AL, Ehlers A, Roper RL (2003) Poxvirus orthologous clusters: toward defining the minimum essential poxvirus genome. J Virol 77: 7590-7600.

25. Lefkowitz EJ, Wang C, Upton C (2006) Poxviruses: past, present and future. Virus Res 117: 105-118.
26. Hollinshead M, Vanderplasschen A, Smith GL, Vaux DJ (1999) Vaccinia virus intracellular mature virions contain only one lipid membrane. J Virol 73: 1503-1517.
27. Moss B (2006) Poxvirus entry and membrane fusion. Virology 344: 48-54.
28. Dales S, Siminovitch L (1961) The development of vaccinia virus in Earle's L strain cells as examined by electron microscopy. J Biophys Biochem Cytol 10: 475-503.
29. Katsafanas GC, Moss B (2007) Colocalization of transcription and translation within cytoplasmic poxvirus factories coordinates viral expression and subjugates host functions. Cell Host Microbe 2: 221-228.
30. Sodeik B, Doms RW, Ericsson M, Hiller G, Machamer CE, van 't Hof W, van Meer G, Moss B, Griffiths G (1993) Assembly of vaccinia virus: role of the intermediate compartment between the endoplasmic reticulum and the Golgi stacks. J Cell Biol 121: 521-541.
31. Roberts KL, Smith GL (2008) Vaccinia virus morphogenesis and dissemination. Trends Microbiol 16: 472-479.
32. Ward BM (2005) The longest micron; transporting poxviruses out of the cell. Cell Microbiol 7: 1531-1538.
33. Doceul V, Hollinshead M, van der Linden L, Smith GL (2010) Repulsion of superinfecting virions: a mechanism for rapid virus spread. Science 327: 873-876.
34. Moss B (2011) Smallpox vaccines: targets of protective immunity. Immunol Rev 239: 8-26.
35. Kennedy RB, Ovsyannikova IG, Jacobson RM, Poland GA (2009) The immunology of smallpox vaccines. Curr Opin Immunol 21: 314-320.
36. Boomker JM, de Leij LF, The TH, Harmsen MC (2005) Viral chemokine-modulatory proteins: tools and targets. Cytokine Growth Factor Rev 16: 91-103.
37. Alcami A (2003) Viral mimicry of cytokines, chemokines and their receptors. Nat Rev Immunol 3: 36-50.
38. Barry M, McFadden G (1997) Virokines and Viroceptors. In: Remick DG, Friedland JS, editors. Cytokines in health and disease. New York: M. Dekker. pp. 251-261.
39. Chang HW, Jacobs BL (1993) Identification of a conserved motif that is necessary for binding of the vaccinia virus E3L gene products to double-stranded RNA. Virology 194: 537-547.
40. Chang HW, Watson JC, Jacobs BL (1992) The E3L gene of vaccinia virus encodes an inhibitor of the interferon-induced, double-stranded RNA-dependent protein kinase. Proc Natl Acad Sci U S A 89: 4825-4829.
41. Davies MV, Elroy-Stein O, Jagus R, Moss B, Kaufman RJ (1992) The vaccinia virus K3L gene product potentiates translation by inhibiting double-stranded-RNA-activated protein kinase and phosphorylation of the alpha subunit of eukaryotic initiation factor 2. J Virol 66: 1943-1950.
42. Dobbelstein M, Shenk T (1996) Protection against apoptosis by the vaccinia virus SPI-2 (B13R) gene product. J Virol 70: 6479-6485.
43. Kettle S, Alcami A, Khanna A, Ehret R, Jassoy C, Smith GL (1997) Vaccinia virus serpin B13R (SPI-2) inhibits interleukin-1beta-converting enzyme and protects virus-infected cells from TNF- and Fas-mediated apoptosis, but does not prevent IL-1beta-induced fever. J Gen Virol 78 (Pt 3): 677-685.

44. Hengartner MO (2000) The biochemistry of apoptosis. Nature 407: 770-776.
45. Lawen A (2003) Apoptosis-an introduction. Bioessays 25: 888-896.
46. Danial NN, Korsmeyer SJ (2004) Cell death: critical control points. Cell 116: 205-219.
47. Ameisen JC (2002) On the origin, evolution, and nature of programmed cell death: a timeline of four billion years. Cell Death Differ 9: 367-393.
48. Kerr JF, Wyllie AH, Currie AR (1972) Apoptosis: a basic biological phenomenon with wide-ranging implications in tissue kinetics. Br J Cancer 26: 239-257.
49. Barry M, Bleackley RC (2002) Cytotoxic T lymphocytes: all roads lead to death. Nat Rev Immunol 2: 401-409.
50. Brandstadter JD, Yang Y (2011) Natural killer cell responses to viral infection. J Innate Immun 3: 274-279.
51. Rudin CM, Thompson CB (1997) Apoptosis and disease: regulation and clinical relevance of programmed cell death. Annu Rev Med 48: 267-281.
52. Taylor RC, Cullen SP, Martin SJ (2008) Apoptosis: controlled demolition at the cellular level. Nat Rev Mol Cell Biol 9: 231-241.
53. Van Cruchten S, Van Den Broeck W (2002) Morphological and biochemical aspects of apoptosis, oncosis and necrosis. Anat Histol Embryol 31: 214-223.
54. Siegel RM (2006) Caspases at the crossroads of immune-cell life and death. Nat Rev Immunol 6: 308-317.
55. Cullen SP, Martin SJ (2009) Caspase activation pathways: some recent progress. Cell Death Differ 16: 935-938.
56. Yuan J, Shaham S, Ledoux S, Ellis HM, Horvitz HR (1993) The C. elegans cell death gene ced-3 encodes a protein similar to mammalian interleukin-1 beta-converting enzyme. Cell 75: 641-652.
57. Nicholson DW (1999) Caspase structure, proteolytic substrates, and function during apoptotic cell death. Cell Death Differ 6: 1028-1042.
58. Stennicke HR, Salvesen GS (1998) Properties of the caspases. Biochim Biophys Acta 1387: 17-31.
59. Peter ME, Krammer PH (2003) The CD95(APO-1/Fas) DISC and beyond. Cell Death Differ 10: 26-35.
60. Riedl SJ, Salvesen GS (2007) The apoptosome: signalling platform of cell death. Nat Rev Mol Cell Biol 8: 405-413.
61. Luthi AU, Martin SJ (2007) The CASBAH: a searchable database of caspase substrates. Cell Death Differ 14: 641-650.
62. Timmer JC, Salvesen GS (2007) Caspase substrates. Cell Death Differ 14: 66-72.
63. Taylor JM, Barry M (2006) Near death experiences: poxvirus regulation of apoptotic death. Virology 344: 139-150.
64. Ashkenazi A, Dixit VM (1998) Death receptors: signaling and modulation. Science 281: 1305-1308.
65. Nagata S (1997) Apoptosis by death factor. Cell 88: 355-365.
66. Smith CA, Farrah T, Goodwin RG (1994) The TNF receptor superfamily of cellular and viral proteins: activation, costimulation, and death. Cell 76: 959-962.
67. Gruss HJ, Dower SK (1995) Tumor necrosis factor ligand superfamily: involvement in the pathology of malignant lymphomas. Blood 85: 3378-3404.
68. Tanaka M, Suda T, Haze K, Nakamura N, Sato K, Kimura F, Motoyoshi K, Mizuki M, Tagawa S, Ohga S, Hatake K, Drummond AH, Nagata S (1996) Fas ligand in human serum. Nat Med 2: 317-322.
69. Nagata S, Golstein P (1995) The Fas death factor. Science 267: 1449-1456.

70. Itoh N, Nagata S (1993) A novel protein domain required for apoptosis. Mutational analysis of human Fas antigen. J Biol Chem 268: 10932-10937.
71. Tartaglia LA, Ayres TM, Wong GH, Goeddel DV (1993) A novel domain within the 55 kd TNF receptor signals cell death. Cell 74: 845-853.
72. Hsu H, Shu HB, Pan MG, Goeddel DV (1996) TRADD-TRAF2 and TRADD-FADD interactions define two distinct TNF receptor 1 signal transduction pathways. Cell 84: 299-308.
73. Hsu H, Xiong J, Goeddel DV (1995) The TNF receptor 1-associated protein TRADD signals cell death and NF-kappa B activation. Cell 81: 495-504.
74. Beg AA, Baltimore D (1996) An essential role for NF-kappaB in preventing TNF-alpha-induced cell death. Science 274: 782-784.
75. Van Antwerp DJ, Martin SJ, Kafri T, Green DR, Verma IM (1996) Suppression of TNF-alpha-induced apoptosis by NF-kappaB. Science 274: 787-789.
76. Wang CY, Mayo MW, Baldwin AS, Jr. (1996) TNF- and cancer therapy-induced apoptosis: potentiation by inhibition of NF-kappaB. Science 274: 784-787.
77. Boldin MP, Varfolomeev EE, Pancer Z, Mett IL, Camonis JH, Wallach D (1995) A novel protein that interacts with the death domain of Fas/APO1 contains a sequence motif related to the death domain. J Biol Chem 270: 7795-7798.
78. Chinnaiyan AM, O'Rourke K, Tewari M, Dixit VM (1995) FADD, a novel death domain-containing protein, interacts with the death domain of Fas and initiates apoptosis. Cell 81: 505-512.
79. Kischkel FC, Hellbardt S, Behrmann I, Germer M, Pawlita M, Krammer PH, Peter ME (1995) Cytotoxicity-dependent APO-1 (Fas/CD95)-associated proteins form a death-inducing signaling complex (DISC) with the receptor. EMBO J 14: 5579-5588.
80. Boldin MP, Goncharov TM, Goltsev YV, Wallach D (1996) Involvement of MACH, a novel MORT1/FADD-interacting protease, in Fas/APO-1- and TNF receptor-induced cell death. Cell 85: 803-815.
81. Muzio M, Chinnaiyan AM, Kischkel FC, O'Rourke K, Shevchenko A, Ni J, Scaffidi C, Bretz JD, Zhang M, Gentz R, Mann M, Krammer PH, Peter ME, Dixit VM (1996) FLICE, a novel FADD-homologous ICE/CED-3-like protease, is recruited to the CD95 (Fas/APO-1) death--inducing signaling complex. Cell 85: 817-827.
82. Boatright KM, Renatus M, Scott FL, Sperandio S, Shin H, Pedersen IM, Ricci JE, Edris WA, Sutherlin DP, Green DR, Salvesen GS (2003) A unified model for apical caspase activation. Mol Cell 11: 529-541.
83. Oberst A, Pop C, Tremblay AG, Blais V, Denault JB, Salvesen GS, Green DR (2010) Inducible dimerization and inducible cleavage reveal a requirement for both processes in caspase-8 activation. J Biol Chem 285: 16632-16642.
84. Hughes MA, Harper N, Butterworth M, Cain K, Cohen GM, MacFarlane M (2009) Reconstitution of the death-inducing signaling complex reveals a substrate switch that determines CD95-mediated death or survival. Mol Cell 35: 265-279.
85. Thome M, Tschopp J (2001) Regulation of lymphocyte proliferation and death by FLIP. Nat Rev Immunol 1: 50-58.
86. Irmler M, Thome M, Hahne M, Schneider P, Hofmann K, Steiner V, Bodmer JL, Schroter M, Burns K, Mattmann C, Rimoldi D, French LE, Tschopp J (1997) Inhibition of death receptor signals by cellular FLIP. Nature 388: 190-195.
87. Shu HB, Halpin DR, Goeddel DV (1997) Casper is a FADD- and caspase-related inducer of apoptosis. Immunity 6: 751-763.

88. Srinivasula SM, Ahmad M, Ottilie S, Bullrich F, Banks S, Wang Y, Fernandes-Alnemri T, Croce CM, Litwack G, Tomaselli KJ, Armstrong RC, Alnemri ES (1997) FLAME-1, a novel FADD-like anti-apoptotic molecule that regulates Fas/TNFR1-induced apoptosis. J Biol Chem 272: 18542-18545.

89. Inohara N, Koseki T, Hu Y, Chen S, Nunez G (1997) CLARP, a death effector domain-containing protein interacts with caspase-8 and regulates apoptosis. Proc Natl Acad Sci U S A 94: 10717-10722.

90. Goltsev YV, Kovalenko AV, Arnold E, Varfolomeev EE, Brodianskii VM, Wallach D (1997) CASH, a novel caspase homologue with death effector domains. J Biol Chem 272: 19641-19644.

91. Darmon AJ, Nicholson DW, Bleackley RC (1995) Activation of the apoptotic protease CPP32 by cytotoxic T-cell-derived granzyme B. Nature 377: 446-448.

92. Atkinson EA, Barry M, Darmon AJ, Shostak I, Turner PC, Moyer RW, Bleackley RC (1998) Cytotoxic T lymphocyte-assisted suicide. Caspase 3 activation is primarily the result of the direct action of granzyme B. J Biol Chem 273: 21261-21266.

93. Medema JP, Toes RE, Scaffidi C, Zheng TS, Flavell RA, Melief CJ, Peter ME, Offringa R, Krammer PH (1997) Cleavage of FLICE (caspase-8) by granzyme B during cytotoxic T lymphocyte-induced apoptosis. Eur J Immunol 27: 3492-3498.

94. Yang X, Stennicke HR, Wang B, Green DR, Janicke RU, Srinivasan A, Seth P, Salvesen GS, Froelich CJ (1998) Granzyme B mimics apical caspases. Description of a unified pathway for trans-activation of executioner caspase-3 and -7. J Biol Chem 273: 34278-34283.

95. Kroemer G, Galluzzi L, Brenner C (2007) Mitochondrial membrane permeabilization in cell death. Physiol Rev 87: 99-163.

96. Ow YP, Green DR, Hao Z, Mak TW (2008) Cytochrome c: functions beyond respiration. Nat Rev Mol Cell Biol 9: 532-542.

97. Parsons MJ, Green DR (2010) Mitochondria in cell death. Essays Biochem 47: 99-114.

98. Newmeyer DD, Farschon DM, Reed JC (1994) Cell-free apoptosis in Xenopus egg extracts: inhibition by Bcl-2 and requirement for an organelle fraction enriched in mitochondria. Cell 79: 353-364.

99. Chipuk JE, Moldoveanu T, Llambi F, Parsons MJ, Green DR (2010) The BCL-2 family reunion. Mol Cell 37: 299-310.

100. Tait SW, Green DR (2010) Mitochondria and cell death: outer membrane permeabilization and beyond. Nat Rev Mol Cell Biol 11: 621-632.

101. Youle RJ, Strasser A (2008) The BCL-2 protein family: opposing activities that mediate cell death. Nat Rev Mol Cell Biol 9: 47-59.

102. Zou H, Henzel WJ, Liu X, Lutschg A, Wang X (1997) Apaf-1, a human protein homologous to C. elegans CED-4, participates in cytochrome c-dependent activation of caspase-3. Cell 90: 405-413.

103. Liu X, Kim CN, Yang J, Jemmerson R, Wang X (1996) Induction of apoptotic program in cell-free extracts: requirement for dATP and cytochrome c. Cell 86: 147-157.

104. Acehan D, Jiang X, Morgan DG, Heuser JE, Wang X, Akey CW (2002) Three-dimensional structure of the apoptosome: implications for assembly, procaspase-9 binding, and activation. Mol Cell 9: 423-432.

105. Hao Z, Duncan GS, Chang CC, Elia A, Fang M, Wakeham A, Okada H, Calzascia T, Jang Y, You-Ten A, Yeh WC, Ohashi P, Wang X, Mak TW (2005) Specific ablation of the apoptotic functions of cytochrome C reveals a differential requirement for cytochrome C and Apaf-1 in apoptosis. Cell 121: 579-591.

106. Zhou P, Chou J, Olea RS, Yuan J, Wagner G (1999) Solution structure of Apaf-1 CARD and its interaction with caspase-9 CARD: a structural basis for specific adaptor/caspase interaction. Proc Natl Acad Sci U S A 96: 11265-11270.

107. Renatus M, Stennicke HR, Scott FL, Liddington RC, Salvesen GS (2001) Dimer formation drives the activation of the cell death protease caspase 9. Proc Natl Acad Sci U S A 98: 14250-14255.

108. Pop C, Timmer J, Sperandio S, Salvesen GS (2006) The apoptosome activates caspase-9 by dimerization. Mol Cell 22: 269-275.

109. Li K, Li Y, Shelton JM, Richardson JA, Spencer E, Chen ZJ, Wang X, Williams RS (2000) Cytochrome c deficiency causes embryonic lethality and attenuates stress-induced apoptosis. Cell 101: 389-399.

110. Vaux DL, Silke J (2003) Mammalian mitochondrial IAP binding proteins. Biochem Biophys Res Commun 304: 499-504.

111. Eckelman BP, Salvesen GS, Scott FL (2006) Human inhibitor of apoptosis proteins: why XIAP is the black sheep of the family. EMBO Rep 7: 988-994.

112. Suzuki Y, Imai Y, Nakayama H, Takahashi K, Takio K, Takahashi R (2001) A serine protease, HtrA2, is released from the mitochondria and interacts with XIAP, inducing cell death. Mol Cell 8: 613-621.

113. Verhagen AM, Ekert PG, Pakusch M, Silke J, Connolly LM, Reid GE, Moritz RL, Simpson RJ, Vaux DL (2000) Identification of DIABLO, a mammalian protein that promotes apoptosis by binding to and antagonizing IAP proteins. Cell 102: 43-53.

114. Du C, Fang M, Li Y, Li L, Wang X (2000) Smac, a mitochondrial protein that promotes cytochrome c-dependent caspase activation by eliminating IAP inhibition. Cell 102: 33-42.

115. Li LY, Luo X, Wang X (2001) Endonuclease G is an apoptotic DNase when released from mitochondria. Nature 412: 95-99.

116. Daugas E, Susin SA, Zamzami N, Ferri KF, Irinopoulou T, Larochette N, Prevost MC, Leber B, Andrews D, Penninger J, Kroemer G (2000) Mitochondrio-nuclear translocation of AIF in apoptosis and necrosis. FASEB J 14: 729-739.

117. Scaffidi C, Fulda S, Srinivasan A, Friesen C, Li F, Tomaselli KJ, Debatin KM, Krammer PH, Peter ME (1998) Two CD95 (APO-1/Fas) signaling pathways. Embo J 17: 1675-1687.

118. Jost PJ, Grabow S, Gray D, McKenzie MD, Nachbur U, Huang DC, Bouillet P, Thomas HE, Borner C, Silke J, Strasser A, Kaufmann T (2009) XIAP discriminates between type I and type II FAS-induced apoptosis. Nature 460: 1035-1039.

119. Gray MW, Burger G, Lang BF (1999) Mitochondrial evolution. Science 283: 1476-1481.

120. Brown JR, Doolittle WF (1997) Archaea and the prokaryote-to-eukaryote transition. Microbiol Mol Biol Rev 61: 456-502.

121. Martin W, Muller M (1998) The hydrogen hypothesis for the first eukaryote. Nature 392: 37-41.

122. Burger G, Gray MW, Lang BF (2003) Mitochondrial genomes: anything goes. Trends Genet 19: 709-716.

123. Taanman JW (1999) The mitochondrial genome: structure, transcription, translation and replication. Biochim Biophys Acta 1410: 103-123.

124. Krishnan KJ, Turnbull DM (2010) Mitochondrial DNA and genetic disease. Essays Biochem 47: 139-151.

125. Malka F, Lombes A, Rojo M (2006) Organization, dynamics and transmission of mitochondrial DNA: focus on vertebrate nucleoids. Biochim Biophys Acta 1763: 463-472.

126. Herrmann JM (2003) Converting bacteria to organelles: evolution of mitochondrial protein sorting. Trends Microbiol 11: 74-79.

127. Rehling P, Pfanner N, Meisinger C (2003) Insertion of hydrophobic membrane proteins into the inner mitochondrial membrane--a guided tour. J Mol Biol 326: 639-657.

128. Rich PR, Marechal A (2010) The mitochondrial respiratory chain. Essays Biochem 47: 1-23.

129. Saraste M (1999) Oxidative phosphorylation at the fin de siecle. Science 283: 1488-1493.

130. Fawcett D (1981) Mitochondria. The Cell. 2nd ed. Munich, Germany: W.B. Saunders Company.

131. Frey TG, Mannella CA (2000) The internal structure of mitochondria. Trends Biochem Sci 25: 319-324.

132. Mannella CA (2006) The relevance of mitochondrial membrane topology to mitochondrial function. Biochim Biophys Acta 1762: 140-147.

133. Shoshan-Barmatz V, De Pinto V, Zweckstetter M, Raviv Z, Keinan N, Arbel N (2010) VDAC, a multi-functional mitochondrial protein regulating cell life and death. Mol Aspects Med 31: 227-285.

134. Shoshan-Barmatz V, Gincel D (2003) The voltage-dependent anion channel: characterization, modulation, and role in mitochondrial function in cell life and death. Cell Biochem Biophys 39: 279-292.

135. Mitchell P, Moyle J (1965) Evidence discriminating between the chemical and the chemiosmotic mechanisms of electron transport phosphorylation. Nature 208: 1205-1206.

136. Mitchell P, Moyle J (1965) Stoichiometry of proton translocation through the respiratory chain and adenosine triphosphatase systems of rat liver mitochondria. Nature 208: 147-151.

137. Lartigue L, Kushnareva Y, Seong Y, Lin H, Faustin B, Newmeyer DD (2009) Caspase-independent mitochondrial cell death results from loss of respiration, not cytotoxic protein release. Mol Biol Cell 20: 4871-4884.

138. Scott I, Youle RJ (2010) Mitochondrial fission and fusion. Essays Biochem 47: 85-98.

139. Suen DF, Norris KL, Youle RJ (2008) Mitochondrial dynamics and apoptosis. Genes Dev 22: 1577-1590.

140. Olichon A, Emorine LJ, Descoins E, Pelloquin L, Brichese L, Gas N, Guillou E, Delettre C, Valette A, Hamel CP, Ducommun B, Lenaers G, Belenguer P (2002) The human dynamin-related protein OPA1 is anchored to the mitochondrial inner membrane facing the inter-membrane space. FEBS Lett 523: 171-176.

141. Rojo M, Legros F, Chateau D, Lombes A (2002) Membrane topology and mitochondrial targeting of mitofusins, ubiquitous mammalian homologs of the transmembrane GTPase Fzo. J Cell Sci 115: 1663-1674.

142. Santel A, Frank S, Gaume B, Herrler M, Youle RJ, Fuller MT (2003) Mitofusin-1 protein is a generally expressed mediator of mitochondrial fusion in mammalian cells. J Cell Sci 116: 2763-2774.

143. Meeusen S, DeVay R, Block J, Cassidy-Stone A, Wayson S, McCaffery JM, Nunnari J (2006) Mitochondrial inner-membrane fusion and crista maintenance requires the dynamin-related GTPase Mgm1. Cell 127: 383-395.

144. Meeusen S, McCaffery JM, Nunnari J (2004) Mitochondrial fusion intermediates revealed in vitro. Science 305: 1747-1752.

145. Koshiba T, Detmer SA, Kaiser JT, Chen H, McCaffery JM, Chan DC (2004) Structural basis of mitochondrial tethering by mitofusin complexes. Science 305: 858-862.

146. James DI, Parone PA, Mattenberger Y, Martinou JC (2003) hFis1, a novel component of the mammalian mitochondrial fission machinery. J Biol Chem 278: 36373-36379.

147. Yoon Y, Krueger EW, Oswald BJ, McNiven MA (2003) The mitochondrial protein hFis1 regulates mitochondrial fission in mammalian cells through an interaction with the dynamin-like protein DLP1. Mol Cell Biol 23: 5409-5420.

148. Smirnova E, Griparic L, Shurland DL, van der Bliek AM (2001) Dynamin-related protein Drp1 is required for mitochondrial division in mammalian cells. Mol Biol Cell 12: 2245-2256.

149. Smirnova E, Shurland DL, Ryazantsev SN, van der Bliek AM (1998) A human dynamin-related protein controls the distribution of mitochondria. J Cell Biol 143: 351-358.

150. Roux A, Uyhazi K, Frost A, De Camilli P (2006) GTP-dependent twisting of dynamin implicates constriction and tension in membrane fission. Nature 441: 528-531.

151. Danino D, Moon KH, Hinshaw JE (2004) Rapid constriction of lipid bilayers by the mechanochemical enzyme dynamin. J Struct Biol 147: 259-267.

152. Chen H, Detmer SA, Ewald AJ, Griffin EE, Fraser SE, Chan DC (2003) Mitofusins Mfn1 and Mfn2 coordinately regulate mitochondrial fusion and are essential for embryonic development. J Cell Biol 160: 189-200.

153. Ishihara N, Nomura M, Jofuku A, Kato H, Suzuki SO, Masuda K, Otera H, Nakanishi Y, Nonaka I, Goto Y, Taguchi N, Morinaga H, Maeda M, Takayanagi R, Yokota S, Mihara K (2009) Mitochondrial fission factor Drp1 is essential for embryonic development and synapse formation in mice. Nat Cell Biol 11: 958-966.

154. Frank S, Gaume B, Bergmann-Leitner ES, Leitner WW, Robert EG, Catez F, Smith CL, Youle RJ (2001) The role of dynamin-related protein 1, a mediator of mitochondrial fission, in apoptosis. Dev Cell 1: 515-525.

155. Estaquier J, Arnoult D (2007) Inhibiting Drp1-mediated mitochondrial fission selectively prevents the release of cytochrome c during apoptosis. Cell Death Differ 14: 1086-1094.

156. Parone PA, James DI, Da Cruz S, Mattenberger Y, Donze O, Barja F, Martinou JC (2006) Inhibiting the mitochondrial fission machinery does not prevent Bax/Bak-dependent apoptosis. Mol Cell Biol 26: 7397-7408.

157. Scorrano L, Ashiya M, Buttle K, Weiler S, Oakes SA, Mannella CA, Korsmeyer SJ (2002) A distinct pathway remodels mitochondrial cristae and mobilizes cytochrome c during apoptosis. Dev Cell 2: 55-67.

158. Arnoult D, Grodet A, Lee YJ, Estaquier J, Blackstone C (2005) Release of OPA1 during apoptosis participates in the rapid and complete release of cytochrome c and subsequent mitochondrial fragmentation. J Biol Chem 280: 35742-35750.

159. Jourdain A, Martinou JC (2009) Mitochondrial outer-membrane permeabilization and remodelling in apoptosis. Int J Biochem Cell Biol 41: 1884-1889.

160. Martinou JC, Youle RJ (2011) Mitochondria in apoptosis: bcl-2 family members and mitochondrial dynamics. Dev Cell 21: 92-101.
161. Sheridan C, Martin SJ (2010) Mitochondrial fission/fusion dynamics and apoptosis. Mitochondrion 10: 640-648.
162. Zoratti M, Szabo I (1995) The mitochondrial permeability transition. Biochim Biophys Acta 1241: 139-176.
163. Marchetti P, Castedo M, Susin SA, Zamzami N, Hirsch T, Macho A, Haeffner A, Hirsch F, Geuskens M, Kroemer G (1996) Mitochondrial permeability transition is a central coordinating event of apoptosis. J Exp Med 184: 1155-1160.
164. Grimm S, Brdiczka D (2007) The permeability transition pore in cell death. Apoptosis 12: 841-855.
165. Kinnally KW, Peixoto PM, Ryu SY, Dejean LM (2011) Is mPTP the gatekeeper for necrosis, apoptosis, or both? Biochim Biophys Acta 1813: 616-622.
166. Green DR, Kroemer G (2004) The pathophysiology of mitochondrial cell death. Science 305: 626-629.
167. Goldstein JC, Waterhouse NJ, Juin P, Evan GI, Green DR (2000) The coordinate release of cytochrome c during apoptosis is rapid, complete and kinetically invariant. Nat Cell Biol 2: 156-162.
168. Waterhouse NJ, Goldstein JC, von Ahsen O, Schuler M, Newmeyer DD, Green DR (2001) Cytochrome c maintains mitochondrial transmembrane potential and ATP generation after outer mitochondrial membrane permeabilization during the apoptotic process. J Cell Biol 153: 319-328.
169. Kluck RM, Bossy-Wetzel E, Green DR, Newmeyer DD (1997) The release of cytochrome c from mitochondria: a primary site for Bcl-2 regulation of apoptosis. Science 275: 1132-1136.
170. Green D, Kroemer G (1998) The central executioners of apoptosis: caspases or mitochondria? Trends Cell Biol 8: 267-271.
171. Ehrenberg B, Montana V, Wei MD, Wuskell JP, Loew LM (1988) Membrane potential can be determined in individual cells from the nernstian distribution of cationic dyes. Biophys J 53: 785-794.
172. Metivier D, Dallaporta B, Zamzami N, Larochette N, Susin SA, Marzo I, Kroemer G (1998) Cytofluorometric detection of mitochondrial alterations in early CD95/Fas/APO-1-triggered apoptosis of Jurkat T lymphoma cells. Comparison of seven mitochondrion-specific fluorochromes. Immunol Lett 61: 157-163.
173. Wiens M, Krasko A, Muller CI, Muller WE (2000) Molecular evolution of apoptotic pathways: cloning of key domains from sponges (Bcl-2 homology domains and death domains) and their phylogenetic relationships. J Mol Evol 50: 520-531.
174. Wiens M, Diehl-Seifert B, Muller WE (2001) Sponge Bcl-2 homologous protein (BHP2-GC) confers distinct stress resistance to human HEK-293 cells. Cell Death Differ 8: 887-898.
175. Petros AM, Olejniczak ET, Fesik SW (2004) Structural biology of the Bcl-2 family of proteins. Biochim Biophys Acta 1644: 83-94.
176. Reed JC, Doctor KS, Godzik A (2004) The domains of apoptosis: a genomics perspective. Sci STKE 2004: re9.
177. Griffiths GJ, Dubrez L, Morgan CP, Jones NA, Whitehouse J, Corfe BM, Dive C, Hickman JA (1999) Cell damage-induced conformational changes of the pro-apoptotic protein Bak in vivo precede the onset of apoptosis. J Cell Biol 144: 903-914.

178. Hsu YT, Wolter KG, Youle RJ (1997) Cytosol-to-membrane redistribution of Bax and Bcl-X(L) during apoptosis. Proc Natl Acad Sci U S A 94: 3668-3672.
179. Nechushtan A, Smith CL, Hsu YT, Youle RJ (1999) Conformation of the Bax C-terminus regulates subcellular location and cell death. Embo J 18: 2330-2341.
180. Wolter KG, Hsu YT, Smith CL, Nechushtan A, Xi XG, Youle RJ (1997) Movement of Bax from the cytosol to mitochondria during apoptosis. J Cell Biol 139: 1281-1292.
181. Hsu YT, Youle RJ (1997) Nonionic detergents induce dimerization among members of the Bcl-2 family. J Biol Chem 272: 13829-13834.
182. Zhang Z, Zhu W, Lapolla SM, Miao Y, Shao Y, Falcone M, Boreham D, McFarlane N, Ding J, Johnson AE, Zhang XC, Andrews DW, Lin J (2010) Bax forms an oligomer via separate, yet interdependent, surfaces. J Biol Chem 285: 17614-17627.
183. Gavathiotis E, Reyna DE, Davis ML, Bird GH, Walensky LD (2010) BH3-triggered structural reorganization drives the activation of proapoptotic BAX. Mol Cell 40: 481-492.
184. Griffiths GJ, Corfe BM, Savory P, Leech S, Esposti MD, Hickman JA, Dive C (2001) Cellular damage signals promote sequential changes at the N-terminus and BH-1 domain of the pro-apoptotic protein Bak. Oncogene 20: 7668-7676.
185. Dewson G, Kratina T, Sim HW, Puthalakath H, Adams JM, Colman PM, Kluck RM (2008) To trigger apoptosis, Bak exposes its BH3 domain and homodimerizes via BH3:groove interactions. Mol Cell 30: 369-380.
186. Dewson G, Kratina T, Czabotar P, Day CL, Adams JM, Kluck RM (2009) Bak activation for apoptosis involves oligomerization of dimers via their alpha6 helices. Mol Cell 36: 696-703.
187. Antonsson B, Montessuit S, Sanchez B, Martinou JC (2001) Bax is present as a high molecular weight oligomer/complex in the mitochondrial membrane of apoptotic cells. J Biol Chem 276: 11615-11623.
188. Wei MC, Lindsten T, Mootha VK, Weiler S, Gross A, Ashiya M, Thompson CB, Korsmeyer SJ (2000) tBID, a membrane-targeted death ligand, oligomerizes BAK to release cytochrome c. Genes Dev 14: 2060-2071.
189. Lindsten T, Ross AJ, King A, Zong WX, Rathmell JC, Shiels HA, Ulrich E, Waymire KG, Mahar P, Frauwirth K, Chen Y, Wei M, Eng VM, Adelman DM, Simon MC, Ma A, Golden JA, Evan G, Korsmeyer SJ, MacGregor GR, Thompson CB (2000) The combined functions of proapoptotic Bcl-2 family members bak and bax are essential for normal development of multiple tissues. Mol Cell 6: 1389-1399.
190. Wei MC, Zong WX, Cheng EH, Lindsten T, Panoutsakopoulou V, Ross AJ, Roth KA, MacGregor GR, Thompson CB, Korsmeyer SJ (2001) Proapoptotic BAX and BAK: a requisite gateway to mitochondrial dysfunction and death. Science 292: 727-730.
191. Shamas-Din A, Brahmbhatt H, Leber B, Andrews DW (2011) BH3-only proteins: Orchestrators of apoptosis. Biochim Biophys Acta 1813: 508-520.
192. Strasser A (2005) The role of BH3-only proteins in the immune system. Nat Rev Immunol 5: 189-200.
193. Willis SN, Adams JM (2005) Life in the balance: how BH3-only proteins induce apoptosis. Curr Opin Cell Biol 17: 617-625.
194. Hemann MT, Lowe SW (2006) The p53-Bcl-2 connection. Cell Death Differ 13: 1256-1259.

195. Puthalakath H, Strasser A (2002) Keeping killers on a tight leash: transcriptional and post-translational control of the pro-apoptotic activity of BH3-only proteins. Cell Death Differ 9: 505-512.

196. O'Connor L, Strasser A, O'Reilly LA, Hausmann G, Adams JM, Cory S, Huang DC (1998) Bim: a novel member of the Bcl-2 family that promotes apoptosis. Embo J 17: 384-395.

197. O'Reilly LA, Cullen L, Visvader J, Lindeman GJ, Print C, Bath ML, Huang DC, Strasser A (2000) The proapoptotic BH3-only protein bim is expressed in hematopoietic, epithelial, neuronal, and germ cells. Am J Pathol 157: 449-461.

198. Puthalakath H, Huang DC, O'Reilly LA, King SM, Strasser A (1999) The proapoptotic activity of the Bcl-2 family member Bim is regulated by interaction with the dynein motor complex. Mol Cell 3: 287-296.

199. Yin XM (2006) Bid, a BH3-only multi-functional molecule, is at the cross road of life and death. Gene 369: 7-19.

200. Barry M, Heibein JA, Pinkoski MJ, Lee SF, Moyer RW, Green DR, Bleackley RC (2000) Granzyme B short-circuits the need for caspase 8 activity during granule-mediated cytotoxic T-lymphocyte killing by directly cleaving Bid. Mol Cell Biol 20: 3781-3794.

201. Li H, Zhu H, Xu CJ, Yuan J (1998) Cleavage of BID by caspase 8 mediates the mitochondrial damage in the Fas pathway of apoptosis. Cell 94: 491-501.

202. Sutton VR, Davis JE, Cancilla M, Johnstone RW, Ruefli AA, Sedelies K, Browne KA, Trapani JA (2000) Initiation of apoptosis by granzyme B requires direct cleavage of bid, but not direct granzyme B-mediated caspase activation. J Exp Med 192: 1403-1414.

203. Eskes R, Desagher S, Antonsson B, Martinou JC (2000) Bid induces the oligomerization and insertion of Bax into the outer mitochondrial membrane. Mol Cell Biol 20: 929-935.

204. Desagher S, Osen-Sand A, Nichols A, Eskes R, Montessuit S, Lauper S, Maundrell K, Antonsson B, Martinou JC (1999) Bid-induced conformational change of Bax is responsible for mitochondrial cytochrome c release during apoptosis. J Cell Biol 144: 891-901.

205. Kluck RM, Esposti MD, Perkins G, Renken C, Kuwana T, Bossy-Wetzel E, Goldberg M, Allen T, Barber MJ, Green DR, Newmeyer DD (1999) The pro-apoptotic proteins, Bid and Bax, cause a limited permeabilization of the mitochondrial outer membrane that is enhanced by cytosol. J Cell Biol 147: 809-822.

206. Tsujimoto Y, Cossman J, Jaffe E, Croce CM (1985) Involvement of the bcl-2 gene in human follicular lymphoma. Science 228: 1440-1443.

207. Bakhshi A, Jensen JP, Goldman P, Wright JJ, McBride OW, Epstein AL, Korsmeyer SJ (1985) Cloning the chromosomal breakpoint of t(14;18) human lymphomas: clustering around JH on chromosome 14 and near a transcriptional unit on 18. Cell 41: 899-906.

208. Cleary ML, Smith SD, Sklar J (1986) Cloning and structural analysis of cDNAs for bcl-2 and a hybrid bcl-2/immunoglobulin transcript resulting from the t(14;18) translocation. Cell 47: 19-28.

209. Vaux DL, Cory S, Adams JM (1988) Bcl-2 gene promotes haemopoietic cell survival and cooperates with c-myc to immortalize pre-B cells. Nature 335: 440-442.

210. Huang DC, Adams JM, Cory S (1998) The conserved N-terminal BH4 domain of Bcl-2 homologues is essential for inhibition of apoptosis and interaction with CED-4. Embo J 17: 1029-1039.

211. Sugioka R, Shimizu S, Funatsu T, Tamagawa H, Sawa Y, Kawakami T, Tsujimoto Y (2003) BH4-domain peptide from Bcl-xL exerts anti-apoptotic activity in vivo. Oncogene 22: 8432-8440.

212. Nguyen M, Millar DG, Yong VW, Korsmeyer SJ, Shore GC (1993) Targeting of Bcl-2 to the mitochondrial outer membrane by a COOH-terminal signal anchor sequence. J Biol Chem 268: 25265-25268.

213. Krajewski S, Tanaka S, Takayama S, Schibler MJ, Fenton W, Reed JC (1993) Investigation of the subcellular distribution of the bcl-2 oncoprotein: residence in the nuclear envelope, endoplasmic reticulum, and outer mitochondrial membranes. Cancer Res 53: 4701-4714.

214. Akao Y, Otsuki Y, Kataoka S, Ito Y, Tsujimoto Y (1994) Multiple subcellular localization of bcl-2: detection in nuclear outer membrane, endoplasmic reticulum membrane, and mitochondrial membranes. Cancer Res 54: 2468-2471.

215. Yang T, Kozopas KM, Craig RW (1995) The intracellular distribution and pattern of expression of Mcl-1 overlap with, but are not identical to, those of Bcl-2. J Cell Biol 128: 1173-1184.

216. Nijhawan D, Fang M, Traer E, Zhong Q, Gao W, Du F, Wang X (2003) Elimination of Mcl-1 is required for the initiation of apoptosis following ultraviolet irradiation. Genes Dev 17: 1475-1486.

217. Wilson-Annan J, O'Reilly LA, Crawford SA, Hausmann G, Beaumont JG, Parma LP, Chen L, Lackmann M, Lithgow T, Hinds MG, Day CL, Adams JM, Huang DC (2003) Proapoptotic BH3-only proteins trigger membrane integration of prosurvival Bcl-w and neutralize its activity. J Cell Biol 162: 877-887.

218. Leber B, Lin J, Andrews DW (2010) Still embedded together binding to membranes regulates Bcl-2 protein interactions. Oncogene 29: 5221-5230.

219. Chipuk JE, Green DR (2008) How do BCL-2 proteins induce mitochondrial outer membrane permeabilization? Trends Cell Biol 18: 157-164.

220. Lindsay J, Esposti MD, Gilmore AP (2011) Bcl-2 proteins and mitochondria--specificity in membrane targeting for death. Biochim Biophys Acta 1813: 532-539.

221. Schinzel A, Kaufmann T, Borner C (2004) Bcl-2 family members: integrators of survival and death signals in physiology and pathology [corrected]. Biochim Biophys Acta 1644: 95-105.

222. Borgese N, Colombo S, Pedrazzini E (2003) The tale of tail-anchored proteins: coming from the cytosol and looking for a membrane. J Cell Biol 161: 1013-1019.

223. Day CL, Chen L, Richardson SJ, Harrison PJ, Huang DC, Hinds MG (2005) Solution structure of prosurvival Mcl-1 and characterization of its binding by proapoptotic BH3-only ligands. J Biol Chem 280: 4738-4744.

224. Hinds MG, Lackmann M, Skea GL, Harrison PJ, Huang DC, Day CL (2003) The structure of Bcl-w reveals a role for the C-terminal residues in modulating biological activity. EMBO J 22: 1497-1507.

225. Suzuki M, Youle RJ, Tjandra N (2000) Structure of Bax: coregulation of dimer formation and intracellular localization. Cell 103: 645-654.

226. Denisov AY, Madiraju MS, Chen G, Khadir A, Beauparlant P, Attardo G, Shore GC, Gehring K (2003) Solution structure of human BCL-w: modulation of ligand binding by the C-terminal helix. J Biol Chem 278: 21124-21128.

227. Zha J, Weiler S, Oh KJ, Wei MC, Korsmeyer SJ (2000) Posttranslational N-myristoylation of BID as a molecular switch for targeting mitochondria and apoptosis. Science 290: 1761-1765.

228. Schafer B, Quispe J, Choudhary V, Chipuk JE, Ajero TG, Du H, Schneiter R, Kuwana T (2009) Mitochondrial outer membrane proteins assist Bid in Bax-mediated lipidic pore formation. Mol Biol Cell 20: 2276-2285.

229. Hekman M, Albert S, Galmiche A, Rennefahrt UE, Fueller J, Fischer A, Puehringer D, Wiese S, Rapp UR (2006) Reversible membrane interaction of BAD requires two C-terminal lipid binding domains in conjunction with 14-3-3 protein binding. J Biol Chem 281: 17321-17336.

230. Weber A, Paschen SA, Heger K, Wilfling F, Frankenberg T, Bauerschmitt H, Seiffert BM, Kirschnek S, Wagner H, Hacker G (2007) BimS-induced apoptosis requires mitochondrial localization but not interaction with anti-apoptotic Bcl-2 proteins. J Cell Biol 177: 625-636.

231. Petit PX, Dupaigne P, Pariselli F, Gonzalvez F, Etienne F, Rameau C, Bernard S (2009) Interaction of the alpha-helical H6 peptide from the pro-apoptotic protein tBid with cardiolipin. FEBS J 276: 6338-6354.

232. Zaltsman Y, Shachnai L, Yivgi-Ohana N, Schwarz M, Maryanovich M, Houtkooper RH, Vaz FM, De Leonardis F, Fiermonte G, Palmieri F, Gillissen B, Daniel PT, Jimenez E, Walsh S, Koehler CM, Roy SS, Walter L, Hajnoczky G, Gross A (2010) MTCH2/MIMP is a major facilitator of tBID recruitment to mitochondria. Nat Cell Biol 12: 553-562.

233. Grinberg M, Schwarz M, Zaltsman Y, Eini T, Niv H, Pietrokovski S, Gross A (2005) Mitochondrial carrier homolog 2 is a target of tBID in cells signaled to die by tumor necrosis factor alpha. Mol Cell Biol 25: 4579-4590.

234. Aouacheria A, Brunet F, Gouy M (2005) Phylogenomics of life-or-death switches in multicellular animals: Bcl-2, BH3-Only, and BNip families of apoptotic regulators. Mol Biol Evol 22: 2395-2416.

235. Moldoveanu T, Liu Q, Tocilj A, Watson M, Shore G, Gehring K (2006) The X-ray structure of a BAK homodimer reveals an inhibitory zinc binding site. Mol Cell 24: 677-688.

236. Muchmore SW, Sattler M, Liang H, Meadows RP, Harlan JE, Yoon HS, Nettesheim D, Chang BS, Thompson CB, Wong SL, Ng SL, Fesik SW (1996) X-ray and NMR structure of human Bcl-xL, an inhibitor of programmed cell death. Nature 381: 335-341.

237. Petros AM, Medek A, Nettesheim DG, Kim DH, Yoon HS, Swift K, Matayoshi ED, Oltersdorf T, Fesik SW (2001) Solution structure of the antiapoptotic protein bcl-2. Proc Natl Acad Sci U S A 98: 3012-3017.

238. Smits C, Czabotar PE, Hinds MG, Day CL (2008) Structural plasticity underpins promiscuous binding of the prosurvival protein A1. Structure 16: 818-829.

239. Herman MD, Nyman T, Welin M, Lehtio L, Flodin S, Tresaugues L, Kotenyova T, Flores A, Nordlund P (2008) Completing the family portrait of the anti-apoptotic Bcl-2 proteins: crystal structure of human Bfl-1 in complex with Bim. FEBS Lett 582: 3590-3594.

240. Chou JJ, Li H, Salvesen GS, Yuan J, Wagner G (1999) Solution structure of BID, an intracellular amplifier of apoptotic signaling. Cell 96: 615-624.

241. McDonnell JM, Fushman D, Milliman CL, Korsmeyer SJ, Cowburn D (1999) Solution structure of the proapoptotic molecule BID: a structural basis for apoptotic agonists and antagonists. Cell 96: 625-634.

242. Czabotar PE, Lee EF, van Delft MF, Day CL, Smith BJ, Huang DC, Fairlie WD, Hinds MG, Colman PM (2007) Structural insights into the degradation of Mcl-1 induced by BH3 domains. Proc Natl Acad Sci U S A 104: 6217-6222.

243. Day CL, Smits C, Fan FC, Lee EF, Fairlie WD, Hinds MG (2008) Structure of the BH3 domains from the p53-inducible BH3-only proteins Noxa and Puma in complex with Mcl-1. J Mol Biol 380: 958-971.

244. Lama D, Sankararamakrishnan R (2008) Anti-apoptotic Bcl-XL protein in complex with BH3 peptides of pro-apoptotic Bak, Bad, and Bim proteins: comparative molecular dynamics simulations. Proteins 73: 492-514.

245. Sattler M, Liang H, Nettesheim D, Meadows RP, Harlan JE, Eberstadt M, Yoon HS, Shuker SB, Chang BS, Minn AJ, Thompson CB, Fesik SW (1997) Structure of Bcl-xL-Bak peptide complex: recognition between regulators of apoptosis. Science 275: 983-986.

246. Liu X, Dai S, Zhu Y, Marrack P, Kappler JW (2003) The structure of a Bcl-xL/Bim fragment complex: implications for Bim function. Immunity 19: 341-352.

247. Grinberg M, Sarig R, Zaltsman Y, Frumkin D, Grammatikakis N, Reuveny E, Gross A (2002) tBID Homooligomerizes in the mitochondrial membrane to induce apoptosis. J Biol Chem 277: 12237-12245.

248. Schendel SL, Azimov R, Pawlowski K, Godzik A, Kagan BL, Reed JC (1999) Ion channel activity of the BH3 only Bcl-2 family member, BID. J Biol Chem 274: 21932-21936.

249. Hinds MG, Smits C, Fredericks-Short R, Risk JM, Bailey M, Huang DC, Day CL (2007) Bim, Bad and Bmf: intrinsically unstructured BH3-only proteins that undergo a localized conformational change upon binding to prosurvival Bcl-2 targets. Cell Death Differ 14: 128-136.

250. Peng J, Tan C, Roberts GJ, Nikolaeva O, Zhang Z, Lapolla SM, Primorac S, Andrews DW, Lin J (2006) tBid elicits a conformational alteration in membrane-bound Bcl-2 such that it inhibits Bax pore formation. J Biol Chem 281: 35802-35811.

251. Dlugosz PJ, Billen LP, Annis MG, Zhu W, Zhang Z, Lin J, Leber B, Andrews DW (2006) Bcl-2 changes conformation to inhibit Bax oligomerization. EMBO J 25: 2287-2296.

252. Kim PK, Annis MG, Dlugosz PJ, Leber B, Andrews DW (2004) During apoptosis bcl-2 changes membrane topology at both the endoplasmic reticulum and mitochondria. Mol Cell 14: 523-529.

253. Garcia-Saez AJ, Ries J, Orzaez M, Perez-Paya E, Schwille P (2009) Membrane promotes tBID interaction with BCL(XL). Nat Struct Mol Biol 16: 1178-1185.

254. Kuwana T, Bouchier-Hayes L, Chipuk JE, Bonzon C, Sullivan BA, Green DR, Newmeyer DD (2005) BH3 domains of BH3-only proteins differentially regulate Bax-mediated mitochondrial membrane permeabilization both directly and indirectly. Mol Cell 17: 525-535.

255. Kuwana T, Mackey MR, Perkins G, Ellisman MH, Latterich M, Schneiter R, Green DR, Newmeyer DD (2002) Bid, Bax, and lipids cooperate to form supramolecular openings in the outer mitochondrial membrane. Cell 111: 331-342.

256. Letai A, Bassik MC, Walensky LD, Sorcinelli MD, Weiler S, Korsmeyer SJ (2002) Distinct BH3 domains either sensitize or activate mitochondrial apoptosis, serving as prototype cancer therapeutics. Cancer Cell 2: 183-192.

257. Simonen M, Keller H, Heim J (1997) The BH3 domain of Bax is sufficient for interaction of Bax with itself and with other family members and it is required for induction of apoptosis. Eur J Biochem 249: 85-91.

258. Chittenden T, Flemington C, Houghton AB, Ebb RG, Gallo GJ, Elangovan B, Chinnadurai G, Lutz RJ (1995) A conserved domain in Bak, distinct from BH1 and BH2, mediates cell death and protein binding functions. EMBO J 14: 5589-5596.

259. Sedlak TW, Oltvai ZN, Yang E, Wang K, Boise LH, Thompson CB, Korsmeyer SJ (1995) Multiple Bcl-2 family members demonstrate selective dimerizations with Bax. Proc Natl Acad Sci U S A 92: 7834-7838.

260. Yin XM, Oltvai ZN, Korsmeyer SJ (1994) BH1 and BH2 domains of Bcl-2 are required for inhibition of apoptosis and heterodimerization with Bax. Nature 369: 321-323.

261. Kawatani M, Imoto M (2003) Deletion of the BH1 domain of Bcl-2 accelerates apoptosis by acting in a dominant negative fashion. J Biol Chem 278: 19732-19742.

262. Gurudutta GU, Verma YK, Singh VK, Gupta P, Raj HG, Sharma RK, Chandra R (2005) Structural conservation of residues in BH1 and BH2 domains of Bcl-2 family proteins. FEBS Lett 579: 3503-3507.

263. van Delft MF, Huang DC (2006) How the Bcl-2 family of proteins interact to regulate apoptosis. Cell Res 16: 203-213.

264. Chen L, Willis SN, Wei A, Smith BJ, Fletcher JI, Hinds MG, Colman PM, Day CL, Adams JM, Huang DC (2005) Differential targeting of prosurvival Bcl-2 proteins by their BH3-only ligands allows complementary apoptotic function. Mol Cell 17: 393-403.

265. Uren RT, Dewson G, Chen L, Coyne SC, Huang DC, Adams JM, Kluck RM (2007) Mitochondrial permeabilization relies on BH3 ligands engaging multiple prosurvival Bcl-2 relatives, not Bak. J Cell Biol 177: 277-287.

266. Willis SN, Chen L, Dewson G, Wei A, Naik E, Fletcher JI, Adams JM, Huang DC (2005) Proapoptotic Bak is sequestered by Mcl-1 and Bcl-xL, but not Bcl-2, until displaced by BH3-only proteins. Genes Dev 19: 1294-1305.

267. Willis SN, Fletcher JI, Kaufmann T, van Delft MF, Chen L, Czabotar PE, Ierino H, Lee EF, Fairlie WD, Bouillet P, Strasser A, Kluck RM, Adams JM, Huang DC (2007) Apoptosis initiated when BH3 ligands engage multiple Bcl-2 homologs, not Bax or Bak. Science 315: 856-859.

268. Fletcher JI, Meusburger S, Hawkins CJ, Riglar DT, Lee EF, Fairlie WD, Huang DC, Adams JM (2008) Apoptosis is triggered when prosurvival Bcl-2 proteins cannot restrain Bax. Proc Natl Acad Sci U S A 105: 18081-18087.

269. Kim H, Rafiuddin-Shah M, Tu HC, Jeffers JR, Zambetti GP, Hsieh JJ, Cheng EH (2006) Hierarchical regulation of mitochondrion-dependent apoptosis by BCL-2 subfamilies. Nat Cell Biol 8: 1348-1358.

270. Gallenne T, Gautier F, Oliver L, Hervouet E, Noel B, Hickman JA, Geneste O, Cartron PF, Vallette FM, Manon S, Juin P (2009) Bax activation by the BH3-only protein Puma promotes cell dependence on antiapoptotic Bcl-2 family members. J Cell Biol 185: 279-290.

271. Ren D, Tu HC, Kim H, Wang GX, Bean GR, Takeuchi O, Jeffers JR, Zambetti GP, Hsieh JJ, Cheng EH (2010) BID, BIM, and PUMA are essential for activation of the BAX- and BAK-dependent cell death program. Science 330: 1390-1393.

272. Certo M, Del Gaizo Moore V, Nishino M, Wei G, Korsmeyer S, Armstrong SA, Letai A (2006) Mitochondria primed by death signals determine cellular addiction to antiapoptotic BCL-2 family members. Cancer Cell 9: 351-365.

273. Bogner C, Leber B, Andrews DW (2010) Apoptosis: embedded in membranes. Curr Opin Cell Biol 22: 845-851.

274. Leber B, Lin J, Andrews DW (2007) Embedded together: the life and death consequences of interaction of the Bcl-2 family with membranes. Apoptosis 12: 897-911.

275. Billen LP, Kokoski CL, Lovell JF, Leber B, Andrews DW (2008) Bcl-XL inhibits membrane permeabilization by competing with Bax. PLoS Biol 6: e147.

276. Lovell JF, Billen LP, Bindner S, Shamas-Din A, Fradin C, Leber B, Andrews DW (2008) Membrane binding by tBid initiates an ordered series of events culminating in membrane permeabilization by Bax. Cell 135: 1074-1084.

277. Billen LP, Shamas-Din A, Andrews DW (2008) Bid: a Bax-like BH3 protein. Oncogene 27 Suppl 1: S93-104.

278. Merino D, Giam M, Hughes PD, Siggs OM, Heger K, O'Reilly LA, Adams JM, Strasser A, Lee EF, Fairlie WD, Bouillet P (2009) The role of BH3-only protein Bim extends beyond inhibiting Bcl-2-like prosurvival proteins. J Cell Biol 186: 355-362.

279. Gavathiotis E, Suzuki M, Davis ML, Pitter K, Bird GH, Katz SG, Tu HC, Kim H, Cheng EH, Tjandra N, Walensky LD (2008) BAX activation is initiated at a novel interaction site. Nature 455: 1076-1081.

280. Edlich F, Banerjee S, Suzuki M, Cleland MM, Arnoult D, Wang C, Neutzner A, Tjandra N, Youle RJ (2011) Bcl-x(L) retrotranslocates Bax from the mitochondria into the cytosol. Cell 145: 104-116.

281. Hsu YT, Youle RJ (1998) Bax in murine thymus is a soluble monomeric protein that displays differential detergent-induced conformations. J Biol Chem 273: 10777-10783.

282. Kim H, Tu HC, Ren D, Takeuchi O, Jeffers JR, Zambetti GP, Hsieh JJ, Cheng EH (2009) Stepwise activation of BAX and BAK by tBID, BIM, and PUMA initiates mitochondrial apoptosis. Mol Cell 36: 487-499.

283. Ruffolo SC, Shore GC (2003) BCL-2 selectively interacts with the BID-induced open conformer of BAK, inhibiting BAK auto-oligomerization. J Biol Chem 278: 25039-25045.

284. Dai H, Smith A, Meng XW, Schneider PA, Pang YP, Kaufmann SH (2011) Transient binding of an activator BH3 domain to the Bak BH3-binding groove initiates Bak oligomerization. J Cell Biol 194: 39-48.

285. Oh KJ, Singh P, Lee K, Foss K, Lee S, Park M, Aluvila S, Kim RS, Symersky J, Walters DE (2010) Conformational changes in BAK, a pore-forming proapoptotic Bcl-2 family member, upon membrane insertion and direct evidence for the existence of BH3-BH3 contact interface in BAK homo-oligomers. J Biol Chem 285: 28924-28937.

286. Dewson G, Kluck RM (2009) Mechanisms by which Bak and Bax permeabilise mitochondria during apoptosis. J Cell Sci 122: 2801-2808.

287. Akgul C (2009) Mcl-1 is a potential therapeutic target in multiple types of cancer. Cell Mol Life Sci 66: 1326-1336.

288. Warr MR, Shore GC (2008) Unique biology of Mcl-1: therapeutic opportunities in cancer. Curr Mol Med 8: 138-147.

289. Leu JI, Dumont P, Hafey M, Murphy ME, George DL (2004) Mitochondrial p53 activates Bak and causes disruption of a Bak-Mcl1 complex. Nat Cell Biol 6: 443-450.

290. Cheng EH, Sheiko TV, Fisher JK, Craigen WJ, Korsmeyer SJ (2003) VDAC2 inhibits BAK activation and mitochondrial apoptosis. Science 301: 513-517.

291. Lazarou M, Stojanovski D, Frazier AE, Kotevski A, Dewson G, Craigen WJ, Kluck RM, Vaux DL, Ryan MT (2010) Inhibition of Bak activation by VDAC2 is dependent on the Bak transmembrane anchor. J Biol Chem 285: 36876-36883.

292. Roy SS, Ehrlich AM, Craigen WJ, Hajnoczky G (2009) VDAC2 is required for truncated BID-induced mitochondrial apoptosis by recruiting BAK to the mitochondria. EMBO Rep 10: 1341-1347.

293. Setoguchi K, Otera H, Mihara K (2006) Cytosolic factor- and TOM-independent import of C-tail-anchored mitochondrial outer membrane proteins. EMBO J 25: 5635-5647.

294. Baines CP, Kaiser RA, Sheiko T, Craigen WJ, Molkentin JD (2007) Voltage-dependent anion channels are dispensable for mitochondrial-dependent cell death. Nat Cell Biol 9: 550-555.

295. Pagliari LJ, Kuwana T, Bonzon C, Newmeyer DD, Tu S, Beere HM, Green DR (2005) The multidomain proapoptotic molecules Bax and Bak are directly activated by heat. Proc Natl Acad Sci U S A 102: 17975-17980.

296. Liu Q, Gehring K (2010) Heterodimerization of BAK and MCL-1 activated by detergent micelles. J Biol Chem 285: 41202-41210.

297. George NM, Evans JJ, Luo X (2007) A three-helix homo-oligomerization domain containing BH3 and BH1 is responsible for the apoptotic activity of Bax. Genes Dev 21: 1937-1948.

298. Munoz-Pinedo C, Guio-Carrion A, Goldstein JC, Fitzgerald P, Newmeyer DD, Green DR (2006) Different mitochondrial intermembrane space proteins are released during apoptosis in a manner that is coordinately initiated but can vary in duration. Proc Natl Acad Sci U S A 103: 11573-11578.

299. Chipuk JE, Bouchier-Hayes L, Green DR (2006) Mitochondrial outer membrane permeabilization during apoptosis: the innocent bystander scenario. Cell Death Differ 13: 1396-1402.

300. Yuan S, Fu Y, Wang X, Shi H, Huang Y, Song X, Li L, Song N, Luo Y (2008) Voltage-dependent anion channel 1 is involved in endostatin-induced endothelial cell apoptosis. FASEB J 22: 2809-2820.

301. Tomasello F, Messina A, Lartigue L, Schembri L, Medina C, Reina S, Thoraval D, Crouzet M, Ichas F, De Pinto V, De Giorgi F (2009) Outer membrane VDAC1 controls permeability transition of the inner mitochondrial membrane in cellulo during stress-induced apoptosis. Cell Res 19: 1363-1376.

302. Tajeddine N, Galluzzi L, Kepp O, Hangen E, Morselli E, Senovilla L, Araujo N, Pinna G, Larochette N, Zamzami N, Modjtahedi N, Harel-Bellan A, Kroemer G (2008) Hierarchical involvement of Bak, VDAC1 and Bax in cisplatin-induced cell death. Oncogene 27: 4221-4232.

303. Vander Heiden MG, Chandel NS, Li XX, Schumacker PT, Colombini M, Thompson CB (2000) Outer mitochondrial membrane permeability can regulate coupled respiration and cell survival. Proc Natl Acad Sci U S A 97: 4666-4671.

304. Feldmann G, Haouzi D, Moreau A, Durand-Schneider AM, Bringuier A, Berson A, Mansouri A, Fau D, Pessayre D (2000) Opening of the mitochondrial permeability transition pore causes matrix expansion and outer membrane rupture in Fas-mediated hepatic apoptosis in mice. Hepatology 31: 674-683.

305. Vander Heiden MG, Li XX, Gottleib E, Hill RB, Thompson CB, Colombini M (2001) Bcl-xL promotes the open configuration of the voltage-dependent anion channel and metabolite passage through the outer mitochondrial membrane. J Biol Chem 276: 19414-19419.

306. Shimizu S, Narita M, Tsujimoto Y (1999) Bcl-2 family proteins regulate the release of apoptogenic cytochrome c by the mitochondrial channel VDAC. Nature 399: 483-487.

307. Tsujimoto Y, Shimizu S (2000) VDAC regulation by the Bcl-2 family of proteins. Cell Death Differ 7: 1174-1181.

308. Zalk R, Israelson A, Garty ES, Azoulay-Zohar H, Shoshan-Barmatz V (2005) Oligomeric states of the voltage-dependent anion channel and cytochrome c release from mitochondria. Biochem J 386: 73-83.

309. Keinan N, Tyomkin D, Shoshan-Barmatz V (2010) Oligomerization of the mitochondrial protein voltage-dependent anion channel is coupled to the induction of apoptosis. Mol Cell Biol 30: 5698-5709.

310. Bernardi P (1999) Mitochondrial transport of cations: channels, exchangers, and permeability transition. Physiol Rev 79: 1127-1155.

311. Tsujimoto Y, Shimizu S (2007) Role of the mitochondrial membrane permeability transition in cell death. Apoptosis 12: 835-840.

312. Yamagata H, Shimizu S, Nishida Y, Watanabe Y, Craigen WJ, Tsujimoto Y (2009) Requirement of voltage-dependent anion channel 2 for pro-apoptotic activity of Bax. Oncogene 28: 3563-3572.

313. Moroy G, Martin E, Dejaegere A, Stote RH (2009) Molecular basis for Bcl-2 homology 3 domain recognition in the Bcl-2 protein family: identification of conserved hot spot interactions. J Biol Chem 284: 17499-17511.

314. Marzo I, Brenner C, Zamzami N, Susin SA, Beutner G, Brdiczka D, Remy R, Xie ZH, Reed JC, Kroemer G (1998) The permeability transition pore complex: a target for apoptosis regulation by caspases and bcl-2-related proteins. J Exp Med 187: 1261-1271.

315. Shimizu S, Konishi A, Kodama T, Tsujimoto Y (2000) BH4 domain of antiapoptotic Bcl-2 family members closes voltage-dependent anion channel and inhibits apoptotic mitochondrial changes and cell death. Proc Natl Acad Sci U S A 97: 3100-3105.

316. Zheng Y, Shi Y, Tian C, Jiang C, Jin H, Chen J, Almasan A, Tang H, Chen Q (2004) Essential role of the voltage-dependent anion channel (VDAC) in mitochondrial permeability transition pore opening and cytochrome c release induced by arsenic trioxide. Oncogene 23: 1239-1247.

317. Kokoszka JE, Waymire KG, Levy SE, Sligh JE, Cai J, Jones DP, MacGregor GR, Wallace DC (2004) The ADP/ATP translocator is not essential for the mitochondrial permeability transition pore. Nature 427: 461-465.

318. Kim TH, Zhao Y, Barber MJ, Kuharsky DK, Yin XM (2000) Bid-induced cytochrome c release is mediated by a pathway independent of mitochondrial permeability transition pore and Bax. J Biol Chem 275: 39474-39481.

319. Eskes R, Antonsson B, Osen-Sand A, Montessuit S, Richter C, Sadoul R, Mazzei G, Nichols A, Martinou JC (1998) Bax-induced cytochrome C release from mitochondria is independent of the permeability transition pore but highly dependent on Mg2+ ions. J Cell Biol 143: 217-224.

320. Choe S, Bennett MJ, Fujii G, Curmi PM, Kantardjieff KA, Collier RJ, Eisenberg D (1992) The crystal structure of diphtheria toxin. Nature 357: 216-222.

321. Saito M, Korsmeyer SJ, Schlesinger PH (2000) BAX-dependent transport of cytochrome c reconstituted in pure liposomes. Nat Cell Biol 2: 553-555.

322. Schendel SL, Xie Z, Montal MO, Matsuyama S, Montal M, Reed JC (1997) Channel formation by antiapoptotic protein Bcl-2. Proc Natl Acad Sci U S A 94: 5113-5118.

323. Schlesinger PH, Gross A, Yin XM, Yamamoto K, Saito M, Waksman G, Korsmeyer SJ (1997) Comparison of the ion channel characteristics of proapoptotic BAX and antiapoptotic BCL-2. Proc Natl Acad Sci U S A 94: 11357-11362.

324. Minn AJ, Velez P, Schendel SL, Liang H, Muchmore SW, Fesik SW, Fill M, Thompson CB (1997) Bcl-x(L) forms an ion channel in synthetic lipid membranes. Nature 385: 353-357.

325. Antonsson B, Conti F, Ciavatta A, Montessuit S, Lewis S, Martinou I, Bernasconi L, Bernard A, Mermod JJ, Mazzei G, Maundrell K, Gambale F, Sadoul R, Martinou JC (1997) Inhibition of Bax channel-forming activity by Bcl-2. Science 277: 370-372.

326. Annis MG, Soucie EL, Dlugosz PJ, Cruz-Aguado JA, Penn LZ, Leber B, Andrews DW (2005) Bax forms multispanning monomers that oligomerize to permeabilize membranes during apoptosis. EMBO J 24: 2096-2103.

327. Terrones O, Etxebarria A, Landajuela A, Landeta O, Antonsson B, Basanez G (2008) BIM and tBID are not mechanistically equivalent when assisting BAX to permeabilize bilayer membranes. J Biol Chem 283: 7790-7803.

328. Ross K, Rudel T, Kozjak-Pavlovic V (2009) TOM-independent complex formation of Bax and Bak in mammalian mitochondria during TNFalpha-induced apoptosis. Cell Death Differ 16: 697-707.

329. Nechushtan A, Smith CL, Lamensdorf I, Yoon SH, Youle RJ (2001) Bax and Bak coalesce into novel mitochondria-associated clusters during apoptosis. J Cell Biol 153: 1265-1276.

330. Zhou L, Chang DC (2008) Dynamics and structure of the Bax-Bak complex responsible for releasing mitochondrial proteins during apoptosis. J Cell Sci 121: 2186-2196.

331. Dejean LM, Martinez-Caballero S, Guo L, Hughes C, Teijido O, Ducret T, Ichas F, Korsmeyer SJ, Antonsson B, Jonas EA, Kinnally KW (2005) Oligomeric Bax is a component of the putative cytochrome c release channel MAC, mitochondrial apoptosis-induced channel. Mol Biol Cell 16: 2424-2432.

332. Kinnally KW, Antonsson B (2007) A tale of two mitochondrial channels, MAC and PTP, in apoptosis. Apoptosis 12: 857-868.

333. Martinez-Caballero S, Dejean LM, Kinnally MS, Oh KJ, Mannella CA, Kinnally KW (2009) Assembly of the mitochondrial apoptosis-induced channel, MAC. J Biol Chem 284: 12235-12245.

334. Dejean LM, Martinez-Caballero S, Kinnally KW (2006) Is MAC the knife that cuts cytochrome c from mitochondria during apoptosis? Cell Death Differ 13: 1387-1395.

335. Dejean LM, Martinez-Caballero S, Manon S, Kinnally KW (2006) Regulation of the mitochondrial apoptosis-induced channel, MAC, by BCL-2 family proteins. Biochim Biophys Acta 1762: 191-201.

336. Westphal D, Dewson G, Czabotar PE, Kluck RM (2011) Molecular biology of Bax and Bak activation and action. Biochim Biophys Acta 1813: 521-531.

337. Basanez G, Nechushtan A, Drozhinin O, Chanturiya A, Choe E, Tutt S, Wood KA, Hsu Y, Zimmerberg J, Youle RJ (1999) Bax, but not Bcl-xL, decreases the lifetime of planar phospholipid bilayer membranes at subnanomolar concentrations. Proc Natl Acad Sci U S A 96: 5492-5497.

338. Basanez G, Sharpe JC, Galanis J, Brandt TB, Hardwick JM, Zimmerberg J (2002) Bax-type apoptotic proteins porate pure lipid bilayers through a mechanism sensitive to intrinsic monolayer curvature. J Biol Chem 277: 49360-49365.

339. Hardwick JM, Polster BM (2002) Bax, along with lipid conspirators, allows cytochrome c to escape mitochondria. Mol Cell 10: 963-965.

340. Terrones O, Antonsson B, Yamaguchi H, Wang HG, Liu J, Lee RM, Herrmann A, Basanez G (2004) Lipidic pore formation by the concerted action of proapoptotic BAX and tBID. J Biol Chem 279: 30081-30091.

341. Karbowski M, Lee YJ, Gaume B, Jeong SY, Frank S, Nechushtan A, Santel A, Fuller M, Smith CL, Youle RJ (2002) Spatial and temporal association of Bax with mitochondrial fission sites, Drp1, and Mfn2 during apoptosis. J Cell Biol 159: 931-938.

342. Montessuit S, Somasekharan SP, Terrones O, Lucken-Ardjomande S, Herzig S, Schwarzenbacher R, Manstein DJ, Bossy-Wetzel E, Basanez G, Meda P, Martinou JC (2010) Membrane remodeling induced by the dynamin-related protein Drp1 stimulates Bax oligomerization. Cell 142: 889-901.

343. Brooks C, Wei Q, Feng L, Dong G, Tao Y, Mei L, Xie ZJ, Dong Z (2007) Bak regulates mitochondrial morphology and pathology during apoptosis by interacting with mitofusins. Proc Natl Acad Sci U S A 104: 11649-11654.

344. Arnoult D, Rismanchi N, Grodet A, Roberts RG, Seeburg DP, Estaquier J, Sheng M, Blackstone C (2005) Bax/Bak-dependent release of DDP/TIMM8a promotes Drp1-mediated mitochondrial fission and mitoptosis during programmed cell death. Curr Biol 15: 2112-2118.

345. Rolland SG, Conradt B (2010) New role of the BCL2 family of proteins in the regulation of mitochondrial dynamics. Curr Opin Cell Biol 22: 852-858.

346. Autret A, Martin SJ (2010) Bcl-2 family proteins and mitochondrial fission/fusion dynamics. Cell Mol Life Sci 67: 1599-1606.

347. Karbowski M, Norris KL, Cleland MM, Jeong SY, Youle RJ (2006) Role of Bax and Bak in mitochondrial morphogenesis. Nature 443: 658-662.

348. Karbowski M, Arnoult D, Chen H, Chan DC, Smith CL, Youle RJ (2004) Quantitation of mitochondrial dynamics by photolabeling of individual organelles shows that mitochondrial fusion is blocked during the Bax activation phase of apoptosis. J Cell Biol 164: 493-499.

349. Yamaguchi R, Lartigue L, Perkins G, Scott RT, Dixit A, Kushnareva Y, Kuwana T, Ellisman MH, Newmeyer DD (2008) Opa1-mediated cristae opening is Bax/Bak and BH3 dependent, required for apoptosis, and independent of Bak oligomerization. Mol Cell 31: 557-569.

350. Kozopas KM, Yang T, Buchan HL, Zhou P, Craig RW (1993) MCL1, a gene expressed in programmed myeloid cell differentiation, has sequence similarity to BCL2. Proc Natl Acad Sci U S A 90: 3516-3520.

351. Bae J, Leo CP, Hsu SY, Hsueh AJ (2000) MCL-1S, a splicing variant of the antiapoptotic BCL-2 family member MCL-1, encodes a proapoptotic protein possessing only the BH3 domain. J Biol Chem 275: 25255-25261.

352. Bingle CD, Craig RW, Swales BM, Singleton V, Zhou P, Whyte MK (2000) Exon skipping in Mcl-1 results in a bcl-2 homology domain 3 only gene product that promotes cell death. J Biol Chem 275: 22136-22146.

353. Puthalakath H, Villunger A, O'Reilly LA, Beaumont JG, Coultas L, Cheney RE, Huang DC, Strasser A (2001) Bmf: a proapoptotic BH3-only protein regulated by interaction with the myosin V actin motor complex, activated by anoikis. Science 293: 1829-1832.

354. Cuconati A, Mukherjee C, Perez D, White E (2003) DNA damage response and MCL-1 destruction initiate apoptosis in adenovirus-infected cells. Genes Dev 17: 2922-2932.

355. Clem RJ, Cheng EH, Karp CL, Kirsch DG, Ueno K, Takahashi A, Kastan MB, Griffin DE, Earnshaw WC, Veliuona MA, Hardwick JM (1998) Modulation of cell death by Bcl-XL through caspase interaction. Proc Natl Acad Sci U S A 95: 554-559.

356. Cheng EH, Kirsch DG, Clem RJ, Ravi R, Kastan MB, Bedi A, Ueno K, Hardwick JM (1997) Conversion of Bcl-2 to a Bax-like death effector by caspases. Science 278: 1966-1968.

357. Datta SR, Dudek H, Tao X, Masters S, Fu H, Gotoh Y, Greenberg ME (1997) Akt phosphorylation of BAD couples survival signals to the cell-intrinsic death machinery. Cell 91: 231-241.

358. Datta SR, Katsov A, Hu L, Petros A, Fesik SW, Yaffe MB, Greenberg ME (2000) 14-3-3 proteins and survival kinases cooperate to inactivate BAD by BH3 domain phosphorylation. Mol Cell 6: 41-51.

359. Breitschopf K, Haendeler J, Malchow P, Zeiher AM, Dimmeler S (2000) Posttranslational modification of Bcl-2 facilitates its proteasome-dependent degradation: molecular characterization of the involved signaling pathway. Mol Cell Biol 20: 1886-1896.

360. Ito T, Deng X, Carr B, May WS (1997) Bcl-2 phosphorylation required for anti-apoptosis function. J Biol Chem 272: 11671-11673.

361. May WS, Tyler PG, Ito T, Armstrong DK, Qatsha KA, Davidson NE (1994) Interleukin-3 and bryostatin-1 mediate hyperphosphorylation of BCL2 alpha in association with suppression of apoptosis. J Biol Chem 269: 26865-26870.

362. Haldar S, Jena N, Croce CM (1995) Inactivation of Bcl-2 by phosphorylation. Proc Natl Acad Sci U S A 92: 4507-4511.

363. Ojala PM, Yamamoto K, Castanos-Velez E, Biberfeld P, Korsmeyer SJ, Makela TP (2000) The apoptotic v-cyclin-CDK6 complex phosphorylates and inactivates Bcl-2. Nat Cell Biol 2: 819-825.

364. Haldar S, Chintapalli J, Croce CM (1996) Taxol induces bcl-2 phosphorylation and death of prostate cancer cells. Cancer Res 56: 1253-1255.

365. Becker EB, Howell J, Kodama Y, Barker PA, Bonni A (2004) Characterization of the c-Jun N-terminal kinase-BimEL signaling pathway in neuronal apoptosis. J Neurosci 24: 8762-8770.

366. Putcha GV, Le S, Frank S, Besirli CG, Clark K, Chu B, Alix S, Youle RJ, LaMarche A, Maroney AC, Johnson EM, Jr. (2003) JNK-mediated BIM phosphorylation potentiates BAX-dependent apoptosis. Neuron 38: 899-914.

367. Ewings KE, Hadfield-Moorhouse K, Wiggins CM, Wickenden JA, Balmanno K, Gilley R, Degenhardt K, White E, Cook SJ (2007) ERK1/2-dependent phosphorylation of BimEL promotes its rapid dissociation from Mcl-1 and Bcl-xL. EMBO J 26: 2856-2867.

368. Ley R, Balmanno K, Hadfield K, Weston C, Cook SJ (2003) Activation of the ERK1/2 signaling pathway promotes phosphorylation and proteasome-dependent degradation of the BH3-only protein, Bim. J Biol Chem 278: 18811-18816.

369. Ley R, Hadfield K, Howes E, Cook SJ (2005) Identification of a DEF-type docking domain for extracellular signal-regulated kinases 1/2 that directs phosphorylation and turnover of the BH3-only protein BimEL. J Biol Chem 280: 17657-17663.

370. Luciano F, Jacquel A, Colosetti P, Herrant M, Cagnol S, Pages G, Auberger P (2003) Phosphorylation of Bim-EL by Erk1/2 on serine 69 promotes its degradation via the proteasome pathway and regulates its proapoptotic function. Oncogene 22: 6785-6793.

371. Weissman AM (2001) Themes and variations on ubiquitylation. Nat Rev Mol Cell Biol 2: 169-178.

372. Hershko A, Ciechanover A (1998) The ubiquitin system. Annu Rev Biochem 67: 425-479.

373. Hoeller D, Hecker CM, Dikic I (2006) Ubiquitin and ubiquitin-like proteins in cancer pathogenesis. Nat Rev Cancer 6: 776-788.

374. Goldstein G, Scheid M, Hammerling U, Schlesinger DH, Niall HD, Boyse EA (1975) Isolation of a polypeptide that has lymphocyte-differentiating properties and is probably represented universally in living cells. Proc Natl Acad Sci U S A 72: 11-15.

375. Ciechanover A, Heller H, Elias S, Haas AL, Hershko A (1980) ATP-dependent conjugation of reticulocyte proteins with the polypeptide required for protein degradation. Proc Natl Acad Sci U S A 77: 1365-1368.

376. Hershko A, Ciechanover A, Heller H, Haas AL, Rose IA (1980) Proposed role of ATP in protein breakdown: conjugation of protein with multiple chains of the polypeptide of ATP-dependent proteolysis. Proc Natl Acad Sci U S A 77: 1783-1786.

377. Li W, Bengtson MH, Ulbrich A, Matsuda A, Reddy VA, Orth A, Chanda SK, Batalov S, Joazeiro CA (2008) Genome-wide and functional annotation of human E3 ubiquitin ligases identifies MULAN, a mitochondrial E3 that regulates the organelle's dynamics and signaling. PLoS One 3: e1487.

378. Reyes-Turcu FE, Ventii KH, Wilkinson KD (2009) Regulation and cellular roles of ubiquitin-specific deubiquitinating enzymes. Annu Rev Biochem 78: 363-397.

379. Ikeda F, Dikic I (2008) Atypical ubiquitin chains: new molecular signals. 'Protein Modifications: Beyond the Usual Suspects' review series. EMBO Rep 9: 536-542.

380. Peng J, Schwartz D, Elias JE, Thoreen CC, Cheng D, Marsischky G, Roelofs J, Finley D, Gygi SP (2003) A proteomics approach to understanding protein ubiquitination. Nat Biotechnol 21: 921-926.

381. Komander D (2009) The emerging complexity of protein ubiquitination. Biochem Soc Trans 37: 937-953.

382. Schrader EK, Harstad KG, Matouschek A (2009) Targeting proteins for degradation. Nat Chem Biol 5: 815-822.

383. Yang WL, Zhang X, Lin HK (2010) Emerging role of Lys-63 ubiquitination in protein kinase and phosphatase activation and cancer development. Oncogene 29: 4493-4503.

384. Scheffner M, Huibregtse JM, Vierstra RD, Howley PM (1993) The HPV-16 E6 and E6-AP complex functions as a ubiquitin-protein ligase in the ubiquitination of p53. Cell 75: 495-505.

385. Huibregtse JM, Scheffner M, Beaudenon S, Howley PM (1995) A family of proteins structurally and functionally related to the E6-AP ubiquitin-protein ligase. Proc Natl Acad Sci U S A 92: 5249.

386. Deshaies RJ, Joazeiro CA (2009) RING domain E3 ubiquitin ligases. Annu Rev Biochem 78: 399-434.

387. Freemont PS (2000) RING for destruction? Curr Biol 10: R84-87.

388. Suzuki Y, Nakabayashi Y, Takahashi R (2001) Ubiquitin-protein ligase activity of X-linked inhibitor of apoptosis protein promotes proteasomal degradation of caspase-3 and enhances its anti-apoptotic effect in Fas-induced cell death. Proc Natl Acad Sci U S A 98: 8662-8667.

389. Petroski MD, Deshaies RJ (2005) Function and regulation of cullin-RING ubiquitin ligases. Nat Rev Mol Cell Biol 6: 9-20.

390. Pintard L, Willems A, Peter M (2004) Cullin-based ubiquitin ligases: Cul3-BTB complexes join the family. EMBO J 23: 1681-1687.

391. Zimmerman ES, Schulman BA, Zheng N (2010) Structural assembly of cullin-RING ubiquitin ligase complexes. Curr Opin Struct Biol 20: 714-721.

392. Cardozo T, Pagano M (2004) The SCF ubiquitin ligase: insights into a molecular machine. Nat Rev Mol Cell Biol 5: 739-751.

393. Ohta T, Michel JJ, Schottelius AJ, Xiong Y (1999) ROC1, a homolog of APC11, represents a family of cullin partners with an associated ubiquitin ligase activity. Mol Cell 3: 535-541.

394. Tan P, Fuchs SY, Chen A, Wu K, Gomez C, Ronai Z, Pan ZQ (1999) Recruitment of a ROC1-CUL1 ubiquitin ligase by Skp1 and HOS to catalyze the ubiquitination of I kappa B alpha. Mol Cell 3: 527-533.

395. Bai C, Sen P, Hofmann K, Ma L, Goebl M, Harper JW, Elledge SJ (1996) SKP1 connects cell cycle regulators to the ubiquitin proteolysis machinery through a novel motif, the F-box. Cell 86: 263-274.

396. Lisztwan J, Marti A, Sutterluty H, Gstaiger M, Wirbelauer C, Krek W (1998) Association of human CUL-1 and ubiquitin-conjugating enzyme CDC34 with the F-box protein p45(SKP2): evidence for evolutionary conservation in the subunit composition of the CDC34-SCF pathway. EMBO J 17: 368-383.

397. Michel JJ, Xiong Y (1998) Human CUL-1, but not other cullin family members, selectively interacts with SKP1 to form a complex with SKP2 and cyclin A. Cell Growth Differ 9: 435-449.

398. Yu ZK, Gervais JL, Zhang H (1998) Human CUL-1 associates with the SKP1/SKP2 complex and regulates p21(CIP1/WAF1) and cyclin D proteins. Proc Natl Acad Sci U S A 95: 11324-11329.

399. Jin J, Cardozo T, Lovering RC, Elledge SJ, Pagano M, Harper JW (2004) Systematic analysis and nomenclature of mammalian F-box proteins. Genes Dev 18: 2573-2580.

400. Cenciarelli C, Chiaur DS, Guardavaccaro D, Parks W, Vidal M, Pagano M (1999) Identification of a family of human F-box proteins. Curr Biol 9: 1177-1179.
401. Winston JT, Koepp DM, Zhu C, Elledge SJ, Harper JW (1999) A family of mammalian F-box proteins. Curr Biol 9: 1180-1182.
402. Fuchs SY, Chen A, Xiong Y, Pan ZQ, Ronai Z (1999) HOS, a human homolog of Slimb, forms an SCF complex with Skp1 and Cullin1 and targets the phosphorylation-dependent degradation of IkappaB and beta-catenin. Oncogene 18: 2039-2046.
403. Latres E, Chiaur DS, Pagano M (1999) The human F box protein beta-Trcp associates with the Cul1/Skp1 complex and regulates the stability of beta-catenin. Oncogene 18: 849-854.
404. Winston JT, Strack P, Beer-Romero P, Chu CY, Elledge SJ, Harper JW (1999) The SCFbeta-TRCP-ubiquitin ligase complex associates specifically with phosphorylated destruction motifs in IkappaBalpha and beta-catenin and stimulates IkappaBalpha ubiquitination in vitro. Genes Dev 13: 270-283.
405. Vuillard L, Nicholson J, Hay RT (1999) A complex containing betaTrCP recruits Cdc34 to catalyse ubiquitination of IkappaBalpha. FEBS Lett 455: 311-314.
406. Finley D (2009) Recognition and processing of ubiquitin-protein conjugates by the proteasome. Annu Rev Biochem 78: 477-513.
407. Sorokin AV, Kim ER, Ovchinnikov LP (2009) Proteasome system of protein degradation and processing. Biochemistry (Mosc) 74: 1411-1442.
408. Groll M, Ditzel L, Lowe J, Stock D, Bochtler M, Bartunik HD, Huber R (1997) Structure of 20S proteasome from yeast at 2.4 A resolution. Nature 386: 463-471.
409. Whitby FG, Masters EI, Kramer L, Knowlton JR, Yao Y, Wang CC, Hill CP (2000) Structural basis for the activation of 20S proteasomes by 11S regulators. Nature 408: 115-120.
410. Borissenko L, Groll M (2007) 20S proteasome and its inhibitors: crystallographic knowledge for drug development. Chem Rev 107: 687-717.
411. Kisselev AF, Akopian TN, Woo KM, Goldberg AL (1999) The sizes of peptides generated from protein by mammalian 26 and 20 S proteasomes. Implications for understanding the degradative mechanism and antigen presentation. J Biol Chem 274: 3363-3371.
412. de Bettignies G, Coux O (2010) Proteasome inhibitors: Dozens of molecules and still counting. Biochimie 92: 1530-1545.
413. Tsukamoto S, Yokosawa H (2009) Targeting the proteasome pathway. Expert Opin Ther Targets 13: 605-621.
414. Rock KL, Gramm C, Rothstein L, Clark K, Stein R, Dick L, Hwang D, Goldberg AL (1994) Inhibitors of the proteasome block the degradation of most cell proteins and the generation of peptides presented on MHC class I molecules. Cell 78: 761-771.
415. Vinitsky A, Michaud C, Powers JC, Orlowski M (1992) Inhibition of the chymotrypsin-like activity of the pituitary multicatalytic proteinase complex. Biochemistry 31: 9421-9428.
416. Prakash S, Tian L, Ratliff KS, Lehotzky RE, Matouschek A (2004) An unstructured initiation site is required for efficient proteasome-mediated degradation. Nat Struct Mol Biol 11: 830-837.

417. Verma R, Aravind L, Oania R, McDonald WH, Yates JR, 3rd, Koonin EV, Deshaies RJ (2002) Role of Rpn11 metalloprotease in deubiquitination and degradation by the 26S proteasome. Science 298: 611-615.

418. Yao T, Cohen RE (2002) A cryptic protease couples deubiquitination and degradation by the proteasome. Nature 419: 403-407.

419. Vucic D, Dixit VM, Wertz IE (2011) Ubiquitylation in apoptosis: a post-translational modification at the edge of life and death. Nat Rev Mol Cell Biol 12: 439-452.

420. Tan M, Gallegos JR, Gu Q, Huang Y, Li J, Jin Y, Lu H, Sun Y (2006) SAG/ROC-SCF beta-TrCP E3 ubiquitin ligase promotes pro-caspase-3 degradation as a mechanism of apoptosis protection. Neoplasia 8: 1042-1054.

421. Jin Z, Li Y, Pitti R, Lawrence D, Pham VC, Lill JR, Ashkenazi A (2009) Cullin3-based polyubiquitination and p62-dependent aggregation of caspase-8 mediate extrinsic apoptosis signaling. Cell 137: 721-735.

422. Dehan E, Bassermann F, Guardavaccaro D, Vasiliver-Shamis G, Cohen M, Lowes KN, Dustin M, Huang DC, Taunton J, Pagano M (2009) betaTrCP- and Rsk1/2-mediated degradation of BimEL inhibits apoptosis. Mol Cell 33: 109-116.

423. Breitschopf K, Zeiher AM, Dimmeler S (2000) Ubiquitin-mediated degradation of the proapoptotic active form of bid. A functional consequence on apoptosis induction. J Biol Chem 275: 21648-21652.

424. Tait SW, de Vries E, Maas C, Keller AM, D'Santos CS, Borst J (2007) Apoptosis induction by Bid requires unconventional ubiquitination and degradation of its N-terminal fragment. J Cell Biol 179: 1453-1466.

425. Kudla G, Montessuit S, Eskes R, Berrier C, Martinou JC, Ghazi A, Antonsson B (2000) The destabilization of lipid membranes induced by the C-terminal fragment of caspase 8-cleaved bid is inhibited by the N-terminal fragment. J Biol Chem 275: 22713-22718.

426. Tan KO, Tan KM, Yu VC (1999) A novel BH3-like domain in BID is required for intramolecular interaction and autoinhibition of pro-apoptotic activity. J Biol Chem 274: 23687-23690.

427. Agrawal SG, Liu FT, Wiseman C, Shirali S, Liu H, Lillington D, Du MQ, Syndercombe-Court D, Newland AC, Gribben JG, Jia L (2008) Increased proteasomal degradation of Bax is a common feature of poor prognosis chronic lymphocytic leukemia. Blood 111: 2790-2796.

428. Liu FT, Agrawal SG, Gribben JG, Ye H, Du MQ, Newland AC, Jia L (2008) Bortezomib blocks Bax degradation in malignant B cells during treatment with TRAIL. Blood 111: 2797-2805.

429. Yu M, Liu FT, Newland AC, Jia L (2008) The alpha-5 helix of Bax is sensitive to ubiquitin-dependent degradation. Biochem Biophys Res Commun 371: 10-15.

430. Fu NY, Sukumaran SK, Kerk SY, Yu VC (2009) Baxbeta: a constitutively active human Bax isoform that is under tight regulatory control by the proteasomal degradation mechanism. Mol Cell 33: 15-29.

431. Azad N, Vallyathan V, Wang L, Tantishaiyakul V, Stehlik C, Leonard SS, Rojanasakul Y (2006) S-nitrosylation of Bcl-2 inhibits its ubiquitin-proteasomal degradation. A novel antiapoptotic mechanism that suppresses apoptosis. J Biol Chem 281: 34124-34134.

432. Thomas LW, Lam C, Edwards SW (2010) Mcl-1; the molecular regulation of protein function. FEBS Lett 584: 2981-2989.

433. Oda E, Ohki R, Murasawa H, Nemoto J, Shibue T, Yamashita T, Tokino T, Taniguchi T, Tanaka N (2000) Noxa, a BH3-only member of the Bcl-2 family and candidate mediator of p53-induced apoptosis. Science 288: 1053-1058.

434. Shibue T, Takeda K, Oda E, Tanaka H, Murasawa H, Takaoka A, Morishita Y, Akira S, Taniguchi T, Tanaka N (2003) Integral role of Noxa in p53-mediated apoptotic response. Genes Dev 17: 2233-2238.

435. Lee EF, Czabotar PE, van Delft MF, Michalak EM, Boyle MJ, Willis SN, Puthalakath H, Bouillet P, Colman PM, Huang DC, Fairlie WD (2008) A novel BH3 ligand that selectively targets Mcl-1 reveals that apoptosis can proceed without Mcl-1 degradation. J Cell Biol 180: 341-355.

436. Wuilleme-Toumi S, Trichet V, Gomez-Bougie P, Gratas C, Bataille R, Amiot M (2007) Reciprocal protection of Mcl-1 and Bim from ubiquitin-proteasome degradation. Biochem Biophys Res Commun 361: 865-869.

437. Warr MR, Acoca S, Liu Z, Germain M, Watson M, Blanchette M, Wing SS, Shore GC (2005) BH3-ligand regulates access of MCL-1 to its E3 ligase. FEBS Lett 579: 5603-5608.

438. Zhong Q, Gao W, Du F, Wang X (2005) Mule/ARF-BP1, a BH3-only E3 ubiquitin ligase, catalyzes the polyubiquitination of Mcl-1 and regulates apoptosis. Cell 121: 1085-1095.

439. Inuzuka H, Shaik S, Onoyama I, Gao D, Tseng A, Maser RS, Zhai B, Wan L, Gutierrez A, Lau AW, Xiao Y, Christie AL, Aster J, Settleman J, Gygi SP, Kung AL, Look T, Nakayama KI, DePinho RA, Wei W (2011) SCF(FBW7) regulates cellular apoptosis by targeting MCL1 for ubiquitylation and destruction. Nature 471: 104-109.

440. Ding Q, He X, Hsu JM, Xia W, Chen CT, Li LY, Lee DF, Liu JC, Zhong Q, Wang X, Hung MC (2007) Degradation of Mcl-1 by beta-TrCP mediates glycogen synthase kinase 3-induced tumor suppression and chemosensitization. Mol Cell Biol 27: 4006-4017.

441. Maurer U, Charvet C, Wagman AS, Dejardin E, Green DR (2006) Glycogen synthase kinase-3 regulates mitochondrial outer membrane permeabilization and apoptosis by destabilization of MCL-1. Mol Cell 21: 749-760.

442. Zhao Y, Altman BJ, Coloff JL, Herman CE, Jacobs SR, Wieman HL, Wofford JA, Dimascio LN, Ilkayeva O, Kelekar A, Reya T, Rathmell JC (2007) Glycogen synthase kinase 3alpha and 3beta mediate a glucose-sensitive antiapoptotic signaling pathway to stabilize Mcl-1. Mol Cell Biol 27: 4328-4339.

443. Benedict CA, Norris PS, Ware CF (2002) To kill or be killed: viral evasion of apoptosis. Nat Immunol 3: 1013-1018.

444. Barry M, Wasilenko ST, Stewart TL, Taylor JM (2004) Apoptosis regulator genes encoded by poxviruses. Prog Mol Subcell Biol 36: 19-37.

445. Hansen TH, Bouvier M (2009) MHC class I antigen presentation: learning from viral evasion strategies. Nat Rev Immunol 9: 503-513.

446. Wilkinson GW, Lehner PJ (2009) Jenner's irony: cowpox taps into T cell evasion. Cell Host Microbe 6: 395-397.

447. Guerin JL, Gelfi J, Boullier S, Delverdier M, Bellanger FA, Bertagnoli S, Drexler I, Sutter G, Messud-Petit F (2002) Myxoma virus leukemia-associated protein is responsible for major histocompatibility complex class I and Fas-CD95 down-regulation and defines scrapins, a new group of surface cellular receptor abductor proteins. J Virol 76: 2912-2923.

448. Mansouri M, Bartee E, Gouveia K, Hovey Nerenberg BT, Barrett J, Thomas L, Thomas G, McFadden G, Fruh K (2003) The PHD/LAP-domain protein M153R of myxomavirus is a ubiquitin ligase that induces the rapid internalization and lysosomal destruction of CD4. J Virol 77: 1427-1440.

449. Dasgupta A, Hammarlund E, Slifka MK, Fruh K (2007) Cowpox virus evades CTL recognition and inhibits the intracellular transport of MHC class I molecules. J Immunol 178: 1654-1661.

450. Alzhanova D, Edwards DM, Hammarlund E, Scholz IG, Horst D, Wagner MJ, Upton C, Wiertz EJ, Slifka MK, Fruh K (2009) Cowpox virus inhibits the transporter associated with antigen processing to evade T cell recognition. Cell Host Microbe 6: 433-445.

451. Byun M, Verweij MC, Pickup DJ, Wiertz EJ, Hansen TH, Yokoyama WM (2009) Two mechanistically distinct immune evasion proteins of cowpox virus combine to avoid antiviral CD8 T cells. Cell Host Microbe 6: 422-432.

452. Byun M, Wang X, Pak M, Hansen TH, Yokoyama WM (2007) Cowpox virus exploits the endoplasmic reticulum retention pathway to inhibit MHC class I transport to the cell surface. Cell Host Microbe 2: 306-315.

453. Gupta S (2002) A decision between life and death during TNF-alpha-induced signaling. J Clin Immunol 22: 185-194.

454. Smith CA, Davis T, Wignall JM, Din WS, Farrah T, Upton C, McFadden G, Goodwin RG (1991) T2 open reading frame from the Shope fibroma virus encodes a soluble form of the TNF receptor. Biochem Biophys Res Commun 176: 335-342.

455. Upton C, Macen JL, Schreiber M, McFadden G (1991) Myxoma virus expresses a secreted protein with homology to the tumor necrosis factor receptor gene family that contributes to viral virulence. Virology 184: 370-382.

456. Smith CA, Davis T, Anderson D, Solam L, Beckmann MP, Jerzy R, Dower SK, Cosman D, Goodwin RG (1990) A receptor for tumor necrosis factor defines an unusual family of cellular and viral proteins. Science 248: 1019-1023.

457. Schreiber M, McFadden G (1994) The myxoma virus TNF-receptor homologue (T2) inhibits tumor necrosis factor-alpha in a species-specific fashion. Virology 204: 692-705.

458. Schreiber M, Rajarathnam K, McFadden G (1996) Myxoma virus T2 protein, a tumor necrosis factor (TNF) receptor homolog, is secreted as a monomer and dimer that each bind rabbit TNFalpha, but the dimer is a more potent TNF inhibitor. J Biol Chem 271: 13333-13341.

459. Macen JL, Graham KA, Lee SF, Schreiber M, Boshkov LK, McFadden G (1996) Expression of the myxoma virus tumor necrosis factor receptor homologue and M11L genes is required to prevent virus-induced apoptosis in infected rabbit T lymphocytes. Virology 218: 232-237.

460. Hu FQ, Smith CA, Pickup DJ (1994) Cowpox virus contains two copies of an early gene encoding a soluble secreted form of the type II TNF receptor. Virology 204: 343-356.

461. Smith CA, Hu FQ, Smith TD, Richards CL, Smolak P, Goodwin RG, Pickup DJ (1996) Cowpox virus genome encodes a second soluble homologue of cellular TNF receptors, distinct from CrmB, that binds TNF but not LT alpha. Virology 223: 132-147.

462. Loparev VN, Parsons JM, Knight JC, Panus JF, Ray CA, Buller RM, Pickup DJ, Esposito JJ (1998) A third distinct tumor necrosis factor receptor of orthopoxviruses. Proc Natl Acad Sci U S A 95: 3786-3791.

463. Reading PC, Khanna A, Smith GL (2002) Vaccinia virus CrmE encodes a soluble and cell surface tumor necrosis factor receptor that contributes to virus virulence. Virology 292: 285-298.

464. Saraiva M, Alcami A (2001) CrmE, a novel soluble tumor necrosis factor receptor encoded by poxviruses. J Virol 75: 226-233.

465. Brunetti CR, Paulose-Murphy M, Singh R, Qin J, Barrett JW, Tardivel A, Schneider P, Essani K, McFadden G (2003) A secreted high-affinity inhibitor of human TNF from Tanapox virus. Proc Natl Acad Sci U S A 100: 4831-4836.

466. Bertin J, Armstrong RC, Ottilie S, Martin DA, Wang Y, Banks S, Wang GH, Senkevich TG, Alnemri ES, Moss B, Lenardo MJ, Tomaselli KJ, Cohen JI (1997) Death effector domain-containing herpesvirus and poxvirus proteins inhibit both Fas- and TNFR1-induced apoptosis. Proc Natl Acad Sci U S A 94: 1172-1176.

467. Hu S, Vincenz C, Buller M, Dixit VM (1997) A novel family of viral death effector domain-containing molecules that inhibit both CD-95- and tumor necrosis factor receptor-1-induced apoptosis. J Biol Chem 272: 9621-9624.

468. Thome M, Schneider P, Hofmann K, Fickenscher H, Meinl E, Neipel F, Mattmann C, Burns K, Bodmer JL, Schroter M, Scaffidi C, Krammer PH, Peter ME, Tschopp J (1997) Viral FLICE-inhibitory proteins (FLIPs) prevent apoptosis induced by death receptors. Nature 386: 517-521.

469. Garvey TL, Bertin J, Siegel RM, Wang GH, Lenardo MJ, Cohen JI (2002) Binding of FADD and caspase-8 to molluscum contagiosum virus MC159 v-FLIP is not sufficient for its antiapoptotic function. J Virol 76: 697-706.

470. Shisler JL, Moss B (2001) Molluscum contagiosum virus inhibitors of apoptosis: The MC159 v-FLIP protein blocks Fas-induced activation of procaspases and degradation of the related MC160 protein. Virology 282: 14-25.

471. Tsukumo SI, Yonehara S (1999) Requirement of cooperative functions of two repeated death effector domains in caspase-8 and in MC159 for induction and inhibition of apoptosis, respectively. Genes Cells 4: 541-549.

472. Barry M, McFadden G (2000) Regulation of Apoptosis by Poxviruses. In: Cunningham MW, Fujinami RS, editors. Effects of Microbes on the Immune System. Philadelphia: Lippincott Williams & Wilkins. pp. 509-520.

473. Silverman GA, Bird PI, Carrell RW, Church FC, Coughlin PB, Gettins PG, Irving JA, Lomas DA, Luke CJ, Moyer RW, Pemberton PA, Remold-O'Donnell E, Salvesen GS, Travis J, Whisstock JC (2001) The serpins are an expanding superfamily of structurally similar but functionally diverse proteins. Evolution, mechanism of inhibition, novel functions, and a revised nomenclature. J Biol Chem 276: 33293-33296.

474. Pickup DJ, Ink BS, Hu W, Ray CA, Joklik WK (1986) Hemorrhage in lesions caused by cowpox virus is induced by a viral protein that is related to plasma protein inhibitors of serine proteases. Proc Natl Acad Sci U S A 83: 7698-7702.

475. Komiyama T, Ray CA, Pickup DJ, Howard AD, Thornberry NA, Peterson EP, Salvesen G (1994) Inhibition of interleukin-1 beta converting enzyme by the cowpox virus serpin CrmA. An example of cross-class inhibition. J Biol Chem 269: 19331-19337.

476. Quan LT, Caputo A, Bleackley RC, Pickup DJ, Salvesen GS (1995) Granzyme B is inhibited by the cowpox virus serpin cytokine response modifier A. J Biol Chem 270: 10377-10379.

477. Ray CA, Black RA, Kronheim SR, Greenstreet TA, Sleath PR, Salvesen GS, Pickup DJ (1992) Viral inhibition of inflammation: cowpox virus encodes an inhibitor of the interleukin-1 beta converting enzyme. Cell 69: 597-604.

478. Zhou Q, Snipas S, Orth K, Muzio M, Dixit VM, Salvesen GS (1997) Target protease specificity of the viral serpin CrmA. Analysis of five caspases. J Biol Chem 272: 7797-7800.

479. Kotwal GJ, Moss B (1989) Vaccinia virus encodes two proteins that are structurally related to members of the plasma serine protease inhibitor superfamily. J Virol 63: 600-606.

480. Smith GL, Howard ST, Chan YS (1989) Vaccinia virus encodes a family of genes with homology to serine proteinase inhibitors. J Gen Virol 70 (Pt 9): 2333-2343.

481. Boursnell ME, Foulds IJ, Campbell JI, Binns MM (1988) Non-essential genes in the vaccinia virus HindIII K fragment: a gene related to serine protease inhibitors and a gene related to the 37K vaccinia virus major envelope antigen. J Gen Virol 69 (Pt 12): 2995-3003.

482. Cameron C, Hota-Mitchell S, Chen L, Barrett J, Cao JX, Macaulay C, Willer D, Evans D, McFadden G (1999) The complete DNA sequence of myxoma virus. Virology 264: 298-318.

483. Bawden AL, Glassberg KJ, Diggans J, Shaw R, Farmerie W, Moyer RW (2000) Complete genomic sequence of the Amsacta moorei entomopoxvirus: analysis and comparison with other poxviruses. Virology 274: 120-139.

484. Afonso CL, Tulman ER, Lu Z, Oma E, Kutish GF, Rock DL (1999) The genome of Melanoplus sanguinipes entomopoxvirus. J Virol 73: 533-552.

485. Deveraux QL, Reed JC (1999) IAP family proteins--suppressors of apoptosis. Genes Dev 13: 239-252.

486. Salvesen GS, Duckett CS (2002) IAP proteins: blocking the road to death's door. Nat Rev Mol Cell Biol 3: 401-410.

487. Li Q, Liston P, Moyer RW (2005) Functional analysis of the inhibitor of apoptosis (iap) gene carried by the entomopoxvirus of Amsacta moorei. J Virol 79: 2335-2345.

488. Li Q, Liston P, Schokman N, Ho JM, Moyer RW (2005) Amsacta moorei Entomopoxvirus inhibitor of apoptosis suppresses cell death by binding Grim and Hid. J Virol 79: 3684-3691.

489. Senkevich TG, Koonin EV, Buller RM (1994) A poxvirus protein with a RING zinc finger motif is of crucial importance for virulence. Virology 198: 118-128.

490. Brick DJ, Burke RD, Schiff L, Upton C (1998) Shope fibroma virus RING finger protein N1R binds DNA and inhibits apoptosis. Virology 249: 42-51.

491. Brick DJ, Burke RD, Minkley AA, Upton C (2000) Ectromelia virus virulence factor p28 acts upstream of caspase-3 in response to UV light-induced apoptosis. J Gen Virol 81: 1087-1097.

492. Huang J, Huang Q, Zhou X, Shen MM, Yen A, Yu SX, Dong G, Qu K, Huang P, Anderson EM, Daniel-Issakani S, Buller RM, Payan DG, Lu HH (2004) The poxvirus p28 virulence factor is an E3 ubiquitin ligase. J Biol Chem 279: 54110-54116.

493. Nerenberg BT, Taylor J, Bartee E, Gouveia K, Barry M, Fruh K (2005) The poxviral RING protein p28 is a ubiquitin ligase that targets ubiquitin to viral replication factories. J Virol 79: 597-601.

494. Gubser C, Bergamaschi D, Hollinshead M, Lu X, van Kuppeveld FJ, Smith GL (2007) A new inhibitor of apoptosis from vaccinia virus and eukaryotes. PLoS Pathog 3: e17.

495. Castanier C, Arnoult D (2011) Mitochondrial localization of viral proteins as a means to subvert host defense. Biochim Biophys Acta 1813: 575-583.

496. Galluzzi L, Brenner C, Morselli E, Touat Z, Kroemer G (2008) Viral control of mitochondrial apoptosis. PLoS Pathog 4: e1000018.

497. Cuconati A, White E (2002) Viral homologs of BCL-2: role of apoptosis in the regulation of virus infection. Genes Dev 16: 2465-2478.

498. Hardwick JM, Bellows DS (2003) Viral versus cellular BCL-2 proteins. Cell Death Differ 10 Suppl 1: S68-76.

499. Sarid R, Sato T, Bohenzky RA, Russo JJ, Chang Y (1997) Kaposi's sarcoma-associated herpesvirus encodes a functional bcl-2 homologue. Nat Med 3: 293-298.

500. Cheng EH, Nicholas J, Bellows DS, Hayward GS, Guo HG, Reitz MS, Hardwick JM (1997) A Bcl-2 homolog encoded by Kaposi sarcoma-associated virus, human herpesvirus 8, inhibits apoptosis but does not heterodimerize with Bax or Bak. Proc Natl Acad Sci U S A 94: 690-694.

501. Henderson S, Huen D, Rowe M, Dawson C, Johnson G, Rickinson A (1993) Epstein-Barr virus-coded BHRF1 protein, a viral homologue of Bcl-2, protects human B cells from programmed cell death. Proc Natl Acad Sci U S A 90: 8479-8483.

502. Marshall WL, Yim C, Gustafson E, Graf T, Sage DR, Hanify K, Williams L, Fingeroth J, Finberg RW (1999) Epstein-Barr virus encodes a novel homolog of the bcl-2 oncogene that inhibits apoptosis and associates with Bax and Bak. J Virol 73: 5181-5185.

503. Wang GH, Garvey TL, Cohen JI (1999) The murine gammaherpesvirus-68 M11 protein inhibits Fas- and TNF-induced apoptosis. J Gen Virol 80 (Pt 10): 2737-2740.

504. Huang Q, Petros AM, Virgin HW, Fesik SW, Olejniczak ET (2002) Solution structure of a Bcl-2 homolog from Kaposi sarcoma virus. Proc Natl Acad Sci U S A 99: 3428-3433.

505. Cross JR, Postigo A, Blight K, Downward J (2008) Viral pro-survival proteins block separate stages in Bax activation but changes in mitochondrial ultrastructure still occur. Cell Death Differ 15: 997-1008.

506. Desbien AL, Kappler JW, Marrack P (2009) The Epstein-Barr virus Bcl-2 homolog, BHRF1, blocks apoptosis by binding to a limited amount of Bim. Proc Natl Acad Sci U S A 106: 5663-5668.

507. Flanagan AM, Letai A (2008) BH3 domains define selective inhibitory interactions with BHRF-1 and KSHV BCL-2. Cell Death Differ 15: 580-588.

508. Bellows DS, Howell M, Pearson C, Hazlewood SA, Hardwick JM (2002) Epstein-Barr virus BALF1 is a BCL-2-like antagonist of the herpesvirus antiapoptotic BCL-2 proteins. J Virol 76: 2469-2479.

509. Kvansakul M, Wei AH, Fletcher JI, Willis SN, Chen L, Roberts AW, Huang DC, Colman PM (2010) Structural basis for apoptosis inhibition by Epstein-Barr virus BHRF1. PLoS Pathog 6: e1001236.

510. Loh J, Huang Q, Petros AM, Nettesheim D, van Dyk LF, Labrada L, Speck SH, Levine B, Olejniczak ET, Virgin HWt (2005) A surface groove essential for viral Bcl-2 function during chronic infection in vivo. PLoS Pathog 1: e10.

511. Huang Q, Petros AM, Virgin HW, Fesik SW, Olejniczak ET (2003) Solution structure of the BHRF1 protein from Epstein-Barr virus, a homolog of human Bcl-2. J Mol Biol 332: 1123-1130.

512. Bellows DS, Chau BN, Lee P, Lazebnik Y, Burns WH, Hardwick JM (2000) Antiapoptotic herpesvirus Bcl-2 homologs escape caspase-mediated conversion to proapoptotic proteins. J Virol 74: 5024-5031.

513. Afonso CL, Neilan JG, Kutish GF, Rock DL (1996) An African swine fever virus Bc1-2 homolog, 5-HL, suppresses apoptotic cell death. J Virol 70: 4858-4863.

514. Chiou SK, Tseng CC, Rao L, White E (1994) Functional complementation of the adenovirus E1B 19-kilodalton protein with Bcl-2 in the inhibition of apoptosis in infected cells. J Virol 68: 6553-6566.

515. Brun A, Rivas C, Esteban M, Escribano JM, Alonso C (1996) African swine fever virus gene A179L, a viral homologue of bcl-2, protects cells from programmed cell death. Virology 225: 227-230.

516. Galindo I, Hernaez B, Diaz-Gil G, Escribano JM, Alonso C (2008) A179L, a viral Bcl-2 homologue, targets the core Bcl-2 apoptotic machinery and its upstream BH3 activators with selective binding restrictions for Bid and Noxa. Virology 375: 561-572.

517. Chen G, Branton PE, Yang E, Korsmeyer SJ, Shore GC (1996) Adenovirus E1B 19-kDa death suppressor protein interacts with Bax but not with Bad. J Biol Chem 271: 24221-24225.

518. Han J, Sabbatini P, Perez D, Rao L, Modha D, White E (1996) The E1B 19K protein blocks apoptosis by interacting with and inhibiting the p53-inducible and death-promoting Bax protein. Genes Dev 10: 461-477.

519. White E, Sabbatini P, Debbas M, Wold WS, Kusher DI, Gooding LR (1992) The 19-kilodalton adenovirus E1B transforming protein inhibits programmed cell death and prevents cytolysis by tumor necrosis factor alpha. Mol Cell Biol 12: 2570-2580.

520. Farrow SN, White JH, Martinou I, Raven T, Pun KT, Grinham CJ, Martinou JC, Brown R (1995) Cloning of a bcl-2 homologue by interaction with adenovirus E1B 19K. Nature 374: 731-733.

521. Han J, Sabbatini P, White E (1996) Induction of apoptosis by human Nbk/Bik, a BH3-containing protein that interacts with E1B 19K. Mol Cell Biol 16: 5857-5864.

522. Revilla Y, Cebrian A, Baixeras E, Martinez C, Vinuela E, Salas ML (1997) Inhibition of apoptosis by the African swine fever virus Bcl-2 homologue: role of the BH1 domain. Virology 228: 400-404.

523. Arnoult D, Bartle LM, Skaletskaya A, Poncet D, Zamzami N, Park PU, Sharpe J, Youle RJ, Goldmacher VS (2004) Cytomegalovirus cell death suppressor vMIA blocks Bax- but not Bak-mediated apoptosis by binding and sequestering Bax at mitochondria. Proc Natl Acad Sci U S A 101: 7988-7993.

524. Poncet D, Larochette N, Pauleau AL, Boya P, Jalil AA, Cartron PF, Vallette F, Schnebelen C, Bartle LM, Skaletskaya A, Boutolleau D, Martinou JC, Goldmacher VS, Kroemer G, Zamzami N (2004) An anti-apoptotic viral protein that recruits Bax to mitochondria. J Biol Chem 279: 22605-22614.

525. Mavinakere MS, Colberg-Poley AM (2004) Dual targeting of the human cytomegalovirus UL37 exon 1 protein during permissive infection. J Gen Virol 85: 323-329.

526. Pauleau AL, Larochette N, Giordanetto F, Scholz SR, Poncet D, Zamzami N, Goldmacher VS, Kroemer G (2007) Structure-function analysis of the interaction between Bax and the cytomegalovirus-encoded protein vMIA. Oncogene 26: 7067-7080.

527. Arnoult D, Skaletskaya A, Estaquier J, Dufour C, Goldmacher VS (2008) The murine cytomegalovirus cell death suppressor m38.5 binds Bax and blocks Bax-mediated mitochondrial outer membrane permeabilization. Apoptosis 13: 1100-1110.

528. Jurak I, Schumacher U, Simic H, Voigt S, Brune W (2008) Murine cytomegalovirus m38.5 protein inhibits Bax-mediated cell death. J Virol 82: 4812-4822.

529. Norris KL, Youle RJ (2008) Cytomegalovirus proteins vMIA and m38.5 link mitochondrial morphogenesis to Bcl-2 family proteins. J Virol 82: 6232-6243.

530. Cam M, Handke W, Picard-Maureau M, Brune W (2010) Cytomegaloviruses inhibit Bak- and Bax-mediated apoptosis with two separate viral proteins. Cell Death Differ 17: 655-665.

531. Afonso CL, Tulman ER, Lu Z, Zsak L, Kutish GF, Rock DL (2000) The genome of fowlpox virus. J Virol 74: 3815-3831.

532. Tulman ER, Afonso CL, Lu Z, Zsak L, Kutish GF, Rock DL (2004) The genome of canarypox virus. J Virol 78: 353-366.

533. Banadyga L, Gerig J, Stewart T, Barry M (2007) Fowlpox virus encodes a Bcl-2 homologue that protects cells from apoptotic death through interaction with the proapoptotic protein Bak. J Virol 81: 11032-11045.

534. Banadyga L, Veugelers K, Campbell S, Barry M (2009) The fowlpox virus BCL-2 homologue, FPV039, interacts with activated Bax and a discrete subset of BH3-only proteins to inhibit apoptosis. J Virol 83: 7085-7098.

535. Everett H, Barry M, Lee SF, Sun X, Graham K, Stone J, Bleackley RC, McFadden G (2000) M11L: a novel mitochondria-localized protein of myxoma virus that blocks apoptosis of infected leukocytes. J Exp Med 191: 1487-1498.

536. Everett H, Barry M, Sun X, Lee SF, Frantz C, Berthiaume LG, McFadden G, Bleackley RC (2002) The myxoma poxvirus protein, M11L, prevents apoptosis by direct interaction with the mitochondrial permeability transition pore. J Exp Med 196: 1127-1139.

537. Su J, Wang G, Barrett JW, Irvine TS, Gao X, McFadden G (2006) Myxoma virus M11L blocks apoptosis through inhibition of conformational activation of Bax at the mitochondria. J Virol 80: 1140-1151.

538. Wang G, Barrett JW, Nazarian SH, Everett H, Gao X, Bleackley C, Colwill K, Moran MF, McFadden G (2004) Myxoma virus M11L prevents apoptosis through constitutive interaction with Bak. J Virol 78: 7097-7111.

539. Kvansakul M, van Delft MF, Lee EF, Gulbis JM, Fairlie WD, Huang DC, Colman PM (2007) A structural viral mimic of prosurvival Bcl-2: a pivotal role for sequestering proapoptotic Bax and Bak. Mol Cell 25: 933-942.

540. Douglas AE, Corbett KD, Berger JM, McFadden G, Handel TM (2007) Structure of M11L: A myxoma virus structural homolog of the apoptosis inhibitor, Bcl-2. Protein Sci 16: 695-703.

541. Banadyga L, Lam SC, Okamoto T, Kvansakul M, Huang DC, Barry M (2011) Deerpox virus encodes an inhibitor of apoptosis that regulates Bak and Bax. J Virol 85: 1922-1934.
542. Afonso CL, Delhon G, Tulman ER, Lu Z, Zsak A, Becerra VM, Zsak L, Kutish GF, Rock DL (2005) Genome of deerpox virus. J Virol 79: 966-977.
543. Westphal D, Ledgerwood EC, Hibma MH, Fleming SB, Whelan EM, Mercer AA (2007) A novel Bcl-2-like inhibitor of apoptosis is encoded by the parapoxvirus ORF virus. J Virol 81: 7178-7188.
544. Westphal D, Ledgerwood EC, Tyndall JD, Hibma MH, Ueda N, Fleming SB, Mercer AA (2009) The orf virus inhibitor of apoptosis functions in a Bcl-2-like manner, binding and neutralizing a set of BH3-only proteins and active Bax. Apoptosis 14: 1317-1330.
545. Wasilenko ST, Meyers AF, Vander Helm K, Barry M (2001) Vaccinia virus infection disarms the mitochondrion-mediated pathway of the apoptotic cascade by modulating the permeability transition pore. J Virol 75: 11437-11448.
546. Goebel SJ, Johnson GP, Perkus ME, Davis SW, Winslow JP, Paoletti E (1990) The complete DNA sequence of vaccinia virus. Virology 179: 247-266, 517-263.
547. Wasilenko ST, Stewart TL, Meyers AF, Barry M (2003) Vaccinia virus encodes a previously uncharacterized mitochondrial-associated inhibitor of apoptosis. Proc Natl Acad Sci U S A 100: 14345-14350.
548. Stewart TL, Wasilenko ST, Barry M (2005) Vaccinia virus F1L protein is a tail-anchored protein that functions at the mitochondria to inhibit apoptosis. J Virol 79: 1084-1098.
549. Taylor JM, Quilty D, Banadyga L, Barry M (2006) The vaccinia virus protein F1L interacts with Bim and inhibits activation of the pro-apoptotic protein Bax. J Biol Chem.
550. Wasilenko ST, Banadyga L, Bond D, Barry M (2005) The vaccinia virus F1L protein interacts with the proapoptotic protein Bak and inhibits Bak activation. J Virol 79: 14031-14043.
551. Postigo A, Cross JR, Downward J, Way M (2006) Interaction of F1L with the BH3 domain of Bak is responsible for inhibiting vaccinia-induced apoptosis. Cell Death Differ 13: 1651-1662.
552. Taylor JM, Quilty D, Banadyga L, Barry M (2006) The vaccinia virus protein F1L interacts with Bim and inhibits activation of the pro-apoptotic protein Bax. J Biol Chem 281: 39728-39739.
553. Zhai D, Yu E, Jin C, Welsh K, Shiau CW, Chen L, Salvesen GS, Liddington R, Reed JC (2010) Vaccinia virus protein F1L is a caspase-9 inhibitor. J Biol Chem 285: 5569-5580.
554. Yu E, Zhai D, Jin C, Gerlic M, Reed JC, Liddington R (2011) Structural Determinants of Caspase-9 Inhibition by the Vaccinia Virus Protein, F1L. J Biol Chem 286: 30748-30758.
555. Kvansakul M, Yang H, Fairlie WD, Czabotar PE, Fischer SF, Perugini MA, Huang DC, Colman PM (2008) Vaccinia virus anti-apoptotic F1L is a novel Bcl-2-like domain-swapped dimer that binds a highly selective subset of BH3-containing death ligands. Cell Death Differ 15: 1564-1571.
556. Jesenberger V, Jentsch S (2002) Deadly encounter: ubiquitin meets apoptosis. Nat Rev Mol Cell Biol 3: 112-121.

557. Lee JC, Peter ME (2003) Regulation of apoptosis by ubiquitination. Immunol Rev 193: 39-47.

558. Wojcik C (2002) Regulation of apoptosis by the ubiquitin and proteasome pathway. J Cell Mol Med 6: 25-48.

559. Yang Y, Yu X (2003) Regulation of apoptosis: the ubiquitous way. FASEB J 17: 790-799.

560. Degenhardt K, Sundararajan R, Lindsten T, Thompson C, White E (2002) Bax and Bak independently promote cytochrome C release from mitochondria. J Biol Chem 277: 14127-14134.

561. Wang GQ, Wieckowski E, Goldstein LA, Gastman BR, Rabinovitz A, Gambotto A, Li S, Fang B, Yin XM, Rabinowich H (2001) Resistance to granzyme B-mediated cytochrome c release in Bak-deficient cells. J Exp Med 194: 1325-1337.

562. Sambrook, Russel (2001) Molecular Cloning: A Laboratory Manual. Cold Spring Harbor, NY: Cold Spring Harbor Laboratory Press.

563. Altschul SF, Gish W, Miller W, Myers EW, Lipman DJ (1990) Basic local alignment search tool. J Mol Biol 215: 403-410.

564. Earl PL, Moss B, Wyatt LS, Carroll MW (1998) Generation of recombinant vaccinia viruses. In: Ausubel FM, Brent R, Kingston RE, Moore DD, Seidman JG et al., editors. Current protocols in molecular biology. New York, N.Y.: Wiley Interscience. pp. 16.17.11-16.17.19.

565. Chakrabarti S, Sisler JR, Moss B (1997) Compact, synthetic, vaccinia virus early/late promoter for protein expression. Biotechniques 23: 1094-1097.

566. Mottet K, Barry M (Unpublished).

567. Han J, Goldstein LA, Gastman BR, Froelich CJ, Yin XM, Rabinowich H (2004) Degradation of Mcl-1 by granzyme B: implications for Bim-mediated mitochondrial apoptotic events. J Biol Chem 279: 22020-22029.

568. Alexander WA, Moss B, Fuerst TR (1992) Regulated expression of foreign genes in vaccinia virus under the control of bacteriophage T7 RNA polymerase and the Escherichia coli lac repressor. J Virol 66: 2934-2942.

569. Fuerst TR, Niles EG, Studier FW, Moss B (1986) Eukaryotic transient-expression system based on recombinant vaccinia virus that synthesizes bacteriophage T7 RNA polymerase. Proc Natl Acad Sci U S A 83: 8122-8126.

570. Taylor J, Barry M (Unpublished).

571. van Buuren N, Couturier B, Xiong Y, Barry M (2008) Ectromelia virus encodes a novel family of F-box proteins that interact with the SCF complex. J Virol 82: 9917-9927.

572. Wilton BA, Campbell S, Van Buuren N, Garneau R, Furukawa M, Xiong Y, Barry M (2008) Ectromelia virus BTB/kelch proteins, EVM150 and EVM167, interact with cullin-3-based ubiquitin ligases. Virology 374: 82-99.

573. van Buuren N, Barry M (Unpublished).

574. Couturier B, Barry M (Unpublished).

575. Thompson JD, Higgins DG, Gibson TJ (1994) CLUSTAL W: improving the sensitivity of progressive multiple sequence alignment through sequence weighting, position-specific gap penalties and weight matrix choice. Nucleic Acids Res 22: 4673-4680.

576. Stewart T, Barry M (Unpublished).

577. Fujimuro M, Sawada H, Yokosawa H (1994) Production and characterization of monoclonal antibodies specific to multi-ubiquitin chains of polyubiquitinated proteins. FEBS Lett 349: 173-180.

578. Shevchenko A, Wilm M, Vorm O, Mann M (1996) Mass spectrometric sequencing of proteins silver-stained polyacrylamide gels. Anal Chem 68: 850-858.

579. Blum H, Beier H, Gross HJ (1987) Improved silver staining of plant proteins, RNA and DNA in polyacrylamide gels. Electrophoresis 8: 93-99.

580. Zong WX, Li C, Hatzivassiliou G, Lindsten T, Yu QC, Yuan J, Thompson CB (2003) Bax and Bak can localize to the endoplasmic reticulum to initiate apoptosis. J Cell Biol 162: 59-69.

581. Heibein JA, Barry M, Motyka B, Bleackley RC (1999) Granzyme B-induced loss of mitochondrial inner membrane potential (Delta Psi m) and cytochrome c release are caspase independent. J Immunol 163: 4683-4693.

582. Samali A, Cai J, Zhivotovsky B, Jones DP, Orrenius S (1999) Presence of a pre-apoptotic complex of pro-caspase-3, Hsp60 and Hsp10 in the mitochondrial fraction of jurkat cells. EMBO J 18: 2040-2048.

583. Koo GC, Peppard JR (1984) Establishment of monoclonal anti-Nk-1.1 antibody. Hybridoma 3: 301-303.

584. Upton C, Schiff L, Rice SA, Dowdeswell T, Yang X, McFadden G (1994) A poxvirus protein with a RING finger motif binds zinc and localizes in virus factories. J Virol 68: 4186-4195.

585. Zhuang J, Brady HJ (2006) Emerging role of Mcl-1 in actively counteracting BH3-only proteins in apoptosis. Cell Death Differ 13: 1263-1267.

586. Callus BA, Moujallad DM, Silke J, Gerl R, Jabbour AM, Ekert PG, Vaux DL (2008) Triggering of apoptosis by Puma is determined by the threshold set by prosurvival Bcl-2 family proteins. J Mol Biol 384: 313-323.

587. Gomez-Bougie P, Wuilleme-Toumi S, Menoret E, Trichet V, Robillard N, Philippe M, Bataille R, Amiot M (2007) Noxa up-regulation and Mcl-1 cleavage are associated to apoptosis induction by bortezomib in multiple myeloma. Cancer Res 67: 5418-5424.

588. Shimazu T, Degenhardt K, Nur EKA, Zhang J, Yoshida T, Zhang Y, Mathew R, White E, Inouye M (2007) NBK/BIK antagonizes MCL-1 and BCL-XL and activates BAK-mediated apoptosis in response to protein synthesis inhibition. Genes Dev 21: 929-941.

589. Yuan Z, Cao K, Lin C, Li L, Liu HY, Zhao XY, Liu L, Deng HX, Li J, Nie CL, Wei YQ (2011) PUMA Chemosensitizes Intrinsically Resistant Ovarian Cancer Cells to Cisplatin by Lowering the Threshold Set by Bcl-x(L) and Mcl-1. Mol Med.

590. Clohessy JG, Zhuang J, de Boer J, Gil-Gomez G, Brady HJ (2006) Mcl-1 interacts with truncated Bid and inhibits its induction of cytochrome c release and its role in receptor-mediated apoptosis. J Biol Chem 281: 5750-5759.

591. Gillissen B, Essmann F, Hemmati PG, Richter A, Oztop I, Chinnadurai G, Dorken B, Daniel PT (2007) Mcl-1 determines the Bax dependency of Nbk/Bik-induced apoptosis. J Cell Biol 179: 701-715.

592. Han J, Goldstein LA, Gastman BR, Rabinovitz A, Rabinowich H (2005) Disruption of Mcl-1.Bim complex in granzyme B-mediated mitochondrial apoptosis. J Biol Chem 280: 16383-16392.

593. Han J, Goldstein LA, Gastman BR, Rabinowich H (2006) Interrelated roles for Mcl-1 and BIM in regulation of TRAIL-mediated mitochondrial apoptosis. J Biol Chem 281: 10153-10163.

594. Han J, Goldstein LA, Hou W, Rabinowich H (2007) Functional linkage between NOXA and Bim in mitochondrial apoptotic events. J Biol Chem 282: 16223-16231.

595. Opferman JT, Letai A, Beard C, Sorcinelli MD, Ong CC, Korsmeyer SJ (2003) Development and maintenance of B and T lymphocytes requires antiapoptotic MCL-1. Nature 426: 671-676.

596. Opferman JT, Iwasaki H, Ong CC, Suh H, Mizuno S, Akashi K, Korsmeyer SJ (2005) Obligate role of anti-apoptotic MCL-1 in the survival of hematopoietic stem cells. Science 307: 1101-1104.

597. Rinkenberger JL, Horning S, Klocke B, Roth K, Korsmeyer SJ (2000) Mcl-1 deficiency results in peri-implantation embryonic lethality. Genes Dev 14: 23-27.

598. Kamada S, Shimono A, Shinto Y, Tsujimura T, Takahashi T, Noda T, Kitamura Y, Kondoh H, Tsujimoto Y (1995) bcl-2 deficiency in mice leads to pleiotropic abnormalities: accelerated lymphoid cell death in thymus and spleen, polycystic kidney, hair hypopigmentation, and distorted small intestine. Cancer Res 55: 354-359.

599. Huntington ND, Puthalakath H, Gunn P, Naik E, Michalak EM, Smyth MJ, Tabarias H, Degli-Esposti MA, Dewson G, Willis SN, Motoyama N, Huang DC, Nutt SL, Tarlinton DM, Strasser A (2007) Interleukin 15-mediated survival of natural killer cells is determined by interactions among Bim, Noxa and Mcl-1. Nat Immunol 8: 856-863.

600. Jourdan M, De Vos J, Mechti N, Klein B (2000) Regulation of Bcl-2-family proteins in myeloma cells by three myeloma survival factors: interleukin-6, interferon-alpha and insulin-like growth factor 1. Cell Death Differ 7: 1244-1252.

601. Jourdan M, Veyrune JL, De Vos J, Redal N, Couderc G, Klein B (2003) A major role for Mcl-1 antiapoptotic protein in the IL-6-induced survival of human myeloma cells. Oncogene 22: 2950-2959.

602. Puthier D, Bataille R, Amiot M (1999) IL-6 up-regulates mcl-1 in human myeloma cells through JAK / STAT rather than ras / MAP kinase pathway. Eur J Immunol 29: 3945-3950.

603. Puthier D, Thabard W, Rapp M, Etrillard M, Harousseau J, Bataille R, Amiot M (2001) Interferon alpha extends the survival of human myeloma cells through an upregulation of the Mcl-1 anti-apoptotic molecule. Br J Haematol 112: 358-363.

604. Kim JH, Sim SH, Ha HJ, Ko JJ, Lee K, Bae J (2009) MCL-1ES, a novel variant of MCL-1, associates with MCL-1L and induces mitochondrial cell death. FEBS Lett 583: 2758-2764.

605. Stewart ML, Fire E, Keating AE, Walensky LD (2010) The MCL-1 BH3 helix is an exclusive MCL-1 inhibitor and apoptosis sensitizer. Nat Chem Biol 6: 595-601.

606. Herrant M, Jacquel A, Marchetti S, Belhacene N, Colosetti P, Luciano F, Auberger P (2004) Cleavage of Mcl-1 by caspases impaired its ability to counteract Bim-induced apoptosis. Oncogene 23: 7863-7873.

607. Michels J, O'Neill JW, Dallman CL, Mouzakiti A, Habens F, Brimmell M, Zhang KY, Craig RW, Marcusson EG, Johnson PW, Packham G (2004) Mcl-1 is required for Akata6 B-lymphoma cell survival and is converted to a cell death molecule by efficient caspase-mediated cleavage. Oncogene 23: 4818-4827.

608. Clohessy JG, Zhuang J, Brady HJ (2004) Characterisation of Mcl-1 cleavage during apoptosis of haematopoietic cells. Br J Haematol 125: 655-665.
609. Menoret E, Gomez-Bougie P, Surget S, Trichet V, Oliver L, Pellat-Deceunynck C, Amiot M (2010) Mcl-1(128-350) fragment induces apoptosis through direct interaction with Bax. FEBS Lett 584: 487-492.
610. Weng C, Li Y, Xu D, Shi Y, Tang H (2005) Specific cleavage of Mcl-1 by caspase-3 in tumor necrosis factor-related apoptosis-inducing ligand (TRAIL)-induced apoptosis in Jurkat leukemia T cells. J Biol Chem 280: 10491-10500.
611. Rogers S, Wells R, Rechsteiner M (1986) Amino acid sequences common to rapidly degraded proteins: the PEST hypothesis. Science 234: 364-368.
612. Lopez H, Zhang L, George NM, Liu X, Pang X, Evans JJ, Targy NM, Luo X (2010) Perturbation of the Bcl-2 network and an induced Noxa/Bcl-xL interaction trigger mitochondrial dysfunction after DNA damage. J Biol Chem 285: 15016-15026.
613. Mei Y, Du W, Yang Y, Wu M (2005) Puma(*)Mcl-1 interaction is not sufficient to prevent rapid degradation of Mcl-1. Oncogene 24: 7224-7237.
614. De Biasio A, Vrana JA, Zhou P, Qian L, Bieszczad CK, Braley KE, Domina AM, Weintraub SJ, Neveu JM, Lane WS, Craig RW (2007) N-terminal truncation of antiapoptotic MCL1, but not G2/M-induced phosphorylation, is associated with stabilization and abundant expression in tumor cells. J Biol Chem 282: 23919-23936.
615. Warr MR, Mills JR, Nguyen M, Lemaire-Ewing S, Baardsnes J, Sun KL, Malina A, Young JC, Jeyaraju DV, O'Connor-McCourt M, Pellegrini L, Pelletier J, Shore GC (2011) Mitochondrion-dependent N-terminal Processing of Outer Membrane Mcl-1 Protein Removes an Essential Mule/Lasu1 Protein-binding Site. J Biol Chem 286: 25098-25107.
616. Schwickart M, Huang X, Lill JR, Liu J, Ferrando R, French DM, Maecker H, O'Rourke K, Bazan F, Eastham-Anderson J, Yue P, Dornan D, Huang DC, Dixit VM (2010) Deubiquitinase USP9X stabilizes MCL1 and promotes tumour cell survival. Nature 463: 103-107.
617. Domina AM, Vrana JA, Gregory MA, Hann SR, Craig RW (2004) MCL1 is phosphorylated in the PEST region and stabilized upon ERK activation in viable cells, and at additional sites with cytotoxic okadaic acid or taxol. Oncogene 23: 5301-5315.
618. Inoshita S, Takeda K, Hatai T, Terada Y, Sano M, Hata J, Umezawa A, Ichijo H (2002) Phosphorylation and inactivation of myeloid cell leukemia 1 by JNK in response to oxidative stress. J Biol Chem 277: 43730-43734.
619. Kobayashi S, Lee SH, Meng XW, Mott JL, Bronk SF, Werneburg NW, Craig RW, Kaufmann SH, Gores GJ (2007) Serine 64 phosphorylation enhances the antiapoptotic function of Mcl-1. J Biol Chem 282: 18407-18417.
620. Morel C, Carlson SM, White FM, Davis RJ (2009) Mcl-1 integrates the opposing actions of signaling pathways that mediate survival and apoptosis. Mol Cell Biol 29: 3845-3852.
621. Ulrich E, Kauffmann-Zeh A, Hueber AO, Williamson J, Chittenden T, Ma A, Evan G (1997) Gene structure, cDNA sequence, and expression of murine Bak, a proapoptotic Bcl-2 family member. Genomics 44: 195-200.
622. Lee DH, Goldberg AL (1998) Proteasome inhibitors: valuable new tools for cell biologists. Trends Cell Biol 8: 397-403.

623. Batista LF, Kaina B, Meneghini R, Menck CF (2009) How DNA lesions are turned into powerful killing structures: insights from UV-induced apoptosis. Mutat Res 681: 197-208.
624. Latonen L, Laiho M (2005) Cellular UV damage responses--functions of tumor suppressor p53. Biochim Biophys Acta 1755: 71-89.
625. Rogakou EP, Boon C, Redon C, Bonner WM (1999) Megabase chromatin domains involved in DNA double-strand breaks in vivo. J Cell Biol 146: 905-916.
626. Rogakou EP, Pilch DR, Orr AH, Ivanova VS, Bonner WM (1998) DNA double-stranded breaks induce histone H2AX phosphorylation on serine 139. J Biol Chem 273: 5858-5868.
627. Weisiger RA, Fridovich I (1973) Mitochondrial superoxide simutase. Site of synthesis and intramitochondrial localization. J Biol Chem 248: 4793-4796.
628. Germain M, Milburn J, Duronio V (2008) MCL-1 inhibits BAX in the absence of MCL-1/BAX Interaction. J Biol Chem 283: 6384-6392.
629. Hinds MG, Day CL (2005) Regulation of apoptosis: uncovering the binding determinants. Curr Opin Struct Biol 15: 690-699.
630. Ku B, Liang C, Jung JU, Oh BH (2011) Evidence that inhibition of BAX activation by BCL-2 involves its tight and preferential interaction with the BH3 domain of BAX. Cell Res 21: 627-641.
631. Denisov AY, Chen G, Sprules T, Moldoveanu T, Beauparlant P, Gehring K (2006) Structural model of the BCL-w-BID peptide complex and its interactions with phospholipid micelles. Biochemistry 45: 2250-2256.
632. Fire E, Gulla SV, Grant RA, Keating AE (2010) Mcl-1-Bim complexes accommodate surprising point mutations via minor structural changes. Protein Sci 19: 507-519.
633. Zha H, Aime-Sempe C, Sato T, Reed JC (1996) Proapoptotic protein Bax heterodimerizes with Bcl-2 and homodimerizes with Bax via a novel domain (BH3) distinct from BH1 and BH2. J Biol Chem 271: 7440-7444.
634. Hanada M, Aime-Sempe C, Sato T, Reed JC (1995) Structure-function analysis of Bcl-2 protein. Identification of conserved domains important for homodimerization with Bcl-2 and heterodimerization with Bax. J Biol Chem 270: 11962-11969.
635. Cheng EH, Levine B, Boise LH, Thompson CB, Hardwick JM (1996) Bax-independent inhibition of apoptosis by Bcl-XL. Nature 379: 554-556.
636. Holinger EP, Chittenden T, Lutz RJ (1999) Bak BH3 peptides antagonize Bcl-xL function and induce apoptosis through cytochrome c-independent activation of caspases. J Biol Chem 274: 13298-13304.
637. Hunter JJ, Bond BL, Parslow TG (1996) Functional dissection of the human Bc12 protein: sequence requirements for inhibition of apoptosis. Mol Cell Biol 16: 877-883.
638. Boya P, Pauleau AL, Poncet D, Gonzalez-Polo RA, Zamzami N, Kroemer G (2004) Viral proteins targeting mitochondria: controlling cell death. Biochim Biophys Acta 1659: 178-189.
639. McCarthy NJ, Hazlewood SA, Huen DS, Rickinson AB, Williams GT (1996) The Epstein-Barr virus gene BHRF1, a homologue of the cellular oncogene Bcl-2, inhibits apoptosis induced by gamma radiation and chemotherapeutic drugs. Adv Exp Med Biol 406: 83-97.
640. Tarodi B, Subramanian T, Chinnadurai G (1994) Epstein-Barr virus BHRF1 protein protects against cell death induced by DNA-damaging agents and heterologous viral infection. Virology 201: 404-407.

641. Rao L, Debbas M, Sabbatini P, Hockenbery D, Korsmeyer S, White E (1992) The adenovirus E1A proteins induce apoptosis, which is inhibited by the E1B 19-kDa and Bcl-2 proteins. Proc Natl Acad Sci U S A 89: 7742-7746.

642. Tarodi B, Subramanian T, Chinnadurai G (1993) Functional similarity between adenovirus e1b 19k gene and bcl2 oncogene - mutant complementation and suppression of cell-death induced by DNA-damaging agents. Int J Oncol 3: 467-472.

643. Goldmacher VS, Bartle LM, Skaletskaya A, Dionne CA, Kedersha NL, Vater CA, Han JW, Lutz RJ, Watanabe S, Cahir McFarland ED, Kieff ED, Mocarski ES, Chittenden T (1999) A cytomegalovirus-encoded mitochondria-localized inhibitor of apoptosis structurally unrelated to Bcl-2. Proc Natl Acad Sci U S A 96: 12536-12541.

644. Fischer SF, Ludwig H, Holzapfel J, Kvansakul M, Chen L, Huang DC, Sutter G, Knese M, Hacker G (2006) Modified vaccinia virus Ankara protein F1L is a novel BH3-domain-binding protein and acts together with the early viral protein E3L to block virus-associated apoptosis. Cell Death Differ 13: 109-118.

645. Poot M, Zhang YZ, Kramer JA, Wells KS, Jones LJ, Hanzel DK, Lugade AG, Singer VL, Haugland RP (1996) Analysis of mitochondrial morphology and function with novel fixable fluorescent stains. J Histochem Cytochem 44: 1363-1372.

646. Khanim F, Dawson C, Meseda CA, Dawson J, Mackett M, Young LS (1997) BHRF1, a viral homologue of the Bcl-2 oncogene, is conserved at both the sequence and functional level in different Epstein-Barr virus isolates. J Gen Virol 78 (Pt 11): 2987-2999.

647. Hart M, Concordet JP, Lassot I, Albert I, del los Santos R, Durand H, Perret C, Rubinfeld B, Margottin F, Benarous R, Polakis P (1999) The F-box protein beta-TrCP associates with phosphorylated beta-catenin and regulates its activity in the cell. Curr Biol 9: 207-210.

648. Hoppe T (2005) Multiubiquitylation by E4 enzymes: 'one size' doesn't fit all. Trends Biochem Sci 30: 183-187.

649. Koegl M, Hoppe T, Schlenker S, Ulrich HD, Mayer TU, Jentsch S (1999) A novel ubiquitination factor, E4, is involved in multiubiquitin chain assembly. Cell 96: 635-644.

650. Breitschopf K, Bengal E, Ziv T, Admon A, Ciechanover A (1998) A novel site for ubiquitination: the N-terminal residue, and not internal lysines of MyoD, is essential for conjugation and degradation of the protein. EMBO J 17: 5964-5973.

651. Ciechanover A, Ben-Saadon R (2004) N-terminal ubiquitination: more protein substrates join in. Trends Cell Biol 14: 103-106.

652. Kirisako T, Kamei K, Murata S, Kato M, Fukumoto H, Kanie M, Sano S, Tokunaga F, Tanaka K, Iwai K (2006) A ubiquitin ligase complex assembles linear polyubiquitin chains. EMBO J 25: 4877-4887.

653. Rahighi S, Ikeda F, Kawasaki M, Akutsu M, Suzuki N, Kato R, Kensche T, Uejima T, Bloor S, Komander D, Randow F, Wakatsuki S, Dikic I (2009) Specific recognition of linear ubiquitin chains by NEMO is important for NF-kappaB activation. Cell 136: 1098-1109.

654. Wang X, Herr RA, Chua WJ, Lybarger L, Wiertz EJ, Hansen TH (2007) Ubiquitination of serine, threonine, or lysine residues on the cytoplasmic tail can induce ERAD of MHC-I by viral E3 ligase mK3. J Cell Biol 177: 613-624.

655. Cadwell K, Coscoy L (2005) Ubiquitination on nonlysine residues by a viral E3 ubiquitin ligase. Science 309: 127-130.

656. Williams C, van den Berg M, Sprenger RR, Distel B (2007) A conserved cysteine is essential for Pex4p-dependent ubiquitination of the peroxisomal import receptor Pex5p. J Biol Chem 282: 22534-22543.

657. Livnat-Levanon N, Glickman MH (2011) Ubiquitin-proteasome system and mitochondria - reciprocity. Biochim Biophys Acta 1809: 80-87.

658. Bartee E, Mansouri M, Hovey Nerenberg BT, Gouveia K, Fruh K (2004) Downregulation of major histocompatibility complex class I by human ubiquitin ligases related to viral immune evasion proteins. J Virol 78: 1109-1120.

659. Yonashiro R, Ishido S, Kyo S, Fukuda T, Goto E, Matsuki Y, Ohmura-Hoshino M, Sada K, Hotta H, Yamamura H, Inatome R, Yanagi S (2006) A novel mitochondrial ubiquitin ligase plays a critical role in mitochondrial dynamics. EMBO J 25: 3618-3626.

660. Nakamura N, Kimura Y, Tokuda M, Honda S, Hirose S (2006) MARCH-V is a novel mitofusin 2- and Drp1-binding protein able to change mitochondrial morphology. EMBO Rep 7: 1019-1022.

661. Karbowski M, Neutzner A, Youle RJ (2007) The mitochondrial E3 ubiquitin ligase MARCH5 is required for Drp1 dependent mitochondrial division. J Cell Biol 178: 71-84.

662. Park YY, Lee S, Karbowski M, Neutzner A, Youle RJ, Cho H (2010) Loss of MARCH5 mitochondrial E3 ubiquitin ligase induces cellular senescence through dynamin-related protein 1 and mitofusin 1. J Cell Sci 123: 619-626.

663. Matsuda A, Suzuki Y, Honda G, Muramatsu S, Matsuzaki O, Nagano Y, Doi T, Shimotohno K, Harada T, Nishida E, Hayashi H, Sugano S (2003) Large-scale identification and characterization of human genes that activate NF-kappaB and MAPK signaling pathways. Oncogene 22: 3307-3318.

664. Zhang B, Huang J, Li HL, Liu T, Wang YY, Waterman P, Mao AP, Xu LG, Zhai Z, Liu D, Marrack P, Shu HB (2008) GIDE is a mitochondrial E3 ubiquitin ligase that induces apoptosis and slows growth. Cell Res 18: 900-910.

665. Gustin JK, Moses AV, Fruh K, Douglas JL (2011) Viral takeover of the host ubiquitin system. Front Microbiol 2: 161.

666. Viswanathan K, Fruh K, DeFilippis V (2010) Viral hijacking of the host ubiquitin system to evade interferon responses. Curr Opin Microbiol 13: 517-523.

667. Zhang L, Villa NY, McFadden G (2009) Interplay between poxviruses and the cellular ubiquitin/ubiquitin-like pathways. FEBS Lett 583: 607-614.

668. Barry M, van Buuren N, Burles K, Mottet K, Wang Q, Teale A (2010) Poxvirus exploitation of the ubiquitin-proteasome system. Viruses 2: 2356-2380.

669. Barry M, Fruh K (2006) Viral modulators of cullin RING ubiquitin ligases: culling the host defense. Sci STKE 2006: pe21.

670. Mercer AA, Fleming SB, Ueda N (2005) F-box-like domains are present in most poxvirus ankyrin repeat proteins. Virus Genes 31: 127-133.

671. Johnston JB, Wang G, Barrett JW, Nazarian SH, Colwill K, Moran M, McFadden G (2005) Myxoma virus M-T5 protects infected cells from the stress of cell cycle arrest through its interaction with host cell cullin-1. J Virol 79: 10750-10763.

672. Werden SJ, Barrett JW, Wang G, Stanford MM, McFadden G (2007) M-T5, the ankyrin repeat, host range protein of myxoma virus, activates Akt and can be functionally replaced by cellular PIKE-A. J Virol 81: 2340-2348.

673. Sonnberg S, Seet BT, Pawson T, Fleming SB, Mercer AA (2008) Poxvirus ankyrin repeat proteins are a unique class of F-box proteins that associate with cellular SCF1 ubiquitin ligase complexes. Proc Natl Acad Sci U S A 105: 10955-10960.

674. Chang SJ, Hsiao JC, Sonnberg S, Chiang CT, Yang MH, Tzou DL, Mercer AA, Chang W (2009) Poxvirus host range protein CP77 contains an F-box-like domain that is necessary to suppress NF-kappaB activation by tumor necrosis factor alpha but is independent of its host range function. J Virol 83: 4140-4152.

675. Sperling KM, Schwantes A, Schnierle BS, Sutter G (2008) The highly conserved orthopoxvirus 68k ankyrin-like protein is part of a cellular SCF ubiquitin ligase complex. Virology 374: 234-239.

676. Mohamed MR, Rahman MM, Lanchbury JS, Shattuck D, Neff C, Dufford M, van Buuren N, Fagan K, Barry M, Smith S, Damon I, McFadden G (2009) Proteomic screening of variola virus reveals a unique NF-kappaB inhibitor that is highly conserved among pathogenic orthopoxviruses. Proc Natl Acad Sci U S A 106: 9045-9050.

677. Kvansakul M (Unpublished).

678. Bonifacino JS, Dell'Angelica EC, Springer TA (2001) Immunoprecipitation. Curr Protoc Immunol Chapter 8: Unit 8 3.

679. Weiss W, Gorg A (2008) Sample solublization buffers for two-dimensional electrophoresis. Methods Mol Biol 424: 35-42.

680. Adams J (2002) Proteasome inhibitors as new anticancer drugs. Curr Opin Oncol 14: 628-634.

681. Giuliano M, D'Anneo A, De Blasio A, Vento R, Tesoriere G (2003) Apoptosis meets proteasome, an invaluable therapeutic target of anticancer drugs. Ital J Biochem 52: 112-121.

682. Furukawa M, Zhang Y, McCarville J, Ohta T, Xiong Y (2000) The CUL1 C-terminal sequence and ROC1 are required for efficient nuclear accumulation, NEDD8 modification, and ubiquitin ligase activity of CUL1. Mol Cell Biol 20: 8185-8197.

683. Tseng M, Palaniyar N, Zhang W, Evans DH (1999) DNA binding and aggregation properties of the vaccinia virus I3L gene product. J Biol Chem 274: 21637-21644.

684. Lin YC, Li J, Irwin CR, Jenkins H, DeLange L, Evans DH (2008) Vaccinia virus DNA ligase recruits cellular topoisomerase II to sites of viral replication and assembly. J Virol 82: 5922-5932.

685. Hannoun Z, Greenhough S, Jaffray E, Hay RT, Hay DC (2010) Post-translational modification by SUMO. Toxicology 278: 288-293.

686. Dunkle A, Dzhagalov I, He YW (2010) Mcl-1 promotes survival of thymocytes by inhibition of Bak in a pathway separate from Bcl-2. Cell Death Differ 17: 994-1002.

687. Pearce AF, Lyles DS (2009) Vesicular stomatitis virus induces apoptosis primarily through Bak rather than Bax by inactivating Mcl-1 and Bcl-XL. J Virol 83: 9102-9112.

688. Schache P, Gurlevik E, Struver N, Woller N, Malek N, Zender L, Manns M, Wirth T, Kuhnel F, Kubicka S (2009) VSV virotherapy improves chemotherapy by triggering apoptosis due to proteasomal degradation of Mcl-1. Gene Ther 16: 849-861.

689. Mohd-Ismail NK, Deng L, Sukumaran SK, Yu VC, Hotta H, Tan YJ (2009) The hepatitis C virus core protein contains a BH3 domain that regulates apoptosis through specific interaction with human Mcl-1. J Virol 83: 9993-10006.

690. Langland JO, Kash JC, Carter V, Thomas MJ, Katze MG, Jacobs BL (2006) Suppression of proinflammatory signal transduction and gene expression by the dual nucleic acid binding domains of the vaccinia virus E3L proteins. J Virol 80: 10083-10095.

691. Zhai D, Jin C, Huang Z, Satterthwait AC, Reed JC (2008) Differential regulation of Bax and Bak by anti-apoptotic Bcl-2 family proteins Bcl-B and Mcl-1. J Biol Chem 283: 9580-9586.

692. Vieira HL, Belzacq AS, Haouzi D, Bernassola F, Cohen I, Jacotot E, Ferri KF, El Hamel C, Bartle LM, Melino G, Brenner C, Goldmacher V, Kroemer G (2001) The adenine nucleotide translocator: a target of nitric oxide, peroxynitrite, and 4-hydroxynonenal. Oncogene 20: 4305-4316.

693. Chen W, Calvo PA, Malide D, Gibbs J, Schubert U, Bacik I, Basta S, O'Neill R, Schickli J, Palese P, Henklein P, Bennink JR, Yewdell JW (2001) A novel influenza A virus mitochondrial protein that induces cell death. Nat Med 7: 1306-1312.

694. Zamarin D, Garcia-Sastre A, Xiao X, Wang R, Palese P (2005) Influenza virus PB1-F2 protein induces cell death through mitochondrial ANT3 and VDAC1. PLoS Pathog 1: e4.

695. Pastorino JG, Hoek JB (2008) Regulation of hexokinase binding to VDAC. J Bioenerg Biomembr 40: 171-182.

696. Zhao G, Droit L, Tesh RB, Popov VL, Little NS, Upton C, Virgin HW, Wang D (2011) The genome of Yoka poxvirus. J Virol 85: 10230-10238.

697. Lin EY, Orlofsky A, Berger MS, Prystowsky MB (1993) Characterization of A1, a novel hemopoietic-specific early-response gene with sequence similarity to bcl-2. J Immunol 151: 1979-1988.

698. Gonzalez JM, Esteban M (2010) A poxvirus Bcl-2-like gene family involved in regulation of host immune response: sequence similarity and evolutionary history. Virol J 7: 59.

699. Cooray S, Bahar MW, Abrescia NG, McVey CE, Bartlett NW, Chen RA, Stuart DI, Grimes JM, Smith GL (2007) Functional and structural studies of the vaccinia virus virulence factor N1 reveal a Bcl-2-like anti-apoptotic protein. J Gen Virol 88: 1656-1666.

700. Bartlett N, Symons JA, Tscharke DC, Smith GL (2002) The vaccinia virus N1L protein is an intracellular homodimer that promotes virulence. J Gen Virol 83: 1965-1976.

701. Aoyagi M, Zhai D, Jin C, Aleshin AE, Stec B, Reed JC, Liddington RC (2007) Vaccinia virus N1L protein resembles a B cell lymphoma-2 (Bcl-2) family protein. Protein Sci 16: 118-124.

702. DiPerna G, Stack J, Bowie AG, Boyd A, Kotwal G, Zhang Z, Arvikar S, Latz E, Fitzgerald KA, Marshall WL (2004) Poxvirus protein N1L targets the I-kappaB kinase complex, inhibits signaling to NF-kappaB by the tumor necrosis factor superfamily of receptors, and inhibits NF-kappaB and IRF3 signaling by toll-like receptors. J Biol Chem 279: 36570-36578.

703. Postigo A, Way M (2011) The Vaccinia Virus Encoded Bcl-2 Homologues Do Not Act as Direct Bax Inhibitors. J Virol.

704. Graham SC, Bahar MW, Cooray S, Chen RA, Whalen DM, Abrescia NG, Alderton D, Owens RJ, Stuart DI, Smith GL, Grimes JM (2008) Vaccinia virus proteins A52 and B14 Share a Bcl-2-like fold but have evolved to inhibit NF-kappaB rather than apoptosis. PLoS Pathog 4: e1000128.

705. Satheshkumar PS, Anton LC, Sanz P, Moss B (2009) Inhibition of the ubiquitin-proteasome system prevents vaccinia virus DNA replication and expression of intermediate and late genes. J Virol 83: 2469-2479.

706. Teale A, Campbell S, Van Buuren N, Magee WC, Watmough K, Couturier B, Shipclark R, Barry M (2009) Orthopoxviruses require a functional ubiquitin-proteasome system for productive replication. J Virol 83: 2099-2108.

707. Benard G, Neutzner A, Peng G, Wang C, Livak F, Youle RJ, Karbowski M (2010) IBRDC2, an IBR-type E3 ubiquitin ligase, is a regulatory factor for Bax and apoptosis activation. EMBO J 29: 1458-1471.

708. Niture SK, Jaiswal AK (2011) INrf2 (Keap1) targets Bcl-2 degradation and controls cellular apoptosis. Cell Death Differ 18: 439-451.

709. Nakamura N, Hirose S (2008) Regulation of mitochondrial morphology by USP30, a deubiquitinating enzyme present in the mitochondrial outer membrane. Mol Biol Cell 19: 1903-1911.

710. Bagola K, Mehnert M, Jarosch E, Sommer T (2011) Protein dislocation from the ER. Biochim Biophys Acta 1808: 925-936.

711. Stewart DP, Koss B, Bathina M, Perciavalle RM, Bisanz K, Opferman JT (2010) Ubiquitin-independent degradation of antiapoptotic MCL-1. Mol Cell Biol 30: 3099-3110.

712. Wiggins CM, Tsvetkov P, Johnson M, Joyce CL, Lamb CA, Bryant NJ, Komander D, Shaul Y, Cook SJ (2011) BIM(EL), an intrinsically disordered protein, is degraded by 20S proteasomes in the absence of poly-ubiquitylation. J Cell Sci 124: 969-977.

713. Szabo I, Soddemann M, Leanza L, Zoratti M, Gulbins E (2011) Single-point mutations of a lysine residue change function of Bax and Bcl-xL expressed in Bax- and Bak-less mouse embryonic fibroblasts: novel insights into the molecular mechanisms of Bax-induced apoptosis. Cell Death Differ 18: 427-438.

714. Szabo I, Bock J, Grassme H, Soddemann M, Wilker B, Lang F, Zoratti M, Gulbins E (2008) Mitochondrial potassium channel Kv1.3 mediates Bax-induced apoptosis in lymphocytes. Proc Natl Acad Sci U S A 105: 14861-14866.

715. McCormick AL, Smith VL, Chow D, Mocarski ES (2003) Disruption of mitochondrial networks by the human cytomegalovirus UL37 gene product viral mitochondrion-localized inhibitor of apoptosis. J Virol 77: 631-641.

716. Poncet D, Pauleau AL, Szabadkai G, Vozza A, Scholz SR, Le Bras M, Briere JJ, Jalil A, Le Moigne R, Brenner C, Hahn G, Wittig I, Schagger H, Lemaire C, Bianchi K, Souquere S, Pierron G, Rustin P, Goldmacher VS, Rizzuto R, Palmieri F, Kroemer G (2006) Cytopathic effects of the cytomegalovirus-encoded apoptosis inhibitory protein vMIA. J Cell Biol 174: 985-996.

717. Wilton S, Mohandas AR, Dales S (1995) Organization of the vaccinia envelope and relationship to the structure of intracellular mature virions. Virology 214: 503-511.

718. Bowie A, Kiss-Toth E, Symons JA, Smith GL, Dower SK, O'Neill LA (2000) A46R and A52R from vaccinia virus are antagonists of host IL-1 and toll-like receptor signaling. Proc Natl Acad Sci U S A 97: 10162-10167.

719. Alcami A, Smith GL (1995) Vaccinia, cowpox, and camelpox viruses encode soluble gamma interferon receptors with novel broad species specificity. J Virol 69: 4633-4639.

720. Spriggs MK, Hruby DE, Maliszewski CR, Pickup DJ, Sims JE, Buller RM, VanSlyke J (1992) Vaccinia and cowpox viruses encode a novel secreted interleukin-1-binding protein. Cell 71: 145-152.

721. Symons JA, Alcami A, Smith GL (1995) Vaccinia virus encodes a soluble type I interferon receptor of novel structure and broad species specificity. Cell 81: 551-560.

722. Graham KA, Lalani AS, Macen JL, Ness TL, Barry M, Liu LY, Lucas A, Clark-Lewis I, Moyer RW, McFadden G (1997) The T1/35kDa family of poxvirus-secreted proteins bind chemokines and modulate leukocyte influx into virus-infected tissues. Virology 229: 12-24.

723. Smith CA, Smith TD, Smolak PJ, Friend D, Hagen H, Gerhart M, Park L, Pickup DJ, Torrance D, Mohler K, Schooley K, Goodwin RG (1997) Poxvirus genomes encode a secreted, soluble protein that preferentially inhibits beta chemokine activity yet lacks sequence homology to known chemokine receptors. Virology 236: 316-327.

724. Blomquist MC, Hunt LT, Barker WC (1984) Vaccinia virus 19-kilodalton protein: relationship to several mammalian proteins, including two growth factors. Proc Natl Acad Sci U S A 81: 7363-7367.

725. Reisner AH (1985) Similarity between the vaccinia virus 19K early protein and epidermal growth factor. Nature 313: 801-803.

726. Comeau MR, Johnson R, DuBose RF, Petersen M, Gearing P, VandenBos T, Park L, Farrah T, Buller RM, Cohen JI, Strockbine LD, Rauch C, Spriggs MK (1998) A poxvirus-encoded semaphorin induces cytokine production from monocytes and binds to a novel cellular semaphorin receptor, VESPR. Immunity 8: 473-482.

727. Howard ST, Chan YS, Smith GL (1991) Vaccinia virus homologues of the Shope fibroma virus inverted terminal repeat proteins and a discontinuous ORF related to the tumor necrosis factor receptor family. Virology 180: 633-647.

728. Colamonici OR, Domanski P, Sweitzer SM, Larner A, Buller RM (1995) Vaccinia virus B18R gene encodes a type I interferon-binding protein that blocks interferon alpha transmembrane signaling. J Biol Chem 270: 15974-15978.

729. Alcami A, Smith GL (1992) A soluble receptor for interleukin-1 beta encoded by vaccinia virus: a novel mechanism of virus modulation of the host response to infection. Cell 71: 153-167.

730. Smith VP, Bryant NA, Alcami A (2000) Ectromelia, vaccinia and cowpox viruses encode secreted interleukin-18-binding proteins. J Gen Virol 81: 1223-1230.

731. Born TL, Morrison LA, Esteban DJ, VandenBos T, Thebeau LG, Chen N, Spriggs MK, Sims JE, Buller RM (2000) A poxvirus protein that binds to and inactivates IL-18, and inhibits NK cell response. J Immunol 164: 3246-3254.

732. Law KM, Smith GL (1992) A vaccinia serine protease inhibitor which prevents virus-induced cell fusion. J Gen Virol 73 (Pt 3): 549-557.

733. Zhou J, Sun XY, Fernando GJ, Frazer IH (1992) The vaccinia virus K2L gene encodes a serine protease inhibitor which inhibits cell-cell fusion. Virology 189: 678-686.

734. Shisler JL, Jin XL (2004) The vaccinia virus K1L gene product inhibits host NF-kappaB activation by preventing IkappaBalpha degradation. J Virol 78: 3553-3560.

735. Gedey R, Jin XL, Hinthong O, Shisler JL (2006) Poxviral regulation of the host NF-kappaB response: the vaccinia virus M2L protein inhibits induction of NF-kappaB activation via an ERK2 pathway in virus-infected human embryonic kidney cells. J Virol 80: 8676-8685.

736. Chen RA, Ryzhakov G, Cooray S, Randow F, Smith GL (2008) Inhibition of IkappaB kinase by vaccinia virus virulence factor B14. PLoS Pathog 4: e22.

737. Bahar MW, Kenyon JC, Putz MM, Abrescia NG, Pease JE, Wise EL, Stuart DI, Smith GL, Grimes JM (2008) Structure and function of A41, a vaccinia virus chemokine binding protein. PLoS Pathog 4: e5.

738. Schroder M, Baran M, Bowie AG (2008) Viral targeting of DEAD box protein 3 reveals its role in TBK1/IKKepsilon-mediated IRF activation. EMBO J 27: 2147-2157.

739. Najarro P, Traktman P, Lewis JA (2001) Vaccinia virus blocks gamma interferon signal transduction: viral VH1 phosphatase reverses Stat1 activation. J Virol 75: 3185-3196.

740. Ng A, Tscharke DC, Reading PC, Smith GL (2001) The vaccinia virus A41L protein is a soluble 30 kDa glycoprotein that affects virus virulence. J Gen Virol 82: 2095-2105.

741. Kotwal GJ, Isaacs SN, McKenzie R, Frank MM, Moss B (1990) Inhibition of the complement cascade by the major secretory protein of vaccinia virus. Science 250: 827-830.

742. Kotwal GJ, Moss B (1988) Vaccinia virus encodes a secretory polypeptide structurally related to complement control proteins. Nature 335: 176-178.

743. Engelstad M, Howard ST, Smith GL (1992) A constitutively expressed vaccinia gene encodes a 42-kDa glycoprotein related to complement control factors that forms part of the extracellular virus envelope. Virology 188: 801-810.

Appendix

A

B
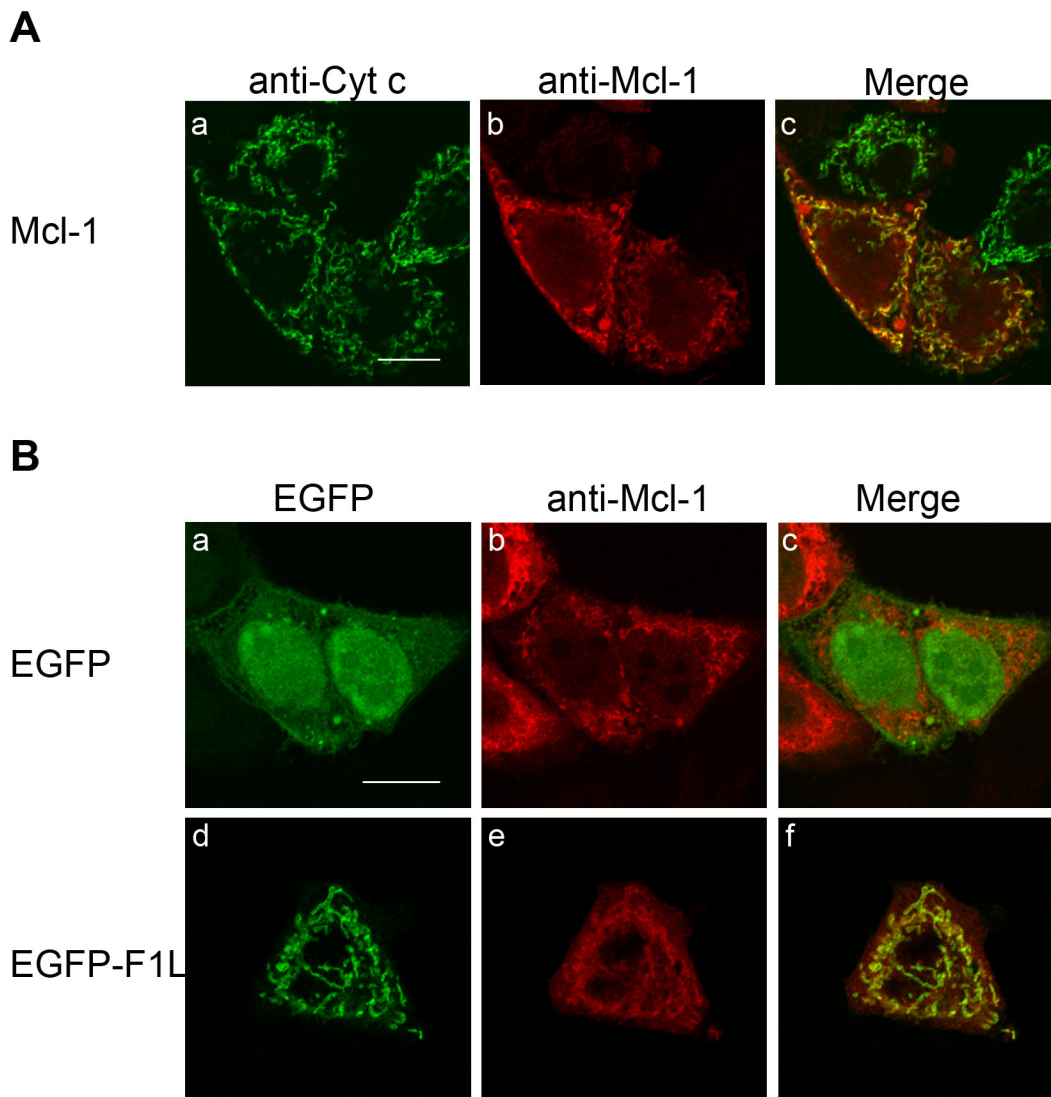
Figure A.1 Mcl-1 and F1L colocalize at mitochondria. A. HeLa cells transfected with pCR3.1-Mcl-1 for 16 hours were fixed and stained with anti-cytochrome c (anti-Cyt c) to visualize mitochondria and anti-Mcl-1 to visualize Mcl-1 by confocal microscopy. **B.** HeLa cells were transfected with pEGFP or pEGFP-F1L and pCR3.1-Mcl-1 for 16 hours before fixing and staining with a polyclonal anti-Mcl-1 antibody. The localization of EGFP and EGFP-F1L was visualized by EGFP fluorescence (**a,d**), while anti-Mcl-1 staining revealed Mcl-1 localization (**b,e**). Merged images demonstrate colocalization of Mcl-1 and EGFP-F1L (**f**), but not Mcl-1 and EGFP (**c**). Bar=15μm.
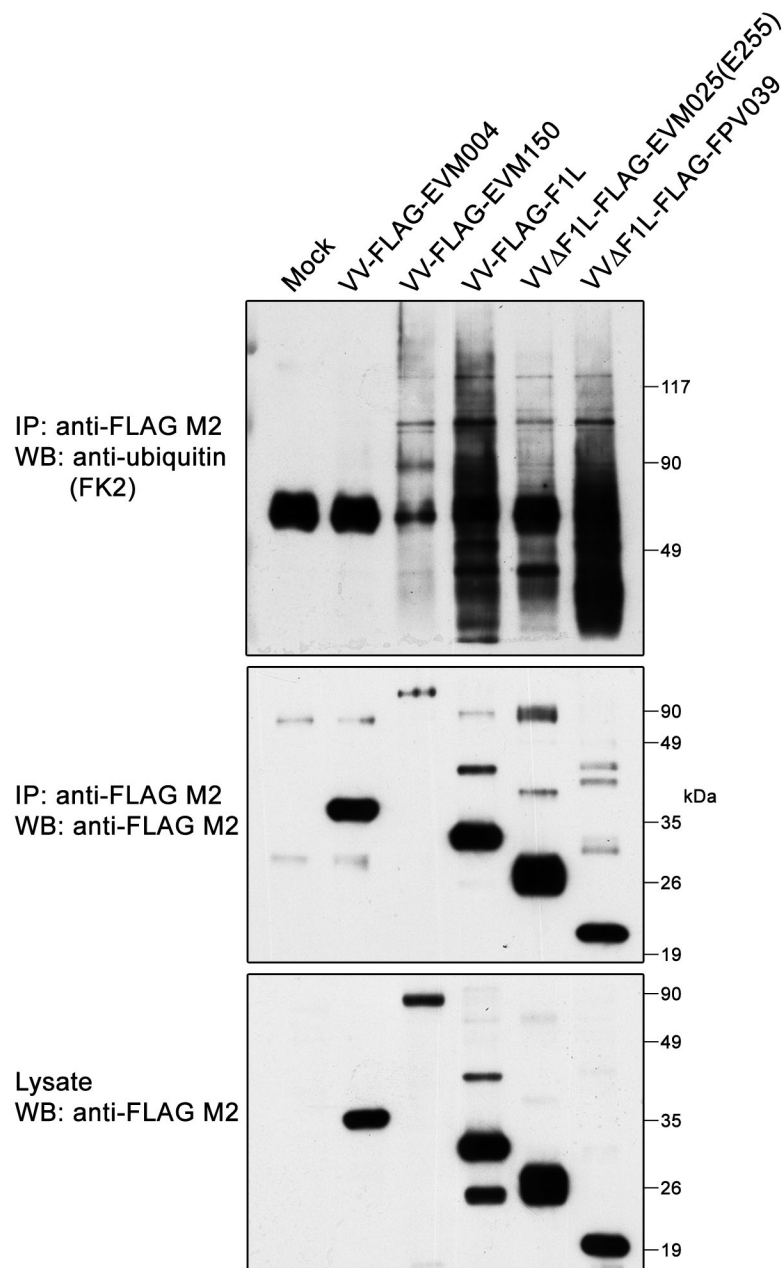
Figure A.2 F1L associates with endogenous conjugated ubiquitin during RIPA lysis. HeLa cells were mock-infected or infected with VV-FLAG-EVM004, VV-FLAG-EVM150, VV-FLAG-F1L, VVΔ F1L-FLAG-EVM025(E255), or VVΔF1L-FLAG-FPV039 for 12 hours. To examine direct conjugation to ubiquitin, cells were lysed in RIPA buffer and subject to anti-FLAG M2 immunoprecipitation. Immunoprecipitates were western blotted with anti-ubiquitin (FK2) and anti-FLAG M2, while lysates were probed with anti-FLAG M2.

	anti-HA	anti-FLAG M2	Merge
VV-FLAG-F1L+ HA-WT-Ub	a	b	c
	d	e	f
	g	h	i
	j	k	l
	m	n	o
	p	q	r
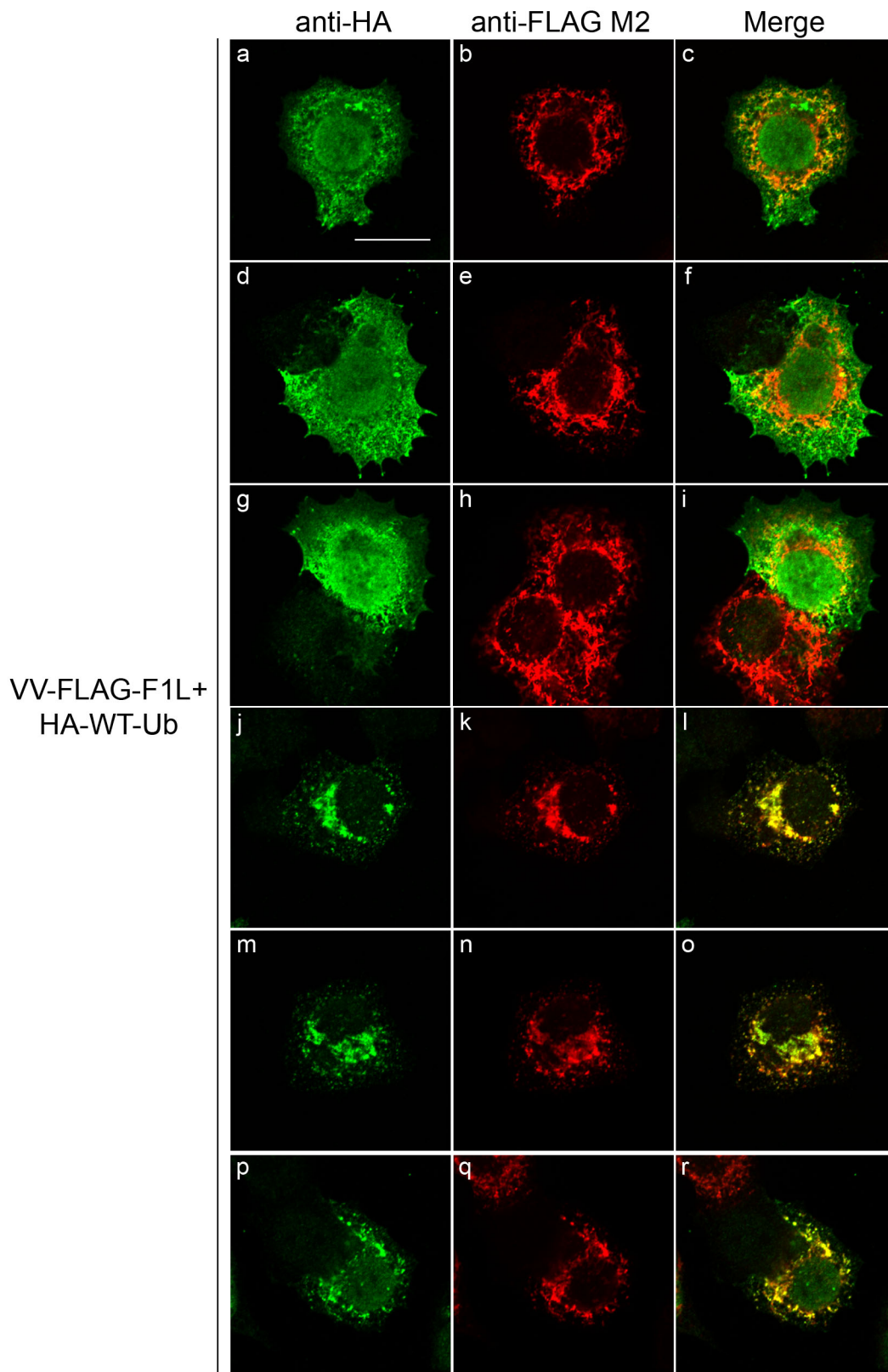
Figure A.3 F1L and ubiquitin colocalize in aggregated and punctuate structures. HeLa cells were co-infected with VV-FLAG-F1L at an MOI of 4 and VVT7 at an MOI of 1 and transfected with pcDNA-HA-ubiquitin (HA-WT-Ub) for fourteen hours. Cells were fixed and stained with anti-HA to visualize HA-ubiquitin and anti-FLAG M2 to detect FLAG-F1L. Cells expressing FLAG-F1L and HA-ubiquitin adopted two distinct phenotypes. Colocalization did not occur when FLAG-F1L was reticular and HA-WT-Ub was diffuse throughout the cell (**a-i**). Colocalization only occurred when FLAG-F1L and HA-WT-Ub were found in punctuate or aggregated regions (**j-r**). Bar=15μm.
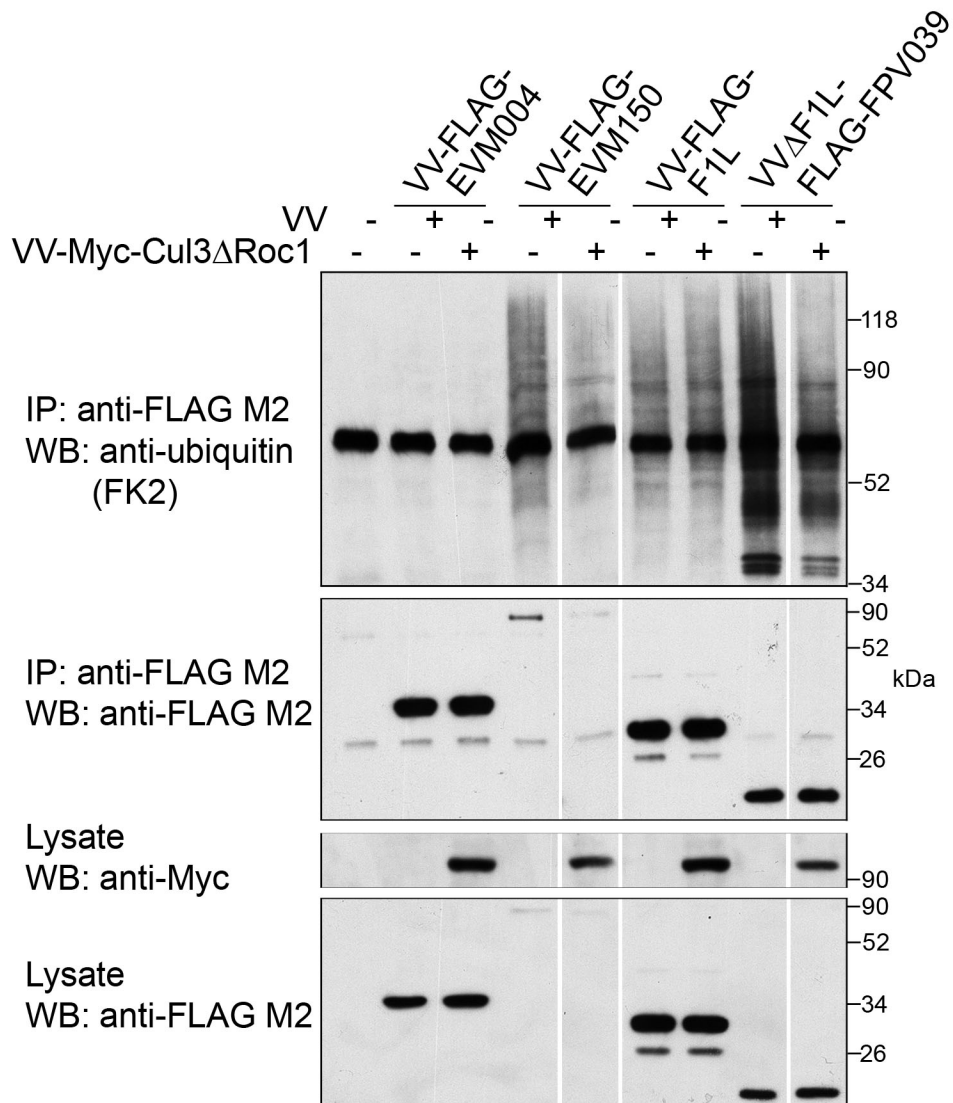
Figure A.4 F1L is not regulated by the cullin-3 ubiquitin ligase. HEK 293T cells were mock-infected or infected with VV-FLAG-EVM004, VV-FLAG-EVM150, VV-FLAG-F1L, or VVΔF1L-FLAG-FPV039 and co-infected with VV or VV-Myc-Cul3 ΔRoc1, each at an MOI of 5. Twelve hours post infection, cells were lysed in 1% NP-40 buffer and immunoprecipitated with anti-FLAG M2. Immunoprecipitates were western blotted with anti-ubiquitin (FK2) and anti-FLAG M2, while lysates were western blotted with anti-Myc and anti-FLAG M2. Note: lane 5 (VV-FLAG-EVM150 + VV-Myc-Cul3ΔRoc1) and lane 9 (VVΔF1L-FLAG-FPV039 + VV-Myc-Cul3ΔRoc1) were cut from the same membrane and exchanged with one another.
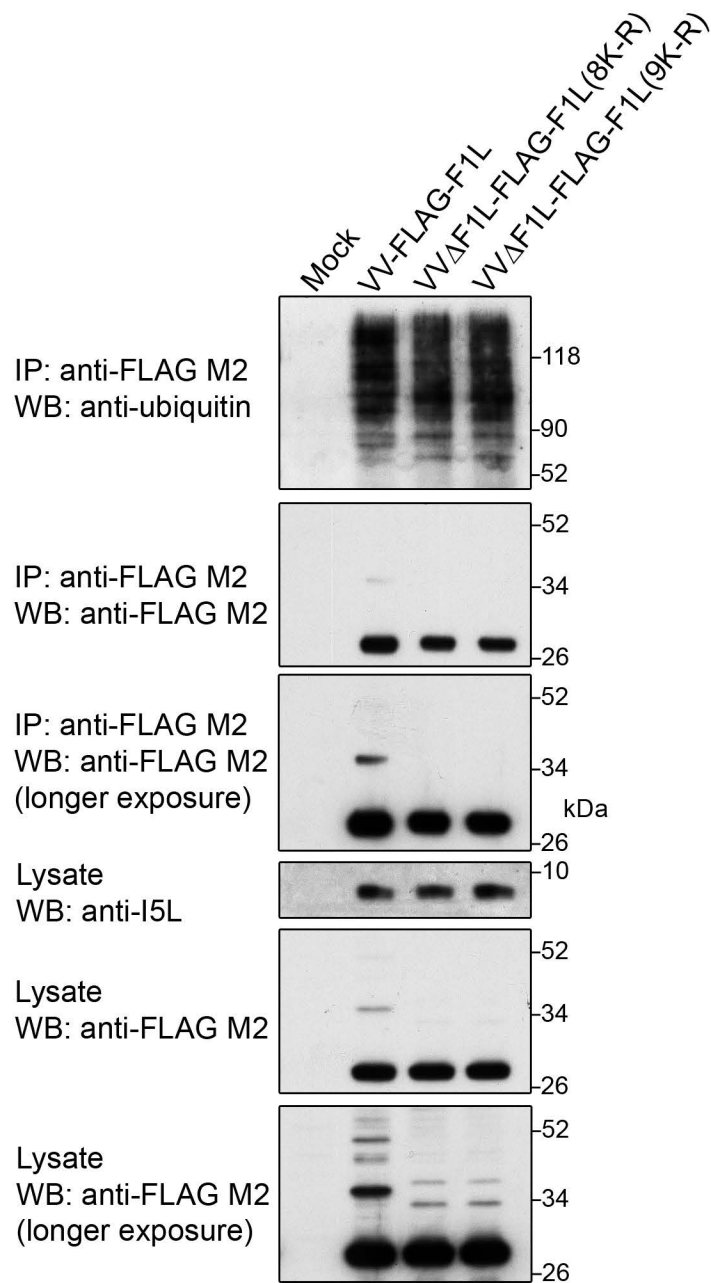
Figure A.5 FLAG-F1L(8K-R) and FLAG-F1L(9K-R) associate with ubiquitin during recombinant virus infection. HeLa cells were mock-infected or infected with VV-FLAG-F1L, VVΔF1L-FLAG-F1L(8K-R), or VVΔF1L-FLAG-F1L(9K-R) at an MOI of 5 for 12 hours. Cells were lysed in RIPA buffer and anti-FLAG M2 was used for immunoprecipitation. Immunoprecipitates were western blotted with rabbit anti-ubiquitin or anti-FLAG M2, while lysates were western blotted with anti-I5L or anti-FLAG M2. Longer exposures were included for immunoprecipitates and lysates western blotted with anti-FLAG M2.

A

anti-FLAG M2

Reticular

Punctate

Aggregated
& Punctate
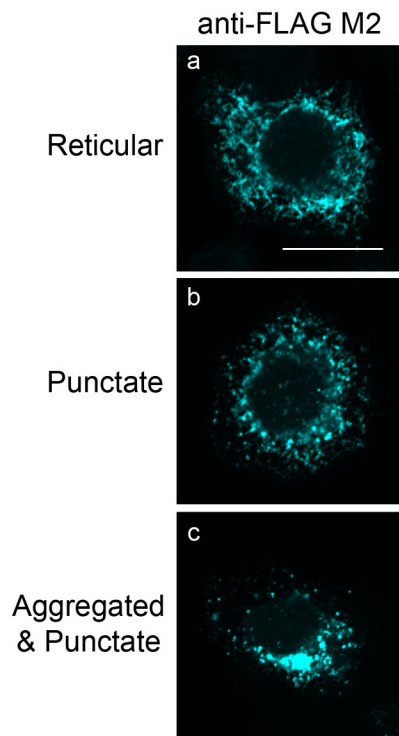
B
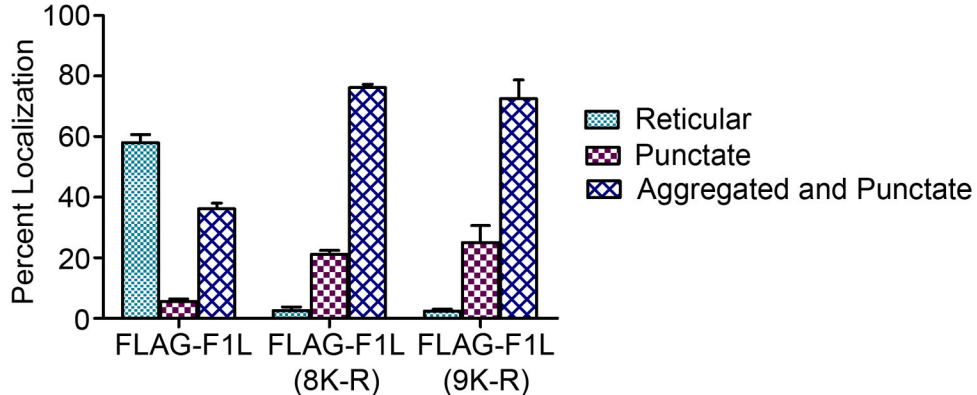
Figure A.6 Mitochondria in VVΔF1L-FLAG-F1L(8K-R)- and VVΔ F1L-FLAG-F1L(9K-R)-infected cells are aggregated and punctate. A. HeLa cells were infected with VV-FLAG-F1L, VVΔF1L-FLAG-F1L(8K-R), or VVΔ F1L-FLAG-F1L(9K-R) for 12 hours at an MOI of 5. Anti-FLAG M2 was used to visualize localization patterns of FLAG-tagged proteins, which were either reticular (**a**), punctate (**b**), or aggregated and punctate (**c**). Bar=15μm. **B.** Quantification of FLAG-F1L, FLAG-F1L(8K-R), and FLAG-F1L(9K-R) localization patterns. Two hundred VV-FLAG-F1L-, VVΔF1L-FLAG-F1L(8K-R)-, and VVΔ F1L-FLAG-F1L(9K-R)-infected cells were counted in triplicate and graphically represented with standard deviations.

A

anti-ubiquitin (FK2) anti-FLAG M2 Merge

No colocalization

Colocalization

B
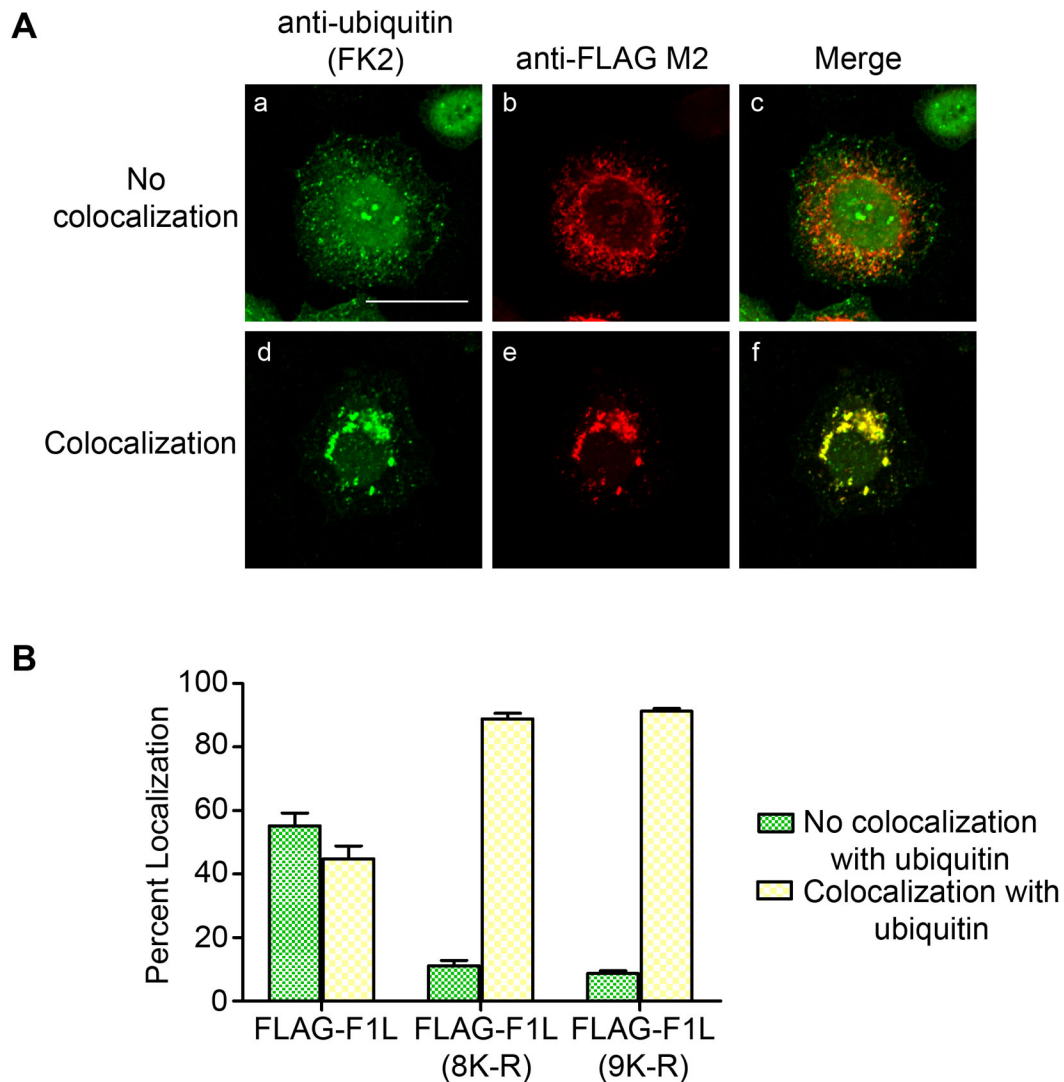
Figure A.7 The majority of cells expressing FLAG-F1L(8K-R) and FLAG-F1L(9K-R) recruit conjugated ubiquitin to mitochondria. A. VV-infected and pSC66-FLAG-F1L-transfected HeLa cells demonstrated two phenotypes. No colocalization was observed between ubiquitin and FLAG-F1L when conjugated ubiquitin was speckled and diffuse throughout the cell and FLAG-F1L was reticular (**a-c**). Colocalization only occurred when both conjugated ubiquitin and FLAG-F1L were punctate and aggregated (**d-f**). Bar=15μm. **B.** Quantification of colocalization between FLAG-F1L, FLAG-F1L(8K-R), and FLAG-F1L(9K-R) and conjugated ubiquitin. Two hundred cells from figure 5.18 were counted in triplicate for colocalization with conjugated ubiquitin.
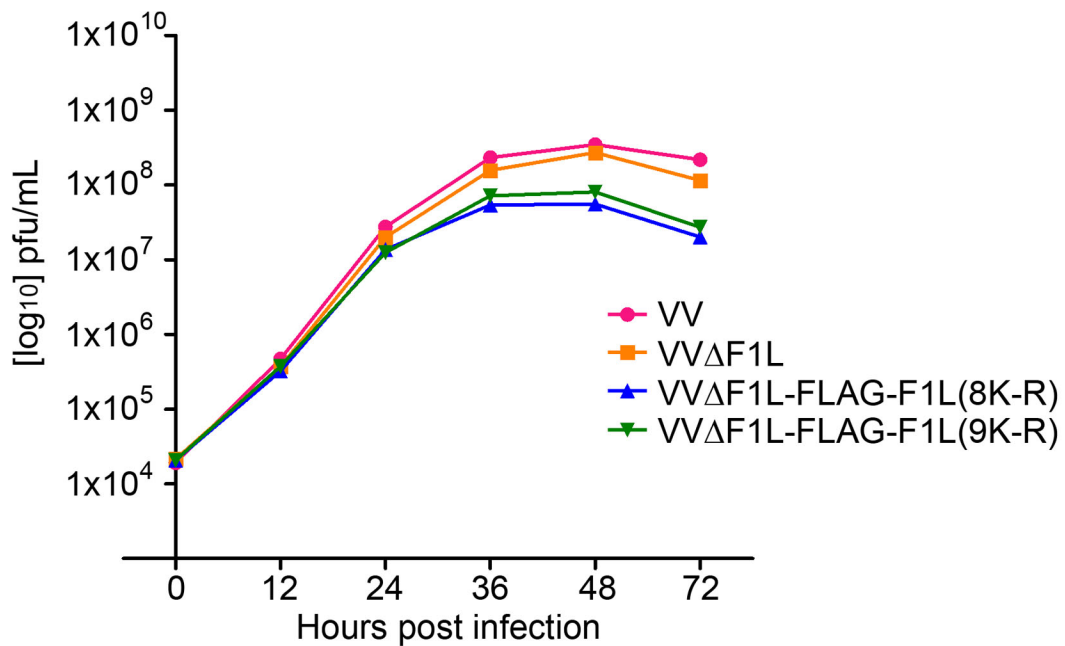
Figure A.8 VVΔF1L-FLAG-F1L(8K-R) and VVΔF1L-FLAG-F1L(9K-R) display late growth defects. Viral growth kinetics were examined by infecting BGMK cells with VV, VVΔF1L, VVΔF1L-FLAG-F1L(8K-R), or VVΔF1L-FLAG-F1L(9K-R) at an MOI of 0.01 in triplicate. Infected cells were harvested up to 72 hours post infection and lysed to release infectious virus. Serial dilutions of harvested virus were plated on BGMK cells in duplicate for 42 hours. Infected monolayers were fixed and stained with crystal violet solution and plaques were counted to generate a multi-step virus growth curve with standard deviations.

IP: anti-FLAG M2

Mock   VV   VV-FLAG-F1L

34 —

— Voltage-dependent anion channel*
— Adenine nucleotide transporter**
— Vaccinia virus F1L
— Immunoglobulin light chain

26 —
kDa

*21.6% peptide coverage
**36.6% peptide coverage
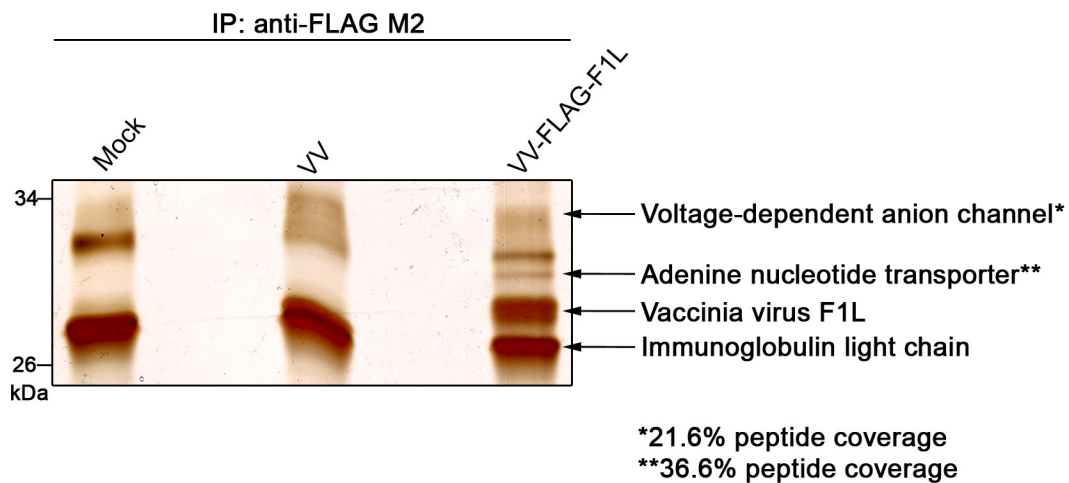
Figure A.9 FLAG-F1L associates with components of the permeability pore during infection. Mock-infected HeLa cells or HeLa cells infected with VV or VV-FLAG-F1L at an MOI of 5 were lysed 12 hours post infection in 1% NP-40 lysis buffer and subject to anti-FLAG M2 immunoprecipitation. Samples were resolved by SDS-PAGE and visualized by silver staining. Unique bands in VV-FLAG-F1L immunoprecipitates were excised and analyzed by mass spectrometry, revealing that FLAG-F1L associates with the voltage-dependent anion channel and adenine nucleotide transporter.